DEVELOPMENT OF MUCOADHESIVE THERMOGELS FOR TREATING ANTERIOR OCULAR CONDITIONS

DEVELOPMENT OF MUCOADHESIVE THERMOGELS FOR TREATING ANTERIOR OCULAR CONDITIONS

By

MITCHELL SCOTT ROSS, B.E.Sc

A Thesis

Submitted to the School of Graduate Studies

In the Partial Fulfillment of the Requirements

for the Degree

Doctor of Philosophy in Chemical Engineering

McMaster University

Doctor of Philosophy (2022) McMaster University

(Chemical Engineering) Hamilton, Ontario

TITLE: Development of Mucoadhesive Thermogels for Treating Anterior Ocular Conditions

AUTHOR: Mitchell Ross, B.E.Sc (McMaster University)

SUPERVISOR: Professor Heather Sheardown

NUMBER OF PAGES: xxix, 242

LAY ABSTRACT

Topical eyedrops are the most utilized treatment option for the vast majority of ocular diseases. However, eyedrops are largely ineffective with less than 5% of an applied dose reaching the desired cite of action. Therefore, eyedrops need to be frequently reapplied. To overcome these limitations, an eyedrop was developed which can be applied as a liquid but gels against the heat of the eye. This gel allows for prolonged drug release over multiple days, greatly increasing drug efficacy as well as patient comfort and compliance. To prevent obstructing vision, these gels can be applied under the lower eyelid. To keep these gels retained under the lower eyelid, they were designed to anchor to the natural mucus layer which covers the surface of eye. The developed eyedrops represent a significant advancement in ocular care; bettering the convenience, comfort, and effectiveness for patients of a topical formulation compared to traditional eyedrops.

ABSTRACT

Most marketed formulations for treating anterior ocular conditions are topical, with conventional eyedrops representing the most utilized modality. However, due to the natural clearance mechanisms of the eye, less than 5% of an applied dose remains bioavailable following administration. To overcome the shortcomings associated with conventional eyedrops, a series of enzymatically degradable, mucoadhesive thermogels were developed. Thermogels can be applied as a solution, like a conventional eyedrops, but gel against the heat of eye. To avoid obstructing vision, these thermogels were designed to be instilled within the inferior fornix of the eye. In these studies, the base thermogelling polymer (pNAM) was crosslinked with the natural polymer chitosan. Not only does crosslinking strengthen the typically weak thermogels, but chitosan can be enzymatically degraded by lysozyme, the highest concentration protein found in tear fluid. Therefore, the developed thermogels can be applied to the inferior fornix and degrade over multiple days. A limitation of applying materials to the inferior fornix is they tend to be poorly retained. To anchor the developed thermogels within the inferior fornix, the mucoadhesive properties were tailored based on the chitosan utilized as well as the inclusion of a disulfide monomer capable of covalently bonding with the natural mucosal layer covering the surface of the eye. The disulfide bridging monomer could be further conjugated with therapeutic components which were released as a function of mucosal interaction. Conjugates investigated included cysteamine for treating cystinosis, n-acetyl cysteine for

treating dry eye, the adhesion peptide RGDC as a model peptide/protein, and polyethylene glycol for modulating material properties. The release of the drugs Ketotifen Fumarate, for treating allergic conjunctivitis, and atropine, for treating myopia, were also investigated. The safety of the developed thermogels were studied both *in vivo* and extensively *in vitro* utilizing both rat and rabbit models.

ACKNOWLEDGEMENTS

First and foremost, I would like to thank my mother for her unwavering support as well as instilling an interest in science and education for myself and my brothers from a young age. No one could ask for a better mom. I would also like to thank by dad for his insights, and the research opportunities he provided me, which helped lead me to where I am now. And of course, my brothers Fraser and Ian for all they have done over this time and long before it.

Next, I would like to thank Heather Sheardown for everything she has done for me over the past four years. I truly believe I couldn't ask for a better, more supportive supervisor, who was always there when I needed her and provided me with so many opportunities along the way. I would also like to thank my committee members Todd Hoare and Judith West-Mays for their support and feedback throughout this process.

I need to thank also thank a lot of my friends for their support over this time. Jenn, who has been my best friend these last few years, provided me with so much support throughout, and listened to me complain more times than can be counted (but she also joined in). Nate as a dedicated co-brewer and an equal within fantasy football. Aristo, who has lived with me all throughout Europe and will continue to be my travel buddy. Taylor and Nicole for their friendship, camping experiences, and general lack of knowledge regarding proper use of an Epipen. Zahan and Matt as my roommates over this time and as fellow soccer stars. Lindsay, for her faithful

two years of service and chauffeuring. And last but not least; Katie, Clare, and Tom, for their years of putting up with me.

Academically my collaborators, Jenn, Emily-Anne, Ben, Jon, Aftab, and Lindsay for their help throughout my thesis. And finally, Lina Liu deserves a special shoutout for her help over these last four years and being someone in the lab I could always count on for a hand and support.

DECLARATION OF ACADEMIC ACHIEVEMENT

a) Thesis Chapters

Ross M, and Sheardown H. (expected submission 2022). Application of Thermogels to the Anterior of the Eye as Alternatives to Conventional Eyedrops.

This review, written entirely by the author of this thesis, was divided across chapter 1: introduction and objectives, and chapter 2: literature review. The review covers the recent advancement in the application of thermogels to the anterior of the eye as well as emerging paradigms within the field.

Ross M, Hicks EA, Rambarran T, and Sheardown H. (2022). Thermo-sensitivity and erosion of chitosan crosslinkedpoly[N-isopropylacrylamide-co-(acrylic acid)-co-(methyl methacrylate)]hydrogels for application to the inferior fornix. Acta Biomaterialia. (141): 151-163.
http://dx.doi.org/https://doi.org/10.1016/j.actbio.2022.01.043

This published manuscript comprises chapter 3 of the thesis. The work described within was conducted entirely by the author of this thesis, aided by Talena Rambarran in initial idea formulation and Emily Anne Hicks for *in vivo* rat testing.

Ross M, Mofford J, Tian J, Muirhead B, Hicks EA, Sheardown L, and Sheardown H (accepted December 1st 2022 to Biomaterials Advances). Thermo-responsive and muco-adhesive gels for treatment of cystinosis.

This accepted manuscript comprises chapter 4 of the thesis. The author of this thesis conducted all data collection and fully wrote this manuscript. Jennifer Tian and Emily Anne Hicks contributed to the rat *in vivo* testing and Benjamin Muirhead, Jonathan Mofford, and Lindsay Sheardown aided with the rabbit *in vivo* testing.

Ross M, Sheardown L, Muirhead B, Mofford J, Tian J, and Sheardown H. (Submitted October 4th 2022 to Journal of Controlled Release). Muco-adhesive thermo-gel platform for treating anterior ocular conditions.

This manuscript to be submitted comprises chapter 5 of the thesis. The author of this manuscript is responsible for all material characterization and wrote the manuscript. Lindsay Sheardown aided in material characterization. Benjamin Muirhead, Jonathan Mofford, and Lindsay Sheardown completed the rabbit *in vivo* testing reported within.

b) Additional Contributions

Ross M, Rambarran T, and Sheardown H

Polymer system for ophthalmic drug delivery – filed 2021/12/09

United States 17/546,645 and Canada 3,141,366.2021/12/09

Ross M, Amaral N, Taiyab A, and Sheardown H. (2022). Delivery of Cells to the Anterior of the Eye Using Synthetic Biomaterials. Cornea. 41: 10. doi: 10.1097/ICO.0000000000003094.

Tian J, Liu L, **Ross M**, and Sheardown H. (expected submission 2022). Hyaluronic acid based therapeutic bandage contact lenses for corneal would healing.

Goostrey T, **Ross M**, Soliman K, and Sheardown H. (expected submission 2022). Preactivated Thiomer Mucoadhesive Micelles for Anterior Ophthalmic Drug Delivery.

Phan C, **Ross M**, Fahmy K, McEwen B, and Jones L. (expected submission 2023). Evaluating viscosity and tear breakup time on an in vitro eye model of various commercial eye drops.

Duarte Campos D, Rhode M, **Ross M**, Anvari P, Blaeser A, Vogt M, Panfil C, Yam G, Mehta J, Fischer H, Walter P, Fuest M. (2019). Corneal bioprinting utilizing collagen-based bioinks and primary human keratocytes. Journal of Biomedical Materials Research Part A. 107A: 1945-1953.
http://dx.doi.org/https://doi.org/10.1002/jbm.a.36702

Kennedy A, Laamanen C, **Ross M**, Vohra R, Boreham D, Scott J, Ross G. (2017). Nerve growth factor inhibitor with novel-binding domain demonstrates nanomolar efficacy in both cell based and cell-free assay systems. Pharmacology Research and Perspectives. 5(5): 1-15. https://doi.org/10.1002/prp2.339

TABLE OF CONTENTS

LIST OF FIGURES

LIST OF TABLES

LIST OF ABBREVIATIONS

^{1}H NMR	Proton nuclear magnetic resonance spectroscopy
2-MP	2-mercaptopyridine
AA	Acrylic acid
AC	Allergic conjunctivitis
ANOVA	Single factor analysis of variance
BGP	β-glycerophosphate
BPO	Benzoyl peroxide
CCN	Covalently crosslinked network
CMC	Carboxymethylcellulose
CMCS	Carboxymethyl chitosan
CTS	Chitosan
D_2O	Deuterated water
DCC	Dicyclohexyl carbodiimide
DCM	Dichloromethane
DDA	Degree of deacetylation
DED	Dry eye disease
DHSe	Di-(1-hydroxylundecyl) selenide
DMSO	Dimethyl sulfoxide
DMSO-D_6	Deuterated dimethyl sulfoxide
EDC	N-(3-Dimethylaminopropyl)-N’ -ethylcarbodiimide hydrochloride
EWC	Equilibrium water content
FTIR	Fourier transform infrared spectroscopy
GPC	Gel permeation chromatography
HA	Hyaluronic acid
H&E	Hematoxylin and eosin stain
HCEC	Human corneal epithelial cell
HGC	Hexanoyl glycol chitosan
HPLC	High performance liquid chromatography
IOP	Intraocular pressure
LCST	Lower critical solution temperature
LYS	Lysozyme
MC	Hydroxypropyl methylcellulose
MES	2-(N-Morpholino)ethanesulfonic acid
MMA	Methyl methacrylate
MMP	Matrix metalloproteinase
MSN	Meso-porous silica nanoparticle
MTT	3-(4,5-dimethylthiazol-2- yl)−2,5-diphenyltetrazolium bromide
MW	Molecular weight
MWCO	Molecular weight cutoff

NAC	N-acetyl cysteine
NIPAAm	N-isopropyl acrylamide
OCT	Optical coherence tomography imaging
P188	Pluronic 188
P407	Pluronic 407
PBS	Phosphate buffered saline
PCL	Poly(caprolactone)
PDSMA	Pyridyl disulfide ethylmethacylate
PDSOH	2-(Pyridin-2-yldisulfaneyl)ethan-1-ol
PEO	Poly(ethylene oxide)
POEGMA	Poly(oligoethylene glycol methacrylate)
POSS	Poly(hedral oligomeric silsesquioxane)
pNAM	Poly(N-isopropylacrylamide-co-acrylic acid-co-methyl methacrylate
pNAMP	Poly(N-isopropylacrylamide-co- acrylic acid-co-methyl methacrylate-co-pyridyl disulfide ethylmethacrylate)
pNIPAAm	Poly(N-isopropylacrylamide)
PEC	Polyelectrolyte complex
PEG	Poly(ethylene glycol)
PLGA	Poly(lactic-co-glycolic acid)
PPM	Parts per million
SD	Standard deviation
SLN	Solid lipid nanoparticle
THF	Tetrahydrofuran
ZO	Zonula occludens

LIST OF SYMBOLS

α	Significance
ABS_x	Absorbance of species X
G'	Storage modulus
G''	Loss modulus
M_D	Mass of dry polymer
M_S (or M_I)	Mass of swollen thermogel
M_t (or M_W)	Mass of thermogel at time t
η_x	Viscosity of component X
$tan\delta$	Damping factor

CHAPTER 1 – Introduction

Adapted from:

Mitchell Ross, and Heather Sheardown. (expected submission 2022). Application of Thermogels to the Anterior of the Eye as Alternatives to Conventional Eyedrops. To be submitted.

Objectives:

This introduction seeks to establish the framework on which the original research described within this thesis is based on. The current landscape of topical formulations that are clinically utilized for treating anterior ocular conditions are outlined as well as emerging technologies from research, with a particular focus on thermogels. The barriers of drug delivery to the anterior of the eye are discussed as well as the complications with replicating these systems on the benchtop. Finally, the overall objectives for the original research of this thesis are outlined.

Author Contributions:

The review paper from which this chapter is adapted was written entirely by Mitchell Ross.

1.1 Current Landscape in Treating Anterior Ocular Conditions

Anatomically, the eye is divided into two sections: the anterior and the posterior. The anterior of the eye interacts with the outside environment and is comprised of the cornea, conjunctiva, sclera, iris, lens, and trabecular meshwork. The anterior of the eye can be affected by many different conditions including, but not limited to, glaucoma, dry eye, physical/chemical burns, allergic conjunctivitis, uveitis, abrasions, and bacterial infection. 70% of prescribed dosage forms for treating ocular conditions are topical eyedrops [1]. In particular, topical treatments comprise 90% of all ocular formulations marketed for treating anterior conditions, where these conventional topical dosage forms can be further categorized into: 62.4% solutions, 17.4% ointments, and 8.7% suspensions [2]. Conventional topical dosage forms dominate the market for treating ocular conditions because they are easy to use, painless, and localize drug absorption/effects compared to systemic administration. Furthermore, topical dosage forms are relatively simple and cheap to manufacture [1, 3]. Topical formulations have a key limitation, in that less than 5% remains bioavailable after administration. As such, conventional topical formulations require frequent instillation, which can affect patient compliance [4] and leads to systemic absorption of the drug [5]. Therefore, current research focuses on producing drug-eluting formulations/materials that can prolong drug release and increase the amount of drug that can pass the natural barriers of the eye to reach the target tissues. A common approach to enhancing drug delivery is utilizing eyedrops with greater viscosity. Enhanced viscosity is

typically achieved through the inclusion of cellulose derivatives, though other natural and synthetic polymers have also been investigated [1, 6]. However, increasing viscosity often results in blurred vision and patient discomfort [6]. Formulations such as emulsions [7], nanoparticles; in particular micelles which can deliver hydrophobic drugs more effectively than conventional formulations [8, 9], ocular inserts [10], and in-situ hydrogels; specifically thermogels, have all also been investigated for improving anterior ocular drug delivery.

In-situ formulations are based on polymeric solutions that undergo a transition into a gel phase upon application of an external stimulus; typically pH, ionic strength, or temperature [11, 12]. Thermogels are defined by having a lower critical solution temperature (LCST), which is the temperature at which the solution transitions to form gel. The LCST of thermogelling polymers can typically be modified by the addition of hydrophilic or hydrophobic comonomers. Thermogels are particularly appealing for anterior ocular applications, as they can be applied by the current clinical standards with conventional drug concentrations but are then able to gel against the heat of the eye, prolonging the drug release profile. However, there are two major drawbacks of thermogel formulations. Firstly, conventional thermogels tend to have poor mechanical properties as a result of the weak hydrophilic/hydrophobic interactions driving gelation [13-15]. Therefore, these systems often need to be chemically modified to improve the mechanical attributes. Secondly, thermogels are typically opaque and would therefore obstruct vision if applied directly to the surface of eye like conventional eyedrops. To avoid

obstructing vision, research on thermogelling formulations has focused on topical application to the inferior fornix or injection into anterior tissue by intravitreal injection or sub-conjunctival injection, as shown in Figure 1.1. Categorically, thermogels are typically based on synthetic poly(N-isopropylacrylamide) (pNIPAAm) or polyethylene glycol (PEG)-based poloxamer polymers but thermogels have also been produced with other synthetic or naturally derived polymers. This review focuses on the various thermogels that have been formulated for application to the anterior of the eye while highlighting ongoing developments in the field with a focus on degradable, composite, and mucoadhesive advancements.

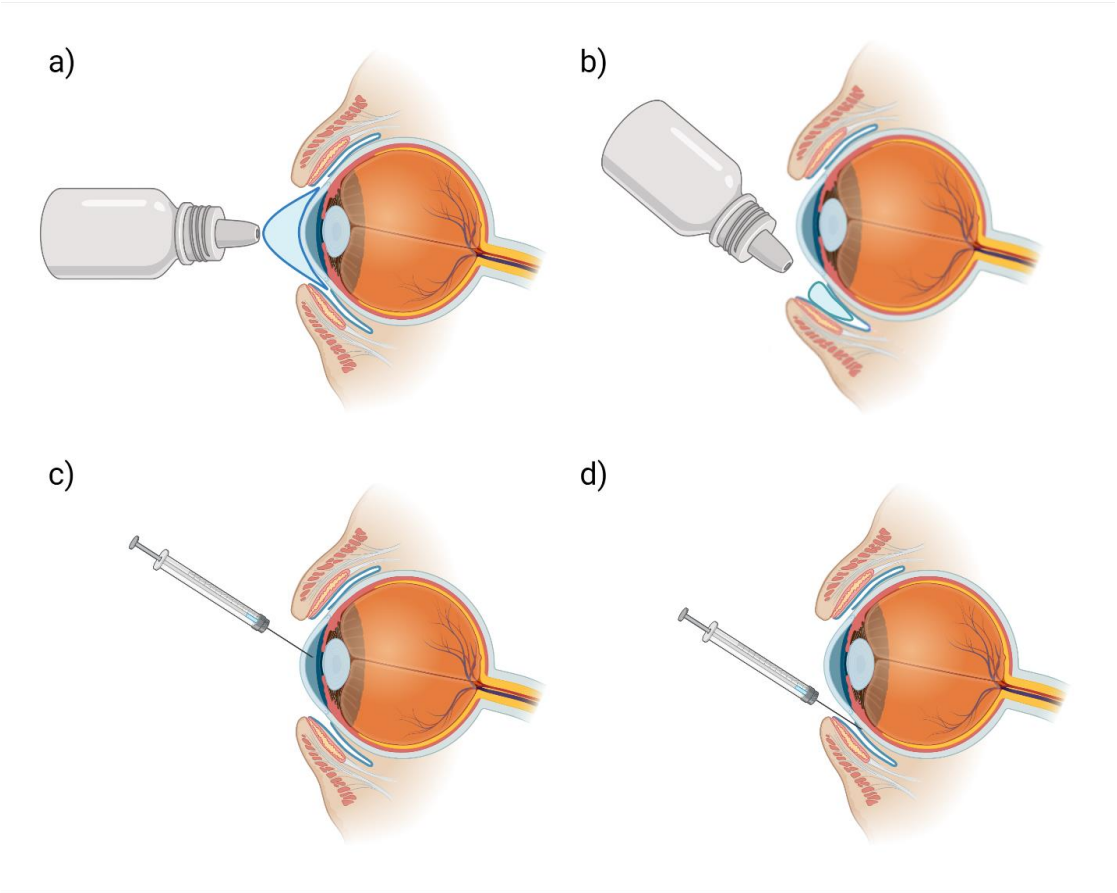

Figure 1.1) Modes of thermogel application to the anterior of the eye a) Topical b) Topical application to inferior fornix c) Intracameral injection and d) Sub-conjunctival injection. Created with BioRender.com.

1.2 Considerations for Anterior Ocular Application

1.2.1 Anterior Anatomy and Barriers to Drug Delivery

Greater than 95% of topical applications are removed by precorneal clearance mechanisms and anatomical barriers before reaching the desired site of action. The anatomy of the anterior of the eye is visualized in Figure 1.2. Upon instillation, the medication is quickly removed by the mechanical barriers of

blinking, lacrimation, and drainage through the nasolacrimal duct, which leads to systemic absorption of the drug [16]. The topical formulation then travels through the tear film, which is constantly undergoing rapid turnover, and is comprised of a thin outer lipid layer (>80 nm) followed by a 3 µm aqueous layer containing various proteins and secreted enzymes, then finally a bound glycocalyx layer of immobilized mucins on the corneal epithelium [17, 18]. The secreted mucins and proteins of the aqueous tear film represent a site of potential drug interaction and the layer of bound mucin represents a physical barrier for drug permeation. Following the tear film, the drug must then penetrate through the cornea. The cornea, roughly 550 µm in thickness, is comprised of five layers: the epithelium, Bowman's layer, stroma, Descement's layer and endothelium. The stratified corneal epithelium consists of outer squamous cells over a layer of wing cells and a basal layer of cuboid cells [19, 20]. The corneal epithelium is lipophilic and contains zonula occludens (ZOs), multiprotein intracellular junction scaffolds, which limit drug permeability, especially for hydrophilic compounds [20, 21]. Hydrophobic drugs that can pass through the corneal epithelium then enter the hydrophilic stroma, the structure of which accounts for greater than 90% of corneal thickness [22].

Besides the cornea, the conjunctiva and sclera also limit drug transport. The conjunctiva is a thin, transparent, connective tissue that covers the sclera and lines the eyelids producing the tear film and mucin. The conjunctiva, similar to the corneal epithelium contains ZOs, though the conjunctiva also has dynamic blood

and lymph flow leading to systemic drug absorption [23]. The hydrophilic sclera anatomically resembles the stroma of the cornea, limiting hydrophobic drug permeation. The sclera, however, has been shown to have greater permeability compared to the cornea, prompting research into transscleral drug delivery [24]. After crossing the surface barriers of the eye, the delivered drug then reaches the anterior chamber in which it is removed by the constant turnover of the aqueous humour. Finally, it is important to note that beyond the static and dynamic physical barriers mentioned thus far, the cornea, iris-ciliary body, and aqueous humour all contain various enzymes capable of drug metabolism [25]. It is the combination of these barriers that results in such small amounts of topically applied drugs reaching the appropriate sites of action.

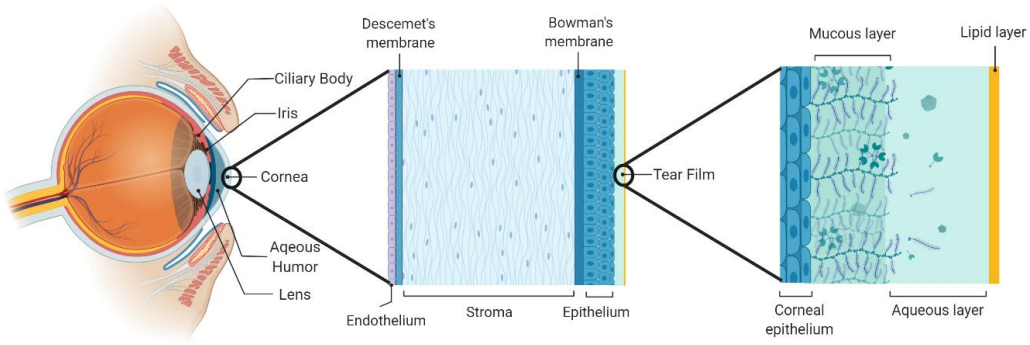

Figure 1.2) Anatomy of the anterior of the eye. Created with BioRender.com.

1.2.2 Development of Anterior Testing

Replication of anterior conditions is difficult for testing during the development of thermogels. For the surface of the eye, the average basal tear flow of 1.2 µL/min can increase roughly five times during reflux flow, with a total tear volume of 7.0 ± 2.0 µL [26, 27]. Upon instillation of topical eyedrops, the tear film and inferior fornix can expand up to 30 µL in volume [28]. For the anterior chamber, the aqueous humour has a turnover rate of 2.4 ± 0.6 µL/min [29] and a total volume of 100 to 200 µL [30-32]. Clinically, intracameral injection into the anterior chamber is used for the administration of antibiotics, with the average volume injected being 100 µL [33]. Replicating these low volumes and turnover rates in laboratory settings is difficult and often overlooked, especially for drug release studies that employ sink conditions for measurement. Recently, models have been produced that employ microfluidics to mimic the flow conditions of the surface of the eye [34, 35]. Of particular note, Seo et al. developed a microfluidic model that incorporates multi-layered tissue structures capable of being used as a dry eye model [35].

Besides anterior flow, there is a significant amount of mechanical force. This mechanical force is typically greatest at the anterior surface due to blinking and globe movement. During *in vitro* degradation studies, the effect of mechanical wear is often not simulated. High speed camera analysis of a mixed age cohort has demonstrated that the average human blink speed is 26±2 mm/s with peak speed of 157±5 mm/s [36]. It is also estimated that the force produced by blinking is 0.2 N and up to 0.8 N for forceful blinking [37, 38]. Therefore, thermogels developed

for application to the ocular surface must withstand such mechanical speed and force. Systems like OcuBlink™, which were developed for visualizing tear film breakup by contact lenses during blinking [39], may be further developed for testing both the effects of mechanical wear and fluid flow on thermogel retention and drug release.

1.2.3 Advancements for Anterior Application

A few key design constraints need to be considered for the successful development of thermogels applied to the anterior of the eye. The first of these considerations, suggested by the authors, is degradability. Degradable thermogels can be removed by the natural clearance mechanisms of the eye following the release of their therapeutic payload. From a clinical standpoint, designed degradation is desirable, as patients do not have to physically remove the applied thermogels themselves after a prescribed period. Most thermogels investigated are based on synthetic pNIPAAm or PEG, which are not degradable. To allow for degradation, comonomers or other polymers can be incorporated, which impart degradation to the thermogelling systems. There are two avenues for designed degradation in the anterior of the eye: hydrolysis, and enzymatic degradation. Hydrolytically degradable poly(oligoethylene glycol methacrylate) (POEGMA) thermogels have been produced by crosslinking with hydrazone bonds [40, 41]. Fitzpatrick et al. produced thermogels capable of hydrolytic degradation over the scale of months by incorporating the monomer dimethyl-γ-butyrolactone acrylate

which undergoes hydrolytic ring opening, increasing polymer hydrophilicity and therefore LCST, allowing the gels to revert back to solution phase over time [42]. Unfortunately, thermogelling systems that degrade via hydrolysis have an inherent storage issue, as the polymer networks require hydration immediately prior to administration to avoid premature degradation. Thermogels can also be designed to undergo enzymatic degradation. The anterior of the eye contains numerous enzymes capable of degrading various natural polymer substrates. Of particular note, lysozyme is the highest concentration enzyme in the tear film at 1.4 mg/mL [43] and is able to degrade chitosan [44-46]. Similarly, matrix metalloproteinase (MMPs), which are involved in ocular inflammation and tissue repair [47], are capable of degrading collagen and its derivative gelatin [48]. Enzymatically degradable thermogels are typically produced by crosslinking synthetic and natural polymers or by grafting thermo-responsive polymer chains to degradable natural polymer substrates.

For application to the anterior of the eye, thermogels need to be designed with the appropriate mechanical properties. Therefore, many studies incorporate viscosity enhancers such as hydroxypropyl methylcellulose (MC), carboxymethyl chitosan (CMCS) and carboxymethylcellulose (CMC) to achieve the desired mechanical attributes and aid in the drug release profiles. For topical eyedrop formulations, a critical viscosity value of 10 mPa.s results in improved retention on the ocular surface [49]. *In vivo* rabbit studies have suggested that a viscosity of 12-15 mPa.s is optimal for topical surface delivery [50]. Finally, formulations with a

viscosity higher than 30 mPa.s have been shown to cause blurring and patient discomfort when applied to the ocular surface [6]. Therefore, in the development of thermogels for direct application to the ocular surface, there is a very narrow constraint of formulation viscosity. For injectable formulations, the thermogelling formulations must have a low enough viscosity at the injection temperature to allow for flow through a fine gauge needle (26-31 G) [51, 52]. The time in which the formulation undergoes transition to the gel state is also important to not clog the needle during injection. Finally, application to the inferior fornix allows for formulations to have a greater solution viscosity and gel stiffness as they do not obstruct vision compared to formulations that are applied directly on the ocular surface.

A key issue with hydrogels applied to the ocular surface or inferior fornix is retention, as the shear produced from blinking and globe movement can cause the applied material to shift [53]. To improve retention, thermogels have been designed to incorporate mucoadhesive components that can bind and anchor the thermogels to the natural mucins found in the tear film and covering epithelial surfaces. Mucoadhesion is typically accomplished through inclusion of monomers/polymers that can interact with ocular mucin in the following ways: moieties that can hydrogen bond with the sugar residues of mucin, cationic components capable of electrostatically interacting with the negatively charged sialic acid residues of mucin, thiolated components that can covalently bond to the

cysteine of mucin through disulfide bridging, and boronic acids that can covalently bind to sugar residues [54].

Another trend to produce thermogels for application to the anterior of the eye is the fabrication of composites that contain either micro or nanoparticles [55, 56]. Incorporating micro or nanoparticles into thermogels can extend the drug release profiles compared to conventional thermogels by adding another layer of diffusion. Additionally, incorporating particles, like micelles or solid lipid particles, allows for drug loading of hydrophobic or lipophilic compounds. Finally, incorporating nanoparticles within thermogel matrices can also have a protective effect for nanoparticles which are designed to penetrate the cornea. Dispersing the nanoparticles within thermogel matrix prevents early clearance of particles and allows them to slowly permeate through the gel and then into the anterior tissue. This review will highlight the recent publications on developing mucoadhesive or composite thermogelling systems for improved retention and drug release within the inferior fornix.

1.3 Thesis Objectives

Based on the current market and research landscapes outlined, the development of thermogels that are capable of releasing drug over multiple days, are of key interest to replacing conventional topicals formulations in the treatment of anterior ocular conditions. Since the formulations that elute drugs over multiple days are typically opaque, thermogels must be applied in such a way as to not

obstruct vision. An objective of this thesis was to design a thermogel specifically for application to the inferior fornix such that vision is not compromised during topical application, and sub-conjunctival or intracameral injection is avoided for patient comfort. When designing formulations for application to the inferior fornix, it is important to consider that retention within this space has been reported to be poor due to the high shear environment [53]. Therefore, another objective of this work was to incorporate tailorable mucoadhesion to the thermogel system. Finally, synthetic thermogels, which are the most studied in literature, tend to be non-degradable. Some non-degradable thermogels have been developed, but these require removal after a set period by the patient [56-58]. Therefore, the final objective of this thesis was to create a thermogel which is degradable over multiple days and can be removed by the natural clearance mechanisms of the eye. The mode of degradation should be site specific and compatible with the development of an aqueous formulation.

In summary, the overall objectives for this thesis were:

1. To create a thermogel to be applied to the inferior fornix for sustained multi-day drug delivery.
2. To have this thermogel be degradable by enzymatic action over a multi-day period.
3. Impart tailorable mucoadhesive properties to the developed thermogels for better anchoring within the inferior fornix.

Although these thermogels were designed specifically for treating anterior ocular conditions, this combination of mucoadhesive thermogels which undergo site specific degradation should be easily translatable to other parts of the body which contain mucosal membranes.

1.4 Thesis Overlap

In accordance with the guidelines for the preparation of a sandwich doctoral thesis set forth by the McMaster University, the author will address any overlap which may be present in the thesis. Synthetically, the formulations developed in Chapters 3, 4, and 5, are similar and therefore the materials utilized are similar. Some of the methods including the production of the PDSMA monomer, polymer synthesis, rheological property determination, and degradation studies contain overlap between the experimental chapters. Inherently, the introduction presented in Chapter 1 and the literature review presented in Chapter 2 will contain some overlap with the individual introductions for Chapter 3, 4, and 5. This overlap is minimal however as each of the chapters based on original research have an overall different goal and focus.

1.5 References

[1] B. Gupta, V. Mishra, S. Gharat, M. Momin, and A. Omri, "Cellulosic Polymers for Enhancing Drug Bioavailability in Ocular Drug Delivery Systems," *Pharmaceuticals,* vol. 14, no. 11, p. 1201, 2021.

[2] R. D. Bachu, P. Chowdhury, Z. H. Al-Saedi, P. K. Karla, and S. H. Boddu, "Ocular drug delivery barriers—role of nanocarriers in the treatment of

anterior segment ocular diseases," *Pharmaceutics,* vol. 10, no. 1, p. 28, 2018.

[3] N. M. Davies, "Biopharmaceutical considerations in topical ocular drug delivery," *Clinical and experimental pharmacology and physiology,* vol. 27, no. 7, pp. 558-562, 2000.

[4] R. Kholdebarin, R. J. Campbell, Y.-P. Jin, Y. M. Buys, and C. C. S. Group, "Multicenter study of compliance and drop administration in glaucoma," *Canadian journal of ophthalmology,* vol. 43, no. 4, pp. 454-461, 2008.

[5] A. Farkouh, P. Frigo, and M. Czejka, "Systemic side effects of eye drops: a pharmacokinetic perspective," *Clinical Ophthalmology (Auckland, NZ),* vol. 10, p. 2433, 2016.

[6] B. McKenzie, G. Kay, K. H. Matthews, R. Knott, and D. Cairns, "Preformulation of cysteamine gels for treatment of the ophthalmic complications in cystinosis," *International journal of pharmaceutics,* vol. 515, no. 1-2, pp. 575-582, 2016.

[7] S. Tamilvanan and S. Benita, "The potential of lipid emulsion for ocular delivery of lipophilic drugs," *European Journal of Pharmaceutics and Biopharmaceutics,* vol. 58, no. 2, pp. 357-368, 2004.

[8] D. R. Janagam, L. Wu, and T. L. Lowe, "Nanoparticles for drug delivery to the anterior segment of the eye," *Advanced drug delivery reviews,* vol. 122, pp. 31-64, 2017.

[9] G. Prosperi-Porta, S. Kedzior, B. Muirhead, and H. Sheardown, "Phenylboronic-acid-based polymeric micelles for mucoadhesive anterior segment ocular drug delivery," *Biomacromolecules,* vol. 17, no. 4, pp. 1449-1457, 2016.

[10] A. Kumari, P. K. Sharma, V. K. Garg, and G. Garg, "Ocular inserts—Advancement in therapy of eye diseases," *Journal of advanced pharmaceutical technology & research,* vol. 1, no. 3, p. 291, 2010.

[11] A. Majeed and N. A. Khan, "Ocular in situ gel: An overview," *Journal of Drug Delivery and Therapeutics,* vol. 9, no. 1, pp. 337-347, 2019.

[12] M. Kouchak, "In situ gelling systems for drug delivery," *Jundishapur journal of natural pharmaceutical products,* vol. 9, no. 3, 2014.

[13] M. A. Haq, Y. Su, and D. Wang, "Mechanical properties of PNIPAM based hydrogels: A review," *Materials Science Engineering C Materials Biological Applications,* vol. 70, no. Pt 1, pp. 842-855, Jan 1 2017, doi: 10.1016/j.msec.2016.09.081.

[14] K. Zhang, K. Xue, and X. J. Loh, "Thermo-responsive hydrogels: from recent progress to biomedical applications," *Gels,* vol. 7, no. 3, p. 77, 2021.

[15] K. Edsman, J. Carlfors, and R. Petersson, "Rheological evaluation of poloxamer as an in situ gel for ophthalmic use," *European journal of pharmaceutical sciences,* vol. 6, no. 2, pp. 105-112, 1998.

[16] R. Gaudana, H. K. Ananthula, A. Parenky, and A. K. Mitra, "Ocular drug delivery," *The AAPS journal,* vol. 12, no. 3, pp. 348-360, 2010.

[17] E. King-Smith, B. Fink, R. Hill, K. Koelling, and J. Tiffany, "The thickness of the tear film," *Current eye research,* vol. 29, no. 4-5, pp. 357-368, 2004.

[18] M. Ruponen and A. Urtti, "Undefined role of mucus as a barrier in ocular drug delivery," *European Journal of Pharmaceutics and Biopharmaceutics,* vol. 96, pp. 442-446, 2015.

[19] G. Pellegrini, C. E. Traverso, A. T. Franzi, M. Zingirian, R. Cancedda, and M. De Luca, "Long-term restoration of damaged corneal surfaces with autologous cultivated corneal epithelium," *The Lancet,* vol. 349, no. 9057, pp. 990-993, 1997.

[20] S. P. Sugrue and J. D. Zieske, "ZO1 in corneal epithelium: association to the zonula occludens and adherens junctions," *Experimental eye research,* vol. 64, no. 1, pp. 11-20, 1997.

[21] K. Cholkar, S. P. Patel, A. D. Vadlapudi, and A. K. Mitra, "Novel strategies for anterior segment ocular drug delivery," *Journal of ocular pharmacology and therapeutics,* vol. 29, no. 2, pp. 106-123, 2013.

[22] T. M. Nejad, C. Foster, and D. Gongal, "Finite element modelling of cornea mechanics: a review," *Arquivos brasileiros de oftalmologia,* vol. 77, pp. 60-65, 2014.

[23] A. Huang, S. Tseng, and K. Kenyon, "Paracellular permeability of corneal and conjunctival epithelia," *Investigative ophthalmology & visual science,* vol. 30, no. 4, pp. 684-689, 1989.

[24] M. R. Prausnitz and J. S. Noonan, "Permeability of cornea, sclera, and conjunctiva: a literature analysis for drug delivery to the eye," *Journal of pharmaceutical sciences,* vol. 87, no. 12, pp. 1479-1488, 1998.

[25] S. Duvvuri, S. Majumdar, and A. K. Mitra, "Role of metabolism in ocular drug delivery," *Current drug metabolism,* vol. 5, no. 6, pp. 507-515, 2004.

[26] R. L. Farris, R. N. Stuchell, and I. D. Mandel, "Basal and reflex human tear analysis: I. Physical measurements: osmolarity, basal volumes, and reflex flow rate," *Ophthalmology,* vol. 88, no. 8, pp. 852-857, 1981.

[27] S. Mishima, A. Gasset, S. Klyce, and J. Baum, "Determination of tear volume and tear flow," *Investigative Ophthalmology & Visual Science,* vol. 5, no. 3, pp. 264-276, 1966.

[28] V. Agrahari *et al.*, "A comprehensive insight on ocular pharmacokinetics," *Drug delivery and translational research,* vol. 6, no. 6, pp. 735-754, 2016.

[29] M. Goel, R. G. Picciani, R. K. Lee, and S. K. Bhattacharya, "Aqueous humor dynamics: a review," *The open ophthalmology journal,* vol. 4, p. 52, 2010.

[30] S. T. Fontana and R. F. Brubaker, "Volume and depth of the anterior chamber in the normal aging human eye," *Archives of Ophthalmology,* vol. 98, no. 10, pp. 1803-1808, 1980.

[31] G. Labiris, M. Gkika, A. Katsanos, M. Fanariotis, E. Alvanos, and V. Kozobolis, "Anterior chamber volume measurements with Visante optical coherence tomography and Pentacam: repeatability and level of agreement," *Clinical & experimental ophthalmology,* vol. 37, no. 8, pp. 772-774, 2009.

[32] D. Wang, M. Qi, M. He, L. Wu, and S. Lin, "Ethnic difference of the anterior chamber area and volume and its association with angle width," *Investigative ophthalmology & visual science,* vol. 53, no. 6, pp. 3139-3144, 2012.

[33] S. A. Arshinoff and M. Modabber, "Dose and administration of intracameral moxifloxacin for prophylaxis of postoperative endophthalmitis," *Journal of Cataract & Refractive Surgery,* vol. 42, no. 12, pp. 1730-1741, 2016.

[34] M. Bajgrowicz, C.-M. Phan, L. N. Subbaraman, and L. Jones, "Release of ciprofloxacin and moxifloxacin from daily disposable contact lenses from an in vitro eye model," *Investigative Ophthalmology & Visual Science,* vol. 56, no. 4, pp. 2234-2242, 2015.

[35] J. Seo *et al.*, "Multiscale reverse engineering of the human ocular surface," *Nature medicine,* vol. 25, no. 8, pp. 1310-1318, 2019.

[36] K.-A. Kwon *et al.*, "High-speed camera characterization of voluntary eye blinking kinematics," *Journal of the Royal Society Interface,* vol. 10, no. 85, p. 20130227, 2013.

[37] P. Edman, “Biopharmaceutics of ocular drug delivery,” *CRC Press*, Boca Raton, FL, 1993.

[38] M. Yamaguchi *et al.*, "Mucoadhesive properties of chitosan-coated ophthalmic lipid emulsion containing indomethacin in tear fluid," *Biological and Pharmaceutical Bulletin,* vol. 32, no. 7, pp. 1266-1271, 2009.

[39] H. Walther, V. W. Chan, C.-M. Phan, and L. W. Jones, "Modelling non-invasive tear break-up times of soft lenses using a sophisticated in vitroblink platform," *Investigative Ophthalmology & Visual Science,* vol. 60, no. 9, pp. 6328-6328, 2019.

[40] N. M. Smeets, E. Bakaic, M. Patenaude, and T. Hoare, "Injectable poly (oligoethylene glycol methacrylate)-based hydrogels with tunable phase transition behaviours: Physicochemical and biological responses," *Acta biomaterialia,* vol. 10, no. 10, pp. 4143-4155, 2014.

[41] D. Sivakumaran, E. Bakaic, S. B. Campbell, F. Xu, E. Mueller, and T. Hoare, "Fabricating degradable thermoresponsive hydrogels on multiple length scales via reactive extrusion, microfluidics, self-assembly, and electrospinning," *JoVE (Journal of Visualized Experiments),* no. 134, p. e54502, 2018.

[42] S. D. Fitzpatrick, M. J. Mazumder, B. Muirhead, and H. Sheardown, "Development of injectable, resorbable drug-releasing copolymer scaffolds for minimally invasive sustained ophthalmic therapeutics," *Acta biomaterialia,* vol. 8, no. 7, pp. 2517-2528, 2012.

[43] E. Aine and P. Morsky, "Lysozyme Concentration in Tears-Assessment of Reference Values in Normal Subjects," *Acta ophthalmologica,* vol. 62, no. 6, pp. 932-938, 1984.

[44] R. J. Nordtveit, K. M. Vårum, and O. Smidsrød, "Degradation of partially N-acetylated chitosans with hen egg white and human lysozyme," *Carbohydrate polymers,* vol. 29, no. 2, pp. 163-167, 1996.

[45] K. Tomihata and Y. Ikada, "In vitro and in vivo degradation of films of chitin and its deacetylated derivatives," *Biomaterials,* vol. 18, no. 7, pp. 567-575, 1997.

[46] J. Ahn, J. Ryu, G. Song, M. Whang, and J. Kim, "Network structure and enzymatic degradation of chitosan hydrogels determined by crosslinking methods," *Carbohydrate polymers,* vol. 217, pp. 160-167, 2019.

[47] J. M. Sivak and M. E. Fini, "MMPs in the eye: emerging roles for matrix metalloproteinases in ocular physiology," *Progress in retinal and eye research,* vol. 21, no. 1, pp. 1-14, 2002.

[48] A. Banerjee, K. Chatterjee, and G. Madras, "Enzymatic degradation of polycaprolactone–gelatin blend," *Materials Research Express,* vol. 2, no. 4, p. 045303, 2015.

[49] H. Zhu and A. Chauhan, "Effect of viscosity on tear drainage and ocular residence time," *Optometry and Vision Science,* vol. 85, no. 8, pp. E715-E725, 2008.

[50] I. D. Rupenthal, C. R. Green, and R. G. Alany, "Comparison of ion-activated in situ gelling systems for ocular drug delivery. Part 1: physicochemical characterisation and in vitro release," *International journal of pharmaceutics,* vol. 411, no. 1-2, pp. 69-77, 2011.

[51] A. Wolf, B. Von Jagow, M. Ulbig, and C. Haritoglou, "Intracameral injection of bevacizumab for the treatment of neovascular glaucoma," *Ophthalmologica,* vol. 226, no. 2, pp. 51-56, 2011.

[52] S. Xia *et al.*, "Shear-thinning viscous materials for subconjunctival injection of microparticles," *AAPS PharmSciTech,* vol. 22, no. 1, pp. 1-8, 2021.

[53] J. Colter, B. Wirostko, and B. Coats, "Finite element design optimization of a hyaluronic acid-based hydrogel drug delivery device for improved retention," *Annals of Biomedical Engineering,* vol. 46, no. 2, pp. 211-221, 2018.

[54] R. S. Dave, T. C. Goostrey, M. Ziolkowska, S. Czerny-Holownia, T. Hoare, and H. Sheardown, "Ocular drug delivery to the anterior segment using nanocarriers: A mucoadhesive/mucopenetrative perspective," *Journal of Controlled Release,* vol. 336, pp. 71-88, 2021.

[55] T. Maeda, "Structures and applications of thermoresponsive hydrogels and nanocomposite-hydrogels based on copolymers with poly (Ethylene glycol) and poly (lactide-co-glycolide) blocks," *Bioengineering,* vol. 6, no. 4, p. 107, 2019.

[56] M. V. Fedorchak, I. P. Conner, J. S. Schuman, A. Cugini, and S. R. Little, "Long term glaucoma drug delivery using a topically retained gel/microsphere eye drop," *Scientific reports,* vol. 7, no. 1, pp. 1-11, 2017.

[57] E. Bellotti, M. V. Fedorchak, S. Velankar, and S. R. Little, "Tuning of thermoresponsive pNIPAAm hydrogels for the topical retention of controlled release ocular therapeutics," *Journal of Materials Chemistry B,* vol. 7, no. 8, pp. 1276-1283, 2019.

[58] J. Jimenez, M. A. Washington, J. L. Resnick, K. K. Nischal, and M. V. Fedorchak, "A sustained release cysteamine microsphere/thermoresponsive gel eyedrop for corneal cystinosis improves drug stability," *Drug Delivery and Translational Research,* vol. 11, no. 5, pp. 2224-2238, 2021.

CHAPTER 2 – Literature Review

Adapted from:

Mitchell Ross, and Heather Sheardown. (expected submission 2022). Application of Thermogels to the Anterior of the Eye as Alternatives to Conventional Eyedrops. To be submitted.

Objectives:

The literature review covers the current developments in the field of utilizing thermogels to treat anterior ocular conditions. The mode of application, type of polymer utilized, as well as trends within the field including designed degradation, mucoadhesion, and composite production, are outlined. This review strives to fully describe the current research landscape and comment on the new areas for development.

Author Contributions:

The review paper on which this chapter is adapted from was written entirely by Mitchell Ross.

2.1 Poly(N-isopropylacrylamide) Thermogels for Anterior Application

Thermogels based on pNIPAAm have been utilized for many different applications, including electronics, robotics, smart displays, drug release, and as cellular scaffolds [1]. For biomaterials applications, pNIPAAm thermogels have been investigated since the 1980s [2]. pNIPAAm polymers have a sharp, reversible, LCST of 32-35℃. The gelation is thermodynamically driven by hydrophilic-hydrophobic interactions between the isopropyl tails of pNIPAAm with the amide groups and water. The LCST of the formulations can be easily modulated by either incorporating hydrophilic comonomers, which raise the LCST, or hydrophobic comonomers, which lower it [1, 3]. Native pNIPAAm thermogels tend to be fragile due to the relatively weak hydrophobic-hydrophilic interactions [4]. Therefore, many studies incorporate other chemical moieties or crosslinkers to improve the mechanical properties [5]. A concern that has arisen with the development of pNIPAAm-based biomaterials is that the monomer has been established to be neurotoxic. However, once polymerized the polymer has been demonstrated to be well-tolerated following intravitreal injection in all ocular tissues with only minimal inflammation at early time points which is a common effect associated with the procedure [6]. Along with poloxamers, pNIPAAm-based thermogels are the most investigated formulation for treatment of anterior ocular conditions. The publications focused on pNIPAAm application to the anterior of the eye are summarized in Table 2.1.

In order to create thermogels that undergo site-specific enzymatic action, short chain pNIPAAm is often grafted to natural polymers, such as chitosan, hyaluronic acid (HA), or gelatin to impart thermogelling properties. For treating anterior ocular conditions, a significant amount of research on grafting pNIPAAm to chitosan or gelatin has been conducted by the Lai group. Gelatin-g-pNIPAAm is produced by first aminating gelatin through the reaction of the carboxylic acids and adipic acid dihydrazide [7]. Short chain pNIPAAm, end-capped with a carboxylic acid, is synthesized by free radical polymerization with mercaptoacetic acid. The end-capped pNIPAAm is then grafted onto the aminated gelatin through dicyclohexyl carbodiimide (DCC) or 1-ethyl-3-(3-dimethyl aminopropyl) carbodiimide hydrochloride (EDC) chemistry. The produced gelatin-g-pNIPAAm can be enzymatically degraded with approximately 50% weight loss following 28-day incubation with 50 ng/mL of MMP-2. Various studies were conducted on the optimization of the thermogelling and enzymatic properties by varying the synthetic compositions. Utilizing shorter molecular weight pNIPAAm resulted in more rapid degradation by MMP-2, likely due to improved enzymatic docking [8]. The effect of varying the degree of gelatin amination was also investigated, with greater degrees of amination resulting in a higher density of positive charge, which led to toxicity issues [9]. Although the previous formulations were intended for intracameral applications, a recent formulation incorporated mucoadhesive lectin *Helix pomatia* agglutinin to improve retention within the inferior fornix [10]. Formulations containing the mucoadhesive component were able to last up to two weeks within

the inferior fornix of rabbits, while base gelatin-g-pNIPAAm was not retained. The study underlies the importance of incorporating mucoadhesive components when designing thermogels to be retained within the inferior fornix. Retention as a factor of the degree of amination was not explored, although mucoadhesion could also be achieved through charge interactions [11].

Like gelatin-g-pNIPAAm, the Lai group developed a series of materials based on chitosan-g-pNIPAAm for intracameral injection and application to the inferior fornix. Synthetically, the carboxylic acid-terminated pNIPAAm can be directly grafted to the primary amines of chitosan. The formulation was further optimized by varying pNIPAAm molecular weight [12], as well as the degree of deacetylation (DDA) of the chitosan [13]. The DDA has a large impact on chitosan degradation by lysozyme, by altering the DDA the authors were able to achieve a tailorable degradation of approximately 30-60% mass loss over 63 days when incubated with lysozyme at a concentration of 1.05 µg/mL [13]. Subsequent publications incorporated benzoic acid derivatives into the thermogelling backbone such as 4-hydroxy-3,5-dimethoxybenzoic acid or Kaempferol for intrinsic treatment of glaucoma in addition to pilocarpine release [14, 15]. Besides grafting, chitosan has also been crosslinked with pNIPAAm-based polymers to create degradable systems for the anterior application. By incorporating the comonomers acrylic acid and methyl methacrylate along with pNIPAAm (resulting polymer denoted as pNAM) the subsequent terpolymer was crosslinked with chitosan either by charge or the use of EDC [16]. The degradation of the crosslinked thermogel could be

tailored from one to four days based on the method of chitosan incorporation. Interestingly, unlike the previous reports, the degradation was found to not be significantly influenced by lysozyme, but rather driven by swelling and subsequent dissolution. The study indicates that not just the material properties of chitosan, like the molecular weight and DDA are important for enzymatic degradation, but also the degree of crosslinking.

In order to prolong the release kinetics of pNIPAAm thermogels, a series of composites containing poly(lactic acid-co-glycolic acid) (PLGA) microspheres have been developed by the DiLeo (Fedorchak) group to treat anterior ocular conditions. Initial investigation of the subconjunctival injection of just brimonidine tartrate PLGA microspheres [17] led to the loading of the drug encapsulated microspheres within a pNIPAAm matrix, shown in Figure 2.1, for topical application to the inferior fornix [18]. Near zero-order release kinetics were achieved with the composite system, with a single dose lowering the intraocular pressure (IOP) of a glaucoma rabbit model comparably to daily eyedrops over a one-month period. From a testing perspective, the study also commented on the importance of removing the nictitating membrane of rabbits prior to testing to achieve gel retention of the scale of days or weeks compared to hours. Additionally, removing the nictitating membrane more closely resembles human physiology. Interestingly, an iteration of the developed thermo-composite system was dispersed in a co-solvent system of water and short chain PEG, where 500 Da PEG is a common ingredient in topical eyedrops. The amount and molecular weight of the PEG co-

solvent could be adjusted to yield the most optimal thermogelling kinetics and rheological properties [19]. The thermo-composite has also been investigated for the treatment of cystinosis, a disease which requires topical reapplication many times a day and could benefit greatly from the improved release kinetics of a composite system [20].

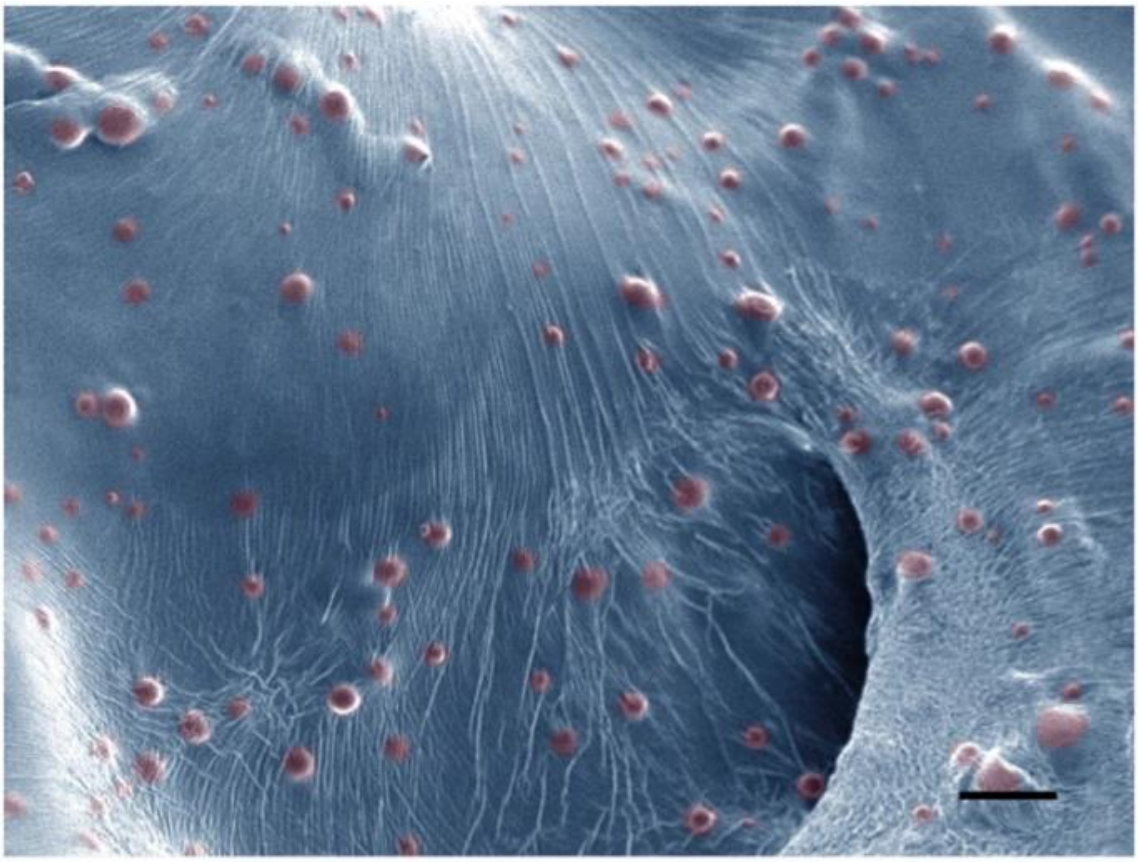

Figure 2.1) Homogeneous suspension of microspheres in gel matrix. This representative scanning electron microscope (SEM) image of pNIPAAm gel (blue, color added) containing embedded, drug loaded PLGA microspheres (red, color added) shows that

microsphere structure [18]. Reproduced without change under terms of Creative Commons License.

Unlike bulk thermogels, micro and nanogels have also be formulated with pNIPAAm for anterior ocular applications. Micro-gels based on aminated hyaluronic acid-g-pNIPAAm were fabricated by sonication and ranged from 165.8-405.4 nm in size based on differing feed ratios [21]. *In vitro*, the produced micro-gels were able to release hydrophobic cyclosporin A over 50 hours. With a rabbit *in vivo* model, micro-gels applied to the inferior fornix resulted in greater drug concentration within the cornea, conjunctiva, and ciliary body after 24 hours compared to conventional eyedrops. Nano-gels have also been fabricated with both heparin and chondroitin sulfate by first conjugating the polysaccharides with the chain transfer agent 2-(dodecylthiocarbonothioylthio)-2-methylpropionic acid and performing subsequent reversible addition−fragmentation chain-transfer polymerization with NIPAAm [22, 23]. The fabricated nano-gels had a hydrodynamic diameter of 2.2 to 6.5 nm [23]. These nanogels were also formulated with the grafted pNIPAAm containing terminal thiol groups capable of covalent mucoadhesion in addition to the ionic mucoadhesion inherent to the use of the anionic polysaccharides. By isothermal titration calorimetry, a greater enthalpic change was noted for heparin-based nano-gels indicating superior mucoadhesive properties. The nano-gels were also loaded with carbonic anhydrase inhibitor and applied topically in a rabbit glaucoma model with improved IOP lowering noted over 8 hours with heparin-based materials [22].

Table 2.1) pNIPAAm Thermogels for Anterior Ocular Application.

Reference	Formulation	Intended Application	Model Drug	Results
pNIPAAm Based Bulk Gels				
[24]	NIPAAm -co-butylacylate or N-tert-butylacrylamide	Injectable	NA	Range of physcially crosslinked thermogels were developed by varying comonomer compositions to yield optimal viscoelastic properties. The sealant properties were tested with both an *ex vivo* pig model and an *in vivo* rabbit model with the latter displaying only early inflammation (less than 12 hours). The developed thermogels were determined to be biocompatible over the month-long study by histological analysis.

pNIPAAm and Natural Polymer Bulk Gels				
[25]	Chitosan-g-pNIPAAm	Inferior fornix	Timolol Maleate	Carboxylic end capped pNIPAAm is grafted to chitosan through DCC crosslinker. Following administration, thermogels showed greater concentration of timolol maleate in rabbit aqueous humour compared to conventional eyedrops over a 2-hour period and a greater reduction in IOP over 10 hours.
[7]	Gelatin-g-pNIPAAm	Intracameral	Pilocarpine	Grafting of carboxylic acid terminated pNIPAAm to aminated gelatin by EDC. Degradation with MMP-2 occurred over 28 days. Pilocarpine release over 14 days. IOP significantly lowered in rabbits with

				developed gel compared to conventional eyedrops over 14 days following injection.
[8]	Gelatin-g-pNIPAAm	Intracameral	Pilocarpine	The effect of varying the molecular weight of carboxylic acid terminated pNIPAAm grafted to gelatin was investigated. The shorter the grafted NIPAAm chain the quicker the degradation by MMP-2 and best lowering of IOP in rabbit model over 14 days.
[26]	Gelatin-g-pNIPAAm	Topical Administration	Epigallocatechin Gallate	Loading of pNIPAAm grafted gelatin with epigallocatechin gallate showed a significant reduction in secreted pro-inflammatory cytokines *in vitro*. Drug loaded thermogel demonstrated a significantly greater effect in reducing dry

				eye symptoms with corneal staining and Schirmer tear secretion test with rabbit model.
[12]	Chitosan-g-pNIPAAm	Intracameral	Pilocarpine	Feed ratio of carboxyl acid terminated pNIPAAm grafted to chitosan was varied to produce varying thermogelling properties. Enzymatic degradation by lysozyme and drug release measured over 42 days. Significant reduction in IOP with rabbit glaucoma model over 28 days following administration.
[13]	Chitosan-g-pNIPAAm	Intracameral	Pilocarpine	Effect of varying the degree of deacetylation of chitosan grafted with pNIPAAm from 60 to 99%. Degree of deacetylation determines rate of lysozyme

				mediated degradation and subsequent drug release. High degrees of deacetylation result in immunogenicity through resulting density of positive charge. Effect of molecular weight not investigated.
[9]	Gelatin-g-pNIPAAm	Intracameral	Pilocarpine	Examination onto NIPAAm grafting on gelatin with different degrees of amination and the resulting thermogelling properties and ultrastructure. Feed of pNIPAAm held constant while degree of gelatin amination changed. Resulting positive charge aided thermogelling properties but led to cell and animal toxicity.

[14]	Chitosan-g-pNIPAAm	Intracameral	Pilocarpine and RGFP966	Increased antioxidant properties by methoxylation effects of chitosan-g-pNIPAAm post conjugated with three different benzoic acid derivatives. Glaucomatous optic neuropathy rabbit demonstrated significant reduction in disease state over entire 70-day testing period.
[10]	Gelatin-g-pNIPAAm	Inferior Fornix	Epigallocatechin Gallate	Incorporated lectin Helix pomatia agglutinin as a mucus binding component with gelatin-g-pNIPAAm. With added mucoadhesion, retention was noted up to 14 days in inferior fornix as compared to controls without mucoadhesion. EGCG

				loaded for antioxidant properties in healing corneal epithelium.
[15]	Chitosan-g-pNIPAAm	Intracameral	Pilocarpine	Chitosan-g-pNIPAAm post modified with phenolic compounds for antioxidant and anti-inflammatory properties to treat glaucoma. Varying phenolic compound concentration, reduction of IOP over 7 days from best formulation and further increase in loaded drug release time with added hydrophobicity.
[27]	Hyaluronic acid-g-pNIPAAm	Inferior Fornix	NA	Anti-inflammatory properties of thiolated HA grafted with amine terminated NIPAAm. Degradation studied in presence of hyaluronidase. *In vivo* dry eye rabbit model showed significant improvement

				following single dosage with repair of corneal defects, supressed inflammation, and prevention of cell apoptosis.
[16]	Chitosan crosslinked pNAM	Inferior Fornix	Ketotifen Fumarate	Production of chitosan crosslinked poly(NIPAAm-co-acrylic acid-co- methyl methacrylate) (pNAM) by ionic or covalent bonding. Degradation tailorable from one to four days with subsequent change in drug release kinetics. Demonstrated importance of chitosan molecular weight, degree of crosslinking and swelling behaviour on degradation with or without lysozyme.
pNIPAAm Composites				

[28]	PLGA loaded pNIPAAm	Inferior Fornix	Moxifloxacin	Release of anti-bacterial noted from PLGA microsphere thermogels over one week testing period. All rabbit eyes treated with the developed drug loaded composite effectively treated endophthalmitis whereas all blanks resulted in disease state.
[18]	PLGA loaded pNIPAAm	Inferior Fornix	Brimonidine tartrate	PLGA microspheres were loaded in pNIPAAm dissolved in a PEG and water co-solvent mixture. Near zero order release of loaded glaucoma drug over 32-day testing period. Reduction of IOP, in rabbit glaucoma model, following single dosage of thermo-composite equal to

				standard free drug drops over month testing period.
[19]	PLGA loaded pNIPAAm	Inferior Fornix	Brimonidine Tartrate	Determination of the optimal thermogelling effects based on PEG co-solvent properties for PLGA microsphere loaded pNIPAAm. All formulations determined to be non-toxic *in vitro* with greater PEG content and higher molecular weight resulting in lower viscosity and quicker gelation kinetics.
[20]	PLGA loaded pNIPAAm	Inferior Fornix	Cysteamine	Cysteamine loaded PLGA microspheres fabricated through spray drying prior to dispersal in pNIPAAm dissolved in water/PEG co-solvents. Sustained cysteamine release noted over 24 hours.

				Thermo-composites applied to rabbit inferior fornix over 24 hours were retained and well tolerated.
pNIPAAm Micro or Nanogels				
[29]	Crosslinked networks of acrylic acid functionalized chitosan and pNIPAAm or blended chitosan and pNIPAAm	NA	Pilocarpine	Nanoparticles produced by reacting carbxoylic functionalized chitosan with NIPAAm by radical-induced co-polymerization or polymer blending. Thermogelling behaviour studied with NIPAAm containing formulations. Formulations with NIPAAm and a low concentration of chitosan were found to be the most mucoadhesive. Lysozyme mediated degradation was a function of chitosan content.

[21]	Hyaluronic acid-g-pNIPAAm	Inferior Fornix	Cyclosporine A	Microgels fabricated by grafting of carboxylic end capped pNIPAAm to hyaluronic acid. Based on rabbit *in vivo* testing the formulations were found not to irritate and after 24-hours the CycA concentrations of rabbit corneas was significantly higher with microgels compared to castor oil or over the counter CycA formulations. Degradation not studied.
[23]	(Heparin or chondroitin sulfate)-g-pNIPAAm	Topical	Dexamethasone	Thermo-sensitive nanogels produced by grafting heparin or chondroitin sulfate with NIPAAm. Nanogels were further crosslinked by reduction of end groups to yield disulfide bridging. Grafting density

				and chain length affected LCST and pH properties. Nanogels were demonstrated to be well tolerated at 0.5 mg/mL with RPE cells. Chondroitin sulfate nanogels resulted in prolonged release of loaded drug up to 12 hours, nearly double the duration of heparin-based materials.
[22]	(Heparin or chondroitin sulfate)-g-pNIPAAm	Topical	Dexamethasone	Thermo-nanogels fabricated through grafting either heparin or chondriotin sulfate with NIPAAm, with or without the addition of disulfide crosslinks. The fabricated nanogels were found to have strong adhesive binding to mucus by isothermal, titration calorimetry. *In vivo* rabbit IOP reduction after 8 hours

				suggests nanogels can prolong carbonic anhydrase inhibitor for treatment of glaucoma.

2.2 Poly(ethylene glycol) and Poloxamer Thermogels for Anterior Application

Polymers based on short-chain PEG can display reversible thermo-gelation [30]. Examples of these polymers include POEGMA and poloxamers (also called Pluronics®, Lutrols®, and Koliphors®). Poloxamers are non-ionic, amphiphilic, A-B-A triblock copolymers comprised of hydrophobic poly(propylene oxide) and hydrophilic poly(ethylene oxide) (PEO). They are commonly used as surfactants or thermogels in the preparation of pharmaceuticals and cosmetics. Poloxamers are popular thermogelling materials as they are simple to use, have a tunable LCST, are easy to blend with other polymers, and are non-toxic. The most used formulations are Poloxamer 407 (P407 or trade name F-127) and Poloxamer 188 (P188 or trade name F-68) which differ based on their ratio of base units. Specifically, P407 and P188 are often utilized for developing ocular thermogelling formulations because of their clarity, high water solubility, shear-thinning properties, tailorable viscosity based on concentration, and demonstrated safety with ocular tissues [31, 32]. Interestingly, poloxamer formulations are known to be somewhat mucoadhesive due to entanglement of the PEG brush structure with mucin [11]. The poloxamer-based systems developed for anterior applications are summarized in Table 2.2.

Poloxamers have been studied for anterior application for the last 20 years, with one of the first studies reporting one hour retention within the inferior fornix of human participants [33]. Though the grafting of pNIPAAm to natural polymers is

well investigated, the grafting of poloxamers is not. An example is the grafting of amine end-capped poloxamer with HA by EDC conjugation for the release of ciprofloxacin [34]. This approach is not well investigated, with most studies focusing on simply blending non-degradable poloxamer analogs together, incorporating viscosity enhancers such as CM, CMC, or HPMC, or adding mucoadhesive polymers such as HA, chitosan, or polyacrylic acid (Carbopols). Frequently, these studies focus on utilizing factorial or central composite design to optimize properties such as gelation temperature, gel viscosity, gelling capacity, spreadability, and drug release kinetics. As an example, the blending of poloxamer analogs P407 and P188 was studied by central composite design, demonstrating that a composition of 21% P407 and 5% P188 (w/w) yielded the optimal gelation temperature and mucoadhesive properties for application to the front of the eye [35]. El-Kamel investigated the blending of P407 with MC, CMC, and HPMC in order to lower the concentration of poloxamer required without compromising gel capabilities [36]. The study found that the best *in vitro* and *in vivo* performance was achieved with 15% P407 and 3% CM (w/w), which also prolonged the drug release. Earlier studies also investigated the use of isotonicity agents, finding that they generally lowered gelation temperatures within the formulations [35, 36]. Despite these early results from El-Kamel, most studies in the field have investigated blending the poloxamers with HPMC. Two different studies based on factorial design found that the optimal formulations were 18% P407 and 0.5% HPMC (w/w) [37] and 8% P407 and 0.8% HPMC (w/w) [38]. When comparing these studies,

there is a large discrepancy in the optimal concentration of P407, which results from the selection of the dependent variables that are optimized, as well as the drug being released. With the 18% P407 and 0.5% HPMC (w/w) formulation, release of the drug benzalkonium chloride was able to steadily decrease the IOP in a rabbit glaucoma model over 8 hours after application to the inferior fornix, compared to a topical eyedrop where the IOP returned to the elevated level after 8 hours [37].

An early investigation into improving mucoadhesion focused on blending HA with P407 and P188 [39]. The study found that increasing HA concentration past 0.3% (w/w) resulted in decreased flowability. However, scintigraphic studies utilizing rabbits demonstrated that HA did not increase retention. In contrast, the incorporation of 0.2% (w/w) of the Carbopol 1342 NF with P407 and P188 did result in increased mucoadhesion as well as the greatest change in IOP following instillation to the inferior fornix in a rabbit model [40]. Gratieri et al., investigated the impact of blending the poloxamers with chitosan [41, 42]. Through Instron measurement, it was determined that increasing the chitosan concentration from 0.5-1.5% (w/w) resulted in an increase in mucoadhesion [42]. Despite this result, a follow-up study demonstrated that the concentration of the loaded fluconazole in the aqueous humour of rabbits was comparable over time between chitosan blended P407 and a simple chitosan solution, suggesting that the incorporation of the thermogel did not aid in drug permeation across the cornea [41]. Most recently, a factorial design found a formula of 22.5% P407 and 0.3% chitosan (w/w) yielded

optimal properties, with the required mucus detachment force being greater than the force of blinking [43]. The study did not investigate the retention time *in vivo* to assess whether the optimal P407 and chitosan blend performed better than either constituent part.

More recently, studies within the field have investigated the addition of micro and nano sized particles within poloxamer matrices. An initial investigation onto poloxamer nano-composites created micelles with the drug diclofenac and dispersed them within P407 yielding a system with near zero-order drug release [44]. By fluorescently tagging the micelles, retention on the ocular surface was demonstrated up to half an hour. Lipid nanoparticles have been investigated in loading lipophilic drugs into aqueous poloxamer systems. It was demonstrated that solid lipid nanoparticles (SLNs) increased in size from roughly 150 to 400 nm when dispersed in a P407/P188 blend and that the particles were able to effectively penetrate through the cornea after 2 hours, as demonstrated by the distribution of fluorescently tagged particles in histological samples [45]. Nanostructured lipid nanoparticles, optimized through central composite design, were dispersed within a blend of P407 and CMCS where the resulting nanocomposite achieving sustained drug release *in vitro* over 3 days [46]. In contrast, nanoliposomes loaded within P407 demonstrated *in vitro* release of senicapoc over 28 days, although retention on the ocular surface was only demonstrated for 60 minutes through fluorescence, as shown in Figure 2.2 [47]. Finally, nanocomposites were fabricated with carbon nanodots derived from HA and CMCS, in order to express CD44

affinity, as the CD44 receptor is often overexpressed in ocular cells under inflammatory conditions [48, 49]. This is a unique strategy as it allows for both sustained drug delivery and active targeting from the dispersed nanoparticles. It was demonstrated that the developed composite resulted in a 3.45-fold increase in the concentration of diclofenac sodium in the aqueous humour of rabbits over 3 hours compared to conventional topical eyedrops [49].

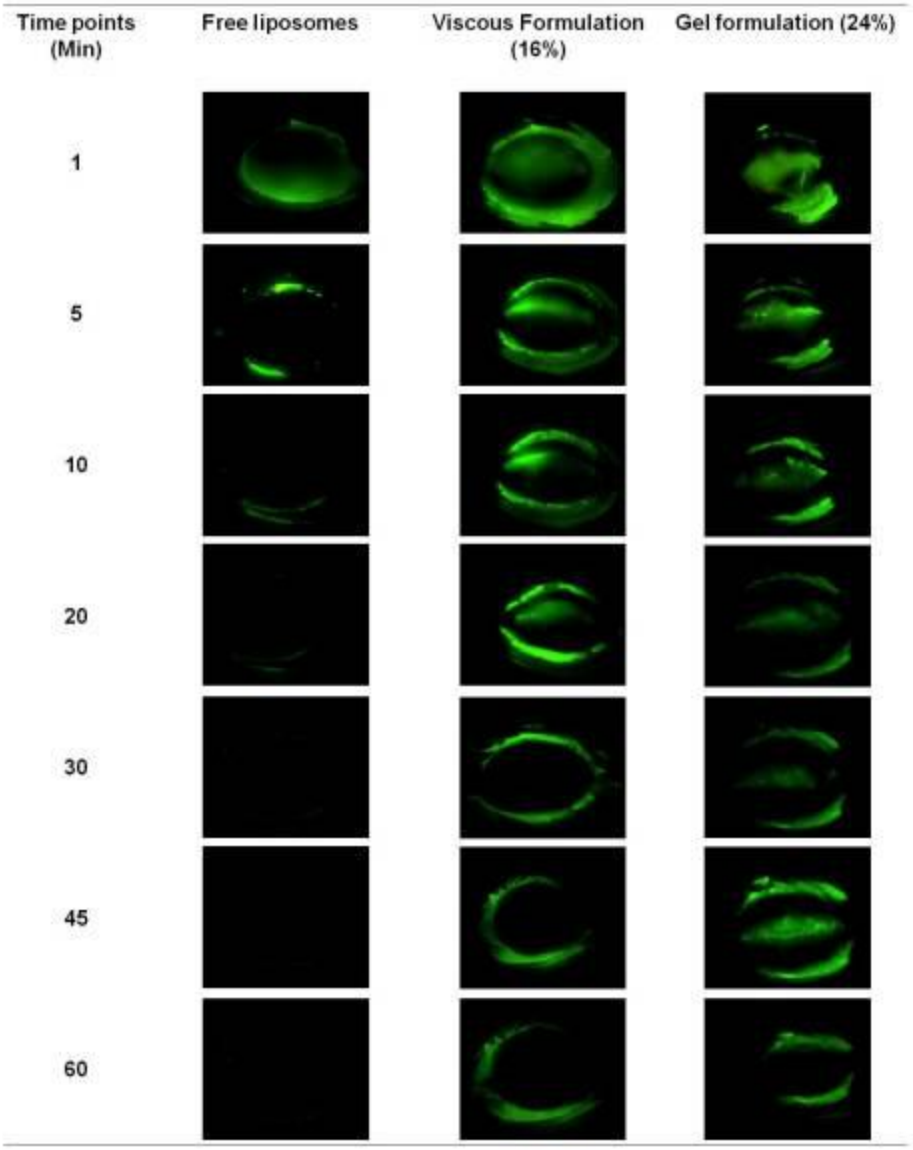

Figure 2.2) Residence images (Micron IV Imaging) of free fluorescein-tagged liposomes and hydrogel formulations in eyes of anesthetized Sprague-Dawley rats. Two rats were used for each formulation [47]. Reproduced without change under terms of Creative Commons License.

Besides poloxamers, thermogelling systems have also been developed based on PEG monomers or PEG oligomers. These thermogels are typically fabricated through ring opening polymerization with hydrolytic components such as poly(caprolactone) (PCL) or PLGA. A recent example was developed based on combining mucoadhesive di-(1-hydroxylundecyl) selenide (DHSe), PEG, and PEO, for delivery of Remdesivir in the ocular treatment of the SARS-CoV-2 virus [50]. Ocular retention of the developed thermogel was noted for over 60 minutes following loading with fluoresceine. An interesting consideration is that the block copolymers fabricated in these studies are often amphiphilic, such that in addition to acting as thermogels, they can also be used to create micelles [51, 52]. Mucoadhesive polyhedral oligomeric silsesquioxane (POSS) was combined with PEG and PEO to create a copolymer capable of self-assembling into micelles, entrapping the drug Tacrolimus, and further acting as a thermogel able to contain these micelles [51]. This synthetic scheme is visualized in Figure 2.3. The resulting drug loaded thermo-composite was able to effectively alleviate symptoms in a mouse dry eye model. Interestingly, micelles of PEG-PCL entrapping pimecrolimus improved the treatment of inflammation in a Keratoconjunctivitis Sicca mouse model, when compared to those same micelles dispersed in a solution of PEG-PCL to act as a thermogelling composite [52]. This is a surprising result, as it is typically hypothesized that incorporating nanoparticles into a thermogel prior to administration to the surface of the eye will result in protection from washout, thus improving drug delivery. The approach has recently been taken

a step further as a thermogelling nanocomposite was developed from a triblock copolymer of PLGA and PEG capable of forming micelles, also incorporating meso-porous silica nanoparticles (MSNs) [53]. This system allows for micelles to entrap one drug, and the MSNs another, before dispersing both particles in the thermogel matrix, yielding a tailorable and selective release profile for multiple drugs. Following sub-conjunctival injection, the developed system was able to significantly lower the concentration of cytokines in the aqueous humour of a rabbit inflammation model compared to conventional eyedrops over a 15-day period.

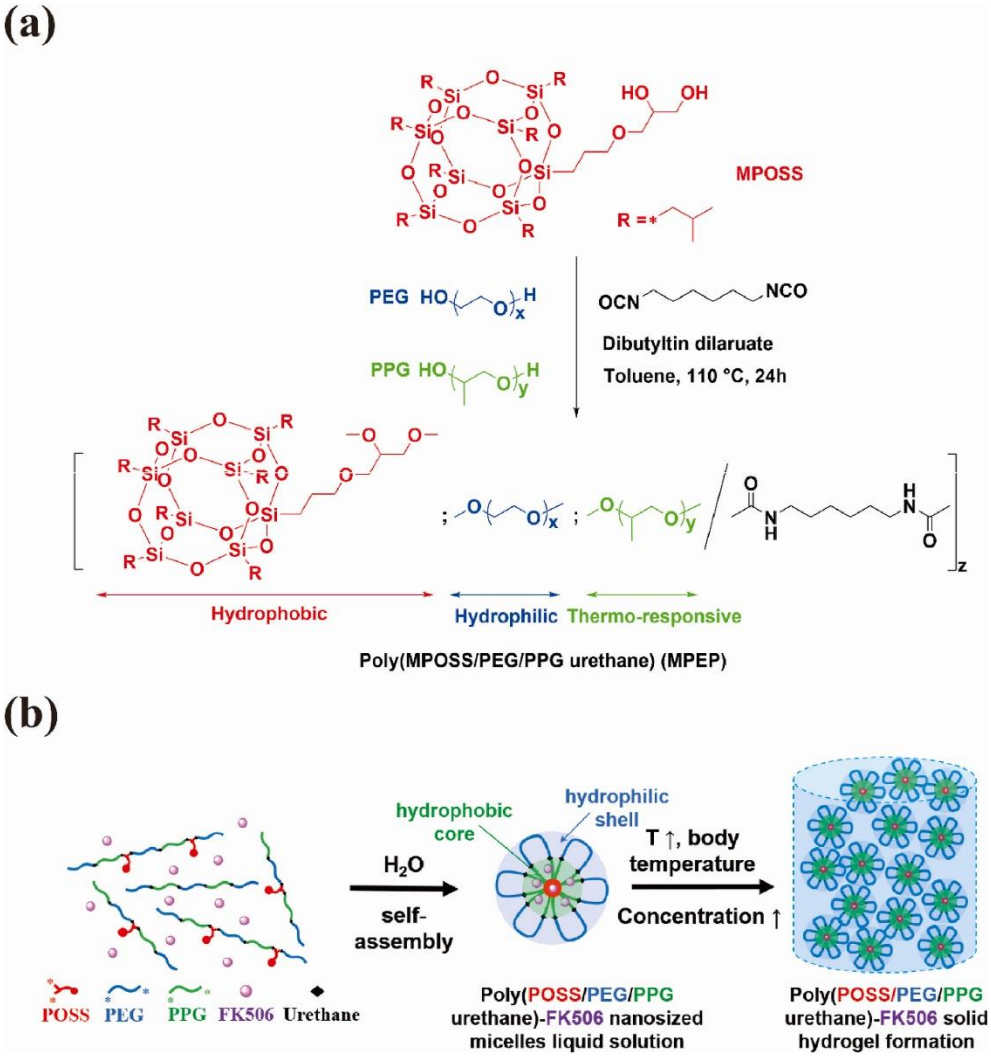

Figure 2.3a) Synthesis of MPEP by polyaddition and (b) illustration of the self-assembly of MPEP and hydrogel formation in water [51]. Reproduced without change under terms of Creative Commons License.

An interesting result when comparing thermogels produced from poloxamers compared to those based on pNIPAAm, is that retention on the surface of the eye or within the inferior fornix is typically much shorter with poloxamers. There are a few possible explanations for this result. Firstly, poloxamers are

optically much clearer, making visualization over time more challenging. Secondly, the retention of poloxamer gels is usually assessed by fluorescence; where either the gel is loaded with a fluorescent dye or is loaded with particles tagged with a fluorescent dye. As the dye or tagged particles diffuse from the thermogel matrix, fluorescent intensity is lost in addition to the quenching over time [50]. Finally, from an experimental design standpoint, many of the studies involving retention within the inferior fornix of rabbits do not mention the removal of nictitating membrane, which is known to drastically shorten retention [18]. Despite these possible sources of error, the very long retention [10, 18] noted in some pNIPAAm-based formulations suggest that it is the superior material to use for application to the ocular surface, in terms of retention over time, compared to poloxamer-based formulations.

Table 2.2) PEG and Poloxamer Based Thermogels for Anterior Ocular Application

Reference	Formulation	Intended Application	Model Drug	Results
Blended Poloxamers				
[36]	P407 with MC, CMC and HPMC	Inferior Fornix	Timolol Maleate	Study compared the concentration of P407 used, the addition of varying isotonicity agents, and the effect of blending with polymer thickening agents. Addition of thickening agents keeps gelling properties constant when lowering the concentration of P407. The formulation with MC was found to have the best rheological and release properties.

[39]	P407 and/or P188 with HA	Topical	NA	Pluronic blends incorporated HA to increase mucoadhesion. Formulations with greater than 0.3% (w/w) HA decreased flowability. Gamma scintigraphy demonstrated that HA incorporation did not improve ocular retention compared to just blended P407 and P188.
[35]	P407 and P188	Inferior Fornix	Puerarin	A two-factor, five-level central composite design was utilized to design a blend of P407 and P188 with optimal thermogelling properties. Optimal formulation was determined as 21% P407 and 5% P188 (w/w). The effect of isotonicity

				agents on gelation temperature was also explored.
[40]	P407 and P188 with carbopol	Inferior Fornix	Puerarin	Carbopol was incorporated with a blend a of poloxamer analogues to improve mucoadhesion. Formulation containing CP1342 demonstrated the greatest mucoadhesive properties and displayed the greatest reduction of IOP over 24 hours in a rabbit glaucoma model.
[42]	P407 with chitosan	Inferior Fornix	NA	Chitosan was incorporated with P407 to increase mucoadhesive properties. As determined by Instron measurement, an increasing concentration of chitosan from 0.5-

				1.5% (w/w) increased mucoadhesion. Scintigraph evaluation demonstrated improved retention in a short-term study with human volunteers although gel distribution was not homogenous.
[41]	P407 with chitosan	Topical	Fluconazole	P407 and chitosan blend compared to a chitosan solution of equal concentration. The aqueous humour concentration of Fluconazole from the rabbit model demonstrated no statistical difference over 6 hours between release of chitosan with or without P407.

[37]	P407 and HPMC	Inferior Fornix	Benzalkonium chloride	3^2 factorial design of blending P407 with HPMC to determine optimal gel viscosity, gelation temperature and drug release. *Ex vivo* goat cornea permeation study demonstrated sustained release of optimal formulation over 5-hour testing period. In vivo rabbit glaucoma model demonstrated continual IOP reduction for 8 hours.
[54]	P407 and P188 with CMC	Inferior Fornix	Voriconazole	Incorporation of CMC with blended poloxamers results in slower release rates of the antimicrobial. Developed formulations were non-irritating in rabbit model and thermogel provided

				greater tear concentration of the drug compared to topical formulations up to 6 hours.
[55]	P407 with HPMC	Inferior Fornix	Olopatadine	Incorporating HPMC into poloxamer formulation aided gelling capacity and slower release kinetics *in vitro*. A sheep model demonstrated significantly higher concentrations of drug in the tear film from developed thermogel compared to topical formulation
[38]	P407 with HPMC	NA	Chloramphenicole	3^2 factorial design of blending P407 with HPMC to determine optimal gelling capacity, pH, and viscosity. A formula of 8% P407 and 0.8%

				HPMC (w/w) was the determined optima. No effect of viscosity on drug release kinetics investigated.
[43]	P407 with chitosan	Topical	Tacrolimus	2-factor-3-level composite design to determine optimal gelation time, temperature, and spreadability for blend. Optimal formulation was 22.5% P407 and 0.3% chitosan (w/w). Optimal formulation capable of sustained release over 4-hour test and were non-irritating *in vivo*.
Poloxamer Composites				
[44]	P407 loaded with diclofenac micelles	Inferior Fornix	Diclofenac	Thermo-composite capable of near zero order release over 6 hours *in vitro*. Retention was noted up to 30

				minutes in the inferior fornix of rabbits by fluorescence staining. Drug concentration in rabbit aqueous humour was sustained up to 24-hours after composite application.
[45]	P407 and P188 with solid lipid nanoparticles	Inferior Fornix	Resina Draconis	Lipophilic drug loaded solid lipid nanoparticles fabricated through melt ultrasonication and dispersed in poloxamer blend. The nanoparticles were demonstrated to penetrate through the poloxamer gel and into the cornea as demonstrated through histological analysis of rabbits treated with fluorescently labeled particles.

[46]	P407 and CMCs with nanostructured lipid carrier	NA	Quercetin	Nanostructured lipid nanocarriers synthetized through melt-emulsification with ultrasonication, and optimized by central composite design, were dispersed in P407 and CMCs crosslinked with genipin. Developed composite achieved sustained release up to 70 hours.
[47]	P407 with nanoliposomes	Sub-conjunctival injection	Senicapoc	Senicapoc loaded nanoliposomes approximately 90 nm were loaded into P407. Composite provided *sustained in vitro* drug release up to 28 days. Fluorescently tagged particles within P407 demonstrated topical residence up to 60 minutes.

[56]	P407 with nanoliposomes	Topical	Propranolol Hydrochloride	Liposomes prepared by solvent evaporation, 170-380 nm in size, were dispersed with P407. Composite system aids in prolonging drug release compared to just nanoliposomes but the effect of *ex vivo* permeation through a rabbit cornea model is not significantly different.
[57]	P407 and P188 with zedoary turmeric oil	Inferior Fornix	Germacrone + Furandadiene	Thermo-sensitive nanoemulsion was produced by compatibilizing zedoary tumeric oil with various other oils and poloxamers. Gels were found to degrade rapidly over 150 minutes, near zero-order kinetic release of the

				loaded drugs. *In vivo* rabbit model demonstrated the produced nanoemulsion gels were not irritating.
[48]	P407, P188 and HPMC with Carbon Dots	Inferior Fornix	Diclofenac sodium	Fabrication of carbon nanodots from HA and CMCS to express CD44. Orthogonal experimental design used to optimize gel matrix. Thermogelling composites prolonged surface retention of fluorescently labeled particles over 30-minute testing period. *In vitro* cellular uptake study showed effective CD44 particle targeting.

[49]	P407, P188 and HPMC with Carbon Dots	Inferior Fornix	Diclofenac sodium	HA and CMCS derived carbon nanodot based composite. Fluorescently tagged particles were distributed through ocular tissues 2 hours after administration. 3.45 increase in drug concentration of rabbit aqueous humour, over 3 hours, from composite compared to topical eyedrops.
PEG Monomer Based Thermogels and Composites				
[58]	Poly(PEG-PCL-PEG)	Inferior Fornix	Diclofenac sodium	Thermogel synthesized through ring opening polymerization. Pharmacokinetic rabbit study demonstrated the developed thermogel had a 1.6-fold increase in

				aqueous humour concentration over 48 hours compared to conventional eyedrops.
[52]	Poly(PEG-PCL) with micelles	Topical	Pimecrolimus	Copolymer of PEG and PCL synthesized by ring opening polymerization and utilized to fabricate both drug loaded micelles and thermo-responsive nanogels. Just micelle application resulted in improved corneal thickness and less inflammatory cells in a Keratoconjunctivitis Sicca mouse model compared to the micelles loaded in the thermogel.

[53]	Poly(PLGA-PEG-PLGA) with MSNs and micelles	Sub-conjunctival injection	Prednisolone acetate and levofloxacin	Thermo-sensitive triblock copolymer of PLGA and PEG synthetized through ring opening polymerization. Resulting composite was capable of loading and selectively releasing both drugs for treatment of ocular inflammation. *In vivo* drug release in rabbits showed a sustained release over 14 days in the aqueous humour following sub-conjunctival injection.
[50]	Poly(DHSe/PEG/PEO urethane)	Topical	Remdesivir	Thermo-responsive polyurethane multi-block copolymer synthesized through condensation reactions. Topical application within a rabbit model demonstrated retention over

				60 minutes by fluorescent measurement. The gel layer forming over the corneal surface was imaged by optical coherence tomography.
[51]	Poly (POSS-PEG-PEO) with micelles	Topical	Tacrolimus	Amphiphilic copolymer synthesized with macro-diols used to encapsulate drug as micelles and additional copolymer utilized for thermogelling properties. Degradation was tailored from 6 to 14 days for the fabricated copolymers with release on the same timeframes. Mucoadhesion was imparted by POSS comonomer. *In vivo* mouse dry eye model demonstrated improved efficacy with

				increased tear production from the developed thermogels.

2.3 Natural Polymer Based Thermogels for Anterior Application

While many studies have combined synthetic and natural polymers to create thermogels with different properties, thermogels have also been produced from just natural polymers. Due to its favorable ocular properties, the most investigated of these systems is chitosan. Chitosan is naturally a thermogel, but its poor solubility causes precipitation above the LCST. Therefore, polyol salts are added to improve the solubility of chitosan at physiological pH [59]. Of these polyol salts, the weak base, β-glycerophosphate (BGP), has been shown to produce thermogels with chitosan that has a high DDA [60-63]. A high concentration of BGP is required in these systems and limited investigation has been conducted into the utilization of other inorganic salts like glycerol disodium [64] and ammonium hydrogen phosphate [65] for the creation of chitosan thermogels. For anterior ocular application, gelatin, chitosan, and BGP were blended to produce a thermogel to release latanoprost as a glaucoma treatment, which was applied to the inferior fornix [66]. The IOP was returned to baseline after one week following a single thermogel dose in a rabbit glaucoma model. A composite of chitosan nanoparticles containing 5-fluorouracil was loaded into thermogels based on BGP with chitosan, quaternary ammonium–chitosan, or thiolated chitosan [67]. Although the mucoadhesion of the different formulations was not quantified, nor was the resulting surface retention with the rabbit model, the chitosan composite thermogels were able to extend the detectable concentration in the aqueous humour from 2 to 8 hours. In a similar study, levofloxacin-loaded chitosan

microspheres were dispersed within a thermogel comprised of chitosan, BGP, and CMCS for application to the inferior fornix [68]. The strictly chitosan-based composite thermogel was retained within the fornix *in vivo* for up to 9 hours by quantification with fluorescein while releasing levofloxacin over an 11-hour period *in vitro*. Finally, a transparent thermogel based on water-soluble quaternized chitosan with BGP and sodium hydrogen carbonate as the gelling agents was developed for the treatment of glaucoma [69]. The developed thermogel delivered a sustained release of timolol maleate over a 3-day period; however, it was demonstrated that an increasing concentration of BGP resulted in a significant increase in cell death *in vitro*. Another important consideration for the usage of BGP and other gelling agents is the concentration of cationic charge associated with chitosan is lowered upon complexation, which reduces mucoadhesive properties of chitosan [70]. Therefore, formulations that utilize chitosan and BGP for mucosal anchoring, particularly on the ocular surface, should incorporate other mucoadhesive components.

Besides complexation with gelling agents to produce chitosan thermogels, simple modifications can also be utilized such as acrylamide [71] or glycol conjugation to chitosan [72, 73]. A particular synthetic strategy that has been utilized for front of the eye applications is the synthesis of thermogelling hexanoyl glycol chitosan (HGC), by the reaction of glycol chitosan with hexanoic anhydride [74, 75]. The produced HGC thermogels were determined to be soft (moduli equal to or under 10 Pa) by rheological measurement and had limited retention of

approximately 90 minutes [74] and 30 minutes [75], as measured by fluorescence, when applied within the inferior fornix of rabbits. Due to the soft nature of these gels, the release of loaded drugs was on the scale of hours. The described HGC thermogels represent an intermediate release profile between micelle or emulsion-based topical formulations, and much stiffer pNIPAAm or poloxamer thermogels.

Very limited studies have described thermogels comprised of natural polymers for anterior ocular application that are not based on chitosan. A notable exception is a thermogel developed from partially enzymatically degraded xyloglucan [76]. Dilute (1-2% w/w) xyloglucan gels were compared to conventional P407 (25% w/w), both loaded with pilocarpine and instilled in the inferior fornix of rabbits. It was shown that the xyloglucan thermogels produced a miotic effect that was not significantly different from P407 formulations, displaying the usability of even dilute glucan systems compared to conventional synthetic systems. Interestingly, other glucans, like curdlan [77], can also be utilized to produce thermogels, though they have not been investigated for application to the anterior of the eye.

2.4 Conclusion

The anterior of the eye is affected by a myriad of diseases, many of which threaten the vision of those afflicted. Unfortunately, nearly all the current marketed therapeutics for treating these diseases are based on topical formulations. Topical formulations are well established to be very ineffective, with only a small fraction,

less than 5%, of each applied dose reaching the desired site of action. One of the major paradigms in ophthalmology is creating formulations that minimize drug loss caused by the natural clearance mechanisms of the eye, while prolonging drug release. One such avenue is through the usage of thermogelling formulations, which can be applied as a solution at room temperature, but gel against the heat of eye. This review has sought to cover the thermogelling formulations that have been developed for treating anterior conditions; namely pNIPAAm, PEG, and natural polymer based systems. This review also focuses on recent the recent developments within the field, such as incorporating degradability, mucoadhesion, and the development of composites containing either micro or nanoparticles.

2.5 References

[1] L. Tang, L. Wang, X. Yang, Y. Feng, Y. Li, and W. Feng, "Poly (N-isopropylacrylamide)-based smart hydrogels: Design, properties and applications," *Progress in Materials Science,* vol. 115, p. 100702, 2021.

[2] A. S. Hoffman, "4. Poly (NIPAAm) revisited-it has been 28 years since it was first proposed for use as a biomaterial: Original research article: Applications of thermally reversible polymers hydrogels in therapeutics and diagnostics, 1987; thermally reversible hydrogels: II. Delivery and selective removal of substances from aqueous solutions, 1986; a novel approach for preparation of pH-sensitive hydrogels for enteric drug delivery, 1991," *Journal of controlled release: official journal of the Controlled Release Society,* vol. 190, p. 36, 2014.

[3] Z. M. Rzaev, S. Dincer, and E. Pişkin, "Functional copolymers of N-isopropylacrylamide for bioengineering applications," *Progress in Polymer Science,* vol. 32, no. 5, pp. 534-595, 2007.

[4] M. A. Haq, Y. Su, and D. Wang, "Mechanical properties of PNIPAM based hydrogels: A review," *Materials Science Engineering C Materials Biological Applications,* vol. 70, no. Pt 1, pp. 842-855, Jan 1 2017, doi: 10.1016/j.msec.2016.09.081.

[5] S. Lanzalaco and E. Armelin, "Poly (N-isopropylacrylamide) and copolymers: a review on recent progresses in biomedical applications," *Gels,* vol. 3, no. 4, p. 36, 2017.

[6] L. H. Lima, Y. Morales, and T. Cabral, "Ocular biocompatibility of poly-N-isopropylacrylamide (pNIPAM)," *Journal of ophthalmology,* vol. 2016, 2016.

[7] J.-Y. Lai and A.-C. Hsieh, "A gelatin-g-poly (N-isopropylacrylamide) biodegradable in situ gelling delivery system for the intracameral administration of pilocarpine," *Biomaterials,* vol. 33, no. 7, pp. 2372-2387, 2012.

[8] J.-Y. Lai, "Biodegradable in situ gelling delivery systems containing pilocarpine as new antiglaucoma formulations: effect of a mercaptoacetic acid/N-isopropylacrylamide molar ratio," *Drug Design, Development and Therapy,* vol. 7, p. 1273, 2013.

[9] L.-J. Luo and J.-Y. Lai, "Amination degree of gelatin is critical for establishing structure-property-function relationships of biodegradable thermogels as intracameral drug delivery systems," *Materials Science and Engineering: C,* vol. 98, pp. 897-909, 2019.

[10] L.-J. Luo, D. D. Nguyen, and J.-Y. Lai, "Long-acting mucoadhesive thermogels for improving topical treatments of dry eye disease," *Materials Science and Engineering: C,* vol. 115, p. 111095, 2020.

[11] R. S. Dave, T. C. Goostrey, M. Ziolkowska, S. Czerny-Holownia, T. Hoare, and H. Sheardown, "Ocular drug delivery to the anterior segment using nanocarriers: A mucoadhesive/mucopenetrative perspective," *Journal of Controlled Release,* vol. 336, pp. 71-88, 2021.

[12] J.-Y. Lai and L.-J. Luo, "Chitosan-g-poly (N-isopropylacrylamide) copolymers as delivery carriers for intracameral pilocarpine administration," *European Journal of Pharmaceutics and Biopharmaceutics,* vol. 113, pp. 140-148, 2017.

[13] L.-J. Luo, C.-C. Huang, H.-C. Chen, J.-Y. Lai, and M. Matsusaki, "Effect of deacetylation degree on controlled pilocarpine release from injectable chitosan-g-poly (N-isopropylacrylamide) carriers," *Carbohydrate polymers,* vol. 197, pp. 375-384, 2018.

[14] L.-J. Luo, D. D. Nguyen, and J.-Y. Lai, "Benzoic acid derivative-modified chitosan-g-poly (N-isopropylacrylamide): Methoxylation effects and pharmacological treatments of Glaucoma-related neurodegeneration," *Journal of Controlled Release,* vol. 317, pp. 246-258, 2020.

[15] D. D. Nguyen, L.-J. Luo, S. J. Lue, and J.-Y. Lai, "The role of aromatic ring number in phenolic compound-conjugated chitosan injectables for

sustained therapeutic antiglaucoma efficacy," *Carbohydrate Polymers,* vol. 231, p. 115770, 2020.

[16] M. Ross, E. A. Hicks, T. Rambarran, and H. Sheardown, "Thermo-sensitivity and erosion of chitosan crosslinked poly [N-isopropylacrylamide-co-(acrylic acid)-co-(methyl methacrylate)] hydrogels for application to the inferior fornix," *Acta Biomaterialia,* 2022.

[17] M. V. Fedorchak, I. P. Conner, C. A. Medina, J. B. Wingard, J. S. Schuman, and S. R. Little, "28-day intraocular pressure reduction with a single dose of brimonidine tartrate-loaded microspheres," *Experimental Eye Research,* vol. 125, pp. 210-216, 2014.

[18] M. V. Fedorchak, I. P. Conner, J. S. Schuman, A. Cugini, and S. R. Little, "Long term glaucoma drug delivery using a topically retained gel/microsphere eye drop," *Scientific reports,* vol. 7, no. 1, pp. 1-11, 2017.

[19] E. Bellotti, M. V. Fedorchak, S. Velankar, and S. R. Little, "Tuning of thermoresponsive pNIPAAm hydrogels for the topical retention of controlled release ocular therapeutics," *Journal of Materials Chemistry B,* vol. 7, no. 8, pp. 1276-1283, 2019.

[20] J. Jimenez, M. A. Washington, J. L. Resnick, K. K. Nischal, and M. V. Fedorchak, "A sustained release cysteamine microsphere/thermoresponsive gel eyedrop for corneal cystinosis improves drug stability," *Drug Delivery and Translational Research,* vol. 11, no. 5, pp. 2224-2238, 2021.

[21] Y. Wu, J. Yao, J. Zhou, and F. Z. Dahmani, "Enhanced and sustained topical ocular delivery of cyclosporine A in thermosensitive hyaluronic acid-based in situ forming microgels," *International journal of nanomedicine,* vol. 8, p. 3587, 2013.

[22] I. Pilipenko *et al.*, "Mucoadhesive properties of nanogels based on stimuli-sensitive glycosaminoglycan-graft-pNIPAAm copolymers," *International Journal of Biological Macromolecules,* vol. 186, pp. 864-872, 2021.

[23] I. Pilipenko, V. Korzhikov-Vlakh, N. Zakharova, A. Urtti, and T. Tennikova, "Thermo-and pH-sensitive glycosaminoglycans derivatives obtained by controlled grafting of poly (N-isopropylacrylamide)," *Carbohydrate Polymers,* vol. 248, p. 116764, 2020.

[24] N. Bayat *et al.*, "A reversible thermoresponsive sealant for temporary closure of ocular trauma," *Science Translational Medicine,* vol. 9, no. 419, p. eaan3879, 2017.

[25] Y. Cao, C. Zhang, W. Shen, Z. Cheng, L. L. Yu, and Q. Ping, "Poly (N-isopropylacrylamide)–chitosan as thermosensitive in situ gel-forming

system for ocular drug delivery," *Journal of controlled release,* vol. 120, no. 3, pp. 186-194, 2007.

[26] L.-J. Luo and J.-Y. Lai, "Epigallocatechin gallate-loaded gelatin-g-poly (N-isopropylacrylamide) as a new ophthalmic pharmaceutical formulation for topical use in the treatment of dry eye syndrome," *Scientific reports,* vol. 7, no. 1, pp. 1-14, 2017.

[27] D. D. Nguyen, L.-J. Luo, and J.-Y. Lai, "Thermogels containing sulfated hyaluronan as novel topical therapeutics for treatment of ocular surface inflammation," *Materials Today Bio,* vol. 13, p. 100183, 2022.

[28] A. Mammen, E. G. Romanowski, M. V. Fedorchak, D. K. Dhaliwal, R. Shanks, and R. P. Kowalski, "Endophthalmitis prophylaxis using a single drop of thermoresponsive controlled-release microspheres loaded with moxifloxacin in a rabbit model," *Translational Vision Science & Technology,* vol. 5, no. 6, pp. 12-12, 2016.

[29] E. Barbu, L. Verestiuc, M. Iancu, A. Jatariu, A. Lungu, and J. Tsibouklis, "Hybrid polymeric hydrogels for ocular drug delivery: nanoparticulate systems from copolymers of acrylic acid-functionalized chitosan and N-isopropylacrylamide or 2-hydroxyethyl methacrylate," *Nanotechnology,* vol. 20, no. 22, p. 225108, 2009.

[30] N. M. Smeets, E. Bakaic, M. Patenaude, and T. Hoare, "Injectable poly (oligoethylene glycol methacrylate)-based hydrogels with tunable phase transition behaviours: Physicochemical and biological responses," *Acta biomaterialia,* vol. 10, no. 10, pp. 4143-4155, 2014.

[31] K. A. Soliman, K. Ullah, A. Shah, D. S. Jones, and T. R. Singh, "Poloxamer-based in situ gelling thermoresponsive systems for ocular drug delivery applications," *Drug Discovery Today,* vol. 24, no. 8, pp. 1575-1586, 2019.

[32] H. Almeida, M. H. Amaral, P. Lobão, and J. M. Sousa Lobo, "Applications of poloxamers in ophthalmic pharmaceutical formulations: an overview," *Expert opinion on drug delivery,* vol. 10, no. 9, pp. 1223-1237, 2013.

[33] K. Edsman, J. Carlfors, and R. Petersson, "Rheological evaluation of poloxamer as an in situ gel for ophthalmic use," *European journal of pharmaceutical sciences,* vol. 6, no. 2, pp. 105-112, 1998.

[34] K. Cho *et al.*, "Release of ciprofloxacin from poloxamer-graft-hyaluronic acid hydrogels in vitro," *International journal of pharmaceutics,* vol. 260, no. 1, pp. 83-91, 2003.

[35] H. Qi, L. Li, C. Huang, W. Li, and C. Wu, "Optimization and physicochemical characterization of thermosensitive poloxamer gel containing puerarin for

ophthalmic use," *Chemical and pharmaceutical bulletin,* vol. 54, no. 11, pp. 1500-1507, 2006.

[36] A. El-Kamel, "In vitro and in vivo evaluation of Pluronic F127-based ocular delivery system for timolol maleate," *International journal of pharmaceutics,* vol. 241, no. 1, pp. 47-55, 2002.

[37] R. Barse, C. Kokare, and A. Tagalpallewar, "Influence of hydroxypropylmethylcellulose and poloxamer composite on developed ophthalmic in situ gel: Ex vivo and in vivo characterization," *Journal of Drug Delivery Science and Technology,* vol. 33, pp. 66-74, 2016.

[38] I. S. Kurniawansyah, T. Rusdiana, I. Sopyan, H. Ramoko, H. A. Wahab, and A. Subarnas, "In situ ophthalmic gel forming systems of poloxamer 407 and hydroxypropyl methyl cellulose mixtures for sustained ocular delivery of chloramphenicole: Optimization study by factorial design," *Heliyon,* vol. 6, no. 11, p. e05365, 2020.

[39] G. Wei, H. Xu, P. T. Ding, and J. M. Zheng, "Thermosetting gels with modulated gelation temperature for ophthalmic use: the rheological and gamma scintigraphic studies," *Journal of Controlled Release,* vol. 83, no. 1, pp. 65-74, 2002.

[40] H. Qi *et al.*, "Development of a poloxamer analogs/carbopol-based in situ gelling and mucoadhesive ophthalmic delivery system for puerarin," *International journal of pharmaceutics,* vol. 337, no. 1-2, pp. 178-187, 2007.

[41] T. Gratieri, G. M. Gelfuso, O. de Freitas, E. M. Rocha, and R. F. Lopez, "Enhancing and sustaining the topical ocular delivery of fluconazole using chitosan solution and poloxamer/chitosan in situ forming gel," *European journal of pharmaceutics and biopharmaceutics,* vol. 79, no. 2, pp. 320-327, 2011.

[42] T. Gratieri, G. M. Gelfuso, E. M. Rocha, V. H. Sarmento, O. de Freitas, and R. F. V. Lopez, "A poloxamer/chitosan in situ forming gel with prolonged retention time for ocular delivery," *European Journal of Pharmaceutics and Biopharmaceutics,* vol. 75, no. 2, pp. 186-193, 2010.

[43] D. Modi *et al.*, "Formulation development, optimization, and in vitro assessment of thermoresponsive ophthalmic pluronic F127-chitosan in situ tacrolimus gel," *Journal of Biomaterials Science, Polymer Edition,* vol. 32, no. 13, pp. 1678-1702, 2021.

[44] X. Li, Z. Zhang, and H. Chen, "Development and evaluation of fast forming nano-composite hydrogel for ocular delivery of diclofenac," *International journal of pharmaceutics,* vol. 448, no. 1, pp. 96-100, 2013.

[45] J. Hao *et al.*, "Fabrication of a composite system combining solid lipid nanoparticles and thermosensitive hydrogel for challenging ophthalmic drug delivery," *Colloids and Surfaces B: Biointerfaces,* vol. 114, pp. 111-120, 2014.

[46] Y. Yu *et al.*, "Nanostructured lipid carrier-based pH and temperature dual-responsive hydrogel composed of carboxymethyl chitosan and poloxamer for drug delivery," *International journal of biological macromolecules,* vol. 114, pp. 462-469, 2018.

[47] J. L. Phua *et al.*, "Topical delivery of senicapoc nanoliposomal formulation for ocular surface treatments," *International Journal of Molecular Sciences,* vol. 19, no. 10, p. 2977, 2018.

[48] L. Wang, H. Pan, D. Gu, P. Li, Y. Su, and W. Pan, "A composite System Combining Self-Targeted Carbon Dots and Thermosensitive Hydrogels for Challenging Ocular Drug Delivery," *Journal of Pharmaceutical Sciences,* 2021.

[49] L. Wang *et al.*, "A Novel Carbon Dots/Thermo-Sensitive In Situ Gel for a Composite Ocular Drug Delivery System: Characterization, Ex-Vivo Imaging, and In Vivo Evaluation," *International journal of molecular sciences,* vol. 22, no. 18, p. 9934, 2021.

[50] S. Xu *et al.*, "Thermosensitive Poly (DHSe/PEG/PPG Urethane)-Based Hydrogel Extended Remdesivir Application in Ophthalmic Medication," *Pharmaceutics,* vol. 14, no. 1, p. 50, 2021.

[51] Y. Han *et al.*, "Effectiveness of an ocular adhesive polyhedral oligomeric silsesquioxane hybrid thermo-responsive FK506 hydrogel in a murine model of dry eye," *Bioactive materials,* vol. 9, pp. 77-91, 2022.

[52] F. Yingfang, B. Zhuang, C. Wang, X. Xu, W. Xu, and Z. Lv, "Pimecrolimus micelle exhibits excellent therapeutic effect for Keratoconjunctivitis Sicca," *Colloids and Surfaces B: Biointerfaces,* vol. 140, pp. 1-10, 2016.

[53] S. Zhang, Y. Fang, J. Sun, Y. Deng, and Y. Lu, "Improved Treatment on Ocular Inflammation with Rationally Designed Thermoresponsive Nanocomposite Formulation," *Advanced Therapeutics,* vol. 4, no. 10, p. 2100088, 2021.

[54] N. Ü. Okur, V. Yozgatlı, M. E. Okur, A. Yoltaş, and P. I. Siafaka, "Improving therapeutic efficacy of voriconazole against fungal keratitis: Thermo-sensitive in situ gels as ophthalmic drug carriers," *Journal of drug delivery science and technology,* vol. 49, pp. 323-333, 2019.

[55] U. M. Güven, M. S. Berkman, B. Şenel, and Y. Yazan, "Development and in vitro/in vivo evaluation of thermo-sensitive in situ gelling systems for ocular allergy," *Brazilian Journal of Pharmaceutical Sciences,* vol. 55, 2019.

[56] B. S. MakhmalZadeh, M. Radpey, and M. R. Abbaspour, "Preparation and Ex-vivo Ocular delivery of Thermo-responsible pluronic F-127 hydrogel containing Propranolol hydrochlorideloaded Liposomes," *Nanomedicine Journal,* vol. 8, no. 1, 2021.

[57] X. Wang, Y. Gu, Y. He, L. Sang, Y. Dai, and D. Wang, "Preparation and optimization formulation of zedoary turmeric oil nanoemulsion based thermo-sensitive gel for improved application in ophthalmology," *Journal of Drug Delivery Science and Technology,* vol. 65, p. 102682, 2021.

[58] Z. Luo *et al.*, "Thermosensitive PEG–PCL–PEG (PECE) hydrogel as an in situ gelling system for ocular drug delivery of diclofenac sodium," *Drug delivery,* vol. 23, no. 1, pp. 63-68, 2016.

[59] V. Grinberg *et al.*, "Thermodynamic insight into the thermoresponsive behavior of chitosan in aqueous solutions: A differential scanning calorimetry study," *Carbohydrate Polymers,* vol. 229, p. 115558, 2020.

[60] C. Chaput and A. R. El Zein, "Mineral-polymer hybrid composition," ed: Google Patents, 2003.

[61] A. Chenite, C. Chaput, D. Wang, and A. Selmani, "Temperature controlled and pH dependent self gelling biopolymeric aqueous solution," ed: Google Patents, 2014.

[62] J. Cho, M.-C. Heuzey, A. Bégin, and P. J. Carreau, "Chitosan and glycerophosphate concentration dependence of solution behaviour and gel point using small amplitude oscillatory rheometry," *Food Hydrocolloids,* vol. 20, no. 6, pp. 936-945, 2006.

[63] J. Cho, M.-C. Heuzey, A. Bégin, and P. J. Carreau, "Effect of urea on solution behavior and heat-induced gelationof chitosan-β-glycerophosphate," *Carbohydrate polymers,* vol. 63, no. 4, pp. 507-518, 2006.

[64] M. Lavertu, D. Filion, and M. D. Buschmann, "Heat-induced transfer of protons from chitosan to glycerol phosphate produces chitosan precipitation and gelation," *Biomacromolecules,* vol. 9, no. 2, pp. 640-650, 2008.

[65] L. S. Nair, T. Starnes, J.-W. K. Ko, and C. T. Laurencin, "Development of injectable thermogelling chitosan–inorganic phosphate solutions for biomedical applications," *Biomacromolecules,* vol. 8, no. 12, pp. 3779-3785, 2007.

[66] Y.-H. Cheng *et al.*, "Thermosensitive chitosan-based hydrogel as a topical ocular drug delivery system of latanoprost for glaucoma treatment," *Carbohydrate polymers,* vol. 144, pp. 390-399, 2016.

[67] A. Fabiano, R. Bizzarri, and Y. Zambito, "Thermosensitive hydrogel based on chitosan and its derivatives containing medicated nanoparticles for transcorneal administration of 5-fluorouracil," *International Journal of Nanomedicine,* vol. 12, p. 633, 2017.

[68] X. Kong, W. Xu, C. Zhang, and W. Kong, "Chitosan temperature-sensitive gel loaded with drug microspheres has excellent effectiveness, biocompatibility and safety as an ophthalmic drug delivery system," *Experimental and Therapeutic Medicine,* vol. 15, no. 2, pp. 1442-1448, 2018.

[69] Y. Pakzad, M. Fathi, Y. Omidi, M. Mozafari, and A. Zamanian, "Synthesis and characterization of timolol maleate-loaded quaternized chitosan-based thermosensitive hydrogel: A transparent topical ocular delivery system for the treatment of glaucoma," *International Journal of Biological Macromolecules,* vol. 159, pp. 117-128, 2020.

[70] O. M. Kolawole, W. M. Lau, and V. V. Khutoryanskiy, "Chitosan/β-glycerophosphate in situ gelling mucoadhesive systems for intravesical delivery of mitomycin-C," *International journal of pharmaceutics: X,* vol. 1, p. 100007, 2019.

[71] F. Ding *et al.*, "Tunable thermosensitive behavior of multiple responsive chitin," *Journal of Materials Chemistry B,* vol. 2, no. 20, pp. 3050-3056, 2014.

[72] F. Lin, H.-R. Jia, and F.-G. Wu, "Glycol chitosan: A water-soluble polymer for cell imaging and drug delivery," *Molecules,* vol. 24, no. 23, p. 4371, 2019.

[73] Z. Li, S. Cho, I. C. Kwon, M. M. Janát-Amsbury, and K. M. Huh, "Preparation and characterization of glycol chitin as a new thermogelling polymer for biomedical applications," *Carbohydrate polymers,* vol. 92, no. 2, pp. 2267-2275, 2013.

[74] I. S. Cho *et al.*, "Thermosensitive hexanoyl glycol chitosan-based ocular delivery system for glaucoma therapy," *Acta Biomaterialia,* vol. 39, pp. 124-132, 2016.

[75] H. Shi *et al.*, "Thermosensitive glycol chitosan-based hydrogel as a topical ocular drug delivery system for enhanced ocular bioavailability," *International Journal of Pharmaceutics,* vol. 570, p. 118688, 2019.

[76] S. Miyazaki, S. Suzuki, N. Kawasaki, K. Endo, A. Takahashi, and D. Attwood, "In situ gelling xyloglucan formulations for sustained release

ocular delivery of pilocarpine hydrochloride," *International journal of pharmaceutics,* vol. 229, no. 1-2, pp. 29-36, 2001.

[77] C. H. Lee and K. B. Chin, "Evaluation of physicochemical and textural properties of myofibrillar protein gels and low-fat model sausage containing various levels of curdlan," *Asian-Australasian Journal of Animal Sciences,* vol. 32, no. 1, p. 144, 2019.

CHAPTER 3 – Thermo-sensitivity and erosion of chitosan crosslinked poly[N-isopropylacrylamide-co-(acrylic acid)-co-(methyl methacrylate)]hydrogels for application to the inferior fornix

Published Manuscript:

Mitchell Ross, Emily Anne Hicks, Talena Rambarran, and Heather Sheardown. (2022). Acta Biomaterialia. (141): 151-163.

Objectives:

To design a degradable thermogel for application to the anterior of the eye. The degradation was designed to occur over several days with release of a loaded anti-allergy medication. Test the safety of the developed thermogels both *in vitro* and *in vivo*.

Author Contributions:

Material development, testing, and subsequent reporting was completed by Mitchell Ross. Emily Anne Hicks aided with *in vitro* rat studies and Talena Rambarran with initial idea formulation.

Thermo-sensitivity and erosion of chitosan crosslinked poly[*N*-isopropylacrylamide-co-(acrylic acid)-co-(methyl methacrylate)] hydrogels for application to the inferior fornix

Mitchell Ross, Emily Anne Hicks, Talena Rambarran, Heather Sheardown

Department of Chemical Engineering, McMaster University, 1280 Main St W, Hamilton, ON L8S 4L8, Canada

Corresponding Author:

Heather Sheardown, sheardow@mcmaster.ca (905) 525-9140, John Hodgins Engineering Building Room 260, 1280 Main St W, Hamilton, ON L8S 4L7

Key words

Thermo-gels, chitosan, rheology, sustained drug release, allergic conjunctivitis

3.1 Abstract

Thermo-gels based on chitosan crosslinked poly(*N*-isopropylacrylamide) were developed as alternatives to conventional eye drops for the sustained release of ketotifen fumarate in the treatment of allergic conjunctivitis. The thermo-gelling properties of the base polymer were altered prior to crosslinking with chitosan by incorporation of the hydrophilic and hydrophobic comonomers acrylic acid and methyl methacrylate respectively. Varying amounts of chitosan were incorporated by ionic interaction to produce polyelectrolyte complexes or by carbodiimide

chemistry to produce covalently crosslinked networks. The lower critical solution temperature of all the chitosan crosslinked thermo-gels produced was below the surface temperature of the eye. All the chitosan crosslinked thermo-gels were found to have greater than 80% equilibrium water contents following gelation. The method and amount of chitosan incorporation allowed for tailor-ability of material rheologic properties, with full degradation occurring over a one-to-four-day period, and tailorable rates of release of 40-60% of the loaded allergy medication ketotifen fumarate. The chitosan crosslinked thermo-gels were demonstrated to be non-toxic both *in vitro* and *in vivo*. It was demonstrated that the synthesized materials could be applied to the inferior fornix of the eye, sustaining a multiple day release of ketotifen fumarate, as an alternative to conventional eyedrops.

3.2 Introduction

Allergic conjunctivitis (AC) is estimated to affect approximately 36% of the US population [1] and 45% of the Japanese population [2], although global estimates vary widely due to variations between countries and geographic regions. The prevalence of AC is expected to only increase due to global warming and air pollution [3, 4]. AC is an umbrella term referring to several hypersensitivity issues affecting the conjunctiva, eyelid and/or cornea [5]. Symptoms of AC include tearing, itching and conjunctival hyperemia. The treatment of anterior ocular conditions, such as AC, is most often accomplished using topical eye drops and ointments which are easy to apply, inexpensive, and non-invasive. However, it is

generally accepted that, with topical eye drops, less than 5% of an applied dose remains bioavailable after administration [6]. There are several barriers that limit the applied dosage including drainage via the nasolacrimal duct, rapid tear turnover and sources of undesirable absorption [7]. Despite these limitations, topical eye drops are the most common treatment method for AC using, for example, decongestants, antihistamines, mast cell stabilizers, nonsteroidal anti-inflammatory drugs (NSAID) and/or corticosteroid solutions [8]. According to the American Academy of Allergy, Asthma, and Immunology, nearly all brand name topical eye drops for the treatment of AC require a minimum of one dose per day.

Chitosan-based hydrogels have been extensively tested as ocular therapies due to their biodegradability, biocompatibility, muco-adhesion, corneal wound healing properties and anti- microbial/fungal effects [9, 10]. The properties of chitosan such as the molecular weight, degree of deacetylation (DDA), and the pattern of repeat units influence solubility by charge distribution, porosity, water uptake and degradation by the enzyme lysozyme [11]. Various sustained release ocular formulations based on chitosan have been developed including in situ gels, inserts, liposomes, microspheres/micelles and nanoparticles [12]. In situ gels at ambient conditions remain as polymeric solutions but, by a tuneable sol-gel transition, form hydrogel networks by the action of an external stimulus. Ocular in situ forming gels based on chitosan generally fall into one of three categories: thermo-responsive, pH-responsive, and ion-sensitive [9, 13]. Ocular thermo-responsive chitosan gels are typically based on the addition of polyol bearing

compounds such as glycerophosphate with chitosan or by combining chitosan with thermo-sensitive synthetic monomers/polymers such poloxamers or *N*-isopropylacrylamide (NIPAAm) [9, 13, 14].

Since their introduction in the 1980s, NIPAAm based hydrogels have been frequently suggested for use in biomedical applications [15, 16]. Poly(*N*-isopropylacrylamide) (pNIPAAM) hydrogels are defined by their reversible thermo-gelation with a lower critical solution temperature (LCST) of approximately 32-35 ℃. The LCST of pNIPAAm-based hydrogel systems can be altered by copolymerization with hydrophilic or hydrophobic comonomers [16]. The degradation of pNIPAAm-based hydrogels is typically accomplished through hydrolysis by the inclusion of various comonomers [17, 18]. The Sheardown research group has previously developed pNIPAAm-based hydrogels incorporating dimethyl-γ-butyrolactone acrylate, which undergoes slow hydrolytic ring opening, allowing for degradation over multiple months. This system was used for posterior eye injection applications [19-22].

pNIPAAm has been grafted with chitosan for many different applications, the most common of which is hydrogel strengthening. pNIPAAm-based hydrogels have been grafted with chitosan through carbodiimide EDC chemistry and have been shown to degrade via incubation with pepsin in simulated gastric fluid at 37 ℃ [23, 24]. As it pertains to ocular formulations, a similar system of chitosan grafted to pNIPAAm by EDC has been used as a platform for intracameral injection for the treatment of glaucoma. This system is enzymatically degraded when

incubated with lysozyme, at the concentrations found in rabbit aqueous humour, at 34 ℃ [25-28].

Drug delivery systems for the treatment of anterior eye conditions, applied to the inferior fornix (also known as the cul-de-sac) have been reported in the literature as alternatives to conventional eye drops [29-31]. These hydrogel systems have the potential for sustained drug delivery offering a major advantage over conventional, once daily, topical eye drops. On average, healthy patients blink between 10 and 25 times per minute and the mechanical load of blinking would lead to rapid deterioration of any hydrogel scaffold applied directly to the eye surface [32]. Therefore, application in the inferior fornix has been investigated with a goal of creating hydrogels that do not deteriorate as quickly during blinking and do not obstruct vision. These systems are typically either non-degradable in-situ gels, degradable pre-set films, or ocular inserts. In this work, it was hypothesized that by incorporating chitosan in pNIPAAm based hydrogels, an in situ thermo-gel with the ability to degrade over multiple days and with degradation by-products that are safely removed by the natural clearance mechanisms of the eye, can be developed to deliver a sustained delivery of loaded drugs for treating various ocular conditions such as AC. Chitosan was selected for its degradation by lysozyme, longer time scale of degradation compared to other natural polymers, and well documented use in ophthalmic preparations. Herein, we describe the incorporation of a hydrophobic comonomer to tailor thermo-gelling properties after chitosan incorporation. The work also investigates and compares the incorporation of

chitosan by either ionic or covalent chemistry and the subsequent effect on material properties and performance which, to the authors knowledge, has not been previously investigated in literature.

3.3 Materials and Methods

3.3.1 Materials

Chitosan (MW = 10-50 kDa, DDA = 70%) was purchased from Heppe Medical Chitosan (Halle, Saxony-Anhalt, Germany) and used as received. *N*-isopropylacrylamide (NIPAAm; 97%) was purchased from Sigma-Aldrich (Oakville, Ontario, Canada) and purified by recrystallization from toluene with n-hexane. Acrylic Acid (AA; 99%) was purchased from Sigma-Aldrich and purified by passing through a packed column containing Sigma-Aldrich inhibitor remover to remove the inhibitor 4-methoxyphenol. Methyl methacrylate (MMA; 99%), Benzoyl Peroxide (BPO; Luperox®, 98%), *N*-(3-Dimethylaminopropyl)-N′-ethylcarbodiimide hydrochloride (EDC; BioXtra), and 2-(*N*-Morpholino)ethanesulfonic acid (MES; free acid) were purchased from Sigma-Aldrich and used as received. 1,4-Dioxane, n-hexane, toluene, anhydrous diethyl ether and tetrahydrofuran (THF) were purchased from VWR (Radnor, Pennsylvania, USA) and used as received. Milli-Q grade deionized water was prepared using a Barnstead Diamond™ water purification system (Thermo Fisher Scientific, Waltham, Massachusetts, USA). 10x Phosphate buffered saline (PBS) was purchased from BioShop® (Burlington, Ontario, Canada) and diluted with

deionized water to 1x (pH 7.4) for all experiments. All other compounds were purchased from Sigma Aldrich (Oakville, Ontario, Canada) unless otherwise specified.

3.3.2 Poly[N-isopropylacrylamide-co-(acrylic acid)-co-(methyl methacrylate)] (pNAM) Synthesis

The free radical pNAM terpolymers were produced by methods similar to those previously reported [19-21]. The free radical synthetic pathway is depicted in Figure 3.1a). Briefly, 3.8 g (33.6 mmol) of recrystalized NIPAAm, 30 mg (0.4 mmol) uninhibited AA, 170 mg (1.7 mmol) of MMA and 18 mg of BPO (0.1 mmol) were dissolved in a round bottom flask containing 40 mL of 1,4-dioxane:deionized water (9:1 v/v) to produce a 10% (m/v) monomer solution. The molar feed ratio was 80:5:15 (NIPAAm:AA:MMA). The flask was sealed, and oxygen was removed by bubbling the solution with nitrogen for 25 minutes; the reaction was then heated to 70 ℃ for 24 hours under constant stirring. Following polymerization, the polymer solution was exposed to oxygen to terminate the reaction and cooled to room temperature. To remove any unreacted monomers, the polymer solution was precipitated twice into 800 mL of chilled anhydrous diethyl ether, separated by vacuum filtration over a fritted funnel and redissolved in THF between precipitations. The resulting pNAM powder was placed in a vacuum oven to dry overnight before being dialyzed for 3 days against 4L of deionized water using a Membra-Cel® 14 kDa MWCO cellulose membrane (Viskase®, Lombard, Illinois,

USA). The pNAM sample was then lyophilized using a Labconco™ FreeZone 2.5L benchtop freeze drier (Kansas City, Missouri, USA) and stored at -20 ℃. The composition of the pNAM polymers was determined by ^{1}H NMR using a Bruker© 600 MHz Spectrometer, operating at 600.13 MHz and 298 K (Billerica, Massachusetts, USA). Samples were analyzed in DMSO-d_6. The pNAM polymer molecular weights were determined at room temperature using a Polymer Laboratories PL-50 gel permeation chromatograph (GPC; Church Streton, Shropshire, UK) fitted with three Phenomenex Phenogel™ columns; pore sizes 100, 500 and 104 Å (Torrance, California, USA), using dimethylformamide containing 5 mM lithium bromide as the eluent. GPC calibrations were performed using linear polyethylene glycol standards provided by Polymer Laboratories. All samples were filtered through a 0.2 μm PTFE syringe filter prior to quantification.

3.3.3 Chitosan Crosslinked pNAM Networks

The production of covalently crosslinked chitosan-graft-pNAM networks (CCN) followed similar methods to those reported in literature, shown in Figure 3.1b) [25, 33, 34]. Three CCN samples were produced containing 1, 3 and 5% (m/m) chitosan/pNAM. These samples are denoted as 1-CCN, 3-CCN and 5-CCN, respectively. To produce 3-CCN, 90 mg chitosan was first dissolved in 10 mM MES buffer, adjusted to pH 4.7 using 0.1 N NaOH, at 1% (m/v) and mixed for 5 hours at 45 ℃ under constant stirring. Once dissolved, the sample was filtered using a 0.2 μm syringe filter to remove any remaining aggregates. 3 g of pNAM was then

added and allowed to dissolve before the dropwise addition of 862 mg (4.5 mmol) of EDC, which was dissolved in a minimal volume of MES buffer. The solution was reacted for 24 hours at room temperature under constant stirring. The CCN samples were then dialyzed for three days against 4 L deionized water using Spectrum Labs 3.5 kDa MWCO Spectra/Por regenerated cellulose dialysis membrane (VWR, Radnor, Pennsylvania, USA) before being lyophilized and stored at -20 ℃. For polyelectrolyte complexes (PEC) of physically crosslinked chitosan to pNAM via ionic interactions, the same procedure was used but without the addition of EDC.

Infrared spectra of the CCN and PEC polymer networks were run on a Nicolet 6700 Fourier Transform Infrared spectrometer (FTIR; Thermo scientific, Waltham, Massachusetts, USA).

a)

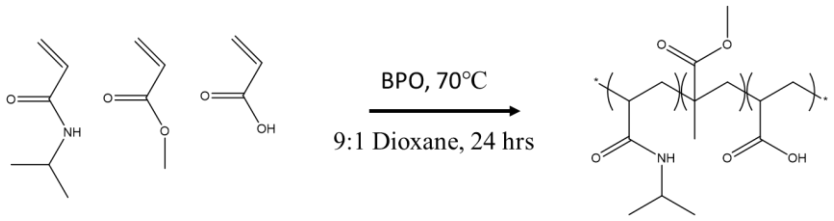

b)

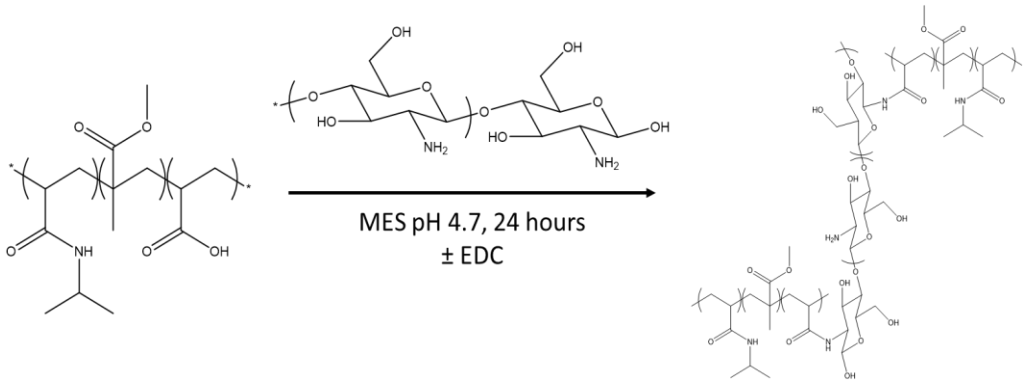

Figure 3.1a) Free radical polymerization of pNAM b) Covalent Crosslinking of pNAM with Chitosan by EDC.

3.3.4 Rheological Analysis

The rheological properties and LCST of polymer samples were determined by a Discovery HR-2 hybrid rheometer (Waters™, Newcastle, Delaware, USA) fitted with a 20 mm parallel aluminum Peltier plate. All samples were dissolved at a concentration of 20% (m/v) in PBS for analysis. Stress sweeps were conducted at 37 ℃ for all samples to determine the range of the linear viscoelastic region (LVE). Temperature ramps were conducted at a rate of 1 ℃/min, ranging from 15-45 ℃, to determine the LCST of polymer samples [14, 35]. The LCST is defined as temperature in which the storage modulus (G') increases above the loss modulus (G'') indicating that the sample is a gel behaving as a viscoelastic solid [36, 37]. Frequency sweeps were conducted at 37 ℃ to determine gel stiffness, the effect of increasing chitosan crosslinking and the effect of grafting chitosan by either covalent conjugation or physical ionic interactions [36].

3.3.5 Equilibrium Water Content

Dry lyophilized polymer samples were dissolved to 20% (m/v) in PBS. The polymer solutions were then weighed (M_l) before being incubated at 37 ℃ for 24 hours. Following incubation any supernatant expelled from the gel was extracted and the samples were carefully blotted dry with tissue paper and the swollen gels

weighed (M_S). The equilibrium water content (EWC) of the thermo-gels was also assessed. The dry polymer mass (M_D) was compared to the swollen gels following supernatant removal. The EWC was determined gravimetrically using equation 3.1.

$$3.1) \quad EWC = \left(\frac{M_S - M_D}{M_S}\right) 100$$

3.3.6 Gravimetric Hydrogel Degradation

Based on their favorable material properties, the degradation of pNAM, 3-CCN and 3-PEC was conducted at 37 ℃. 100 mg polymer samples were dissolved at 20% (m/v) in PBS and subsequently allowed to gel for 1 hour. Following the initial incubation time, any supernatant was extracted, and the swollen samples were weighed (M_I). The gels were then incubated with either 0.5 mL PBS as a control or PBS containing 1.4 mg/mL hen egg white lysozyme to simulate the physiological protein concentration [38]. At predetermined time intervals, the supernatants were extracted, and the remaining gels weighed (M_W) to determine the degradation by mass loss. The degradation of the polymer samples was then calculated by equation 3.2.

$$3.2) \quad Mass\ Remaining\ (\%) = \left(\frac{M_W}{M_I}\right) 100$$

3.3.7 Drug Release

100 mg samples of pNAM, 3-CCN and 3-PEC were dissolved at 20% (m/v) in PBS containing 0.35 mg/mL Ketotifen Fumarate (KF). The unstirred samples were then gelled at 37 ℃ and allowed to swell for 1 hour before the addition of 0.5 mL pre-warmed PBS (pH 7.4) supernatant release medium to yield sink conditions. 200 µL aliquots were removed at set time intervals and replaced with an equal volume of release medium. Following collection, the samples were frozen and subsequently lyophilized. The amount of KF released was analyzed by an Agilent 1260 Infinity II high performance liquid chromatographer (HPLC; Santa Clara, California, USA). The mobile phase consisted of 60:40 10 mM ammonium acetate (pH 3.5): methanol (HPLC grade) and was passed over a Pall® Life Sciences 0.45 µm nylon filter (Port Washington, New York, USA) prior to use [39]. Freeze dried samples were dissolved in 10 mM ammonium acetate (pH 3.5) and passed through a 0.2 µm Nylon filter (Agilent) prior to HPLC quantification. The concentration values determined were assessed against a KF calibration curve with a wavelength maximum of 300 nm. The percent cumulative release of KF was determined as the cumulative mass of KF released at a set time interval to the total mass of KF loaded.

The first 60% of the release profiles of KF from the thermo-gels were fitted to the Ritger–Peppas and Korsmeyer–Peppas (Power law) model [40-42]. The semi-empirical model is shown in equation 3.3.

$$\frac{M_t}{M_\infty} = kt^n \quad (3.3)$$

Where M_t/M_∞ is the cumulative fractional drug release, *t* is time, *k* the release velocity constant and *n* the exponent of release.

3.3.8 *In Vitro* Cytotoxicity Assays

Human corneal epithelial cells (HCECs) were cultured in keratinocyte serum free medium (Gibco™, Thermo Fisher Scientific) containing 25 mg of bovine pituitary extract and 2.5 µg human recombinant epidermal growth factor (Thermo Fisher Scientific) at 37 ℃ and 5% CO_2. The culture medium was changed every 2 days with cells reaching confluence after 7 to 10 days. The cells were passaged at 80-90% confluence.

The cytotoxicity of pNAM, 3-CCN and 3-PEC polymers was assessed using an MTT assay [43]. HCECs were plated into 96-well microtiter plates at a density of 20,000 cells/well. After 24 hours, the culture medium was replaced with 200 µL of medium containing pNAM, 3-CCN or 3-PEC (n=4) at a concentration of 1% (m/v), passed through a 0.2 µm syringe filter and UV treated for minimum 12 hours prior to cell exposure. A thermo-gel concentration of 1% (m/v) was used to prevent film formation over the cells, which can negatively affect metabolic activities. Fresh medium served as a control. To assess acute toxicity, after 24 or 48 hours, the gel and media were removed, and the cells washed gently with PBS. The negative control was produced by incubating cells with 0.25% (v/v) Triton X-100 for three minutes after which the surfactant was removed, and the cells washed three times with PBS. 3-(4,5-dimethylthiazol-2-yl)-2,5-diphenyltetrazolium bromide (MTT)

powder was first dissolved to 5 mg/mL in sterile PBS. 100 µL of medium containing 10% (v/v) MTT solution was added to each well. After 3 hours, any unreacted MTT was removed and replaced with 200 µL of DMSO for 15 minutes. The cell viability was quantified by a SpectraMax® ABS Plus UV-vis micro-plate reader (Molecular Devices, San Jose, California, USA) at a wavelength of 570 nm. Cell viability was calculated by absorbance using equation 3.4.

$$3.4) \quad Cell\ Viability = \frac{Abs_{sample}}{Abs_{control}}$$

Polymer cytotoxicity was also assessed by Live/Dead staining. Cells were plated and treated as described above for 24 hours. The cells were then stained with a calcein-AM/ethidium homodimer-1 fluorescence kit (Thermo Fisher Scientific) and visualized with an Olympus IX51 inverted fluorescent microscope (Shinjuku, Tokyo, Japan). The viability of treated cells was assessed following visualization using open-source ImageJ (NIH) software to count the fluorescently stained cells.

3.3.9 *In Vivo* Safety Analysis

Animal studies were performed in compliance with protocols approved by the Animal Research Ethics Board at McMaster University in accordance with the regulations of the Animals for Research Act of the Province of Ontario and the guidelines of the Canadian Council on Animal Care. Five, 9-month-old female Brown Norway Rats (Charles River, Wilmington, Massachusetts, USA) were utilized to test the *in vivo* compatibility of pNAM, 3-CCN and 3-PEC gels. The rats

were anesthetized with gaseous isoflurane before the application of 10 µL of pNAM, 3-CCN, 3-PEC or PBS as a control to both eyes of one rat. The thermo-gel samples were UV treated for 12 hours prior to application. The samples were allowed to gel against the surface of the rat eyes for a minimum of a half hour prior to the reversal of anaesthesia and the onset of blinking. After 24 hours, the rats were euthanized, and the eyes were harvested and fixed in 4% paraformaldehyde overnight at 4 ℃ and then stored in 70% ethanol. Samples were processed (Core Histology Department, McMaster University) and embedded in paraffin (Paraplast Tissue Embedding Media, Thermo Fisher Scientific). Finally, serial sections were cut to 4 µm in thickness and used for hematoxylin and eosin (H&E) staining and visualized with an Olympus BX51 inverted microscope. Corneal thickness measurements were taken from H&E-stained slides using ImageJ software.

3.3.10 Statistical Analysis

Error bars represent the standard deviation (SD) of n=3 except for *in vitro* cell studies which utilized an n=4. Single factor analysis of variance (ANOVA) followed by Tukey or Dunnett's post-hoc analysis, Two-Way ANOVA or Student's t-test based on two tailed distribution and unequal variance was used to determine statistical significance for material/rheological properties, degradation, and cytotoxicity analysis.

3.4 Results

3.4.1 Synthesis and characterization of pNAM

The ^{1}H NMR spectrum of pNAM, shown in Figure 3.2), was used to determine the molar composition of the polymer. The tertiary NH associated with the isopropyl tail of the NIPAAm units is present at 3.84 ppm (A), the hydroxyl group of AA at 12 ppm (B) and the methyl tail of MMA as a doublet at 3.54 and 3.50 ppm (C). The free radical polymerization of pNAM was found to be highly reproducible with a molar composition of 80.28 ± 0.07, 4.10 ± 0.06 and 15.61 ± 0.08 of NIPAAm:AA:MMA across all 9 batches. The GPC analysis of pNAM terpolymers determined that the average polymer molecular weight was 61,500 ± 5,300 g/mol across all pNAM batches with a polydispersity index of 2.8 ± 0.1.

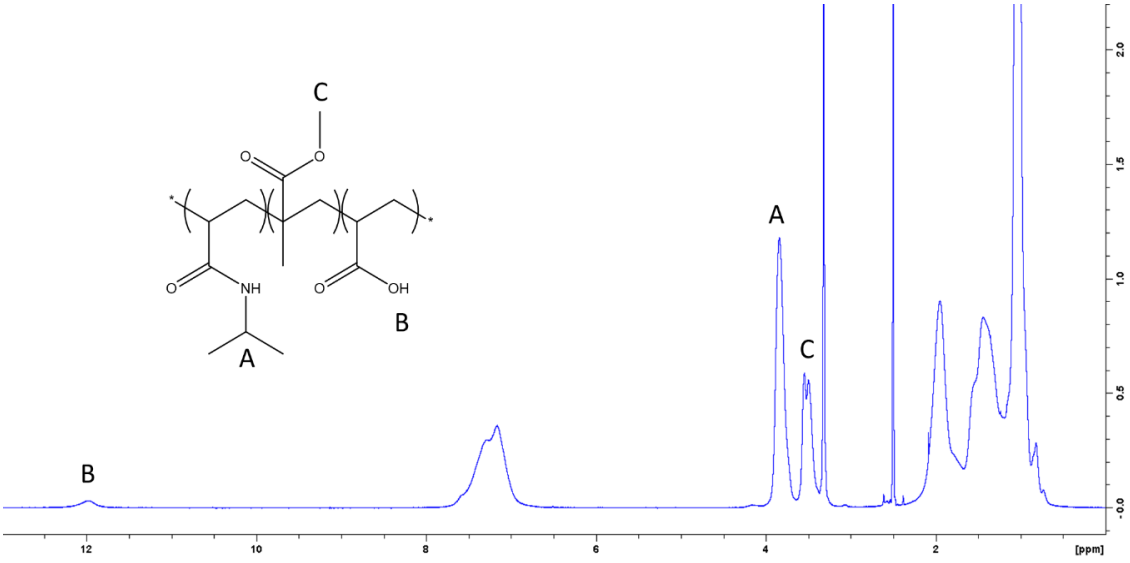

Figure 3.2) ^{1}H NMR analysis of pNAM.

3.4.2 Synthesis and characterization of chitosan crosslinked pNAM

Hydrogel compositions were characterized by FTIR analysis with a wavenumber range of 400 to 4000 cm^{-1}. The FTIR spectra for chitosan, pNAM, 3-CCN and 3-PEC are shown in Figure 3.3. The pNAM control spectra shares some peaks with chitosan because of the nature of the NIPAAm monomer: 3300 cm^{-1} (NH stretch), 1640 cm^{-1} (C=O stretch, amide I) and 1530 cm^{-1} (NH bend, amide II). Incorporation of AA is seen at 1730 cm^{-1} (carbonyl C=O stretch) and MMA at 1171 cm^{-1} (ester C-O) and 1130 cm^{-1} (unconjugated ester -CO-O-CH_3 stretch) [44]. With the 3-CCN and 3-PEC samples, two new subtle peaks are observed at 1077 and 1039 cm^{-1} which reflect the slightly shifted C-O-C and C-O stretches of the incorporated chitosan, respectively. However, the signal change is very small so additional characterization methods were used to confirm the incorporation of chitosan.

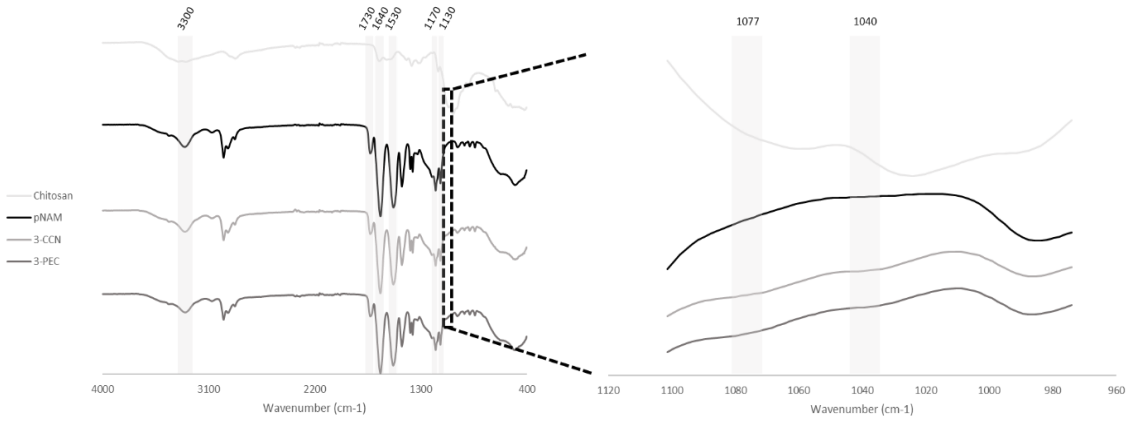

Figure 3.3) FTIR spectra of Chitosan, pNAM, 3-CCN and 3-PEC thermo-gels. Peaks corresponding to chitosan incorporation are highlighted and magnified.

The crosslinking of pNAM with chitosan was accomplished by either the covalent conjugation of carboxylic acid groups in pNAM to the primary amines of chitosan via EDC chemistry or by physical ionic interactions of those same species without the addition of EDC. Due to the pH and thermo-sensitive nature of pNAM, the incorporation of chitosan affects the pH of polymer network solutions. pH measurements for the polymer networks dissolved at 20% (m/v) in PBS are shown in Table 3.1. The pNAM base polymer had a pH of 4.37 when dissolved in solution, reflecting the pKa of acrylic acid. With the addition of chitosan, the pH of solution increased regardless of whether the chitosan was incorporated through covalent or ionic means. The incorporation of chitosan by EDC conjugation results in a linear (R^2 = 0.995) increase of solution pH with chitosan concentration. The concentration of EDC used scaled directly with the concentration of chitosan incorporated into the CCNs. Greater amounts of chitosan presumably led to a higher number of carboxylic acid units reacted from pNAM, with steric limitations. The pH of 6.5 which is seen with 5-CCN theoretically represents the highest pH that can be achieved with chitosan before it is precipitated out of solution [45]. Without the addition of EDC, the blending of chitosan and pNAM creates polyelectrolyte complexes [46]. It can be seen from the samples 3-CCN and 3-PEC that the use of EDC conjugation results in a higher solution pH than the natural ionic interactions as expected because EDC conjugation allows for the actual reaction of the carboxylic acid groups in pNAM and any unreacted groups remain available for ionic interactions.

Table 3.1) pH measurement of thermo-gel networks dissolved in PBS.

Polymer Network	Batch pH
pNAM	4.37 ± 0.2
1-CCN	4.94 ± 0.1
3-CCN	5.68 ± 0.1
3-PEC	5.03 ± 0.0
5-CCN	6.51 ± 0.1

3.4.3 Rheological Results

Rheological analysis of pNIPAAm samples is difficult because of the weak hydrophobic/hydrophilic interactions between polymer chains that are present during physical gelation [47, 48]. The strain sweeps of control pNAM, all CCN and 3-PEC samples are shown in Figure 3.4. The hydrogel samples failed after an applied oscillation strain of greater than 10%, so an oscillation strain of 0.1% was used for all subsequent rheological testing as it was well within the linear viscoelastic region of all the samples.

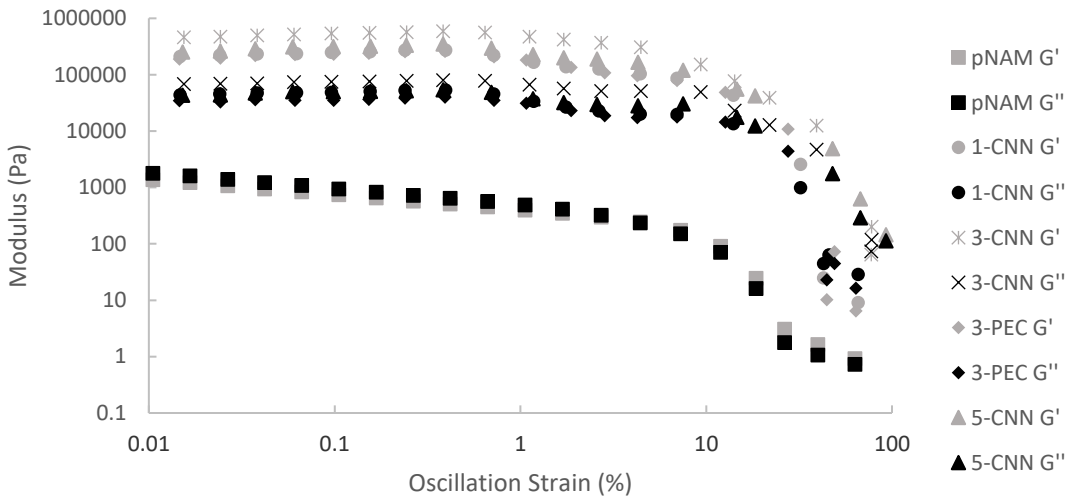

Figure 3.4) Stress Strain Analysis of pNAM, 1-CCN, 3-CCN, 3-PEC and 5-CCN polymer networks.

The LCST of base pNAM and covalently crosslinked networks containing 1, 3 and 5% (m/m) chitosan were tested; the results are shown in Figure 3.5a). The base pNAM polymer had an LCST of 21.0 ± 0.6 ℃, notably lower than the volume phase transition temperature of 27 ℃ reported by Okudan and Altay determined by gravimetric analysis for pNAM of the same molar composition [49]. It can be seen from Figure 3.5a) that the LCST increases with the amount of covalently conjugated chitosan, as was expected. The LCST comparison between covalently crosslinked networks and polyelectrolyte complexes of chitosan and pNAM is shown in Figure 3.5b). Both 3-CCN and 3-PEC have a higher LCST than the base pNAM polymer. Predictably, 3-PEC has a slightly higher LCST when compared to 3-CCN as the blended polymers contain more hydrophilic groups compared to the

case of covalent grafting. The change in LCST of the hydrogels prepared, based on the incorporation of chitosan, was significant ($p < 0.05$) between all groups except for 3-CCN and 5-CCN.

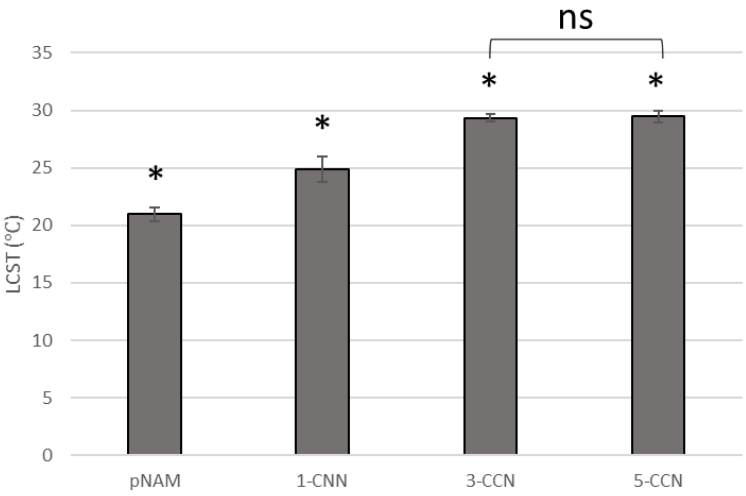

a)

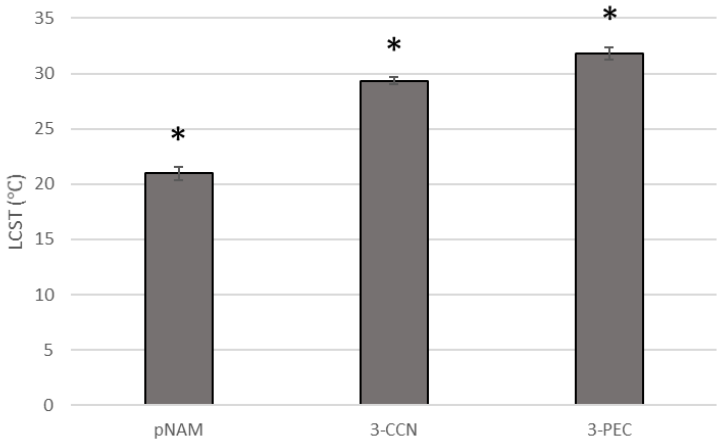

b)

Figure 3.5) LCST determination of a) Covalently crosslinked networks of varying chitosan concentration, statistical significance amongst LCST means except between 3-CCN and 5-CCN and b) Covalent Vs physical ionic incorporation of chitosan, statistical significance amongst LCST means. Data presented as mean ± SD (n = 3), significance determined by

single factor ANOVA analysis followed by Tukey post-hoc analysis. '*' indicates significant difference ($p < 0.05$) and 'ns' indicates no significant difference ($p > 0.05$).

Frequency sweeps were used to determine the effect of chitosan concentration and incorporation on material properties, either by covalent conjugation or physical ionic interactions. The frequency sweeps of pNAM, all CCN and 3-PEC samples are shown in Figure 3.6a). Figure 3.6b) shows the relationship between G' and G'' at a constant angular frequency of 1 rad/s. Examining the frequency sweeps at a lower set angular frequency, such as 1 rad/s, allows for direct comparison of moduli values. Control pNAM samples had very low G' and G'' results with high error, reflective of the weak hydrophilic/hydrophobic interactions between polymer strands [47]. The incorporation of chitosan resulted in higher moduli among all samples with 40-85x higher storage and 25-35x higher loss moduli in comparison to the pNAM control. The higher the concentration of chitosan added, generally the higher the measured storage and loss moduli. The loss moduli of all chitosan crosslinked thermo-gels was significantly higher ($p < 0.05$) when compared to the base uncrosslinked pNAM. Importantly, due to the high absolute error of some of the chitosan crosslinked thermo-gels storage moduli, only 5-CCN was significantly different compared to base pNAM. It is important to note the high storage and loss moduli of 3-PEC, similar to 3-CCN, it would be expected that the covalently conjugated chitosan would have a greater

modulus in comparison to the polymer network based on ionic interactions, due to the higher relative strength of the bonds.

With the storage and loss modulus for a given polymer the damping factor, δ, can be determined by equation 3.5.

$$3.5) \quad tan\delta = \frac{G''}{G'}$$

The damping factor is another comparative tool for examining the physical properties of the polymer networks. When the damping factor approaches 0° the material acts ideally elastically and as the damping factor approaches 90° the polymer behaves ideally viscous. The pNAM control and 3-CCN have damping factors of 41° implying the materials are more viscous when compared to 1-CCN, 3-PEC and 5-CCN which have damping factors of 24°, 25°, and 22°, respectively. It is important to note that 3-CCN, despite the covalent conjugation, is more viscous than the ionically crosslinked 3-PEC. Along with the intermediate LCST, the slightly more viscous nature of 3-CCN is desirable for spreading and comfort when applied to the inferior fornix. Therefore, 3-CCN and 3-PEC were selected for subsequent thermo-gel testing including degradation, drug release and cytotoxicity testing.

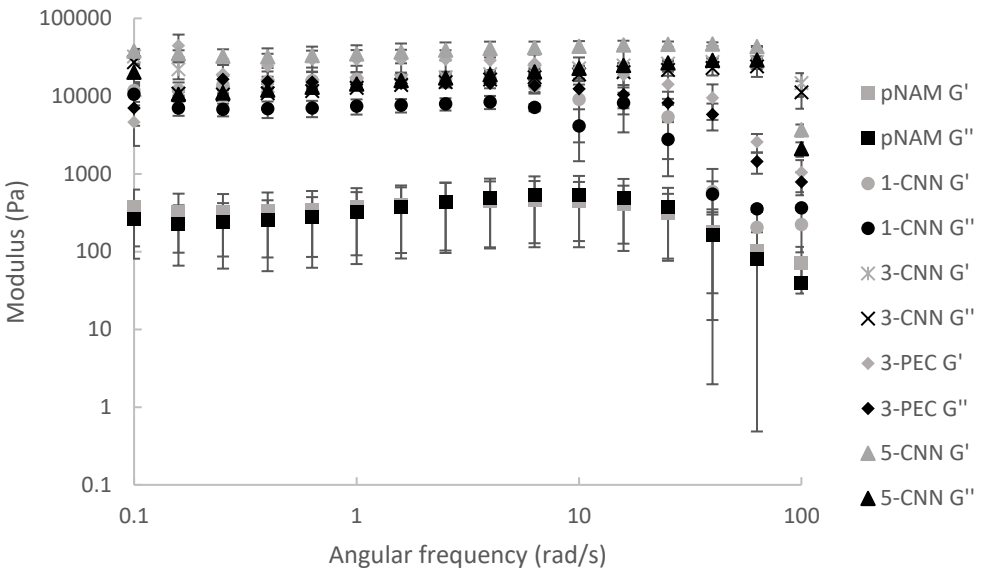

a)

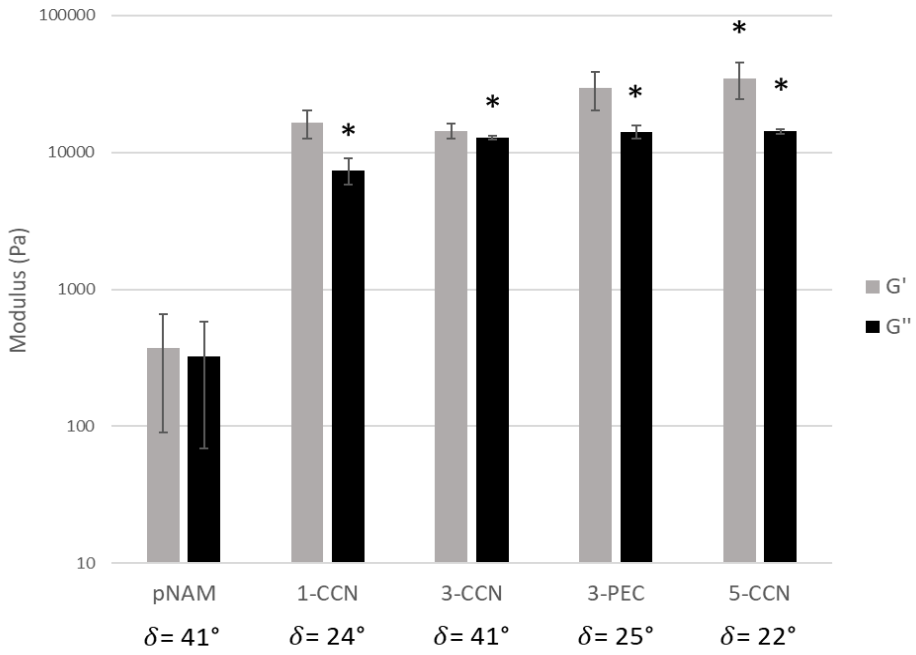

b)

Figure 3.6a) Thermo-gel frequency sweep analysis of pNAM, 1-CCN, 3-CCN, 3-PEC and 5-CCN polymer networks b) Thermo-gel moduli and damping factor (δ) comparison at 1 rad/s of pNAM, 1-CCN, 3-CCN, 3-PEC and 5-CCN polymer networks. Increase of minimum 25x for modulus values following crosslinking either by covalent conjugation or

physical interaction. For storage moduli, only 5-CCN is significantly higher from base pNAM while for the loss moduli, all chitosan crosslinked networks display a significant increase compared to base pNAM. Data presented as mean ± SD (n = 3), significance determined by single factor ANOVA analysis followed by Dunnett's post-hoc analysis comparing the chitosan crosslinked thermo-gels to the base pNAM. '*' indicates significant difference ($p < 0.05$).

3.4.4 EWC

The EWC of the polymer networks are shown in Figure 3.7. The crosslinking of pNAM with chitosan results in a thermo-gel which undergoes a slight change in volume upon gelation, where all crosslinked networks retain greater than 80% of water content upon gelation. The mass of water retention of the swollen polymer, at a solution concentration of 20% (m/v), is a minimum of 10x higher with the incorporation of chitosan. The high EWC is consistent with previously published work on chitosan crosslinked thermo-gels [26, 50, 51]. All chitosan crosslinked thermo-gels had a significant ($p < 0.05$) increase in EWC compared to base pNAM. Amongst crosslinked thermo-gels there was no significant difference in EWC except between 1-CCN and 5-CCN.

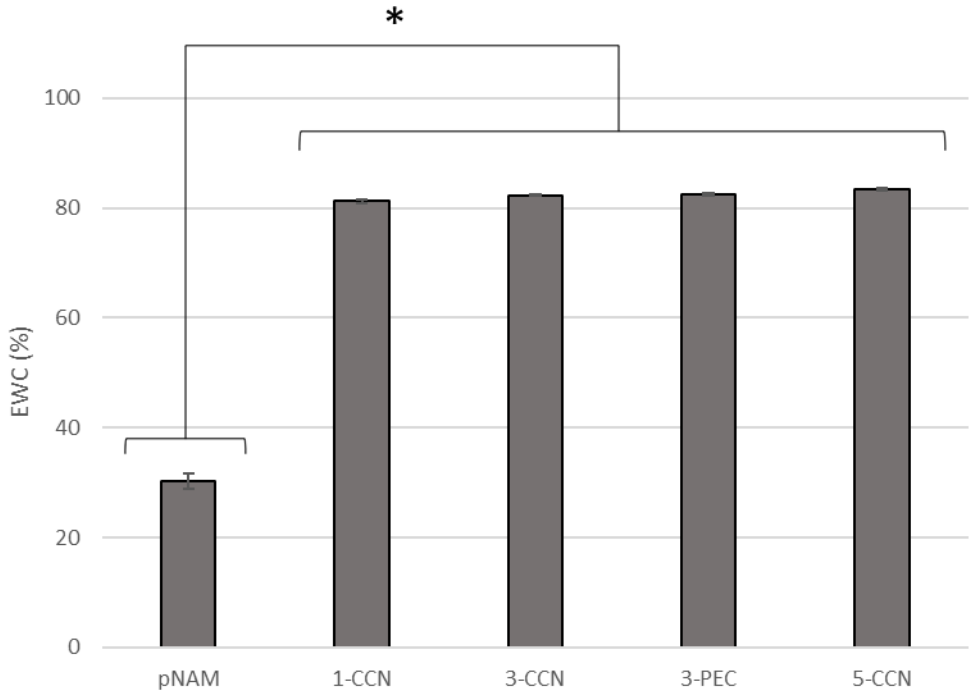

Figure 3.7) EWC of pNAM, 1-CCN, 3-CCN, 3-PEC and 5-CCN thermo-gels. All water swollen crosslinked networks had significantly higher water content than the uncrosslinked base pNAM. Data presented as mean ± SD (n = 3), significance determined by single factor ANOVA analysis followed by Tukey post-hoc analysis. '*' indicates significant difference ($p < 0.05$).

3.4.5 Aqueous Polymer Degradation

Since chitosan has been shown to be degraded in the presence of lysozyme, the impact of the enzyme on the gels was studied. Figure 3.8 shows the degradation of pNAM, 3-CCN and 3-PEC over time in the presence or absence of lysozyme (abbreviated to Lys on graph). Despite the gel mechanical strength, the ionic interactions of 3-PEC hydrogels were quickly degraded in the aqueous

environment, over a period of approximately 24 hours. Comparatively, the base pNAM thermo-gel degraded over 60 hours. The 3-CCN samples degraded over a period of 96 hours in the aqueous environment, four times longer than 3-PEC and over 1.5 times longer than pNAM. No statistical difference was observed for the chitosan containing thermo-gels 3-CCN, or 3-PEC for degradation with or without the enzyme lysozyme.

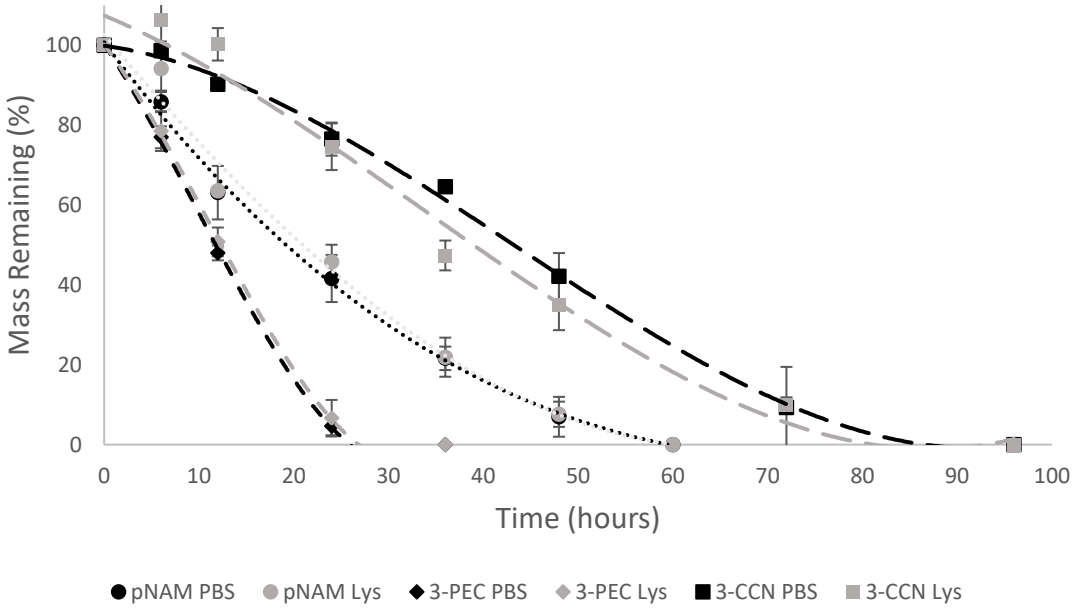

Figure 3.8) Degradation of pNAM, 3-CCN and 3-PEC thermo-gels incubated with and without lysozyme (Lys) over 96 hours. No statistical difference in any group for degradation with or without lysozyme. All data sets fitted with a cubic trendline. 3-CCN thermo-gels outlasted uncrosslinked pNAM or 3-PEC. Data presented as mean ± SD (n = 3), significance determined by Two-Way ANOVA with $\alpha = 0.05$.

3.4.6 Drug Release

The release of KF from base pNAM polymer, 3-CCN and 3-PEC over seven days, shown in Figure 3.9, demonstrated that more drug is released from 3-PEC hydrogels, 59.5 ± 0.5%, compared with the base pNAM or 3-CCN at 50.2 ± 2.5% and 43.3 ± 5.5% respectively. This result was expected as 3-PEC degrades more quickly than the other hydrogels. 3-CCN released the lowest amount of KF over the testing period as expected based on degradation profiles. In all cases, the controlled release of KF observed from the thermo-gels represents a significant improvement of the burst noted with conventional topical eyedrops.

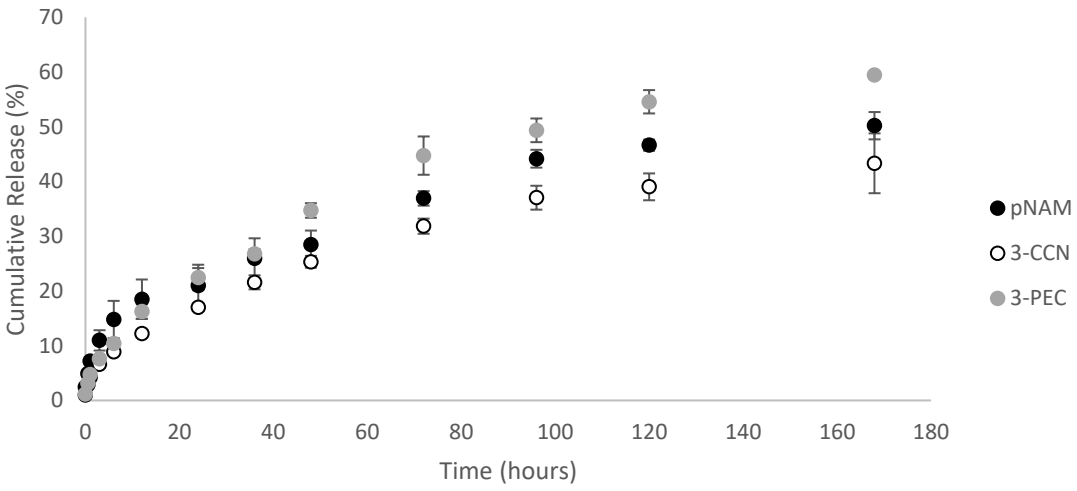

Figure 3.9) Release of Ketotifen Fumarate from pNAM, 3-CCN and 3-PEC thermo-gels over 168 hours, measured by HPLC. Overall, 3-CCN releases less Ketotifen Fumarate compared to pNAM and 3-PEC. Data presented as mean ± SD (n = 3).

The results of the fitting of the first 60% of the observed KF release profiles to the Ritger–Peppas and Korsmeyer–Peppas model is summarized in Table 3.2. The determined exponent of release, n, is utilized to characterize the transport phenomena of the drug through the hydrogel. For release from cylindrical hydrogels, the transport phenomena can be classified into four cases: for n = 0.45 (Case 1) the release is governed by Fickian diffusion, when 0.45 < n < 0.89 the driving force is anomalous transport or non-Fickian and drug transport diffusion and are comparable, n = 0.89 describes non-Fickian zero-order release (Case 2) governed by hydrogel swelling and polymer relaxation, and n > 0.89 Super Case 2 where the drug release rate is a function of hydrogel crazing [40, 42, 52]. For the base pNAM the mechanism of drug release is Fickian diffusion. For the chitosan crosslinked 3-CCN and 3-PEC the release of KF from the hydrogels is found to be a function of diffusion and swelling.

Table 3.2) Model Fitting of KF Release Profiles.

Thermo-gel	**k**	**n**	**R^2 (%)**
pNAM	0.070 ± 0.007	0.37 ± 0.04	97.3 ± 0.3
3-CCN	0.040 ± 0.001	0.46 ± 0.01	99.6 ± 0.2
3-PEC	0.045 ± 0.004	0.51 ± 0.02	98.8 ± 0.5

3.4.7 *In Vitro* Cytotoxicity

The cytotoxicity of the pNAM, 3-CCN and 3-PEC polymers as determined by MTT assay is shown in Figure 3.10. From the MTT assay it can be determined that the thermo-gelling polymers had low cytotoxicity. At the 24 and 48-hour time points, the 3-CCN and 3-PEC samples were not significantly different from the negative control ($p > 0.05$). Notably, the pNAM base polymer yielded a significantly higher cell viability ($p < 0.05$) than the negative control or 3-CCN and 3-PEC samples suggesting the cell-gel interactions are favorable for growth in the given conditions.

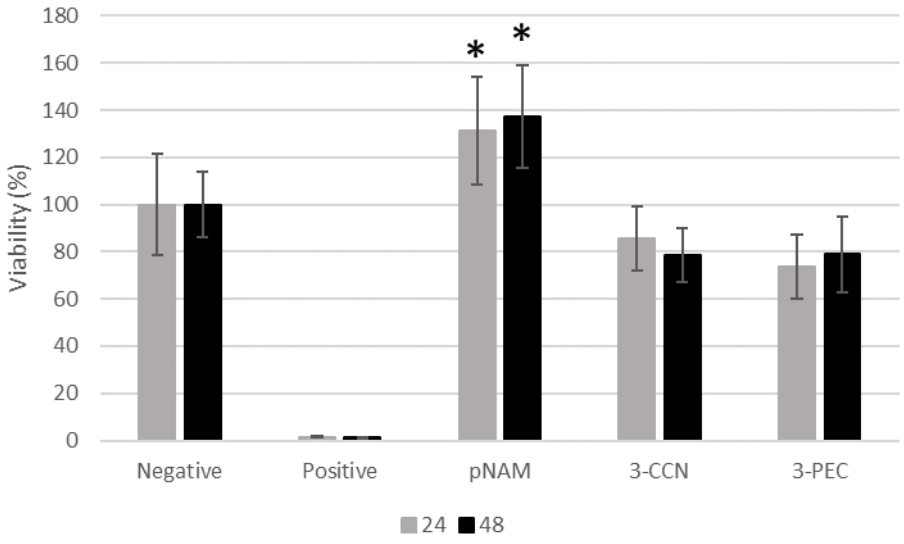

Figure 3.10) MTT Cytotoxicity Assay of pNAM, 3-CCN and 3-PEC thermo-gels after 24 and 48 hours of incubation. Uncrosslinked pNAM gels produced a significantly higher viability compared to negative control over 24 and 48 hours. 3-CCN and 3-PEC gels were not significantly different from negative controls at 24 or 48 hours. Data presented as mean

± SD (n = 4), significance determined by single factor ANOVA analysis followed by Dunnett's post-hoc analysis comparing the thermo-gels to the negative control. '*' indicates significant difference ($p < 0.05$).

The response of HCEC cells following thermo-gel treatment is visualized in Figure 3.11a) with Live/Dead staining. It is important to note that following incubation with 3-CCN, visually the cell morphology is more spherical compared to the other gel and control samples. The number of Live/Dead fluorescently stained cells was quantified, and the viability is shown in Figure 3.11b). pNAM and 3-PEC treated cells resulted in a viability which was not significantly different from the negative control ($p > 0.05$). 3-CCN treated cells had a significantly lower viability compared to negative control. The morphology and wide distribution of cellular viability suggests that the cells are in a more stressed state following treatment with 3-CCN which reflects a change in cellular transport phenomena as the cells are covered by the covalently crosslinked thermo-gel.

a)

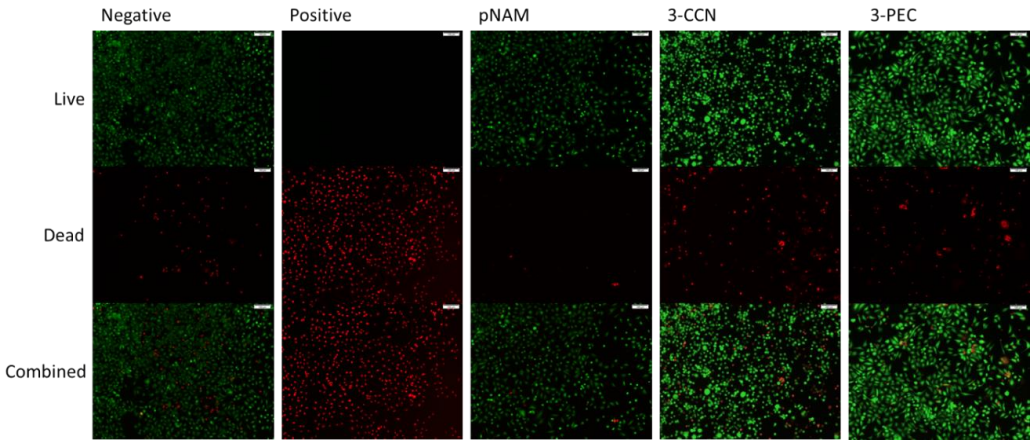

b)

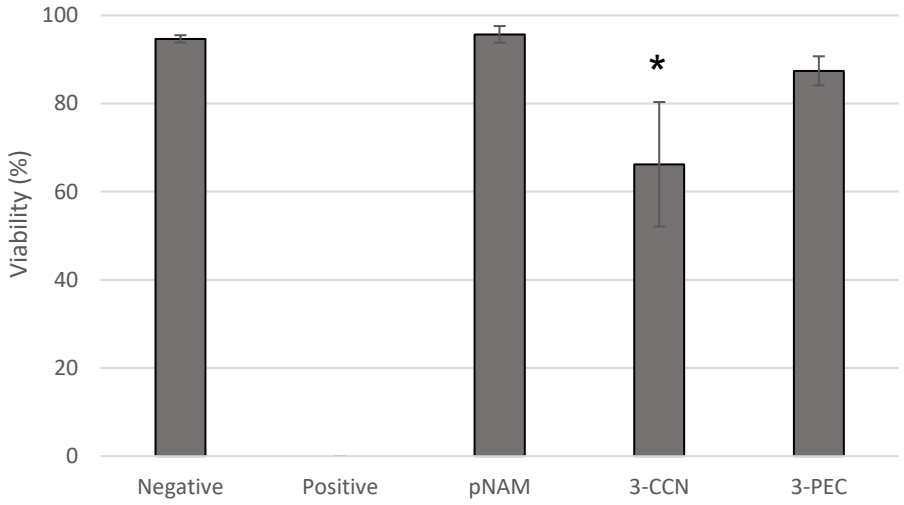

Figure 3.11a) Live/Dead Staining of HCEC gels with pNAM, 3-CCN and 3-PEC thermo-gels after 24 hours. The morphology of HCECs was more spherical after incubation with 3-CCN suggesting some degree of cellular stress. Scale bars represent 100 µm and b) Cell viability determined by Live/Dead Staining. pNAM and 3-PEC thermo-gels did not result in a significant change in cell viability compared to negative control. The viability of cells treated with 3-CCN were significantly lower compared to negative control. Data presented as mean ± SD (n = 4), significance determined by single factor ANOVA analysis followed by Dunnett's post-hoc analysis comparing the thermo-gels to the negative control. '*' indicates significant difference ($p < 0.05$).

3.4.8 *In Vivo* Cytotoxicity

The effect of the thermo-gels on rat corneas was assessed by H&E staining (Figure 3.12). From the histological staining, it is observed that there is no difference in inflammation or appearance of inflammatory cells in the cornea and anterior chamber between PBS treated controls (12A, B) and thermo-gel treated

(12C-H) rats after 24 hours. Based on measurement of the corneal epithelium, stroma, and Descemet's membrane and endothelium, there was no apparent difference in morphology of control corneas or those treated with pNAM, 3-CCN or 3-PEC thermo-gels. From these results, the thermo-gels do not produce an inflammatory response or induce morphological change from short term application.

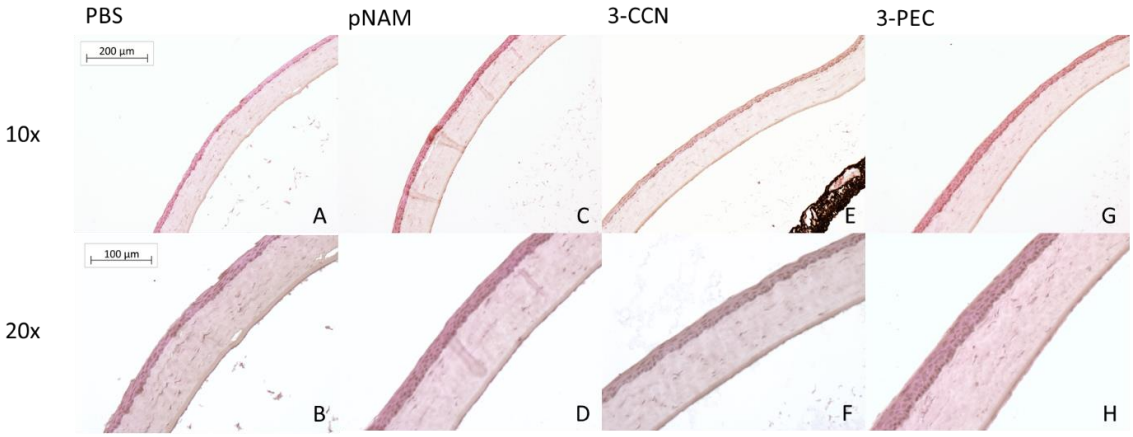

Figure 3.12) Histological H&E staining of Brown Norway Rat Corneas following 24-hour incubation with pNAM, 3-CCN and 3-PEC thermo-gels. Top row 10x objective magnification, scale bars represent 200 µm. Bottom row 20x objective magnification, scale bars represent 100 µm. No observable difference in corneal inflammation or morphology following short term thermo-gel treatment.

3.5 Discussion

It was hypothesized that the crosslinking of pNAM with chitosan, by either covalent conjugation or ionic interaction, would raise the thermo-gels LCST due to

the hydrophilicity of chitosan. Therefore, a base polymer with a lower LCST was used to maximize the amount of chitosan that could be incorporated, which has not been previously investigated in the literature. Okudan and Altay developed a series of pNAM gel terpolymers, with and without *N*-tertbutylacrylamide crosslinker [49]. Due to its documented use and ease of incorporation, MMA was chosen as the hydrophobic monomeric component of the polymer to lower the LCST. It is important to note, with the incorporation of AA directly into the polymer backbone, the base pNAM polymer is both a pH and thermo-sensitive polymer [53-55]. When dissolved in solution at 20% (m/v), pNAM has a pH of 4.37, reflecting the pKa value of acrylic acid.

By synthesizing pNAM, a base polymer in which the carboxylic acid units are distributed along the polymer chain, we were able to investigate and compare for the first time the properties of chitosan incorporation either as a PEC or CCN. Most studies that graft chitosan on pNIPAAm chains, particularly in the ophthalmic space, use a synthetic scheme in which pNIPAAm chains are end-capped with a carboxylic acid rather than incorporating carboxylic acid units throughout the polymer backbone [25, 26, 29, 56]. The end-capped pNIPAAm polymer chains are then covalently grafted to chitosan by use of a carbodiimide. By synthesizing pNAM, wherein the carboxylic acid groups are incorporated throughout the polymer backbone, there will be an intrinsic difference in both base polymer properties and the hydrogel properties, once crosslinked with chitosan. By incorporating carboxylic acid moieties along the polymer, both chitosan and pNAM

can be conjugated anywhere along their polymer chains, limited only by carbodiimide concentration, amine/carboxylic acid concentration and steric hinderance. This contrasts with end-capped pNIPAAm which can only be conjugated at those terminal moieties. Therefore, it is hypothesized that these chitosan-pNAM hydrogels will be stiffer due to the higher degree of possible conjugation between the two polymer chains compared to hydrogels produced from end-capped pNIPAAm. Unlike hydrogels based on end-capped pNIPAAm, the resulting chitosan-pNAM will be pH-sensitive based on the concentration of unreacted carboxylic acid groups on the polymer backbone. For application to the anterior of the eye, a solution pH > 4, and as close to neutral as possible is required to avoid irritation. For instance, antibiotic Ofloxacin eyedrops have a pH of 4.5 which have been documented to cause a burning or stinging sensation with some users [57]. Experiments demonstrated that, importantly, the pH of all polymer networks could be adjusted with base to a pH of approximately 6.5 before chitosan precipitation.

By reacting a higher number of the primary amines, and neutralizing those remaining by ionic interactions, chitosan becomes a predominantly hydrophilic crosslinker and therefore raises the LCST of the system. There are conflicting reports on the LCST of chitosan grafted with end-capped pNIPAAm. Cao et al. [29] noted a decrease in the LCST with the inclusion of chitosan while Rejinold et al. [56] noted a nonlinear increase of LCST with varying concentrations of chitosan. The LCST of the hydrogels is a function of solution concentration, degree of

grafting and chitosan properties. Luo et al. [26] demonstrated an increase in LCST corresponding to an increase of the DDA of chitosan grafted with end-capped pNIPAAM. For application to the inferior fornix of the eye, the thermo-gel must be able to withstand temperatures which are slightly below physiologic, as low as 34 ℃ at the surface of the eye, up to 37 ℃ [25]. From the LCST data, all the thermo-gels produced were suitable, with LCSTs below 34 ℃. From this data, a nonlinear increase in LCST was observed.

For material degradation, shown in Figure 3.8, the 3-CCN gels lasted longer than pNAM and 3-PEC respectively. This result was expected due to the stronger covalent bonds holding the thermo-gels together. For application to the anterior of the eye, gel survival for 4 days marks a vast improvement compared to conventional, daily use eyedrops. Ideally, the thermo-gels should last for as long as possible in order to alleviate the need for reapplication and delivery the most sustained release of the loaded drug. As can be seen from the Figure 3.8, the 3-CCN samples initially gain mass as the gels swell in supernatant. This swelling effect, as well as the shear effect encountered with supernatant removal and replacement, may cause rapid mechanical degradation of the crosslinked thermo-gels. Since mechanical forces are a significant factor in the inferior fornix of the eye with globe movement and tear renewal/drainage, it is hypothesized that these gels will undergo a similar timescale of degradation in this environment [30].

Importantly, the driving force for thermo-gel degradation was not the enzymatic action of lysozyme, as has been reported in other chitosan crosslinked

materials [25, 26]. This result was corroborated by rheologic measurement of the thermo-gels after incubation with lysozyme (Supplementary Figure 3.S-1). Lysozyme is the highest concentration tear enzyme at 1.4 mg/mL [38] and enzymatically degrades chitosan based on its material properties. The chitosan used in this study had a low DDA of 70% and a low molecular weight of 10-50 kDa, both of which are attributes that theoretically promote enzymatic breakdown of chitosan by lysozyme. However, the pattern of chitosan repeat units is also a crucial attribute as lysozyme docking has been described to only occur on sites with a minimum of three sequential acetylated units [11, 58]. It is hypothesized that with the high degree of polymer interaction with our chitosan-pNAM, as well as the low molecular weight of chitosan utilized, lysozyme was unable to effectively interact with the bound chitosan to degrade it. Future studies will seek to determine the impact of chitosan with different properties on the enzymatic degradation of chitosan-pNAM thermo-gels.

For the release of KF, shown in Figure 3.9, an increase in the release profiles were observed with the pNAM and 3-PEC, corresponding to times of major hydrogel breakdown (occurring at approximately 72 hours) previously shown by the aqueous degradation studies, Figure 3.8. From modeling of the release rates, (up to 48 hours) it was found that pNAM was governed by Fickian diffusion while 3-CCN and 3-PEC was governed by diffusion and swelling. This result was expected based on the swelling and degradation profiles of the thermo-gels as 3-CCN and 3-PEC continually absorb water which affects the drug release profile.

The Power Law model was utilized to fit the experimental release data since in this study because it is often applied to hydrogel systems (compared to the Higuchi model) to determine the mechanism of release. In this study, cylindrical thermogels were utilized for drug release and this geometry was reflected during the interpretation of the Power Law model fitting. Future studies will seek to fit other drug models specifically for hydrogel modeling. The Hopfenberg model is utilized for erosive polymeric systems although the dimensions of the formulation must be known which is difficult to measure with thermogels following syneresis.

The release of KF from 3-CCN represents the most optimal profile by yielding the most sustained release with the longest degradation profile. As the hydrogels erode and disperse into the supernatant, the solution became turbid with thermo-gel particles which continue to release drug. This phenomenon accounts for the drug releases being longer than the measured degradation times and is a limitation of the *in vitro* drug release. Under physiological conditions, these small soft particles produced through gel degradation would be removed by tear drainage without causing patient discomfort. Another factor to consider is that KF, a weak base, has been shown to interact with chitosan [59, 60]. For this reason, the release of Ketotifen Fumarate from chitosan-containing hydrogels or charged polymers may be heavily based on the degradation profile of the gel, which theoretically accounts for the 40-60% of unreleased KF observed in this study. For this study, sink conditions were utilized for determining the drug release profiles of KF from the produced thermo-gels, future studies will therefore focus on *in vivo*

pharmacokinetic studies to measure the drug release profiles and tissue distribution to provide data more specific to the anterior of the eye.

From the *in vitro* cytotoxicity assays, Figure 3.10 and 3.11, and the *in vitro* histology results, Figure 3.12, the produced thermo-gels are not cytotoxic based on short term application. Following incubation with pNAM, a significant increase in cellular viability as measured by MTT was demonstrated although this result was not observed by live/dead staining. The increase in metabolic activity may be attributable to the HCECs digesting the pNAM polymer although further studies would be required to verify this conclusion. It is important to note from Figure 3.11 that the 3-CCN application does result in a change in HCEC morphology to a spherical shape and a lower viability, suggesting that the material may be causing a degree of stress by possibly interrupting cellular transport phenomena. However, by MTT analysis as well as histology following application to the cornea of rats, no negative response was noted for any of the produced thermo-gels. Also, from the *in vivo* testing, no visible discomfort such as excessive blinking, eye scratching or excessive grooming was noted for any of the rats following thermo-gel treatment suggesting the applied thermo-gel doses were also well tolerated. The amount of KF which was loaded into the gels is the same concentration as commercially available eyedrops of KF and therefore, the effect of drug loading on cytotoxicity was not considered as it is assumed to be negligible.

By synthesizing thermo-gels based on ionic or covalent incorporation of chitosan, we were able to measure and compare the properties of the resulting

PECs and CCNs. By varying the method and amount of chitosan incorporated the mechanical properties, degradation rate and drug release profiles could be easily tailored for application to the inferior fornix.

3.6 Conclusion

A series of thermo-gelling polymers containing chitosan were developed in this study for application to the inferior fornix in the treatment of surface ocular diseases such as AC. These drug eluting thermo-gels can provide sustained therapeutic release over multiple days and thus may eliminate the frequent reapplication necessary with conventional topical eyedrops. In this study, chitosan was used as a crosslinker for the base thermo-gelling pNAM because of its established beneficial ophthalmic properties, to improve mechanical attributes and to provide a possible means of degradation, either by covalent conjugation or ionic interaction. By varying the properties of the base pNAM it was possible to have a greater degree of control of the LCST after crosslinking. The final water swollen network pH, as well as the mechanical properties, were improved by the inclusion of varying concentrations of chitosan. It was found that driving force of hydrogel degradation was by physical forces such as swelling. The degradation of the hydrogels could be easily tailored over multiple days through the incorporation of chitosan by covalent conjugation or ionic interaction. Future studies will examine the effect of using chitosan with different physical properties on thermo-gel degradation by lysozyme. It was found that the thermo-gels provided sustained

release of the loaded anti-allergy drug Ketotifen Fumarate for about one-week period. The materials were found not to be cytotoxic by *in vitro* MTT and Live/Dead staining as well as *in vivo* histological analysis. These safety studies suggest that these materials warrant larger scale investigation *in vivo*. An issue commonly encountered with drug eluting materials applied to the front of the eye is retention due to the higher shearing forces produced by blinking and ocular globe movement. Future studies will therefore examine mucosal anchoring of the chitosan-pNAM thermo-gels in addition to studying whether these muco-adhesion properties can be tailored for greater material retention.

3.7 Acknowledgements

We acknowledge The Natural Sciences and Engineering Research Council of Canada (NSERC Discovery) and Ontario Research Fund (C20/20 ORF-RE Round 8) for funding this research.

3.8 Appendix – Supplementary Information

3.8.1 Rheologic Hydrogel Degradation

The degradation of pNAM, 3-CCN and 3-PEC through just the action of lysozyme was assessed by comparing gel stiffness after incubation. 100 mg polymer samples were dissolved at 20% (m/v), in either PBS, PBS containing 1.4 mg/mL of lysozyme to reflect physiological concentration, or PBS containing 14 mg/mL (10x physiological) lysozyme and incubated at 37 ℃ for 48 hours. 48 hours

was selected based on the half-life of lysozyme [61]. Following incubation, the samples were cooled to 4 ℃ overnight to re-dissolve the hydrogels and frequency sweeps were conducted at 37 ℃ to determine gel stiffness and compare the effect of incubating the chitosan-based hydrogels with lysozyme.

Figure 3.S-1 compares the moduli from frequency sweeps of pNAM, 3-CCN and 3-PEC after incubation, examined at 1 rad/s. From the data there was no statistical impact on hydrogel mechanical properties after incubation with either the physiological concentration of lysozyme, or 10x the tear fluid concentration of lysozyme, after 48 hours for pNAM and 3-CCN. 3-PEC incubated with 1x the physiological concentration of lysozyme had a significantly higher ($p < 0.05$) storage and loss modulus compared to PBS incubated controls and 3-PEC incubated with 10x the physiological concentration of lysozyme had a significantly lower ($p > 0.05$) storage and loss modulus compared to PBS controls. This data corroborates that the hydrogel degradation by lysozyme is minimal over this time frame.

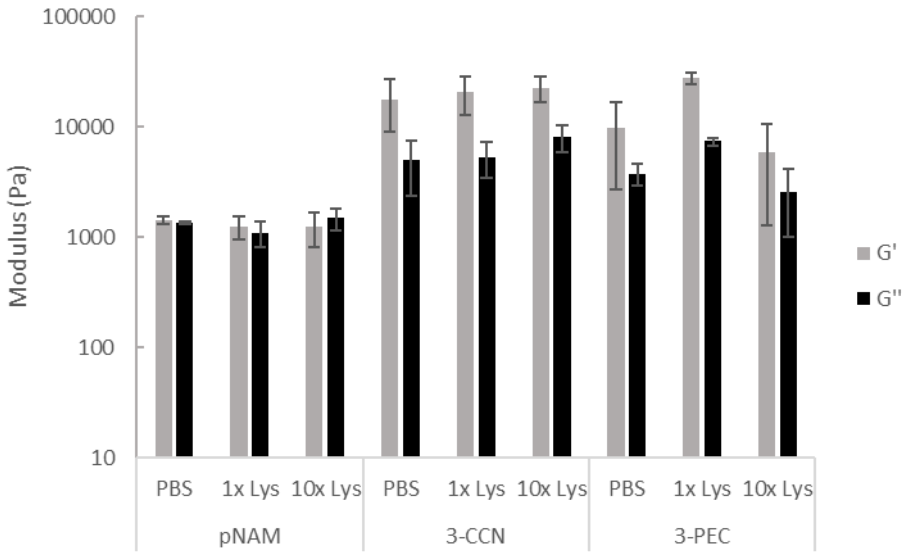

Figure 3.S- 1. Rheological analysis of thermo-gel properties following 48-hour incubation with lysozyme (Lys). No significant change of material properties for pNAM or 3-CCN. 3-PEC modulus values following lysozyme incubation were significant compared to PBS controls but displayed no correlation with the concentration of lysozyme added. Data presented as mean ± SD (n = 3), significance determined by single factor ANOVA analysis followed by Dunnett's post-hoc analysis comparing the lysozyme incubated thermo-gels to the PBS incubated controls. '*' indicates significant difference ($p < 0.05$).

3.9 References:

[1] M. Shaker, E. Salcone, An update on ocular allergy, Current Opinion in Allergy and Clinical Immunology 16(5) (2016) 505-510.

[2] D. Miyazaki, K. Fukagawa, A. Fukushima, H. Fujishima, E. Uchio, N. Ebihara, J. Shoji, E. Takamura, K. Namba, Y. Ohashi, Air pollution significantly associated with severe ocular allergic inflammatory diseases, Scientific reports 9(1) (2019) 1-9.

[3] A.W. Chan, K. Hon, T. Leung, M.H. Ho, J. Sou Da Rosa Duque, T. Lee, The effects of global warming on allergic diseases, Hong Kong Medical Journal (2018).

[4] D. Miyazaki, K. Fukagawa, S. Okamoto, A. Fukushima, E. Uchio, N. Ebihara, J. Shoji, K. Namba, Y. Shimizu, Epidemiological aspects of allergic conjunctivitis, Allergology International 69(4) (2020) 487-495.

[5] A. Leonardi, L. Quintieri, Olopatadine: a drug for allergic conjunctivitis targeting the mast cell, Expert Opinion on Pharmacotherapy 11(6) (2010) 969-981.

[6] A.F. Clark, T. Yorio, Ophthalmic drug discovery, Nature Reviews Drug Discovery 2(6) (2003) 448-459.

[7] J.W. Shell, Pharmacokinetics of topically applied ophthalmic drugs, Survey of ophthalmology 26(4) (1982) 207-218.

[8] A.A. Azari, N.P. Barney, Conjunctivitis: a systematic review of diagnosis and treatment, Jama 310(16) (2013) 1721-1730.

[9] T. Irimia, C.E. Dinu-Pirvu, M.V. Ghica, D. Lupuleasa, D.L. Muntean, D.I. Udeanu, L. Popa, Chitosan-Based In Situ Gels for Ocular Delivery of Therapeutics: A State-of-the-Art Review, Marine Drugs 16(10) (2018).

[10] E. Szymańska, K. Winnicka, Stability of chitosan—a challenge for pharmaceutical and biomedical applications, Marine drugs 13(4) (2015) 1819-1846.

[11] D.L. Roman, V. Ostafe, A. Isvoran, Deeper inside the specificity of lysozyme when degrading chitosan. A structural bioinformatics study, Journal of Molecular Graphics and Modelling 100 (2020) 107676.

[12] L. Popa, M.V. Ghica, C.E. Dinu-Pîrvu, T. Irimia, Chitosan: A Good Candidate for Sustained Release Ocular Drug Delivery Systems, Chitin-Chitosan-Myriad Functionalities in Science and Technology (2018) 283-310.

[13] P. Sacco, F. Furlani, G. De Marzo, E. Marsich, S. Paoletti, I. Donati, Concepts for Developing Physical Gels of Chitosan and of Chitosan Derivatives, Gels 4(3) (2018).

[14] Y.H. Cheng, T.H. Tsai, Y.Y. Jhan, A.W. Chiu, K.L. Tsai, C.S. Chien, S.H. Chiou, C.J. Liu, Thermosensitive chitosan-based hydrogel as a topical ocular drug delivery system of latanoprost for glaucoma treatment, Carbohydrate Polymers 144 (2016) 390-9.

[15] A.S. Hoffman, 4. Poly (NIPAAm) revisited-it has been 28 years since it was first proposed for use as a biomaterial: Original research article: Applications of thermally reversible polymers hydrogels in therapeutics and diagnostics, 1987; thermally reversible hydrogels: II. Delivery and selective removal of substances from aqueous solutions, 1986; a novel approach for preparation of pH-sensitive hydrogels for enteric drug delivery, 1991, Journal of controlled release: official journal of the Controlled Release Society 190 (2014) 36.

[16] S. Lanzalaco, E. Armelin, Poly (n-isopropylacrylamide) and copolymers: A review on recent progresses in biomedical applications, Gels 3(4) (2017) 36.

[17] Z. Cui, B.H. Lee, C. Pauken, B.L. Vernon, Degradation, cytotoxicity, and biocompatibility of NIPAAm-based thermosensitive, injectable, and bioresorbable polymer hydrogels, Journal of Biomedical Materials Research A 98(2) (2011) 159-66.

[18] M. Patenaude, T. Hoare, Injectable, Degradable Thermoresponsive Poly(N-isopropylacrylamide) Hydrogels, ACS Macro Letters 1(3) (2012) 409-413.

[19] S.D. Fitzpatrick, M. Jafar Mazumder, F. Lasowski, L.E. Fitzpatrick, H. Sheardown, PNIPAAm-grafted-collagen as an injectable, in situ gelling, bioactive cell delivery scaffold, Biomacromolecules 11(9) (2010) 2261-2267.

[20] S.D. Fitzpatrick, M.J. Mazumder, B. Muirhead, H. Sheardown, Development of injectable, resorbable drug-releasing copolymer scaffolds for minimally invasive sustained ophthalmic therapeutics, Acta biomaterialia 8(7) (2012) 2517-2528.

[21] M.J. Mazumder, S.D. Fitzpatrick, B. Muirhead, H. Sheardown, Cell-adhesive thermogelling PNIPAAm/hyaluronic acid cell delivery hydrogels for potential application as minimally invasive retinal therapeutics, Journal of biomedical materials research Part A 100(7) (2012) 1877-1887.

[22] B. Muirhead, S. Fitzpatrick, K. Gregory-Evans, M. Bhatia, H. Sheardown, NIPAAm Based Cell Delivery Scaffolds for Posterior Segment Therapeutics, Investigative Ophthalmology & Visual Science 54(15) (2013) 4627-4627.

[23] Y. Yu, X. Chang, H. Ning, S. Zhang, Synthesis and characterization of thermoresponsive hydrogels cross-linked with chitosan, Central European Journal of Chemistry 6(1) (2008) 107-113.

[24] Y. Yu, Y. Li, C. Zhu, L. Liu, Synthesis and characterization of temperature-sensitive and biodegradable hydrogel based on N-isopropylacrylamide, Open Chemistry 8(2) (2010) 426-433.

[25] J.Y. Lai, L.J. Luo, Chitosan-g-poly(N-isopropylacrylamide) copolymers as delivery carriers for intracameral pilocarpine administration, European Journal Pharmaceutics and Biopharmaceutics 113 (2017) 140-148.

[26] L.J. Luo, C.C. Huang, H.C. Chen, J.Y. Lai, M. Matsusaki, Effect of deacetylation degree on controlled pilocarpine release from injectable chitosan-g-poly(N-isopropylacrylamide) carriers, Carbohydrate Polymers 197 (2018) 375-384.

[27] L.J. Luo, D.D. Nguyen, J.Y. Lai, Benzoic acid derivative-modified chitosan-g-poly(N-isopropylacrylamide): Methoxylation effects and pharmacological treatments of Glaucoma-related neurodegeneration, Journal of Controlled Release 317 (2020) 246-258.

[28] D.D. Nguyen, L.J. Luo, S.J. Lue, J.Y. Lai, The role of aromatic ring number in phenolic compound-conjugated chitosan injectables for sustained therapeutic antiglaucoma efficacy, Carbohydrate Polymers 231 (2020) 115770.

[29] Y. Cao, C. Zhang, W. Shen, Z. Cheng, L.L. Yu, Q. Ping, Poly(N-isopropylacrylamide)-chitosan as thermosensitive in situ gel-forming system for ocular drug delivery, Jounral of Controlled Release 120(3) (2007) 186-94.

[30] J. Colter, B. Wirostko, B. Coats, Finite element design optimization of a hyaluronic acid-based hydrogel drug delivery device for improved retention, Annals of Biomedical Engineering 46(2) (2018) 211-221.

[31] M.V. Fedorchak, I.P. Conner, J.S. Schuman, A. Cugini, S.R. Little, Long term glaucoma drug delivery using a topically retained gel/microsphere eye drop, Scientific reports 7(1) (2017) 1-11.

[32] L. Leinonen, S.-L. Joutsiniemi, M.-L. Laakso, N. Lindblom, M. Kaski, Automatic blink detection: a method for differentiation of wake and sleep of intellectually disabled and healthy subjects in long-term ambulatory monitoring, Sleep 26(4) (2003) 473-479.

[33] Y. Cao, C. Zhang, W. Shen, Z. Cheng, L.L. Yu, Q. Ping, Poly (N-isopropylacrylamide)–chitosan as thermosensitive in situ gel-forming system for ocular drug delivery, Journal of controlled release 120(3) (2007) 186-194.

[34] T. Saitoh, Y. Sugiura, K. Asano, M. Hiraide, Chitosan-conjugated thermo-responsive polymer for the rapid removal of phenol in water, Reactive and Functional Polymers 69(10) (2009) 792-796.

[35] Y. Wen, J. Ban, Z. Mo, Y. Zhang, P. An, L. Liu, Q. Xie, Y. Du, B. Xie, X. Zhan, L. Tan, Y. Chen, Z. Lu, A potential nanoparticle-loaded in situ gel for enhanced and sustained ophthalmic delivery of dexamethasone, Nanotechnology 29(42) (2018) 425101.

[36] O. Guaresti, C. Garcia-Astrain, R.H. Aguirresarobe, A. Eceiza, N. Gabilondo, Synthesis of stimuli-responsive chitosan-based hydrogels by Diels-Alder cross-linking `click reaction as potential carriers for drug administration, Carbohydrate Polymers 183 (2018) 278-286.

[37] N. Yang, Y. Wang, Q. Zhang, L. Chen, Y. Zhao, In situ formation of poly (thiolated chitosan-co-alkylated β-cyclodextrin) hydrogels using click cross-linking for sustained drug release, Journal of Materials Science 54(2) (2018) 1677-1691.

[38] E. Aine, P. Morsky, Lysozyme Concentration in Tears-Assessment of Reference Values in Normal Subjects, Acta ophthalmologica 62(6) (1984) 932-938.

[39] S. Muralidharan, L.B. Han, Y. Ming, J. Lau, K. Sailishni, S. Arumugam, Simple and accurate estimation of ketotifen fumarate by RP-HPLC, International Journal of Pharmaceutical, Chemical and Biological Sciences 2(3) (2012) 392-396.

[40] R.W. Korsmeyer, R. Gurny, E. Doelker, P. Buri, N.A. Peppas, Mechanisms of solute release from porous hydrophilic polymers, International journal of pharmaceutics 15(1) (1983) 25-35.

[41] N. Peppas, P. Bures, W. Leobandung, H. Ichikawa, Hydrogels in pharmaceutical formulations, European journal of pharmaceutics and biopharmaceutics 50(1) (2000) 27-46.

[42] P.L. Ritger, N.A. Peppas, A simple equation for description of solute release II. Fickian and anomalous release from swellable devices, Journal of controlled release 5(1) (1987) 37-42.

[43] M. Korogiannaki, J. Zhang, H. Sheardown, Surface modification of model hydrogel contact lenses with hyaluronic acid via thiol-ene “click” chemistry for enhancing surface characteristics, Journal of Biomaterials Applications 32(4) (2017) 446-462.

[44] V.M. Varghese, V. Raj, K. Sreenivasan, T.V. Kumary, In vitro cytocompatibility evaluation of a thermoresponsive NIPAAm-MMA copolymeric surface using L929 cells, Journal of Materials Science Materials in Medicine 21(5) (2010) 1631-9.

[45] J. Leuba, P. Stossel, Chitosan and other polyamines: antifungal activity and interaction with biological membranes, Chitin in nature and technology, Springer 1986, pp. 215-222.

[46] T.T. Nge, M. Yamaguchi, N. Hori, A. Takemura, H. Ono, Synthesis and characterization of chitosan/poly (acrylic acid) polyelectrolyte complex, Journal of applied polymer science 83(5) (2002) 1025-1035.

[47] M.A. Haq, Y. Su, D. Wang, Mechanical properties of PNIPAM based hydrogels: A review, Materials Science Engineering C Materials Biological Application 70(Pt 1) (2017) 842-855.

[48] Q.V. Nguyen, D.P. Huynh, J.H. Park, D.S. Lee, Injectable polymeric hydrogels for the delivery of therapeutic agents: A review, European Polymer Journal 72 (2015) 602-619.

[49] A. Okudan, A. Altay, Investigation of the Effects of Different Hydrophilic and Hydrophobic Comonomers on the Volume Phase Transition Temperatures and Thermal Properties of N-Isopropylacrylamide-Based Hydrogels, International Journal of Polymer Science 2019 (2019) 1-12.

[50] K. Varaprasad, K. Vimala, S. Ravindra, N.N. Reddy, G.S.M. Reddy, K.M. Raju, Biodegradable chitosan hydrogels for in vitro drug release studies of 5-flurouracil an anticancer drug, Journal of Polymers and the Environment 20(2) (2012) 573-582.

[51] S.W. Wu, X. Liu, A.L. Miller, 2nd, Y.S. Cheng, M.L. Yeh, L. Lu, Strengthening injectable thermo-sensitive NIPAAm-g-chitosan hydrogels using chemical cross-linking of disulfide bonds as scaffolds for tissue engineering, Carbohydrate Polymers 192 (2018) 308-316.

[52] M.L. Bruschi, Mathematical models of drug release, Strategies to modify the drug release from pharmaceutical systems 63 (2015).

[53] S.J. Lue, C.-H. Chen, C.-M. Shih, Tuning of Lower Critical Solution Temperature (LCST) of Poly(N-Isopropylacrylamide-co-Acrylic acid) Hydrogels, Journal of Macromolecular Science, Part B 50(3) (2011) 563-579.

[54] Y. Pei, J. Chen, L. Yang, L. Shi, Q. Tao, B. Hui, J. Li, The effect of pH on the LCST of poly(N-isopropylacrylamide) and poly(N-isopropylacrylamide-co-acrylic acid), Journal of Biomateria Science Polymer Edition 15(5) (2004) 585-94.

[55] N. Seddiki, D. Aliouche, Synthesis, rheological behavior and swelling properties of copolymer hydrogels based on poly(N-isopropylacrylamide) with hydrophilic monomers, Bulletin of the Chemical Society of Ethiopia 27(3) (2013).

[56] N.S. Rejinold, P.R. Sreerekha, K.P. Chennazhi, S.V. Nair, R. Jayakumar, Biocompatible, biodegradable and thermo-sensitive chitosan-g-poly (N-isopropylacrylamide) nanocarrier for curcumin drug delivery, International Journal of Biological Macromolecules 49(2) (2011) 161-72.

[57] C. Roberts, Comparison of the ocular comfort of ofloxacin 0.3% ophthalmic solution and lubricant eye drops, Clinical pediatrics 41(3) (2002) 151-154.

[58] R.J. Nordtveit, K.M. Vårum, O. Smidsrød, Degradation of partially N-acetylated chitosans with hen egg white and human lysozyme, Carbohydrate polymers 29(2) (1996) 163-167.

[59] K.A. Alkhamis, M.S. Salem, M.S. Khanfar, The sorption of ketotifen fumarate by chitosan, Aaps Pharmscitech 9(3) (2008) 866-869.

[60] S. Guerrero, C. Teijón, E. Muñiz, J.M. Teijón, M.D. Blanco, Characterization and in vivo evaluation of ketotifen-loaded chitosan microspheres, Carbohydrate Polymers 79(4) (2010) 1006-1013.

[61] R. Kashani, S. Fariba, M. Aminlari, R. Ramezani, Effects of high and low temperature on inactivation of lysozyme in pasteurized milk, Online Journal of Veterinary Research 17 (2013) 300-309.

CHAPTER 4 – Thermo-responsive and mucoadhesive gels for the treatment of cystinosis.

Submitted Manuscript:

Mitchell Ross, Jonathan Mofford, Jennifer JingYuan Tian, Benjamin Muirhead, Emily Anne Hicks, Lindsay Sheardown, and Heather Sheardown. Accepted to Biomaterials Advances on December 1st 2022.

Objectives:

To design a degradable and mucoadhesive thermogel for application to the anterior of the eye. Test the effect of altering mucoadhesive properties versus retention within the inferior fornix. Explore the conjugation of cysteamine for mucosal mediated drug delivery in treating cystinosis.

Author Contributions:

Material development, testing, and subsequent reporting was completed by Mitchell Ross. All listed co-authors contributed to either *in vivo* rat or rabbit testing.

Thermo-responsive and mucoadhesive gels for the treatment of cystinosis.

Mitchell Ross, Jonathan Mofford, Jennifer JingYuan Tian, Benjamin Muirhead, Emily Anne Hicks, Lindsay Sheardown, and Heather Sheardown

Department of Chemical Engineering, McMaster University, 1280 Main St W, Hamilton, ON L8S 4L8, Canada

Corresponding Author:
Heather Sheardown, sheardow@mcmaster.ca (905) 525-9140, John Hodgins Engineering Building Room 260, 1280 Main St W, Hamilton, ON L8S 4L7

Declaration of Interest

The work which has been reported herein is covered by the patent Polymer System for Ophthalmic Drug Delivery pending to authors Mitchell Ross and Heather Sheardown. The authors declare that there are no further declarations of interest.

Highlights

- Development of a mucoadhesive and natively degradable thermogel for application to the inferior fornix.

- Release of cysteamine from the developed thermogel is modulated by mucosal interaction.
- The sustained release of cysteamine is noted over several days compared to current topical formulations which required reinstallation four times per day.
- The developed thermogel formulation can be reformulated for any mucosal surface.

Key words

Thermogels, mucoadhesion, sustained drug release, cystinosis, degradation, inferior fornix

Abbreviations

2-MP, 2-mercaptopyridine; AA, acrylic acid; ABS, absorbance; ANOVA, single factor analysis of variance; BPO, benzoyl peroxide; CTS, chitosan; DCM, dichloromethane; EDC, 1-ethyl-3-(3-dimethylaminopropyl)carbodiimide; EWC, equilibrium water content; FTIR, Fourier transform infrared spectroscopy; GPC, gel permeation chromatography; LCST, lower critical solution temperature; MES, 2-(N-Morpholino)ethanesulfonic acid; MMA, methyl methacrylate; NMR, nuclear magnetic resonance; OCT, optical coherence tomography; PBS, phosphate buffered saline; PDSOH, 2-(Pyridin-2-yldisulfaneyl)ethan-1-ol; PDSMA, pyridyl disulfide ethylmethacylate; PK, pharmacokinetics; PLGA, poly(lactic-co-glycolic

acid); pNAMP, poly(N-isopropylacrylamide-co-acrylic acid-co-methyl methacrylate-co-pyridyl disulfide ethylmethacrylate); pNIPAAm, n-isopropylacrylamide; SD, standard deviation; THF, tetrahydrofuran.

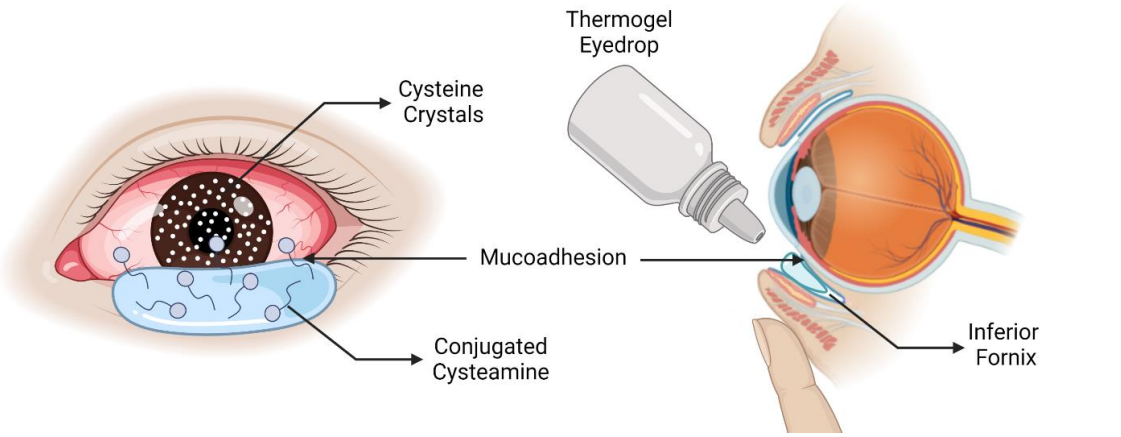

Graphical Abstract: Created with BioRender.com

4.1 Abstract

Mucoadhesive thermogels were developed by crosslinking poly(n-isopropylacrylamide) based polymers with chitosan and incorporating disulfide bridges, capable of releasing cysteamine upon interaction with mucin, for the treatment of cystinosis. Through crosslinking with chitosan and incorporating varying concentrations of the disulfide monomer into the polymer backbone, the extent of how mucoadhesive the developed thermogels were could be controlled. Through disulfide bridging with mucin, the thermogels released 6 to 10 µg of the conjugate model 2-mercaptopyridine over five days. Utilizing chitosan as the crosslinker, the developed thermogels were shown to degrade to a significantly

higher extent following incubation with lysozyme, the highest concentration tear enzyme, by gravimetric and rheologic analysis. The developed thermogels were extensively tested *in vivo* utilizing a rat model in which materials were applied directly to the corneal surface and a rabbit model in which thermogels were applied to the inferior fornix. With the developed models, there was no adverse reactions or visual discomfort incurred following application of the thermogels. It has been demonstrated that the thermogels produced can be applied to the inferior fornix and release the stable conjugated payload over several days. The developed thermogel was designed to improve upon the current clinical treatment options for ocular cystinosis which are acidic topical formulations that require reapplication multiple times a day.

4.2 Introduction

Of the more than 10,000 inherited genetic disorders known to affect humans, a disproportionate number impact the eye [1]. It is estimated that one in every 500-1000 individuals is affected by a single-gene ophthalmic disorder [2]. Cystinosis is a multisystem recessive genetic disorder that is characterized by a buildup of crystals consisting of the amino acid cysteine in various tissues throughout the body. The intracellular accumulation of cysteine and subsequent crystal formation is caused by defective action of the lysosomal transmembrane protein cystinosin. It is approximated that cystinosis affects one in every 100,000-200,000 live births and has been shown to affect all ethnic groups globally, though

not equally [3]. There are over 100 pathogenic mutations that have been reported to be associated with cystinosis [4]. Cysteine crystals have been shown to develop within the liver, kidneys, brain, pancreas, as well as the eyes. Ocular diagnosis is typically accomplished by slit-lamp examination of crystal buildup within the cornea in patients greater than 16 months old, although the conjunctiva, iris, ciliary body, lens capsule, choroid, and retinal pigment epithelium are afflicted as well [5]. The accumulation of cysteine crystals in these ocular tissues can lead to clinical symptoms and disorders including, but not limited to, photophobia, epithelial erosion, vision impairment, scarring, corneal neovascularization, secondary glaucoma, pigmentary retinopathy, and central vision loss [6].

The only clinical treatment option available for treating cystinosis is the aminothiol cysteamine, which can reduce cysteine crystals via the disulfide reaction. The resulting mixed disulfide cysteine-cysteamine is then transported out of the lysosome by the cationic lysine transport system [5]. Oral cysteamine is utilized to treat most of the symptoms associated with cystinosis but is ineffective at treating ocular tissues. Therefore, either topical eyedrops or lubricating gels are used to treat the eye. The major drawback for the utilization of cysteamine topical eyedrops is that they require frequent reapplication, as often as 10-12 times per day [4, 5]. Furthermore, to prevent rapid oxidation of cysteamine, hydrochloride salt is used. It has a low solution pH of 4.2, leading to stinging and burning sensation for the patient upon application. Due to rapid oxidation once opened, commercial cysteamine drops are only stable for one week, requiring frequent

replacement [7]. To overcome these limitations, various materials have been explored to prolong cysteamine release. In particular, the lubricating gel Cystadrops® (Orphan Europe, Puteaux, France), approved by the European Medicines Agency, has been shown to reduce reapplication frequency to four times per day by incorporating the thickening agent carboxymethylcellulose [8]. Other publications have investigated alternative thickening agents including hydroxypropylmethylcellulose [9, 10], polyacrylic acid [10, 11], hydroxyethyl cellulose [10], xantham gum [10], hyaluronic acid [10, 12], and an ion-sensitive blend of deacylated gellan gum and kappa carrageenan [12]. Cysteamine-loaded contact lenses [13-15], as well as polyvinyl alcohol nano-wafers [16] have been explored in literature to control cysteamine release. Of particular interest, Jiminez et al., recently reported the release of cysteamine from loaded poly(lactic-co-glycolic acid) (PLGA) microparticles within a thermogelling poly(N-isopropylacrylamide) (pNIPAAm)-polyethylene glycol thermosensitive hydrogel matrix, capable of a sustained, 24-hour release [17]. Furthermore, by fabricating the cysteamine-loaded PLGA microspheres through spray drying, the stability of the formulation was increased to 7 weeks.

Regardless, all these treatments continue to require frequent reapplication. Mucin, which is a critical component of the tear film, coats the surface of the eye and acts as both lubrication and a barrier [18]. It has been investigated as an anchorage point for drug eluting materials. Mucus layers present throughout the body have proven to be a promising avenue for drug release technologies [19-22].

Therefore, for improving thermogel retention within the inferior fornix, mucoadhesive properties can be galvanized for improved anchorage.

Recently, thiol-bearing polymers/moieties have been formulated to develop mucoadhesive systems that are able to covalently bond via disulfide linkages with the cysteine residues of mucin [23, 24]. Furthermore, these preactivated thiomers can be conjugated with therapeutic ligands that release during disulfide bonding with the cystine residues of mucin. The Sheardown research group has previously developed chitosan-crosslinked pNIPAAm-based thermogels for the treatment of allergic conjunctivitis [25]. Herein we hypothesize that by incorporating a preactivated thiomer monomer into these thermogels, the mucoadhesive properties can be altered, and the materials easily conjugated with thiol-containing small molecules like cysteamine. Therefore, in this study, the goal was to conjugate cysteamine to the previously developed thermogelling formulations to improve shelf life, by eliminating the possibility of oxidation, and have the pH of the formulations closer to neutral to prevent stinging upon application. As a model, cysteamine can be conjugated onto the polymers to create a platform material that can be easily applied to the inferior fornix, will have high retention while releasing cysteamine over multiple days at a physiological pH ultimately for the treatment of cystinosis. It is important to note, although these mucoadhesive thermogels are currently being validated for the surface of the eye, these degradable materials can be utilized in other mucous membranes, including nasal, buccal, or vaginal

drug delivery pathways, as lysozyme is secreted by the serous cells of all sub-mucosal glands [26].

4.3 Materials and Methods

4.3.1 Materials

Chitosan (MW = 80-200 kDa, degree of deacetylation = 70%) was purchased from Heppe Medical Chitosan (Halle, Saxony-Anhalt, Germany) and used as received. N-isopropylacrylamide (NIPAAm; 97%) was purchased from Sigma-Aldrich (Oakville, Ontario, Canada) and purified by recrystallization from toluene with n-hexane. Acrylic Acid (AA; 99%) and methyl methacrylate (MMA; 99%) was purchased from Sigma-Aldrich and was purified by passing through a packed column containing inhibitor remover, obtained from Sigma-Aldrich to remove the inhibitor 4-methoxyphenol. 1,4-Dioxane, n-hexane, toluene, anhydrous diethyl ether and tetrahydrofuran (THF) were purchased from VWR (Radnor, Pennsylvania, USA) and used as received. Milli-Q grade deionized water was prepared using a Barnstead Diamond™ water purification system (Thermo Fischer Scientific, Waltham, Massachusetts, USA). 10x Phosphate buffered saline (PBS) was purchased from BioShop® (Burlington, Ontario, Canada) and diluted with deionized water to 1x (pH 7.4) for all experiments. All other compounds were purchased from Sigma-Aldrich (Oakville, Ontario, Canada) unless otherwise specified.

4.3.2 Pyridyl Disulfide Ethylmethacylate (PDSMA) Monomer Synthesis

The PDSMA monomer was synthesized based on protocols previously reported in literature [27, 28]. Briefly, one gram of pyridyl disulfide was dissolved in methanol to a concentration of 83.3 mg/mL. 7.7 molar equivalents of acetic acid were then added dropwise followed by 0.72 molar equivalents of mercaptoethanol dissolved to 0.43 mM in ethanol. The reaction then proceeded overnight with constant stirring. Following the reaction, the intermediate 2-(Pyridin-2-yldisulfaneyl)ethan-1-ol (PDSOH) was extracted and column purified. Purified PDSOH was then dissolved in anhydrous dichloromethane (DCM) to a concentration of 25 mg/mL. 2 molar equivalents of N,N-diisopropylethylamine was then added to the reaction mixture before being placed in an ice bath. Finally, 1.2 molar equivalents of methacryloyl chloride dissolved in an equal volume of anhydrous DCM was added to the reaction mixture dropwise and reacted for 12 hours. The pyridyl disulfide ethyl methacrylate product was extracted and column purified.

4.3.3 Poly(N-isopropylacrylamide-co-acrylic acid-co-methyl methacrylate-co-pyridyl disulfide ethylmethacrylate) (pNAMP) Synthesis

The free radical synthesis of the base terpolymer pNAM and functional tetrapolymer pNAMP followed our previously established protocols [25]. The

synthetic scheme of pNAMP synthesis is depicted in Figure 4.1a. Four polymers were produced containing 0, 1, 2 and 3 mol% PDSMA. These samples are denoted as pNAM, pNAMP-1, pNAMP-2, and pNAMP-3 respectively. To produce pNAMP-3, 834.2 mg (7.34 mmol) of recrystallized NIPAAm, 12.5 mg (0.17 mmol) uninhibited AA, 86.8 mg (0.87 mmol) of MMA, 66.4 mg (0.26 mmol) of PDSMA and 21.0 mg of BPO (0.1 mmol) were dissolved in a round bottom flask containing 10 mL of 1,4-dioxane:deionized water (9:1 v/v) to produce a 10% (wt/v) monomer solution. The flask was then sealed and purged with nitrogen for 25 minutes to remove oxygen. The reaction proceeded at 70℃ for 24 hours. Following polymerization, the polymer was precipitated twice into 800 mL of chilled anhydrous diethyl ether. The resulting pNAMP-3 powder was collected by vacuum filtration and dialyzed against 4L of deionized water using a Membra-Cel® 14 kDA MWCO cellulose membrane (Viskase®, Lombard, Illinois, USA), changing once per day for three days. After dialysis, the polymer was lyophilized using a Labconco™ FreeZone 2.5 benchtop freeze drier (Kansas City, Missouri, USA) and stored at -20℃. The composition of the polymers was determined by ^{1}H NMR using a Bruker© 600 MHz Spectrometer, operating at 600.13 MHz and 298 K (Billerica, Massachusetts, USA). All samples were dissolved in DMSO-D_6 for analysis. The pNAMP polymer molecular weight as well as the polydispersity index (PDI) was determined by a Polymer Laboratories PL-50 gel permeation chromatograph (GPC; Church Streton, Shropshire, UK) fitted with three Phenomenex Phenogel™ columns; pore sizes 100, 500 and 104 Å (Torrance,

California, USA) at room temperature. Dimethylformamide containing 5 mM lithium bromide was used as the eluent. All samples were filtered through a 0.2 µm PTFE syringe filter prior to quantification. Linear polyethylene glycol standards provided by Polymer Laboratories were utilized for molecular weight calibration.

4.3.4 Synthesis of Chitosan crosslinked Thermogelling Networks

The synthesis of covalently crosslinked chitosan networks of pNAMP (CTS-pNAMP) followed similar protocols to those previously established [25] as shown in Figure 4.1b. To crosslink the polymer, a concentration of 3% (wt/wt) chitosan/pNAMP was utilized. Briefly, 30 mg of chitosan was dissolved in 30 mL of 10 mM of 2-(N-morpholino)ethanesulfonic acid (MES) buffer, adjusted to pH 4.7 with 0.1 N NaOH, and heated at 45℃ under constant stirring. After 5 hours, the chitosan solution was passed through a 0.45 µm syringe filter to remove any large aggregates, then 1g of pNAMP powder was dissolved into the solution. Finally, 61.6 mg (0.32 mmol) of 1-ethyl-3-(3-dimethylaminopropyl)carbodiimide (EDC) was dissolved in a minimum volume of MES buffer and added dropwise to the chitosan/pNAMP solution and reacted for 24 hours under constant stirring. The CTS-pNAMP product was then dialyzed against 4L of deionized water using Spectrum Labs 3.5 kDa MWCO Spectra/Por Grade regenerated cellulose dialysis membrane (Spectrum Laboratories, Rancho Dominguez, CA, USA) changing once per day for three days. Samples were then lyophilized and stored at -20℃.

The CTS-pNAMP networks were characterized by ^{1}H NMR, using D_2O as a solvent, and as solids by a Nicolet 6700 Fourier Transform Infrared spectrometer (FTIR; Thermo Scientific, Waltham, Massachusetts, USA).

4.3.5 Analysis of CTS-pNAMP Thermogel Mucoadhesive Properties

The mucoadhesive properties of the prepared thermogels were determined by rheological synergism [19, 29]. Rheological synergism is calculated by equation 4.1.

$$\eta_{synergism} = \eta_{mix} - \left(\eta_{thermogel} + \eta_{mucin}\right) \quad 4.1)$$

Where η_x is the viscosity of a given component x.

An equal volume of 6% (wt/wt) mucin dispersion was mixed by shaking with either dissolved thermogel at 20% (wt/v) or buffer as control for one hour prior to testing (final mucin concentration of 3% (wt/wt) and thermogel 10% (wt/v), respectively) [29-31]. Viscosity was measured by a flow sweep at a shear rate of 0.1 to 100 s^{-1} utilizing a Discovery HR-2 hybrid rheometer (Waters™, Newcastle, Delaware, USA) fitted with a 20 mm 1° cone and Peltier plate assembly at 4℃. Viscosity measurement was conducted for all the thermogels prior to cysteamine conjugation.

The extent of pNAMP adhesion to mucin was assessed by the evolution of 2-mercaptopyridine (2-MP) using a SpectraMax® ABS Plus UV-vis micro-plate reader (Molecular Devices, San Jose, California, USA). 0.05% (wt/v) pNAMP was mixed with either PBS, 0.015% (wt/wt) mucin, or an equimolar concentration of the

small thiol bearing compound mercaptoethanol. The amount of 2-mercaptopyridine released by disulfide exchange with mucin was compared to the control mercaptoethanol as described in equation 4.2.

$$2-\text{Mercapto}pyridine\ Evolution = \left(\frac{Abs_{Mucin}}{Abs_{Mercaptoethanol}}\right)100 \quad 4.2)$$

Where ABS_x is the absorbance of a given component x. The evolution of 2-MP was quantified by UV-visible spectroscopy at a wavelength of 343 nm.

4.3.6 2-MP Release of CTS-pNAMP Thermogels from Mucin

The release of 2-MP from the CTS-pNAMP thermogels following incubation with mucin was measured using an Agilent 1260 Infinity II high performance liquid chromatographer (HPLC; Santa Clara, California, USA). 0.995 mL of 6% (wt/wt) mucin was added to a 1 mL Spectra/Por Float-A-Lyzer® G2 (Spectrum Laboratories, Rancho Dominguez, CA, USA) with a 3.5-5 kDa MWCO placed in a 5 mL of PBS and incubated at 37℃. 50 µL of thermogel dissolved at 10% (wt/v) was then pipetted into the mucin solution and allowed to gel. 1 mL of PBS supernatant was removed at set time intervals and replaced with an equal volume of PBS. The mobile phase consisted of 90% Milli-Q, 10% acetonitrile, and 0.1% phosphoric acid and was passed over a Pall® Life Sciences 0.45 µm nylon filter (Port Washington, New York, USA) prior to use. The release samples were filtered through a 0.2 µm Nylon filter (Agilent) prior to quantification. Sample concentration was determined against a calibration curve of 2-MP at a wavelength of 343 nm.

4.3.7 Cysteamine Conjugation of CTS-pNAMP (CTS-pNAMP-C)

Cysteamine was conjugated to CTS-pNAMP thermogels by a disulfide exchange reaction to produce CTS-pNAMP-C, as depicted in Figure 4.1c. To produce CTS-pNAMP-C2, 1g of CTS-pNAMP-2 was dissolved to a concentration of 3% (wt/v). 67.2 mg (0.87mmol; 1.5 molar excess to PDSMA concentration) of cysteamine was dissolved (10 mg/mL) in Milli-Q and the pH adjusted to 6.5 using 0.1 M HCl. The cysteamine was added dropwise to the CTS-pNAMP solution under constant stirring and allowed to react for 24 hours. The resulting CTS-pNAMP-C was then dialyzed against 4 L of deionized water using Spectrum Labs 3.5 kDa MWCO Spectra/Por Grade regenerated cellulose dialysis membrane as described above. Samples were then lyophilized and stored at -20℃. The conjugation of cysteamine was measured by the evolution of 2-MP using UV-vis at a wavelength of 343 nm. For accurate measurement by UV-vis samples were diluted 200x prior to the absorbance reading and the background of dissolved polymer was subtracted from samples to ensure the reading was just reflective of the release of 2-MP.

Rheological temperature ramps were conducted at a rate of 1℃/min from 15 to 45℃, utilizing a 20 mm 1° cone and Peltier plate assembly. The LCST was defined as the temperature in which both the storage and loss modulus begin to increase by orders of magnitude above the baseline measurement. Temperature ramps were conducted on the base pNAM and CTS-pNAM as well as the final

cysteamine conjugated networks CTS-pNAMP-C1, CTS-pNAMP-C2 and CTS-pNAMP-C3.

a)

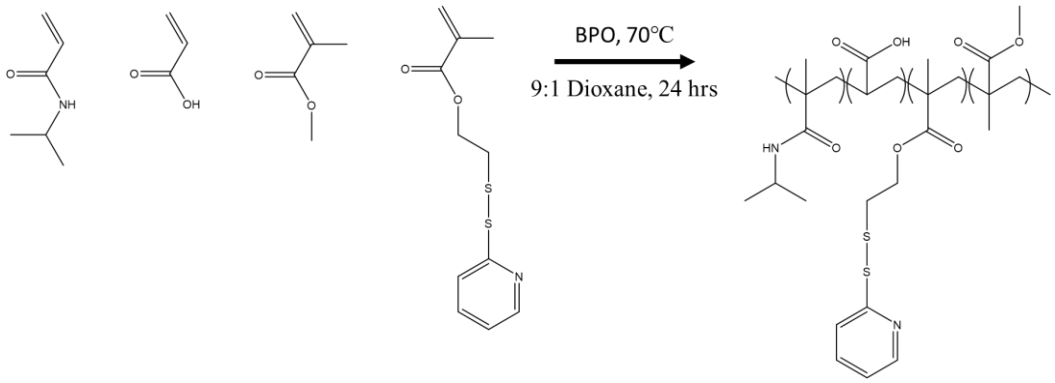

b)

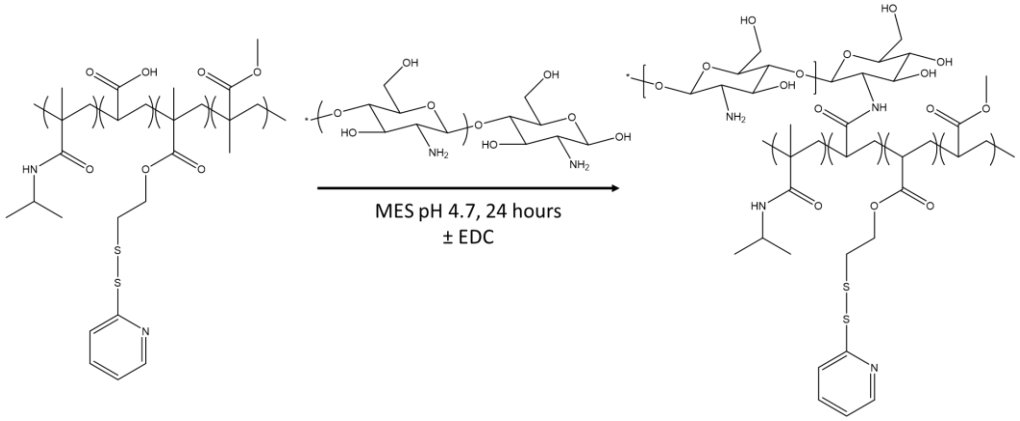

c)

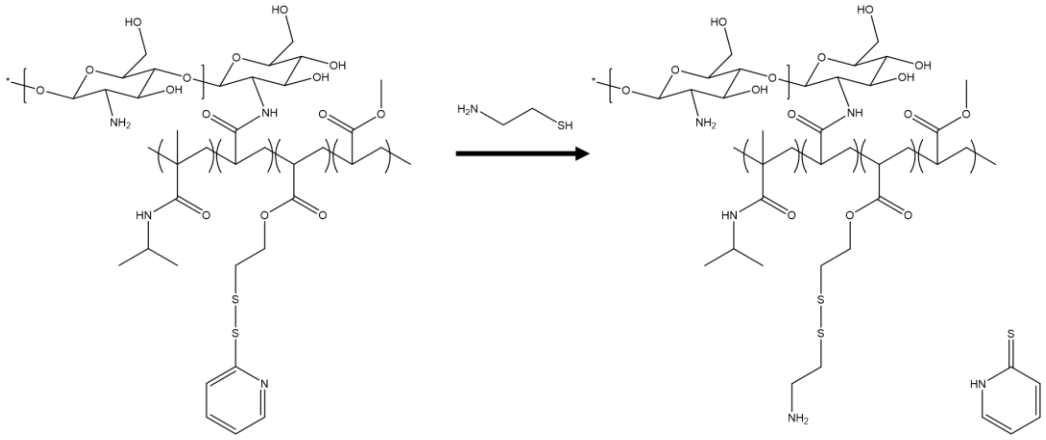

Figure 4.1a) Free radical polymerization of pNAMP, b) Crosslinking of pNAMP with chitosan and c) Conjugation of cysteamine to CTS-pNAMP.

4.3.8 Rheological Analysis of Materials Properties

All samples were tested at a concentration 10% (w/v) in PBS. Stress and frequency sweeps were conducted utilizing a 20 mm parallel Peltier plate. Stress sweeps were utilized to determine the linear viscoelastic region of the base pNAM and CTS-pNAM at 37℃. Frequency sweeps were conducted to quantify the effect of chitosan crosslinking, as well as cysteamine conjugation on pNAM, CTS-pNAM and CTS-pNAMP-C.

4.3.9 Thermogel Equilibrium Water Content

The equilibrium water content (EWC) of the various hydrogels were assessed gravimetrically. 50 mg of the respective material (M_D) were dissolved to a concentration of 10% (wt/v) in PBS at room temperature. The dissolved solutions were then allowed to gel at 37℃. After 24 hours, the gels were blotted dry using a lintless paper wipe and reweighed (M_S). The EWC was calculated using equation 4.3.

$$EWC\ (\%) = \left(\frac{M_S - M_D}{M_S}\right) 100 \qquad 4.3)$$

4.3.10 Determination of Thermogel Enzymatic Degradation

The gravimetric degradation of the thermogels was conducted at 37℃. 50 mg of the thermogel was dissolved to 10% (wt/v) in PBS and allowed to gel for 24 hours prior to testing. Following the initial incubation (t=0), the samples were blotted dry using a lintless paper wipe, and the initial mass measured (M_S). The dry gels were then incubated with 0.5 mL of either PBS or PBS containing 1.4 mg/mL of hen egg white lysozyme, to simulate physiologic tear concentration. At given time intervals, the supernatants were extracted, and the gel mass measured (M_t). The percent degradation of the thermogels was calculated as a mass at a predetermined time interval to the initial gel mass as described in equation 4.4.

$$4.4) \quad Degradation\ (\%) = \left(\frac{M_t}{M_S}\right) 100$$

The action of lysozyme on the degradation of the thermogels was also quantified by measurement of the viscosity following incubation with the protein. 50 mg of the thermogel was dissolved at 10% (wt/v) in either PBS or PBS containing a physiologic concentration of lysozyme. The samples were then gelled at 37℃ for 48 hours. After incubation, the samples were cooled back to a liquid and the viscosity measured by rheometric analysis utilizing a flow sweep with a 20 mm 1° cone and Peltier plate at 4℃.

4.3.11 *In Vivo* Safety and Tolerability

Animal studies were performed in compliance with protocols approved by the Animal Research Ethics Board at McMaster University in accordance with the

regulations of the Animals for Research Act of the Province of Ontario and the guidelines of the Canadian Council on Animal Care. 12, nineteen-week-old female Brown Norway Rats (Charles River, Wilmington, Massachusetts, USA) were used to test the safety of pNAM, CTS-pNAM and CTS-pNAMP-C2 thermogels. The thermogel samples were UV treated for 12 hours prior to application. The rats were anesthetized with gaseous isoflurane before the application of 10 µL of PBS, pNAM, CTS-pNAM or CTS-pNAMP-C2 everyday for one week, with three rats per testing group. The materials were allowed to gel and remained on the surface of the eye for one hour prior to the reversal of anesthesia and the onset of rat blinking. At days 1, 3, and 5, the cornea was assessed utilizing Phoenix MICRON™ Optical Coherence Tomography imaging system (OCT; Owens Drive, Pleasanton, California, USA) as well as by fluorescence staining to measure corneal disruption. OCT was utilized to visualize the cornea as well as measure corneal thickness over time to ensure that applied gels were not producing an inflammatory response. After one week, the rats were euthanized, and the eyes harvested. Eyes were fixed in 4% paraformaldehyde overnight at 4℃, then stored in 70% ethanol. Samples were processed (Core Histology Department, McMaster University) and embedded in paraffin (Paraplast Tissue Embedding Media, Thermo Fischer Scientific). 4 µm thick serial sections were cut from the cornea, stained with hematoxylin and eosin (H&E) and visualized with an Olympus BX51 inverted microscope. Corneal thickness measurements were taken from H&E-stained slides using open-source ImageJ (NIH) software.

4.3.12 *In Vivo* Rabbit Retention Study

9, thirty-week-old female New Zealand White rabbits (Charles River, Wilmington, Massachusetts, USA) were used to study the retention of various thermogel formulations with a range of mucoadhesive properties within the inferior fornix. One week prior to use, the nictitating membranes of the rabbits were surgically removed. To ensure sterility, the thermogel samples were UV treated for 12 hours prior to application. The rabbits were anesthetized with gaseous isoflurane before assessment of baseline corneal health by slit-lamp imaging, fluorescent staining, and OCT imaging. 50 µL of pNAM, CTS-pNAM or CTS-pNAMP-C2 was then placed into the inferior fornix of the rabbits using a 1 mL syringe while awake. The thermogels were then assessed every 24 hours to establish if altering the mucoadhesive properties resulted in improved retention within the inferior fornix.

4.3.13 *In Vivo* Rabbit Safety Study

To assess the safety of the developed thermogels when applied to the inferior fornix, an acute rabbit model was utilized. Following the retention study, the same 9-rabbit cohort, with removed nictitating membranes, received 50 µL of pNAM, CTS-pNAM or CTS-pNAMP-C2, applied to the inferior fornix, without anesthesia. After 24-hours, the study was stopped, and the ocular health of all animals was reassessed by slit-lamp imaging, fluorescent staining, and OCT imaging to evaluate any possible negative effects.

4.3.14 Statistical Analysis

Error bars represent the standard deviation. Student T-tests with two tailed distribution and unequal variance were utilized to compare paired OCT values. Single factor analysis of variance (ANOVA) followed by Tukey's post-hoc analysis was utilized to compare gel water content, LCSTs, and *in vivo* safety. Two-Way ANOVA with replication was utilized to compare rheological properties, degradation, and drug release.

4.4 Results and Discussion

4.4.1 Synthesis and Characterization of pNAMP

The composition of the base thermogelling polymer was determined utilizing ^{1}H NMR. The structure of pNAMP-3 is shown in Figure 4.2; the tertiary amine of the isopropyl tail of NIPAAm occurs at 3.84 ppm (A), the hydroxyl of AA at 12.0 ppm (B), the aromatic 2-MP of PDMSA as multiple peaks from 7.25-8.50 ppm (C-E) and the methyl tail of MMA as a doublet at 3.49 and 3.50 (F). The C and D peaks associated with PDSMA are not appropriate for integration due to the influence of the NH peak of NIPAAm in the same region. The composition of the polymers was determined by integrating peaks A, B, E, and F.

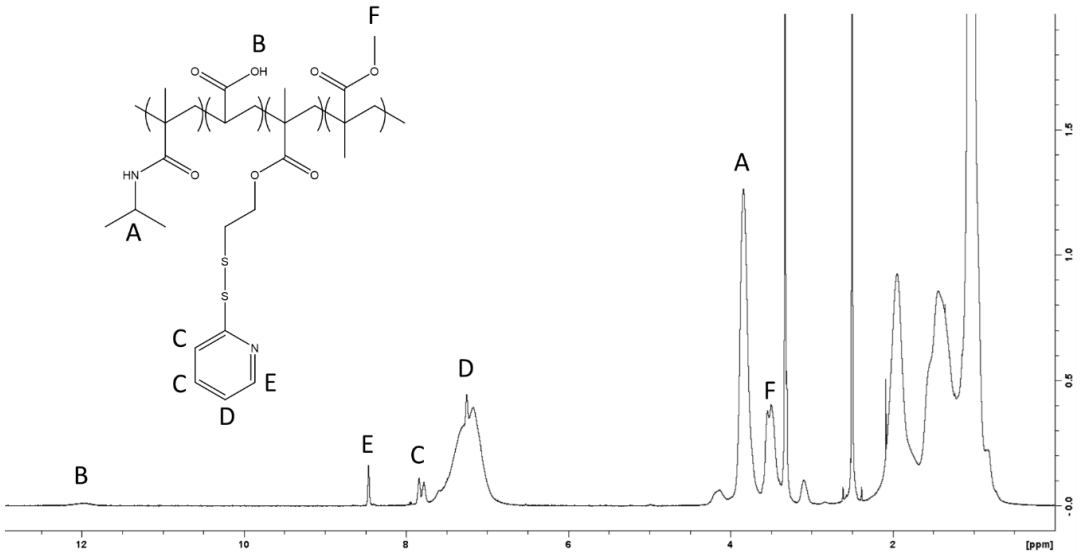

Figure 4.2) ^{1}H NMR analysis of developed base thermogelling pNAMP-3 tetrapolymer.

The composition, determined by ^{1}H NMR, and molecular weight, as determined by GPC, of the thermogels is listed in Table 4.1.

Table 4.1) Molecular Composition of pNAMP Polymers and Molecular Weights.

Polymer	Theoretical Composition	Determined Composition	Molecular Weight (kDA)	PDI
pNAM	88: 2: 10	86.9: 1.5: 11.6	57.7	1.9
pNAMP-1	87: 2: 10: 1	87.2: 1.5: 10.7: 0.6	60.7	3.0
pNAMP-2	86: 2: 10: 2	85.6: 1.5: 11.2: 1.7	49.7	3.0
pNAMP-3	85: 2: 10: 3	84.4: 1.6: 11.4: 2.6	43.3	3.3

4.4.2 Characterization of Chitosan Crosslinking

The crosslinking of chitosan to the base pNAM or pNAMP thermogel was accomplished by the covalent conjugation of the primary amines of chitosan to the carboxylic acids of AA through the carbodiimide crosslinker EDC. AA was incorporated into the base polymer backbone to facilitate crosslinking with chitosan. As the carboxylic acids of AA along the polymer backbone are conjugated to chitosan, the pH of the polymer networks increased. When dissolved at a concentration of 10% (wt/v) the base thermogelling polymers had a pH of 5.17, which is low due to the pKa of AA, while the chitosan crosslinked CTS-pNAM networks had a pH of 6.53. Of note, a pH of 6.53 is close to the maximum pH achievable for a chitosan-containing network without causing the precipitation of chitosan [32]. In this work, a chitosan concentration of 3% (wt/wt) chitosan/pNAMP was utilized because of the favorable mechanical and thermogelling properties established from previous work by the Sheardown lab [25]. From the previous investigation, a higher concentration of AA was incorporated into the base polymer backbone, 5 mol% compared to 2 mol%. This higher concentration of AA led to lower solution pH values for both the base and chitosan crosslinked thermogels. By lowering the amount of AA in the base polymer backbone, higher pH values were closer to physiologic.

4.4.3 Characterization of the Mucoadhesive Properties of the Produced CTS-pNAMP Thermogels

The rheological synergism of the thermogels is shown in Figure 4.3. Comparing the uncrosslinked polymers containing various concentrations of PDSMA, there was not a large impact of PDSMA concentration on mucoadhesive properties compared to base pNAM. Comparing base pNAM to CTS-pNAM, it is clear that the incorporation of chitosan improved the mucoadhesive properties by greater than a full order of magnitude. This result was expected as chitosan is well established to be mucoadhesive through charge interaction. By varying the concentration of PDSMA after chitosan crosslinking a further improvement of mucoadhesive properties was demonstrated. Both CTS-pNAMP-2 and CTS-pNAMP-3 increased the mucoadhesion by another full order of magnitude when compared to CTS-pNAM. CTS-pNAMP-1 did not significantly increase the mucoadhesion when compared to CTS-pNAM. Although changing the concentration of PDSMA in the base polymer did not have a significant impact on mucoadhesion, changing the concentration after crosslinking with chitosan did have a significant effect, showing that these two different mucoadhesive properties also display synergism when combined.

These results demonstrate that the mucoadhesive properties of these thermogels can be increased by incorporation of chitosan or the disulfide monomer PDSMA. In addition, the degree of mucoadhesion can be controlled by changing the concentration of these components. This an important result for designing a

material to be applied to the surface of the eye, or any other mucosal surface, as adhesion should directly impact retention. It is important to note that when utilizing rheological synergism, the properties had to be measured as mixed solutions rather than in the gel phase. Therefore, these results represent the maximum amount of mucoadhesion possible; the gels will likely display less adhesion due to the mucin bound to the surface rather than throughout the polymer matrix.

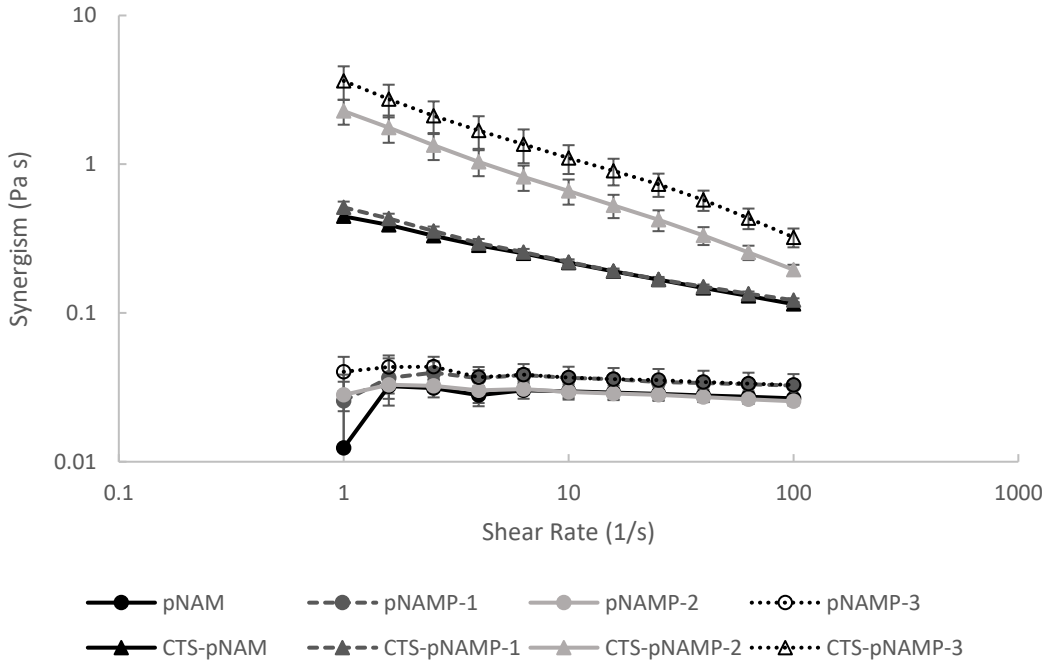

Figure 4.3) Mucoadhesive properties of the produced thermogels determined by rheological synergism. Incorporating disulfide linkages into the thermo-gel has a minimal effect on the measured mucoadhesion. Crosslinking with chitosan results in an order of magnitude increase in mucoadhesive performance. Combining chitosan crosslinking and disulfide linkages resulted in a synergistic effect between those components further increasing mucoadhesive properties. Data presented as mean ± SD (n = 3).

The degree of polymer interaction with mucin by disulfide bonding was measured through 2-MP evolution. The release of 2-MP occurs during the disulfide exchange reaction between the CTS-pNAMP and the residual cysteine residues of mucin. 2-MP forms a stable leaving group in polar solvents, such as water, which prevents further disulfide exchange from occurring and allows for simple quantification of the amount of 2-MP which leaves [33]. Comparing the amount of 2-MP released after mixing with mucin to that after mixing with mercaptoethanol yields an estimate for interaction. The value of 2-MP release is summarized in Table 4.2. From these results, at least half of the pyridine is released following incubation with mucin. The amount of 2-MP released did scale with the concentration of PDSMA in the polymer backbone (although the percent released did not), such that an increase in PDSMA results in an increase of disulfide bonding with mucin. It was found that just by varying the amount of PDSMA in the pNAMP backbone that a significant increase in mucoadhesion was not observed. A threshold value of interaction between conjugation or ionic interaction may be required to improve rheological synergism with the developed model. This would explain why varying PDSMA did not significantly increase mucoadhesion although crosslinking with chitosan and crosslinking with chitosan while varying PDSMA did significantly increase mucoadhesion. In this study a mucin solution was utilized for testing the rheologic synergism, utilizing a solution may yield a conservative estimate of mucoadhesion as the mucins are not forming a gel like structure.

Future studies will investigate utilizing harvested mucins from an animal source for testing mucoadhesive properties.

Table 4.2) Evolution of 2-MP from incubation with mucin compared to mercaptoethanol.

Thermogel	Pyridine Evolution (%)
pNAM	0
pNAMP-1	48.4
pNAMP-2	70.3
pNAMP-3	60.7

4.4.4 Determination of 2-MP Release Profile with Mucin

The amount of 2-MP produced from the thermogels is shown in Figure 4.4. From the analysis, it can be observed that in the gel phase, the disulfide bridging of the gel with mucin did not occur quickly, but rather occurred over several hours for detection to be possible. Furthermore, the release of 2-MP was sustained over the first three days before the release plateaued. As shown in Figure 4.4a the amount of 2-MP released across the gels was similar ranging from 6 to 10 µg. As shown in Figure 4.4b, the theoretical amount of 2-MP which was released was much greater, at 10%, for the material which contained the lowest molar concentration of the disulfide containing monomer (CTS-pNAMP-1) compared to CTS-pNAMP-3 at 2% theoretical release which contained the highest molar concentration of disulfide. The similarity between the release of 2-MP between the

three thermogels suggests that as mucin is bound to the surface, it may prevent all possible sites from reacting. Following the five-day study, the gels were recoverable from within the mucin core, even at temperatures below their LCST (data not shown). This result suggests that as mucin is covalently bound to the surface, it likely prevents the docking of lysozyme and subsequent degradation. Without degradation, a significant amount of possible disulfide bridging may not occur, accounting for the relatively low amount of theoretical 2-MP release.

Another key consideration is that Cystadrops®, the current most advanced treatment modality on the market for the treatment of cystinosis, contains 5.5 mg/mL of cysteamine. Based on an equal volume of 50 µL and applying the conservative 95% drug loss which is incurred with conventional eyedrops [34, 35], it can be approximated that less than 14 µg of cysteamine would reach the desired tissues for the treatment of cystinosis. This value is equivalent to our final 2-MP value following sustained release as measured by our *in vitro* release model, based on a single dose of each formulation. Furthermore, topical gels such as Cystadrops®, which contains carboxymethylcellulose as the viscous agent, can lead to blurring. It is approximated that formulation viscosities which are above 30 mPa.s lead to discomfort and patient non-compliance [10]. Given the high viscosity of the 5.5 mg/mL cysteamine Cystadrop® formulation [36], there is a significant benefit in utilizing a thermogel designed to be placed in the inferior fornix which will not impede patient vision or comfort.

In comparison with previous work by Jimenez et al. where cysteamine spray dried PLGA microparticles loaded in a pNIPAAm/PEG matrix, sustained release of up to 2.5 mg of cysteamine was observed over a 24-hour period [17]. Despite the differences in the amount of cysteamine released (2.5 mg over 24 hours versus 10 µg over 4 days), it is important to consider how much cysteamine penetrates the cornea as the system in this study measures release through mucin suspension, which is a considerable barrier. An *in vivo* pharmacokinetic (PK) study will be required to assess the release from these conjugated gels by disulfide bridging and intraocular penetration. There are important differences between an *in vivo* PK and an *in vitro* release study. The disulfide bridging of the gels is a function of thermogel surface area; in an eye, the gels produce thin films, which cup the ocular surface while in this release model, the gels form in a spherical shape when added to the mucin core. This change in surface-to-volume will lead to a lower release of 2-MP in the theoretical model compared to a clinical setting. Furthermore, this release study employs a much greater volume of mucin than that which would be encountered on the surface of the eye, which would trap 2-MP, significantly limiting the amount of drug released.

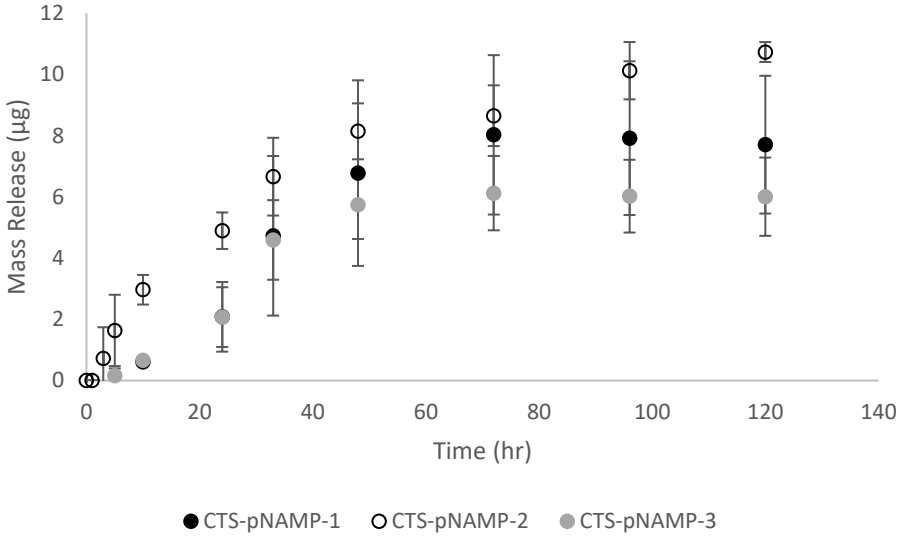

a)

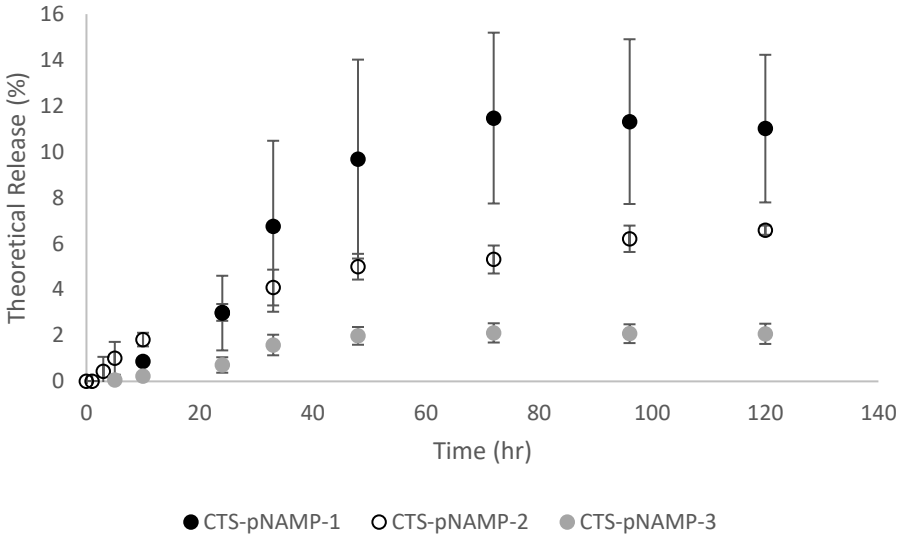

b)

Figure 4.4) Release of 2-MP over time from CTS-pNAMP-1, CTS-pNAMP-2, and CTS-pNAMP-3 in terms of a) ug and b) theoretical release measured by HPLC. A similar amount of 2-MP was released by the three formulations over 5 days. Data presented as mean ± SD (n = 3).

4.4.5 Characterization of Cysteamine Conjugation to CTS-pNAMP Thermogels

The chitosan-crosslinked CTS-pNAMP-3 and subsequent conjugation of cysteamine to produce CTS-pNAMP-C3 was characterized utilizing ^{1}H NMR and is shown in Figure 4.5. Successful conjugation of chitosan is shown in both spectra by the secondary amine peak at 2.83 ppm (A), although this peak was not utilized for quantification of chitosan. CTS-pNAMP-3 contains the aromatic peaks of 2-MP occurring at 7.27-8.37 ppm (B). The successful conjugation of cysteamine is visualized by the reduction of aromatic peaks as 2-MP is removed and the incorporation of the peaks at 2.95 (C) and 3.34 (D) ppm corresponding to carbons adjacent to the thiol and tertiary amine of cysteamine, respectively. The conjugation of cysteamine was also measured by absorbance due to the evolution of the stable 2-MP leaving group during disulfide-thiol exchange. The crosslinking of CTS-pNAMP-C by intra-polymer disulfide bridging is unlikely to occur. Despite the disulfide reaction being a dynamic covalent conjugation, following the reaction and subsequent purification there should be no free thiols which are unconjugated allowing for crosslinking by disulfide bridging.

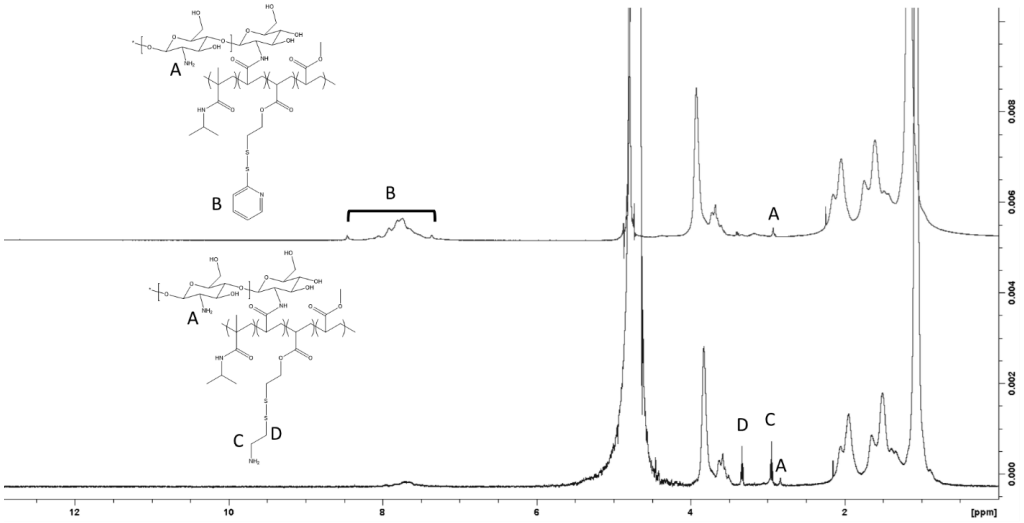

Figure 4.5) ^{1}H NMR analysis of CTS-pNAMP-3 (top) and CTS-pNAMP-C3 (bottom).

The LCST of the base pNAM and CTS-pNAM as well as the cysteamine modified thermogels was determined by temperature ramps. The LCST values are displayed in Figure 4.6a. For pNAM, CTS-pNAM, CTS-pNAMP-C1, CTS-pNAMP-C2, and CTS-pNAMP-C3 the LCSTs were determined as 24.5 ± 0.5, 25.5 ± 0.1, 25.1 ± 0.6, 26.0 ± 0.4, and 26.6 ± 0.4℃ respectively. The LCST of the thermogel increased after crosslinking with chitosan, although this was not significant (p = 0.085). Further conjugation of cysteamine after chitosan crosslinking resulted in an increased LCST; however, only CTS-pNAMP-C3 had a significantly higher LCST compared to CTS-pNAM while both CTS-pNAMP-C1 and CTS-pNAMP-C2 were not significantly different from CTS-pNAM. It was found that conjugating cysteamine up to 5% (CTS-pNAMP-C5) resulted in a thermogel with an LCST significantly higher than the 34℃ cutoff for the front of the eye (data not shown).

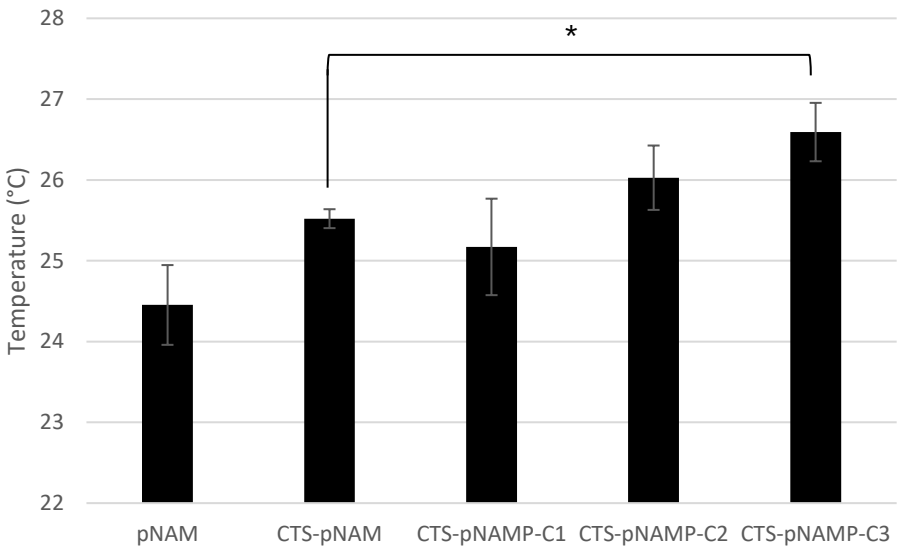
28
27
26
25
24
23
22
Temperature (°C)
*
pNAM
CTS-pNAM
CTS-pNAMP-C1
CTS-pNAMP-C2
CTS-pNAMP-C3

a)

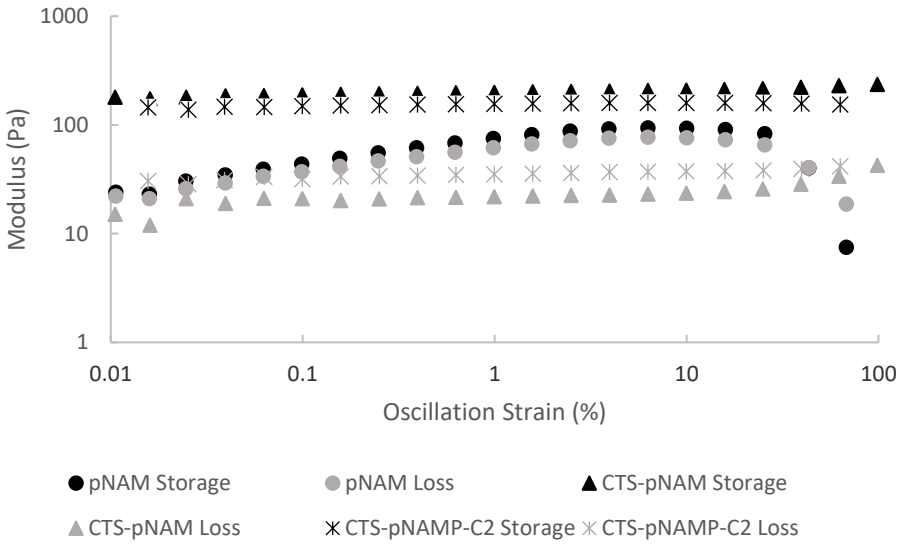
1000
100
10
1
Modulus (Pa)
0.01
0.1
1
10
100
Oscillation Strain (%)
pNAM Storage
pNAM Loss
CTS-pNAM Storage
CTS-pNAM Loss
CTS-pNAMP-C2 Storage
CTS-pNAMP-C2 Loss

b)

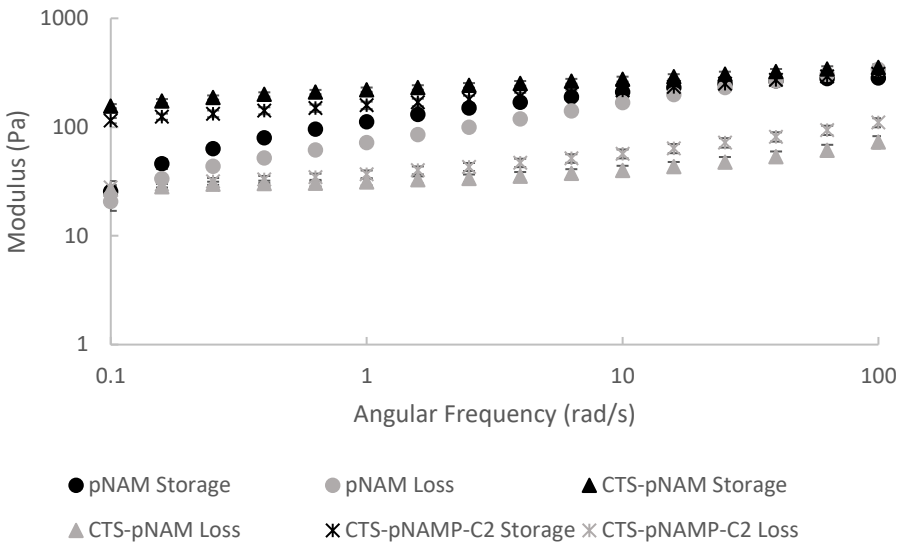
1000
100
10
1
Modulus (Pa)
0.1
1
10
100
Angular Frequency (rad/s)
pNAM Storage
pNAM Loss
CTS-pNAM Storage
CTS-pNAM Loss
CTS-pNAMP-C2 Storage
CTS-pNAMP-C2 Loss

c)

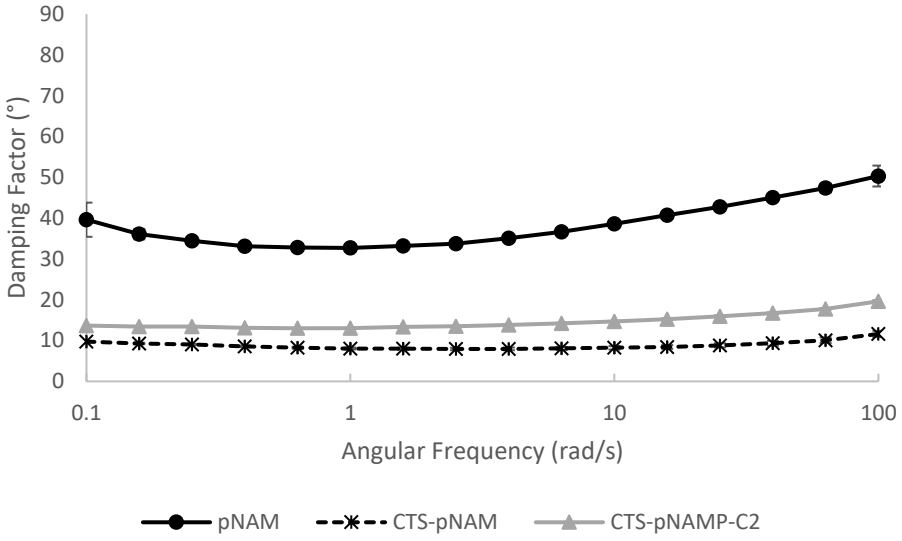
90
80
70
60
50
40
30
20
10
0
Damping Factor (°)
0.1
1
10
100
Angular Frequency (rad/s)
pNAM
CTS-pNAM
CTS-pNAMP-C2

d)

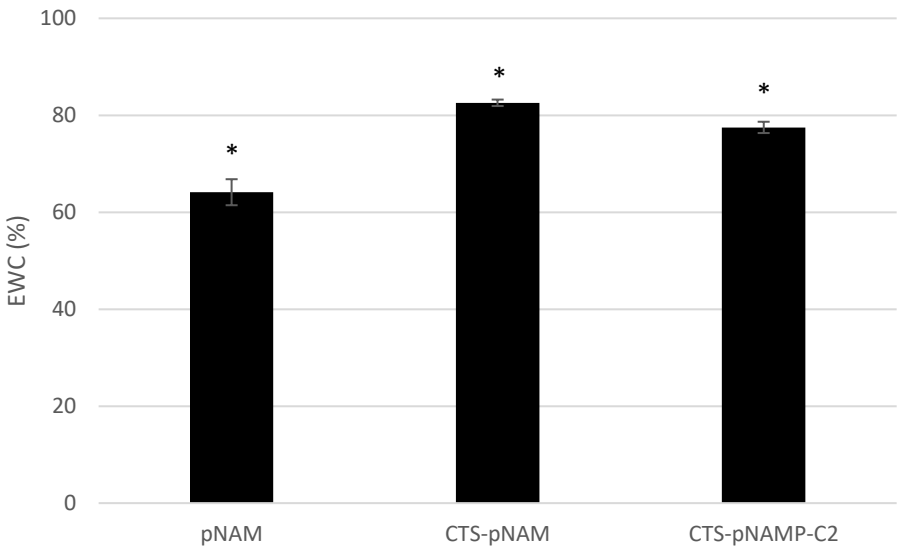

e)

Figure 4.6) Properties of the developed thermogels. a) Determination of thermogel LCST. Chitosan crosslinking did not result in a statistical difference in LCST ($p > 0.05$). Conjugation with 3% cysteamine did result in a significant change in LCST between CTS-pNAMP-C3 and CTS-pNAM ($p = 0.04$). Rheological analysis of pNAM, CTS-pNAM, and CTS-pNAMP-C2 with b) strain sweep analysis c) strain sweep analysis and d) damping factor as determined by frequency sweep analysis. From the strain sweep analysis, the linear viscoelastic region is increased following chitosan crosslinking. The damping factor of all the produced thermogels are significantly different ($p < 0.05$), crosslinking with chitosan results in approximately a third reduction in damping factor. e) EWC of pNAM, CTS-pNAM, and CTS-pNAMP-C2. EWC's were significantly different ($p < 0.05$) between the developed thermogels. Data presented as mean ± SD ($n = 3$), significance determined by single factor ANOVA analysis followed by Tukey's post-hoc analysis comparing the thermo-gels. '$*$' indicates significant difference ($p < 0.05$).

From the LCST analysis, conjugating cysteamine from 1-3% resulted in thermogels that had a transition temperature well below the 34℃ cutoff for the front of the eye. Therefore, any of these formulations could be used for the delivery of cysteamine in the treatment of cystinosis. Based on the measurement of mucoadhesive properties, formulations containing 2-3% of the disulfide monomer produce the greatest mucoadhesive effects. From the release studies, the release of the conjugate will likely be similar across different formulations. Cystadrops®, which are the current best formulation for sustained release, contains 5.5 mg/mL of cysteamine hydrochloride, which is equivalent to 3.8 mg/mL of cysteamine [5, 36]. Based on ^{1}H NMR, the formulation CTS-pNAMP-C2 contains approximately 3.9 mg/mL of cysteamine. Therefore, for further investigations CTS-pNAMP-C2 was focused on as the primary conjugate because it has a similar loading of cysteamine compared to the current industry standard while displaying high mucoadhesive properties.

4.4.6 Rheologic Properties of the Developed Thermogels

Strain sweeps and frequency sweeps were conducted on the pNAM, CTS-pNAM, and CTS-pNAMP-C2 thermogels to study the effect of chitosan crosslinking. The strain sweep analysis is shown in Figure 4.6b. From the strain sweep analysis, the base pNAM polymer failed after an applied oscillation strain of approximately 15% while the crosslinked CTS-pNAM and CTS-pNAMP-C2 did not fail up to 100% applied oscillation strain. For subsequent testing, an oscillation

strain of 0.1% was used as it was well within the linear viscoelastic region of both thermogels. Frequency sweeps were conducted to further assess the influence of chitosan crosslinking, as shown in Figure 4.6c. The uncrosslinked pNAM displays an increase in modulus with angular frequency while the properties of CTS-pNAM and CTS-pNAMP-C2 remained independent of angular frequency. The CTS-pNAM and CTS-pNAMP-C2 have greater modulus values compared to pNAM especially at lower angular frequencies. The damping factor (δ) was determined from storage (G') and loss (G'') modulus by equation 4.5:

$$4.5) \quad tan\delta = \frac{G''}{G'}$$

The damping factor relates modulus values to material behavior; when the damping factor approaches 90° the polymer behaves at an ideal viscosity and as the damping factor approaches 0° the material acts ideally elastic. The damping factor for pNAM and CTS-pNAM calculated from the frequency sweep is shown in Figure 4.6d. pNAM has an average damping factor of 38° compared to the 8° of CTS-pNAM and 14° of CTS-pNAMP-C2, illustrating that following chitosan crosslinking the thermogels behave much more elastically. Interestingly, following conjugation with cysteamine, CTS-pNAMP-C2 has a significantly higher damping factor than CTS-pNAM illustrating that the amount and type of material conjugated to disulfide bridges for delivery has an impact on material properties.

Our previous study examined the effect of chitosan crosslinking with a short chitosan crosslinker (10-50 kDa), and the subsequent rheologic properties. In this study utilizing a larger chitosan, 80-200 kDa, with a scaled concentration of the

EDC crosslinker, the resulting networks were found to have lower modulus values. From a previous study by the Sheardown lab, CTS-pNAM containing 3% (wt/wt) of the shorter chitosan had a storage and loss modulus of greater than 10 000 and 100 Pa, respectively. In the current study, which utilizes the larger molecular weight chitosan the storage and loss modulus are greater than 100 and 10 Pa, respectively [25]. This decrease in mechanical properties is attributable to the lower degree of crosslinking produced when using a larger molecular weight chitosan and keeping the moles of EDC per chitosan polymer constant. Importantly, thermogels produced through physical ionic interactions using the lower molecular weight chitosan had similar modulus values to those produced through EDC chemistry, a full order of magnitude greater than the thermogels produced in this study. Therefore, the physical properties of the chitosan, particularly the molecular weight, have a significant impact on mechanical properties.

4.4.7 EWC of the Thermogels

The EWC of pNAM, CTS-pNAM and CTS-pNAMP-C2 are shown in Figure 4.6e. Following chitosan crosslinking, CTS-pNAM and CTS-pNAMP-C2 have significantly greater EWC holding 82.5% and 77.5% of the water volume compared to 64.1% of pNAM without crosslinking. These materials underwent significantly more syneresis compared to our previously developed thermogels, which were close to fully totally volume retentive [25]. This result suggests that chitosan

properties, as well as the degree of crosslinking, plays a large role in gel syneresis. Interestingly, following conjugation of cysteamine the gels have a significantly lower EWC compared to no conjugation.

4.4.8 Degradation Profiles and Enzymatic Action

Figure 4.7 shows the degradation of pNAM, CTS-pNAM, and CTS-pNAMP-C2, in both PBS and PBS containing the physiological concentration of lysozyme. Both the chitosan crosslinked networks had a significantly greater extent of degradation following incubation with lysozyme. With both materials degradation plateaued after 4 days. Furthermore, following conjugation with cysteamine, the thermogels degraded to a lesser degree, approximately 50% less compared to the unconjugated chitosan crosslinked CTS-pNAM which degraded to less than 20%. This result may suggest that the conjugate may have a role in the degradation of the gels by lysozyme. It is also important to note that the uncrosslinked pNAM showed significant degradation compared to just PBS. None of the gels degraded beyond 50% when incubated in just PBS. The degradation noted in PBS is likely attributable to surface dissolution.

To further delineate the effect of lysozyme on the thermogels, the rheologic properties were measured following 48 hours of incubation (Figure 4.8). The viscosity of the pNAM solution was not significantly different at this time, whereas the CTS-pNAM and CTS-pNAMP-C2 solution viscosities were significantly reduced after incubation with lysozyme. From Figures 4.7 and 4.8, it can be

concluded that lysozyme had enzymatic interactions with CTS-pNAM and CTS-pNAMP-C2, but not pNAM.

For pNAM, the degradation noted by lysozyme likely has to do with the charge interaction between positively charged lysozyme and negatively charged pNAM. As hydrophilic lysozyme associates with and penetrates the pNAM thermogel, it increases the LCST, causing rapid overall degradation. Incubating pNAM with lysozyme results in a small, but insignificant, increase in viscosity attributable to charge interaction. For CTS-pNAM and CTS-pNAMP-C2, consistent loss of mass is observed during testing. Furthermore, the chitosan-crosslinked gels resulted in a significant, near full order of magnitude, reduction of viscosity following incubation with lysozyme.

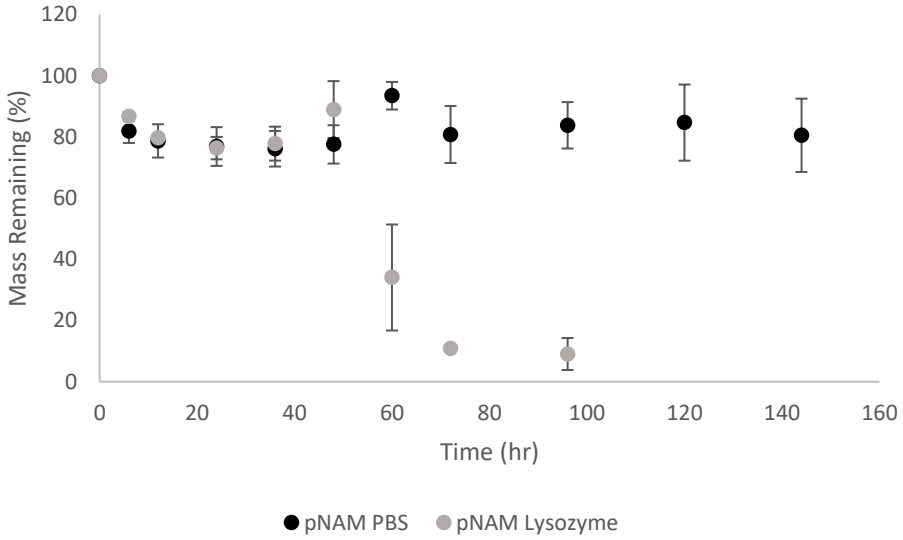

a)

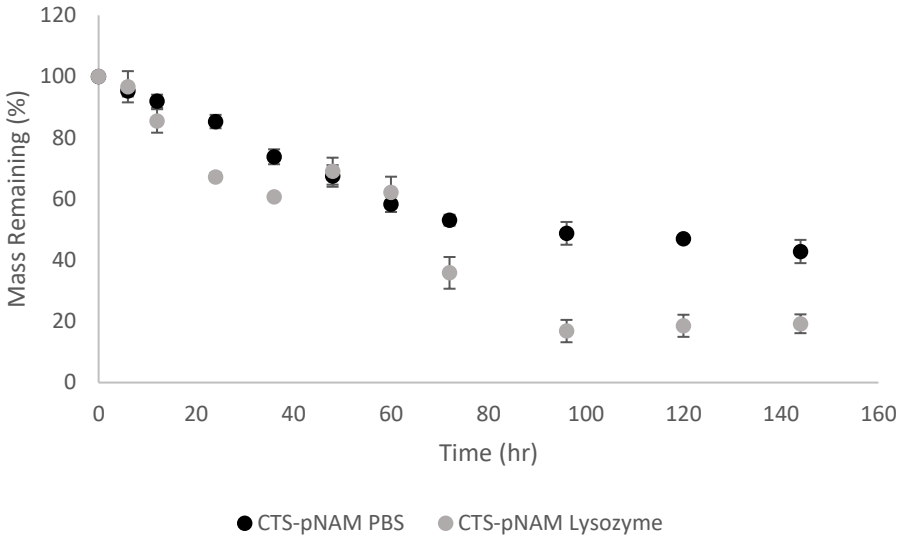

b)

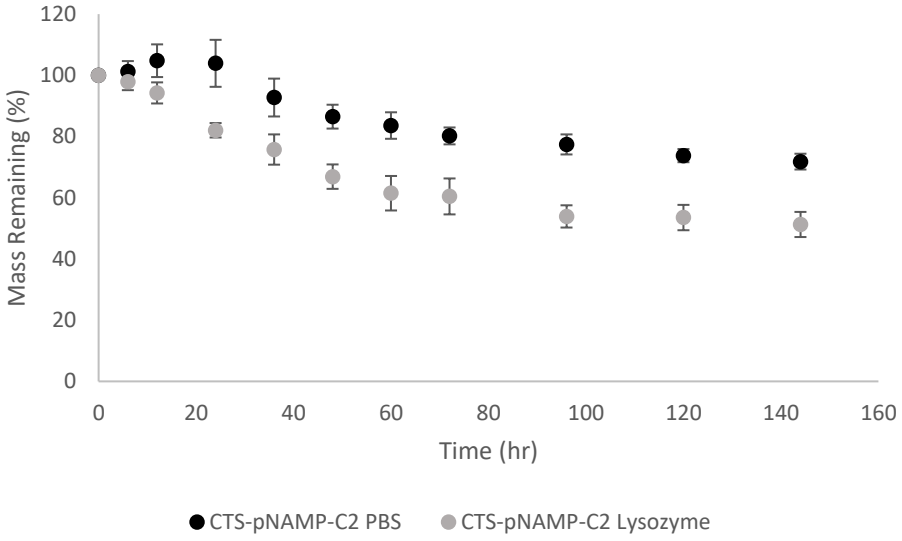

c)

Figure 4.7) Degradation of a) pNAM, b) CTS-pNAM, or c) CTS-pNAMP-C2 in either PBS or in PBS containing the physiologic concentration of lysozyme. All the thermogels demonstrated a significant increase in degradation following incubation with lysozyme ($p < 0.05$). Data presented as mean ± SD ($n = 3$), significance determined by two-way ANOVA analysis comparing incubation with or without lysozyme.

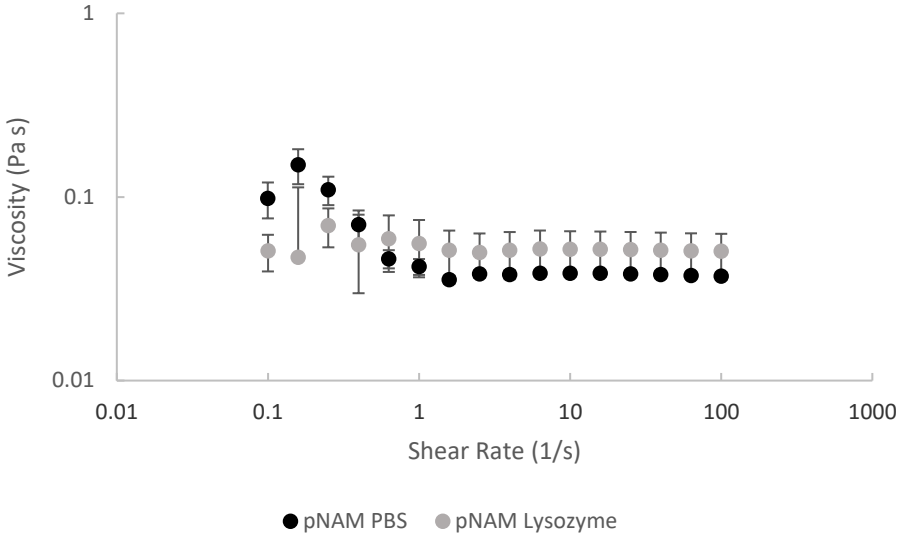
1
0.1
0.01
Viscosity (Pa s)
0.01
0.1
1
10
100
1000
Shear Rate (1/s)
pNAM PBS
pNAM Lysozyme

a)

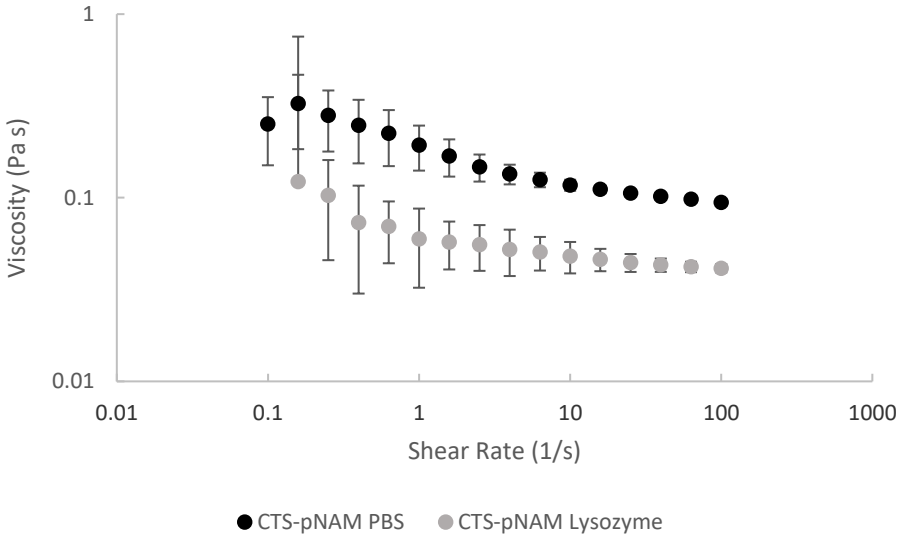
1
0.1
0.01
Viscosity (Pa s)
0.01
0.1
1
10
100
1000
Shear Rate (1/s)
CTS-pNAM PBS
CTS-pNAM Lysozyme

b)

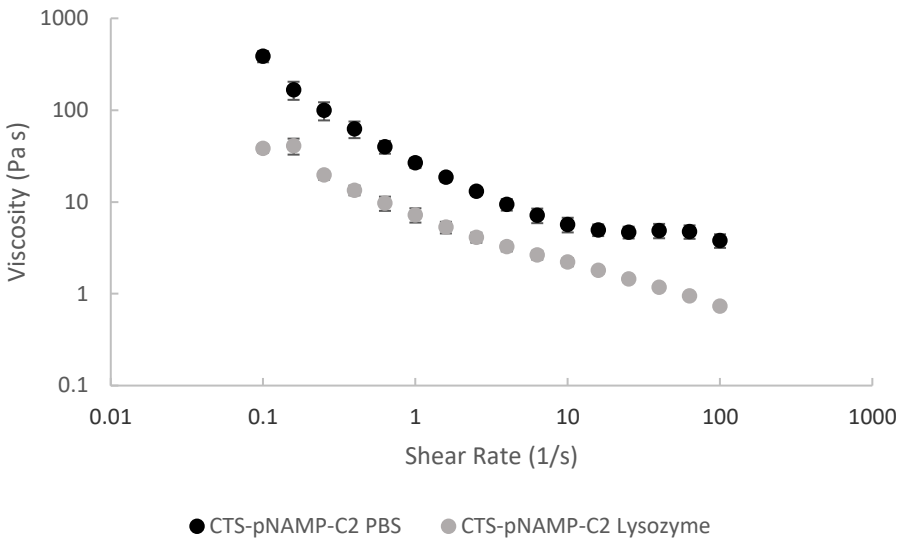

c)

Figure 4.8) Rheologic determination of thermogel degradation by lysozyme a) pNAM, b) CTs-pNAM, and d) CTS-pNAMP-C2. No statistical difference was observed for pNAM ($p > 0.05$) while the viscosity of CTS-pNAM and CTS-pNAMP-C2 was significantly lower ($p < 0.05$) following lysozyme incubation. Data presented as mean ± SD ($n = 3$), significance determined by two-way ANOVA analysis comparing incubation with or without lysozyme.

Compared to the previous study, using a chitosan crosslinker with a higher molecular weight, while keeping the amount of EDC added constant, resulted in enzymatic degradation by lysozyme while a lower chitosan molecular weight did not result in degradation [25]. This agrees with the results in the literature [37, 38]. From previous research, utilizing a higher molecular weight chitosan promotes lysozyme mediated degradation, likely attributable to promoting lysozyme docking by reducing the number of crosslinks between chitosan and the base pNAM polymer. It is important to consider that concentration of lysozyme may be reduced

for individuals suffering from cystinosis which may have an effect on the degradation rate of the developed thermogels. An *in vivo* study would be required to verify if there is a change in degradation rate.

4.4.9 *In Vivo* Safety Analysis

The safety and tolerability of the pNAM, CTS-pNAM, and CTS-pNAMP-C2 thermogels was evaluated using a rat model. 10 µL of each gel was applied to the cornea of the rats once a day for one week. During the study the thickness of the rat corneas was measured by OCT (Figure 4.9a). It was found that were was no statistical difference ($p > 0.05$) in corneal thickness between thermogel groups and PBS controls at a given time interval. There was also no statistical difference ($p > 0.05$) comparing thermogel treatment to the respective baseline measurement. Following the one-week trial, the rats were euthanized, and the eyes collected for histological analysis. The H&E-stained tissues (Figure 4.9b) showed no statistical difference in corneal thickness, nor was there any appearance of corneal damage or infiltration of inflammatory cells within the anterior chamber. It is clear therefore, that these thermogels are well tolerated on the ocular surface. However, a larger animal model was required to test application to the inferior fornix.

a)

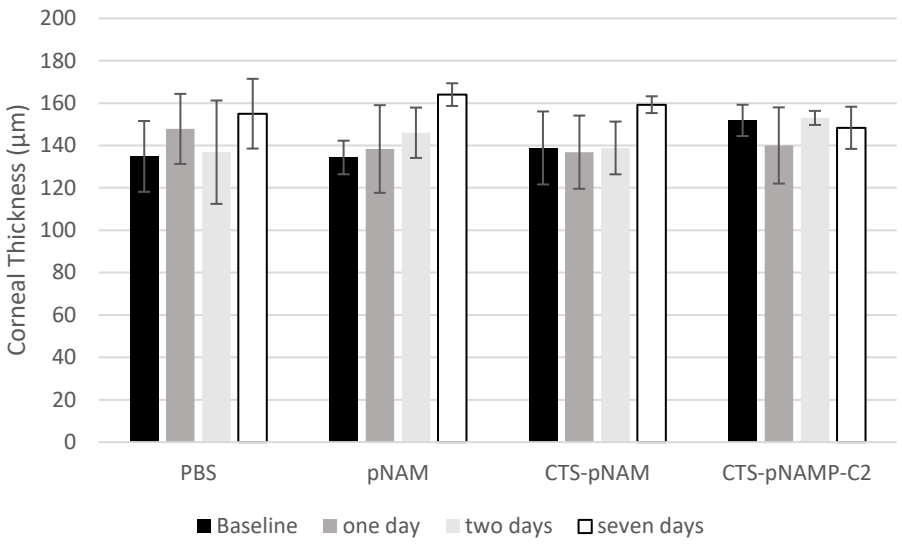

b)

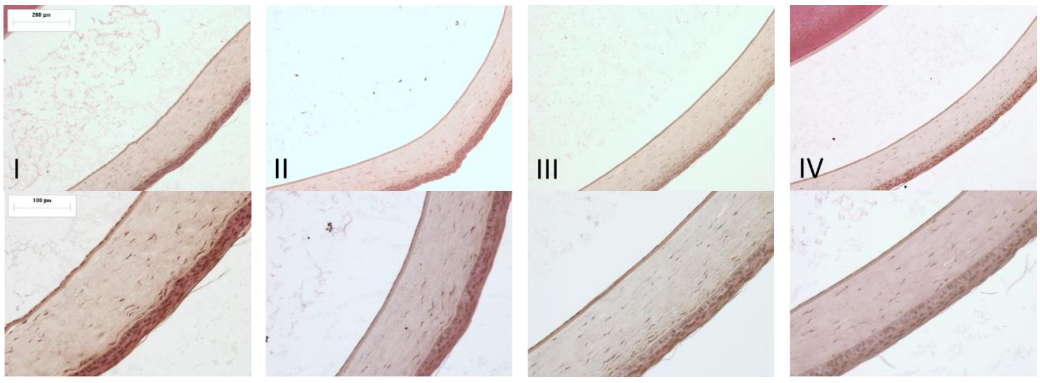

Figure 4.9a) Rat corneal thickness over one week trial as determined by OCT measurement. No statistical difference ($p > 0.05$) in corneal thickness comparing to PBS controls or baseline measurements. Data presented as mean ± SD ($n = 6$), significance determined by single factor ANOVA analysis followed by Tukey's post-hoc analysis comparing the thermo-gels. b) H&E-stained corneas following one-week daily application of PBS (I), pNAM (II), CTS-pNAM (III), and CTS-pNAMP-C2 (III) to rat corneal surfaces. Top images are 10x magnificent (scale bars 200 µm) and bottom images are 10x magnificent (scale bars 100 µm). No damage to the cornea, or infiltration of inflammatory cells to the anterior chamber was observed.

4.4.10 Rabbit *In Vivo* Retention Study

Representative images of the retention of the thermogels in the inferior fornix of the rabbits is shown in Figure 4.10. Approximately 50 µL of each gel variation was applied to inferior fornix of the unsedated rabbits. For each material, three rabbits were utilized with 5 eyes receiving a dosage and one eye remaining as a control. After 24 hours, two pNAM, three CTS-pNAM and 1 CTS-pNAMP-C2 gel remained within the fornix. After 72 hours only one CTS-pNAM gel remained retained from the entire trial. The greatest retention noted among all trials was 96 hours. As it can be seen in Figure 4.10, shifting of the gels was noted over time for those that remained within the eye. Though the experiment was conducted several times with varying approaches, similar retention results were documented each time. However, based on observations, this was a function of animal behavior with losses due to grooming rather than blinking, despite attempts to hold the eyelids shut. Interestingly removal of the nictitating membrane helped but did not alleviate the problem of removal. Therefore, although the model demonstrated successful retention up to four days, it was not able to delineate whether modulating mucoadhesive properties influenced thermogel retention. Other studies have been able to show long term retention of thermogels with the inferior fornix up to two weeks [39] or one month [40]. Future studies will look to investigate retention utilizing a model which minimizes behavioral effects.

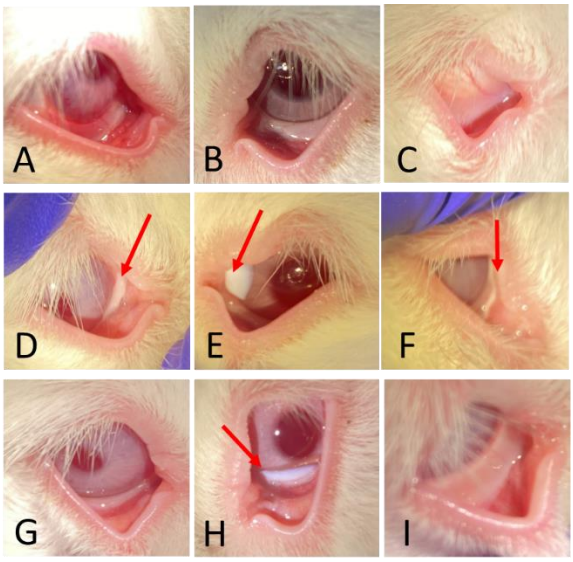

Figure 4.10) Representative images of thermogel retention within the inferior fornix of rabbits. Images were taken for baseline (A-C), 24 hours after application (D-F) and 72 hours after application (G-I). Animals were treated with pNAM (A, D, and G), CTS-pNAM (B, E, and H), or CTS-pNAMP-C2 (C, F, and I). After 24 hours 6 of the 15 applied gels were retained within the inferior fornix. After 72 hours one of the applied gels was retained.

4.4.11 Rabbit *In Vivo* Acute Toxicity Study

To assess the impact of the thermogels on ocular health, the rabbit models were assessed 24 hours post instillation. Approximately 50 µL of each gel variation was applied to inferior fornix of the rabbits while awake. For each material three rabbits were used with 5 eyes receiving a dosage and one eye remaining as a control. Slit-lamp, fluorescent staining, and OCT imagery were completed to assess ocular health. A 24-hour study was used based on the retention study. The baseline images utilized represent ocular health one week following nictitating

membrane removal and prior to any thermogel application. Figure 4.11a shows representative images of the baseline and 24-hours after treatment of the thermogels to the inferior fornix. From the images, the gels do not negatively impact corneal health or increase staining. Figure 4.11b shows the corneal thickness of all treated eyes as measured by OCT. It was found that there was no statistical change ($p > 0.05$) in corneal thickness with thermogel instillation, except for pNAM which was significantly thicker ($p = 0.02$) increasing from 361 ± 6 µm to 372 ± 6 µm after 24-hours. This approximately 3% thickening for the cornea following pNAM treatment is not likely attributable to an immunological response or damage but natural changes which occur over the day. Overall, the acute rabbit model demonstrated that the gels are not toxic. Future studies will focus on safety for a longer duration. Based on our retention results, to best assess safety while retaining all of the applied gels, a tarsorrhaphy procedure may need to be utilized [41].

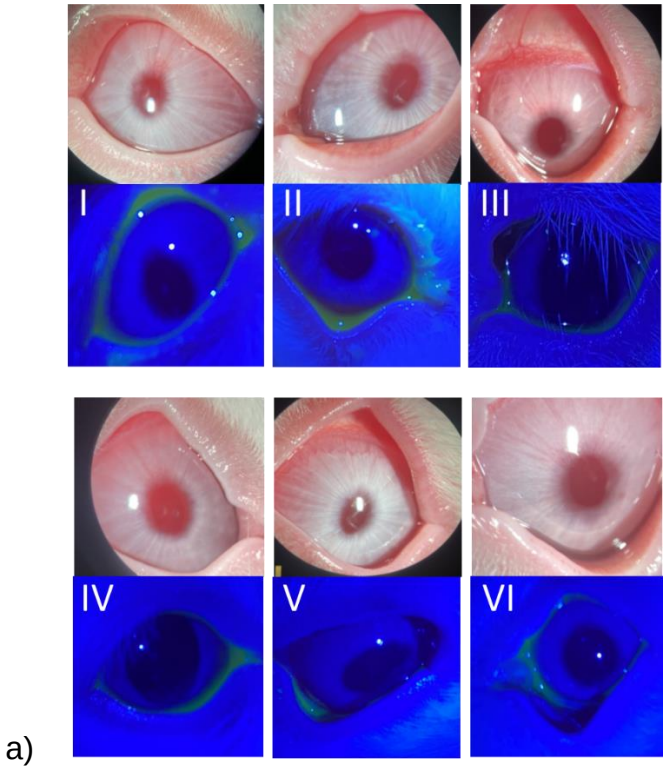

a)

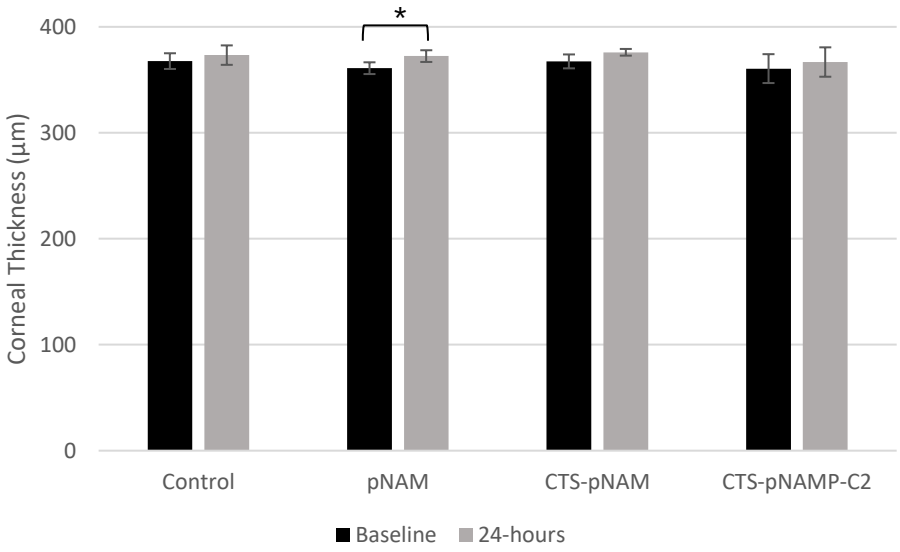

b)

Figure 4.11a) Representative slit lamp and fluorescein staining images of ocular health before (I-III) and after 24-hour treatment with developed thermogels (IV-VI). Animals were treated with pNAM (I and IV), CTS-pNAM (II and V), and CTS-pNAMP-C2 (III and VI). No

negative impacts on corneal health were observed. b) OCT analysis of corneal thickness before and after 24-hour application of developed thermogels to the inferior fornix of rabbits. The corneal thickness was not significantly different ($p > 0.05$) following thermogel application except for pNAM ($p = 0.02$). Data presented as mean ± SD ($n = 3$ for control and $n = 5$ for a given thermogel), significance determined by Student T-test analysis using a two tailed distribution and unequal variance comparing the corneal thickness for a group between the two time points. '$*$' indicates significant difference ($p < 0.05$).

4.5 Conclusions

A platform mucoadhesive thermogel was designed for application to mucosal surfaces. By incorporating the mucoadhesive monomer PDSMA into a base thermogel and then subsequently crosslinking with chitosan, the mucoadhesive properties could be tailored. Using an incorporated preactivated thiomer, the materials were conjugated with cysteamine with a goal of treating cystinosis. By conjugating cysteamine into the system, oxidation can be prevented, which would increase the shelf life and remove the need for acidic salts, creating a solution with a pH much closer to physiologic. A large range of tailorable mucoadhesive properties were displayed, with the conservative release model demonstrated a sustained release of 6 to 10 µg of 2-MP over a 4-day period. The chitosan crosslinked thermogels were shown to be enzymatically degradable by lysozyme through gravimetric and rheological analysis. This illustrates that the novel thermogelling system can be applied to mucosal systems and display both adhesion and site-specific degradation by lysozyme. Extensive *in vivo* studies

were conducted to evaluate the safety and retention of the gels. In rabbits, it was demonstrated that the gels can be retained up to four days, though retention was found to be largely affected by animal behavior. Both the one-week rat and 24-hour rabbit safety studies demonstrated the safety of the materials with no adverse effects documented over the testing period. Further studies are required to assess this platform technology with other conjugates to treat various diseases. Besides therapeutic payloads, future studies will examine creating materials with tailorable rheologic properties as well as gels capable of acting as cellular scaffolds.

Data Availability

The raw/processed data required to reproduce these findings cannot be shared at this time as the data also forms part of an ongoing study.

CRediT authorship contribution statement

Mitchell Ross: Conceptualization, Methodology, Data curation, Formal analysis, Investigation, Validation, Writing – original draft. **Jonathan Mofford:** Methodology, Investigation. **Jennifer Tian:** Investigation. **Benjamin Muirhead:** Methodology, Investigation. **Emily Anne Hicks:** Methodology, Investigation. **Lindsay Sheardown:** Investigation. **Heather Sheardown:** Conceptualization, Supervision, Writing – review & editing.

4.6 Acknowledgements

We acknowledge The Natural Sciences and Engineering Research Council of Canada (NSERC Discovery) and Ontario Research Fund (C20/20 ORF-RE Round 8) for funding this research.

4.7 References

[1] I. MacDonald, P. Haney, and M. Musarella, "Summary of ocular genetic disorders and inherited systemic conditions with eye findings," *Ophthalmic genetics,* vol. 19, no. 1, pp. 1-17, 1998.

[2] T. Rosenberg, "Epidemiology of hereditary ocular disorders," *Genetics in ophthalmology,* vol. 37, pp. 16-33, 2003.

[3] G. Nesterova and W. A. Gahl, "Cystinosis: the evolution of a treatable disease," *Pediatric nephrology,* vol. 28, no. 1, pp. 51-59, 2013.

[4] M. A. Elmonem, K. R. Veys, N. A. Soliman, M. van Dyck, L. P. van den Heuvel, and E. Levtchenko, "Cystinosis: a review," *Orphanet journal of rare diseases,* vol. 11, no. 1, pp. 1-17, 2016.

[5] S. Biswas, M. Gaviria, L. Malheiro, J. P. Marques, V. Giordano, and H. Liang, "Latest clinical approaches in the ocular management of cystinosis: a review of current practice and opinion from the Ophthalmology Cystinosis Forum," *Ophthalmology and therapy,* vol. 7, no. 2, pp. 307-322, 2018.

[6] A. K. Makuloluwa and F. Shams, "Cysteamine hydrochloride eye drop solution for the treatment of corneal cystine crystal deposits in patients with cystinosis: an evidence-based review," *Clinical Ophthalmology (Auckland, NZ),* vol. 12, p. 227, 2018.

[7] N. Huynh, W. A. Gahl, and R. J. Bishop, "Cysteamine ophthalmic solution 0.44% for the treatment of corneal cystine crystals in cystinosis," *Expert Review of Ophthalmology,* vol. 8, no. 4, pp. 341-345, 2013.

[8] A. Labbé *et al.*, "A new gel formulation of topical cysteamine for the treatment of corneal cystine crystals in cystinosis: the Cystadrops OCT-1 study," *Molecular genetics and metabolism,* vol. 111, no. 3, pp. 314-320, 2014.

[9] S. Bozdağ, K. Gümüş, Ö. Gümüş, and N. Ünlü, "Formulation and in vitro evaluation of cysteamine hydrochloride viscous solutions for the treatment of corneal cystinosis," *European journal of pharmaceutics and biopharmaceutics,* vol. 70, no. 1, pp. 260-269, 2008.

[10] B. McKenzie, G. Kay, K. H. Matthews, R. Knott, and D. Cairns, "Preformulation of cysteamine gels for treatment of the ophthalmic complications in cystinosis," *International journal of pharmaceutics,* vol. 515, no. 1-2, pp. 575-582, 2016.

[11] B. Buchan, G. Kay, A. Heneghan, K. H. Matthews, and D. Cairns, "Gel formulations for treatment of the ophthalmic complications in cystinosis," *International journal of pharmaceutics,* vol. 392, no. 1-2, pp. 192-197, 2010.

[12] A. Luaces-Rodríguez *et al.*, "Cysteamine polysaccharide hydrogels: study of extended ocular delivery and biopermanence time by PET imaging," *International journal of pharmaceutics,* vol. 528, no. 1-2, pp. 714-722, 2017.

[13] P. Dixon, K. Christopher, S. Hazra, N. Maity, C. Plummer, and A. Chauhan, "In vitro and ex vivo implantation of cystine crystals and treatment by contact lens," *Colloids and Surfaces A: Physicochemical and Engineering Aspects,* vol. 562, pp. 229-236, 2019.

[14] P. Dixon, R. C. Fentzke, A. Bhattacharya, A. Konar, S. Hazra, and A. Chauhan, "In vitro drug release and in vivo safety of vitamin E and cysteamine loaded contact lenses," *International journal of pharmaceutics,* vol. 544, no. 2, pp. 380-391, 2018.

[15] K.-H. Hsu, R. C. Fentzke, and A. Chauhan, "Feasibility of corneal drug delivery of cysteamine using vitamin E modified silicone hydrogel contact lenses," *European Journal of Pharmaceutics and Biopharmaceutics,* vol. 85, no. 3, pp. 531-540, 2013.

[16] D. C. Marcano *et al.*, "Synergistic cysteamine delivery nanowafer as an efficacious treatment modality for corneal cystinosis," *Molecular pharmaceutics,* vol. 13, no. 10, pp. 3468-3477, 2016.

[17] J. Jimenez, M. A. Washington, J. L. Resnick, K. K. Nischal, and M. V. Fedorchak, "A sustained release cysteamine microsphere/thermoresponsive gel eyedrop for corneal cystinosis improves drug stability," *Drug Delivery and Translational Research,* pp. 1-15, 2021.

[18] H. J. Davidson and V. J. Kuonen, "The tear film and ocular mucins," *Veterinary ophthalmology,* vol. 7, no. 2, pp. 71-77, 2004.

[19] R. S. Dave, T. C. Goostrey, M. Ziolkowska, S. Czerny-Holownia, T. Hoare, and H. Sheardown, "Ocular drug delivery to the anterior segment using nanocarriers: A mucoadhesive/mucopenetrative perspective," *Journal of Controlled Release,* 2021.

[20] C. Menzel, M. Jelkmann, F. Laffleur, and A. Bernkop-Schnürch, "Nasal drug delivery: design of a novel mucoadhesive and in situ gelling polymer," *International journal of pharmaceutics,* vol. 517, no. 1-2, pp. 196-202, 2017.

[21] C. Federer, M. Kurpiers, and A. Bernkop-Schnürch, "Thiolated chitosans: a multi-talented class of polymers for various applications," *Biomacromolecules,* vol. 22, no. 1, pp. 24-56, 2020.

[22] S.-J. Hwang, H. Park, and K. Park, "Gastric retentive drug-delivery systems," *Critical Reviews™ in Therapeutic Drug Carrier Systems,* vol. 15, no. 3, 1998.

[23] A. Bernkop-Schnürch, V. Schwarz, and S. Steininger, "Polymers with thiol groups: a new generation of mucoadhesive polymers?," *Pharmaceutical research,* vol. 16, no. 6, pp. 876-881, 1999.

[24] J. Iqbal, G. Shahnaz, S. Dünnhaupt, C. Müller, F. Hintzen, and A. Bernkop-Schnürch, "Preactivated thiomers as mucoadhesive polymers for drug delivery," *Biomaterials,* vol. 33, no. 5, pp. 1528-1535, 2012.

[25] M. Ross, E. A. Hicks, T. Rambarran, and H. Sheardown, "Thermo-sensitivity and erosion of chitosan crosslinked pNAM hydrogel based eyedrops for application to the inferior fornix," *Acta Biomaterialia - Under Review,* 2021.

[26] R. Dajani *et al.*, "Lysozyme secretion by submucosal glands protects the airway from bacterial infection," *American journal of respiratory cell and molecular biology,* vol. 32, no. 6, pp. 548-552, 2005.

[27] N. Boehnke, *Degradable Hydrogels and Nanogels for the Delivery of Cells and Therapeutics*. University of California, Los Angeles, 2017.

[28] X. Huang, D. Appelhans, P. Formanek, F. Simon, and B. Voit, "Tailored synthesis of intelligent polymer nanocapsules: an investigation of controlled permeability and pH-dependent degradability," *ACS nano,* vol. 6, no. 11, pp. 9718-9726, 2012.

[29] S. Rossi, B. Vigani, M. C. Bonferoni, G. Sandri, C. Caramella, and F. Ferrari, "Rheological analysis and mucoadhesion: A 30 year-old and still active combination," *Journal of pharmaceutical and biomedical analysis,* vol. 156, pp. 232-238, 2018.

[30] H. Hägerström and K. Edsman, "Limitations of the rheological mucoadhesion method: the effect of the choice of conditions and the rheological synergism parameter," *European journal of pharmaceutical sciences,* vol. 18, no. 5, pp. 349-357, 2003.

[31] D. Ivarsson and M. Wahlgren, "Comparison of in vitro methods of measuring mucoadhesion: Ellipsometry, tensile strength and rheological measurements," *Colloids and Surfaces B: Biointerfaces,* vol. 92, pp. 353-359, 2012.

[32] C. K. Pillai, W. Paul, and C. P. Sharma, "Chitin and chitosan polymers: Chemistry, solubility and fiber formation," *Progress in polymer science,* vol. 34, no. 7, pp. 641-678, 2009.

[33] P. Beak, J. B. Covington, S. G. Smith, J. M. White, and J. M. Zeigler, "Displacement of protomeric equilibriums by self-association: hydroxypyridine-pyridone and mercaptopyridine-thiopyridone isomer pairs," *The Journal of Organic Chemistry,* vol. 45, no. 8, pp. 1354-1362, 1980.

[34] D. Achouri, K. Alhanout, P. Piccerelle, and V. Andrieu, "Recent advances in ocular drug delivery," *Drug development and industrial pharmacy,* vol. 39, no. 11, pp. 1599-1617, 2013.

[35] O. L. Lanier *et al.*, "Review of approaches for increasing ophthalmic bioavailability for eye drop formulations," *Aaps Pharmscitech,* vol. 22, no. 3, pp. 1-16, 2021.

[36] H. Liang, A. Labbé, J. Le Mouhaër, C. Plisson, and C. Baudouin, "A new viscous cysteamine eye drops treatment for ophthalmic cystinosis: an open-label randomized comparative phase III pivotal study," *Investigative Ophthalmology & Visual Science,* vol. 58, no. 4, pp. 2275-2283, 2017.

[37] J. Li, Y. Du, and H. Liang, "Influence of molecular parameters on the degradation of chitosan by a commercial enzyme," *Polymer Degradation and Stability,* vol. 92, no. 3, pp. 515-524, 2007.

[38] K. Tomihata and Y. Ikada, "In vitro and in vivo degradation of films of chitin and its deacetylated derivatives," *Biomaterials,* vol. 18, no. 7, pp. 567-575, 1997.

[39] L.-J. Luo, D. D. Nguyen, and J.-Y. Lai, "Long-acting mucoadhesive thermogels for improving topical treatments of dry eye disease," *Materials Science and Engineering: C,* vol. 115, p. 111095, 2020.

[40] M. V. Fedorchak, I. P. Conner, J. S. Schuman, A. Cugini, and S. R. Little, "Long term glaucoma drug delivery using a topically retained gel/microsphere eye drop," *Scientific reports,* vol. 7, no. 1, pp. 1-11, 2017.

[41] C. Anderson, S. Moretti, and R. G. Gieser, "The effect of tarsorrhaphy on normal healing of corneal epithelial defects in a rabbit model," *Cornea,* vol. 10, no. 6, pp. 478-482, 1991.

CHAPTER 5 – Mucoadhesive thermogel platform for treating anterior ocular conditions.

Submitted Manuscript:

Mitchell Ross, Lindsay Sheardown, Benjamin Muirhead, Jonathan Mofford, Jennifer JingYuan Tian, and Heather Sheardown. Submitted to Journal of Controlled Release on November 4th 2022.

Objectives:

To design a mucoadhesive and degradable thermogel for application to the inferior fornix of the eye. Explore the effect of conjugating prodrugs, peptides (and proteins), and property modifiers on thermogel performance and *in vivo* safety. Test the ability to release drugs both by diffusion and mucosal interaction.

Author Contributions:

Material development, testing, and subsequent reporting was completed by Mitchell Ross aided by Lindsay Sheardown. All listed co-authors contributed to *in vivo* rabbit testing.

Mucoadhesive thermogel platform for treating anterior ocular conditions

Mitchell Ross, Lindsay Sheardown, Benjamin Muirhead, Jonathan Mofford, Jennifer (JingYuan) Tian, and Heather Sheardown.

Department of Chemical Engineering, McMaster University, 1280 Main St W, Hamilton, ON L8S 4L8, Canada

Corresponding Author:
Heather Sheardown, sheardow@mcmaster.ca (905) 525-9140, John Hodgins Engineering Building Room 260, 1280 Main St W, Hamilton, ON L8S 4L7

Declaration of Interest

The work which has been reported herein is covered by the patent Polymer System for Ophthalmic Drug Delivery pending to authors Mitchell Ross and Heather Sheardown. The authors declare that there are no further declarations of interest.

Highlights

- Development of a natively degradable and mucoadhesive thermogel platform for application to the inferior fornix in treating anterior ocular diseases.

- The thermogel platform was conjugated with a model prodrug, peptide, and a material property modifier.
- The sustained release of loaded atropine was studied over five days with linear release over the first eight hours and plateauing of the release after one day.
- The developed thermogel formulation can be reformulated with different conjugates and loaded drugs for any mucosal surface in the body.

Abbreviations

AA, acrylic acid; Abs, absorbance; ANOVA, single factor analysis of variance; BPO, benzoyl peroxide; CTS, chitosan; DCM, dichloromethane; DED, dry eye disease; DMSO, dimethyl sulfoxide; EDC, 1-ethyl-3-(3-dimethylaminopropyl)carbodiimide; EWC, equilibrium water content; H&E, hematoxylin and eosin; HPLC, high performance liquid chromatography; LCST, lower critical solution temperature; LVE, linear viscoelastic region; MES, 2-(N-Morpholino)ethanesulfonic acid; MMA, methyl methacrylate; MTT, 3-(4,5-dimethylthiazol-2-yl)-2,5-diphenyltetrazolium bromide; NAC, n-acetyl cysteine; NMR, nuclear magnetic resonance; OCT, optical coherence tomography; PBS, phosphate buffered saline; PDSMA, pyridyl disulfide ethylmethacylate; PEG, polyethylene glycol; pNAMP, poly(N-isopropylacrylamide-co-acrylic acid-co-methyl methacrylate-co-pyridyl disulfide ethylmethacrylate); pNIPAAm, n-isopropylacrylamide; SD, standard deviation; THF, tetrahydrofuran.

Key words

Thermogels, mucoadhesion, sustained drug release, atropine, degradation, inferior fornix

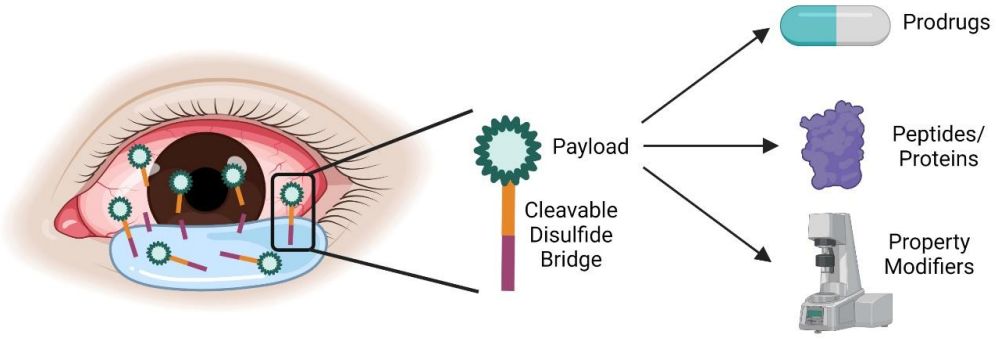

Graphical Abstract: Created with BioRender.com

5.1 Abstract

A platform mucoadhesive and thermogelling eyedrop was developed for application to the inferior fornix for the treatment of various anterior segment ocular conditions. The poly(n-isopropylacrylamide) polymers (pNIPAAm), containing a disulfide bridging monomer, were crosslinked with chitosan to yield a modifiable, mucoadhesive, and natively degradable thermogelling system. Three different conjugates were studied including a small molecule for treating dry eye, an adhesion peptide for modeling delivery of peptides/proteins to the anterior eye, and a material property modifier to create gels with different rheologic characteristics. Based on the conjugate used, different material properties such as solution

viscosity and lower critical solution temperature (LCST) were produced. In addition to releasing the conjugates through disulfide bridging with ocular mucin, the thermogels were shown to deliver atropine, with 70-90% being released over 24-hours, depending on the formulation studied. The results illustrate that these materials can deliver multiple therapeutic payloads at one time and release them through various mechanisms. Finally, the safety and tolerability of the thermogels was demonstrated both *in vitro* and *in vivo*. The gels were instilled into the inferior fornix of rabbits and were shown to not produce any adverse effects over four days. These materials were shown to be highly tunable, creating a platform that could be easily modified to deliver various therapeutic agents to treat a multitude of ocular diseases and have the potential to be an alternative to conventional eyedrops.

5.2 Introduction

For the treatment of conditions of the anterior eye, 90% of all marketed formulations are topical, with conventional eyedrops accounting for greater than 60% [1]. It is, however, well established that topical eyedrops are largely ineffective, with greater than 95% of an applied dose being lost to ocular barriers, including blinking, drainage, and spill onto the cheeks. This results in the need for frequent reapplication of high concentrations of the therapeutic, leading to potentially dangerous systemic drug absorption, patient discomfort, and non-compliance. *In-situ* gels, solutions which are applied as liquids, but then transition

to gels in response to a physical stimulus, have been proposed as alternatives to traditional eyedrops. These materials have the potential to act as drug reservoirs capable of controlled drug release over several days [2, 3]. Thermogels, a subset of *in-situ* gels that transition when triggered by temperature, have received particular attention for ocular surface applications [4-9]. Many of these systems have been designed to be applied to the inferior fornix, also known as the cul-de-sac of the eye, such that they do not obstruct vision following gel phase transition and subsequent drug release. An issue with such application, particularly for degradable materials, is their poor retention within this space due to the high degree of shearing forces associated with blinking and ocular globe movement [10, 11].

We have previously reported on a thermogelling eyedrop, consisting of chitosan crosslinked pNIPAAm based polymers, for the treatment of allergic conjunctivitis [12]. These gels are degradable and are designed to be removed by the natural clearance mechanisms of the eye, while sustaining the release of an anti-allergy drug over several days. Particularly, chitosan was utilized as the crosslinking agent in this system due to its favorable biocompatibility, but also because chitosan can be degraded by lysozyme, which is the highest concentration enzyme in tear fluid [13-17]. These gels were further modified with a disulfide-containing monomer to create a mucoadhesive thermogel for the treatment of cystinosis [18].

Mucoadhesive materials are typically based on covalent conjugation, ionic interaction, hydrogen bonding, Van der Waals forces, mechanical interlocking and/or diffusion interpenetration [19-21]. Chitosan has been established to be mucoadhesive primarily as a result of electrostatic interactions as well as by hydrophobic effects and hydrogen bonding [22]. Several studies have investigated the development of mucoadhesive thermogels based on either pNIPAAm [23-26] or poloxamer blends [27-29]. Mucoadhesive micelles have been fabricated by grafting pNIPAAm chains to chitosan [24]. To improve retention within the inferior fornix, muco-adhesive lectin Helix pomatia agglutinin was incorporated into a pNIPAAm grafted gelation formulation [26]. The formulations containing the added mucoadhesive component were retained up to two weeks in the inferior fornix, significantly longer than formulations without the binding lectin.

In this study, we sought to demonstrate the applicability of a novel thermogelling and mucoadhesive platform material for the treatment of various anterior ocular conditions. N-acetyl cysteine (NAC) and polyethylene glycol (PEG) were both tested as potential conjugates due to their use in the treatment of dry eye disease (DED) [30, 31]. PEG was also utilized as a modifier of material properties as previously documented with thermogels [9, 32, 33]. Additionally, the thiolated adhesion peptide Arg-Gly-Asp-Cys (RGDC) was incorporated to create a thermogel that could deliver peptides/proteins to the ocular surface. Furthermore, incorporating RGDC has the potential to create a thermogel capable of cell delivery which may be useful in the eye in corneal wound healing applications or for the

treatment of limbal stem cell deficiency [34] or in numerous other applications where cell delivery is required. Although the platform described in this study was created for anterior ocular applications, the system could be easily adapted to treat other mucosal surfaces within the body including the mouth, nose, intestines, and vagina.

5.3 Materials and Methods

5.3.1 Materials

Chitosan (MW = 80-200 kDa, DDA = 70%) was purchased from Heppe Medical Chitosan (Halle, Saxony-Anhalt, Germany) and used as received. N-isopropylacrylamide (NIPAAm; 97%) was purchased from Sigma-Aldrich (Oakville, Ontario, Canada) and purified by recrystallization from toluene with n-hexane. Acrylic acid (AA; 99%) was purchased from Sigma-Aldrich and was purified by passing through a packed column containing Sigma-Aldrich inhibitor remover to remove the inhibitor, 4-methoxyphenol. Methyl methacrylate (MMA; 99%), benzoyl peroxide (BPO; Luperox®, 98%), N-(3-dimethylaminopropyl)-N′-ethylcarbodiimide hydrochloride (EDC; BioXtra), and 2-(N-morpholino)ethanesulfonic acid (MES; free acid) were purchased from Sigma-Aldrich and used as received. 1,4-Dioxane, n-hexane, toluene, anhydrous diethyl ether and tetrahydrofuran (THF) were purchased from VWR (Radnor, Pennsylvania, USA) and used as received. Milli-Q grade deionized water was prepared using a Barnstead Diamond™ water purification system (Thermo Fisher

Scientific, Waltham, Massachusetts, USA). 10x Phosphate buffered saline (PBS) was purchased from BioShop® (Burlington, Ontario, Canada) and diluted with deionized water to 1x (pH 7.4) for all experiments. All other compounds were purchased from Sigma Aldrich (Oakville, Ontario, Canada) unless otherwise specified.

5.3.2 Pyridyl Disulfide Ethyl Methacrylate (PDSMA) Monomer Synthesis

The disulfide containing PDSMA monomer was synthesized as in our previous work [35, 36]. To produce the intermediate, 1 g of pyridyl disulfide was dissolved (83.8 mg/mL) in methanol. To this, 7.7 molar equivalents of glacial acetic acid was added dropwise. Finally, mercaptoethanol was dissolved (0.43 mM) in ethanol and 0.72 molar equivalents were added dropwise to the solution. The reaction proceeded overnight. The intermediate was first aqueous extracted, and column purified. To produce PDSMA, the purified intermediate was dissolved (25 mg/mL) in anhydrous dichloromethane (DCM) before the addition of 2 molar equivalents of N,N-diisopropylethylamine. The solution was then placed in an ice bath prior to the dropwise addition of 1.2 molar equivalents methacryloyl chloride dissolved in an equal volume of anhydrous DCM. The reaction proceeded for 12 hours. The resulting PDSMA monomer was then purified by aqueous extraction and column purification.

5.3.3 Poly(n-isopropylacrylamide -co- acrylic acid -co- methyl methacrylate -co- pyridyl disulfide ethylmethacrylate) (pNAMP) Synthesis

The base thermogelling polymer, pNAMP, was synthesized as previously reported [18]. The base polymer contained either 1, 2 or 3 mol% PDSMA denoted as pNAMP-1, pNAMP-2, and pNAMP-3 respectively. Briefly, to produce 1 g of pNAMP-2, 854.5 mg of recrystallized NIPAAm, 12.7 mg of AA, 87.9 mg MMA, 44.8 mg of PDSMA, and 21.3 mg of BPO were dissolved in 10 mL of 9: 1 v/v 1,4-dioxane: Milli-Q water. The reaction vessel was then sealed and purged with nitrogen gas before reacting for 24 hours at 70℃. The resulting pNAMP-2 polymer was purified by precipitation three times in 800 mL of chilled anhydrous diethyl ether and collected by vacuum filtration. The polymer was then dialyzed against 4 L of Milli-Q per day for three days using a Membra-Cel® 14 kDA MWCO cellulose membrane (Viskase®, Lombard, Illinois, USA). The purified pNAMP-2 polymer was lyophilized using a Labconco™ FreeZone 2.5 benchtop freeze drier (Kansas City, Missouri, USA) and stored at -20℃.

To determine the composition of the pNAMP polymers, samples were dissolved at a concentration of approximately 20 mg/mL in deuterated dimethyl sulfoxide (DMSO-D_6) and analyzed by ^{1}H NMR using a Bruker© 600 MHz Spectrometer, operating at 600.13 MHz and 298 K (Billerica, Massachusetts, USA). Polymer molecular weights were determined by first dissolving samples at approximately 5 mg/mL in dimethylformamide 5 mM lithium bromide, filtering with

a 0.2 µm PTFE syringe filter, and then analyzed by gel permeation chromatography (Polymer Laboratories PL-50 gel permeation chromatograph, Church Streton, Shropshire, UK) fitted with three Phenomenex Phenogel™ columns; pore sizes 100, 500 and 104 Å (Torrance, California, USA). Linear PEG standards (provided by Polymer Laboratories) were used for molecular weight calibration.

5.3.4 Chitosan Crosslinked pNAMP Networks

The crosslinking of pNAMP polymers with chitosan (CTS-pNAMP) was conducted based on our previous protocols [18]. For all cases, a crosslinking concentration of 3% (wt/wt) of chitosan/pNAMP was employed. To produce 1 g of CTS-pNAMP-2, 30 mg of chitosan was first dissolved in 30 mL of 10 mM MES buffer, adjusted to pH 4.7 with 0.1 N NaOH, with heating (45℃) for 5 hours. Once dissolved, the chitosan solution was filtered with a 0.45 µm syringe filter. The chitosan solution was then added to 1 g of pNAMP-2 lyophilized powder. 61.6 mg of EDC dissolved in a minimal volume of the 10 mM MES buffer was added dropwise to the reaction vessel once both polymers were fully dissolved, and the reaction proceeded for 24 hours at room temperature. The crosslinked material was then dialyzed against 4 L of Milli-Q per day for three days using a Spectrum Labs 3.5 kDa MWCO Spectra/Por Grade regenerated cellulose dialysis membrane (VWR, Radnor, Pennsylvania, USA). Following dialysis, the samples were lyophilized and stored at -20℃. To determine the composition of the crosslinked

polymers produced, samples were dissolved at a concentration of approximately 20 mg/mL in D_2O and analyzed by ^1H NMR.

5.3.5 Conjugation of CTS-pNAMP

To produce thermogels with different mucoadhesion-mediated leaving groups, NAC, PEG, and RGDC were conjugated to CTS-pNAMP thermogels by a disulfide exchange reaction, denoted as CTS-pNAMP-NAC, CTS-pNAMP-PEG and CTS-pNAMP-RGDC, respectively. CTS-pNAMP samples were first dissolved to a concentration of 3% (wt/v) in 1x PBS. NAC, PEG, or RGDC, were then dissolved to a concentration of 10 mg/mL in 1x PBS. A 1.5 molar excess (conjugate to PDSMA) of NAC, PEG, or RGDC, was then added dropwise to the CTS-pNAMP solution under constant stirring and allowed to react for 24 hours. The resulting conjugated samples were dialyzed against 4 L of Milli-Q per day for three days using Spectrum Labs 3.5 kD MWCO Spectra/Por Grade regenerated cellulose dialysis membrane. Samples were then lyophilized and stored at -20°C. The extent of conjugation was measured by the evolution of 2-mercaptopyridine leaving group using a SpectraMax® ABS Plus UV-vis micro-plate reader (Molecular Devices, San Jose, California, USA) at a wavelength of 343 nm. The CTS-pNAMP thermogel, as well as the three conjugates studied are depicted in Figure 5.1.

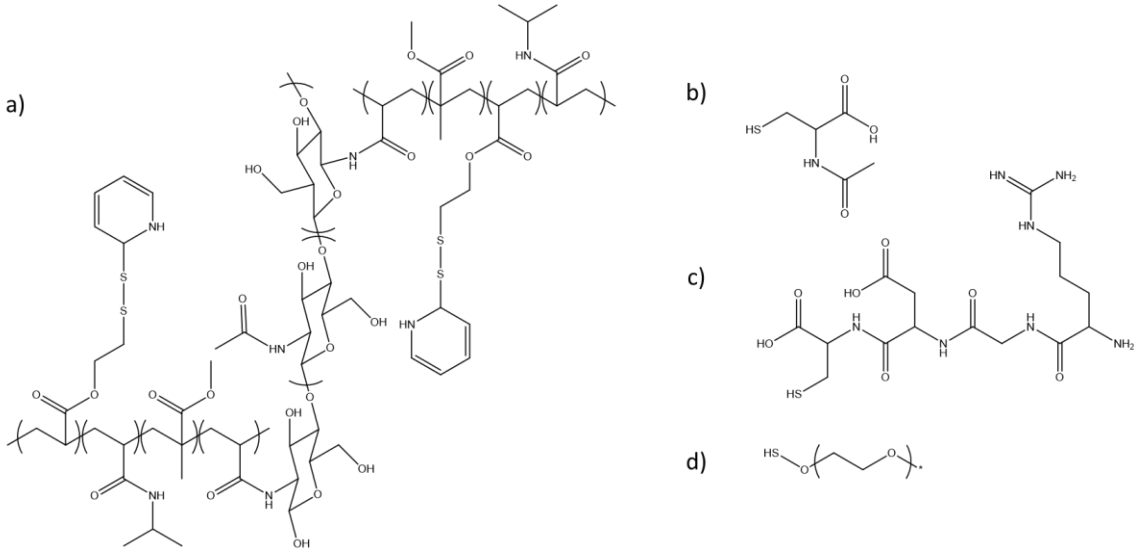

Figure 5.1) Chemical structure of a) CTS-pNAMP as well as the conjugates b) NAC, c) RGDC, and d) PEG-SH.

5.3.6 Rheological Analysis of Materials Properties

The material properties of the various thermogels were studied using a Discovery HR-2 hybrid rheometer (Waters™, Newcastle, Delaware, USA). All samples were tested at a concentration 10% (w/v) in 1x PBS. All measurements were performed in triplicate.

Temperature ramps were conducted at a rate of 1℃/min from 15 to 45℃, utilizing a 20 mm 1° cone and Peltier plate assembly. The LCST was defined as the temperature in which both the storage and loss modulus significantly increased above the baseline measurement. Temperature ramps were conducted on all the thermogels to assess which formulations had the optimal material properties.

Formulation solution viscosity was also studied using the 20 mm 1° cone and Peltier plate assembly, maintained at 4℃. Viscosity was determined with a flow sweep analysis using a shear rate of 0.1 to 100 s^{-1} to assess which formulations were most compatible with conventional topical application.

Gel properties were assessed by both stress and frequency sweep analysis. The measurements were conducted at 37℃ utilizing a 20 mm parallel Peltier plate assembly. Stress sweeps were utilized to determine the linear viscoelastic region of all formulations. Frequency sweeps were conducted to quantify the effect of conjugating various leaving groups on material properties. From the frequency sweeps, the damping factor was determined by equation 5.1 using the storage (G') and loss modulus (G'').

$$5.1) \quad tan\delta = \frac{G''}{G'}$$

The damping factor is utilized to quantify material behaviour using the measured storage and loss moduli. As the damping factor approaches 0° the material acts ideally elastic and when the damping factor approaches 90° the polymer behaves ideally viscous.

5.3.7 Thermogel Swelling and Degradation

The equilibrium water content (EWC) and enzymatic degradation of the various thermogels were assessed gravimetrically. 50 mg of the appropriate thermogel (M_D) was dissolved at 10% (wt/v) in 1x PBS or 1 M NaCl. The samples

were then heated to 37℃. After 24 hours the collapsed gels were blotted dry and weighed (M_S). The equilibrium water content was calculated using equation 5.2.

$$5.2) \quad EWC\ (\%) = \left(\frac{M_S - M_D}{M_S}\right) 100$$

After the 24-hour EWC determination, the same dried gels (t=0) were then incubated with either 1x PBS or 1x PBS containing a physiologic amount (1.4 mg/mL) of lysozyme. At a given time interval, the supernatant was removed, the gels were blotted dry, and the mass was recorded (M_T). The degradation profiles of the thermogels were determined by calculating the ratio of the mass at a given time point to the initial mass as shown in equation 5.3.

$$5.3) \quad Degradation = \left(\frac{M_T}{M_S}\right) 100$$

5.3.8 Rheological Analysis of Degradation

The effect of lysozyme on the various thermogels was also studied by analysis of the rheologic properties before and after enzyme incubation. 25 mg of the thermogel was dissolved at 10% (wt/v) in 1x PBS or 1 M NaCl, or 1x PBS or 1 M NaCl containing 1.4 mg/mL of lysozyme. The samples were then heated to 37℃ and incubated for 48 hours. Following incubation, the samples were cooled back to the solution phase and the viscosity was determined by flow sweep analysis using a shear rate of 0.1 to 100 s^{-1} with a 20 mm 1° cone and Peltier plate assembly, maintained at 4℃.

5.3.9 Atropine Release

The release of the drug Atropine from the produced thermogels was analyzed by an Agilent 1260 Infinity II high performance liquid chromatographer (HPLC; Santa Clara, California, USA). 50 mg of the respective thermogel was dissolved at 10% (wt/v) in either PBS or 1M NaCl containing 1 mg/mL atropine and gelled for one hour at 37℃ before the addition of 2 mL of prewarmed PBS containing the physiologic concentration of lysozyme (t=0). At set time intervals, 1 mL of supernatant was removed and replaced with an equal volume of prewarmed release media. The release samples were passed through a 0.2 µm Nylon filter (Agilent) prior to quantification. A buffer comprised of 50 mM sodium acetate, 15 mM tetrabutylammonium hydrogen sulfate, and 5% (v/v) acetonitrile, was adjusted to pH 5.5 with 1N NaOH and utilized as the mobile phase. The mobile phase was filtered with a Pall® Life Sciences 0.45 µm nylon filter (Port Washington, New York, USA) prior to use. Sample concentration was determined against a calibration curve of atropine measured at 254 nm.

5.3.10 *In Vitro* Cytotoxicity Analysis

The potential cytotoxicity of CTS-pNAMP-NAC3, CTS-pNAMP-RGDC3, and CTS-pNAMP-PEG2 thermogels was assessed by Live/Dead staining as well as metabolic MTT assay. Human corneal epithelial cells (HCECs) were cultured in keratinocyte serum free medium (Gibco™, Thermo Fisher Scientific) containing 25 mg of bovine pituitary extract and 2.5 µg human recombinant epidermal growth

factor (Thermo Fisher Scientific) at 37 ℃ and 5% CO_2. The thermogels were dissolved at 10% (w/v) in either sterile 1x PBS or sterile 1M NaCl and UV treated for 12 hours prior to use. For both assays, HCECs were plated into a 24-well pretreated plate at a density of 40 000 cells/well. After 24 hours, the medium was replaced. Each of the thermogels was tested in triplicate. To each treatment well a 0.4 µm filter insert (Falcon, VWR) was added along with 300 µL of fresh medium and 50 µL of the respective thermogel sample. Filter inserts were utilized to prevent the gels from forming films atop the adhered cells, which can negatively impact natural cellular transport phenomena. For both assays, the potential cytotoxicity of the thermogels were assessed after 24 hours. Wells containing only media without filter inserts served as controls. The negative controls remained untreated while the positive control was produced by incubating cells with 0.25% (v/v) Triton X-100 for three minutes after which the surfactant was removed, and the cells washed three times with sterile 1x PBS at a given timepoint.

For the MTT assay, 3-(4,5-dimethylthiazol-2-yl)-2,5-diphenyltetrazolium bromide (MTT) powder was first dissolved to 5 mg/mL in sterile 1x PBS. 500 µL of medium containing 10% (v/v) MTT solution was added to each well and allowed to incubate for 3 hours. Following incubation, the MTT solution was removed and the produced formazan crystals dissolved in 1 mL of DMSO for 15 minutes. The metabolic cell viability was determined by a SpectraMax® ABS Plus UV-vis micro-plate reader at a wavelength of 570 nm by calculating viability through absorbance (Abs) using equation 5.4.

$$5.4) \quad Cell\ Viability = \frac{Abs_{sample}}{Abs_{control}}$$

For Live/Dead staining, at the given timepoints the cells were stained using a calcein-AM/ethidium homodimer-1 fluorescence kit (Thermo Fisher Scientific) and visualized with an Olympus IX51 inverted fluorescent microscope (Shinjuku, Tokyo, Japan) using the same controls as with the MTT assay.

5.3.11 *In Vivo* Safety and Tolerability

Animals were cared for and analyzed in compliance with protocols approved by the Animal Research Ethics Board at McMaster University in accordance with the regulations of the Animals for Research Act of the Province of Ontario and the guidelines of the Canadian Council on Animal Care. 6, 35-week-old female New Zealand White rabbits (Charles River, Wilmington, Massachusetts, USA) were used to study thermogel retention in the inferior fornix. One-week prior to use, the nictitating membranes of the rabbits were surgically removed [37]. The thermogel samples were dissolved at 10% (wt/v) in either sterile 1x PBS or sterile 1M NaCl and were UV treated for 12 hours prior to application. The rabbits were anesthetized with gaseous isoflurane before assessment of baseline corneal health by fluorescein staining, and OCT imaging. 50 µL of CTS-pNAMP-PEG2, CTS-pNAMP-NAC3 or CTS-pNAMP-RGDC3 were then pipetted into the inferior fornix of the right eye of the rabbits (n = 2). The right eye was then partially closed by the application of an interrupted horizontal mattress suture, 5 mm from the nasal side of the right eye. The left eyes were left untreated as controls. After 4 days, the

sutures were removed and the thermogels recovered. The ocular health was reassessed by fluorescein staining, and OCT imaging to evaluate any possible negative effects of thermogel treatment. Following imaging, the rabbits were euthanized, and the eyes harvested. The eyes were fixed in 4% paraformaldehyde overnight at 4 ℃ and then stored in 70% ethanol. Samples were processed (Core Histology Department, McMaster University) and embedded in paraffin (Paraplast Tissue Embedding Media, Thermo Fisher Scientific). Serial sections of the embedded eyes were cut to 4 µm in thickness and were stained with hematoxylin and eosin (H&E) prior to visualization with an Olympus BX51 inverted microscope. Corneal thickness measurements were taken from H&E-stained slides using ImageJ software.

5.3.12 Statistical Analysis

Error bars represent the standard deviation. Student T-tests with two tailed distribution and unequal variance were utilized to compare paired OCT values. Single factor analysis of variance (ANOVA) followed by Tukey post-hoc analysis was utilized to compare LCSTs, gel water content, *in vitro* cytotoxicity, and *in vivo* safety. Two-Way ANOVA with replication was utilized to compare rheological properties and degradation.

5.4 Results and Discussion

5.4.1 Characterization of Chitosan Crosslinking and Cysteamine Conjugation to pNAMP

The synthesis and characterization of the base thermogelling polymer pNAMP and the effect crosslinking with chitosan are outlined in our previous report [18]. The chitosan crosslinking and subsequent conjugation of NAC, PEG, or RGDC, was characterized utilizing ^{1}H NMR (Figure 5.2). The conjugation of chitosan is shown in both spectra by the presence of the secondary amine peak at 2.83 ppm. CTS-pNAMP-3 contains the aromatic peaks of 2-mercaptopyridine occurring at 7.27-8.37 ppm. The successful conjugations were also confirmed by the reduction of the aromatic peaks as 2-mercaptopyridine.

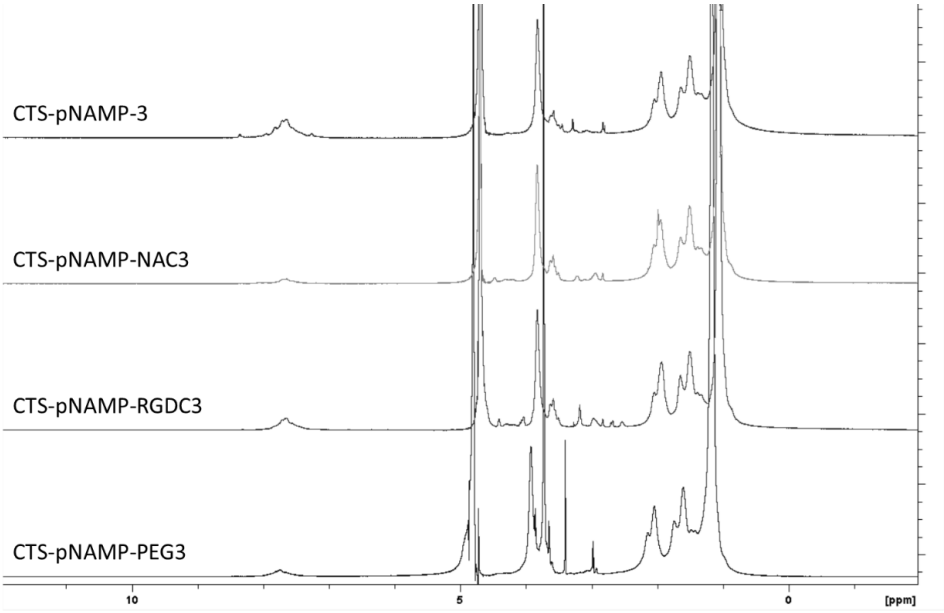

Figure 5.2) ^{1}H NMR analysis of CTS-pNAMP-3 (top), CTS-pNAMP-NAC3 (top-middle), CTS-pNAMP-RGDC3 (bottom-middle), and CTS-pNAMP-PEG3 (bottom).

5.4.2 Conjugate Material Properties

Following conjugation with charged species such as NAC or RGDC, dissolution can become difficult due to an increase of ionic crosslinking in the thermogels. Therefore, to improve dissolution, the NAC and RGDC thermogels were dissolved with 1M NaCl. The pH, viscosity, and LCST of the resulting thermogels are shown in Table 5.1. However, even in 1M NaCl only one NAC containing formulation was able to be fully dispersed. Of note, increasing NaCl concentration, which is an isotonicity agent, is well established to decrease the LCST of thermogelling formulations as observed in Table 5.1 [38].

Table 5.1) Properties of Thermogels. Data presented as mean ± SD (n = 3).

Conjugate	**Solution**	**Material**	**pH**	**Viscosity (Pa.s) at 1 (1/s)**	**LCST (°C)**
NAC	1M NaCl	CTS-pNAMP-NAC1	Could not dissolve		
		CTS-pNAMP-NAC2	Could not dissolve		
		CTS-pNAMP-NAC3	5.51	0.96 ± 0.28	20.55 ± 0.52
RGDC	1M NaCl	CTS-pNAMP-RGDC1	6.26	20.63 ± 1.75	19.35 ± 0.98

		CTS-pNAMP-RGDC2	5.71	4.26 ± 1.01	20.31 ± 0.39
		CTS-pNAMP-RGDC3	5.46	1.69 ± 0.30	19.49 ± 1.09
PEG	1x PBS	CTS-pNAMP-PEG1	6.84	0.76 ± 0.39	27.31 ± 0.75
		CTS-pNAMP-PEG2	6.76	12.13 ± 0.90	28.20 ± 0.04
		CTS-pNAMP-PEG3	6.64	32.67 ± 5.02	28.83 ± 0.10

To determine the usability of the thermogels, the viscosity of the formulations was evaluated by flow sweeps. The results are shown in Figure 5.3. Interestingly, it can be observed that between PEG and RGDC conjugated materials, there is an inverse effect on viscosity based on the concentration of the leaving group conjugated. As the concentration of PEG increases, so does the viscosity, which is to be expected as an increasing amount of PEG results in a greater density of comb-like polymers whose interaction will increase viscosity. Comparatively, an increasing concentration of RGDC reduces solution viscosity which can be attributed to more uniform ionic interaction between the polymer chains reducing the repulsive interactions of the amino groups of chitosan. This same explanation can describe the dissolution properties of NAC conjugated

materials. The thermogels were also compared to the commercial ointment product HYLO Night® which is designed as a gel to be placed in the inferior fornix. The viscosity analysis is shown in Figure 5.3a) and it can be seen at 4℃, this formulation had a higher viscosity than any of the thermogels, suggesting that these materials are within an acceptable viscosity range to be used with conventional application techniques.

The solution viscosity results indicate that for each species to be conjugated, there is an optimal amount which yields the best solution properties and usability. Based on the LCST analysis as well as the solution viscosity analysis and qualitative usability, the thermogels CTS-pNAMP-NAC3, CTS-pNAMP-PEG2, and CTS-pNAMP-RGDC3 were selected for further material testing.

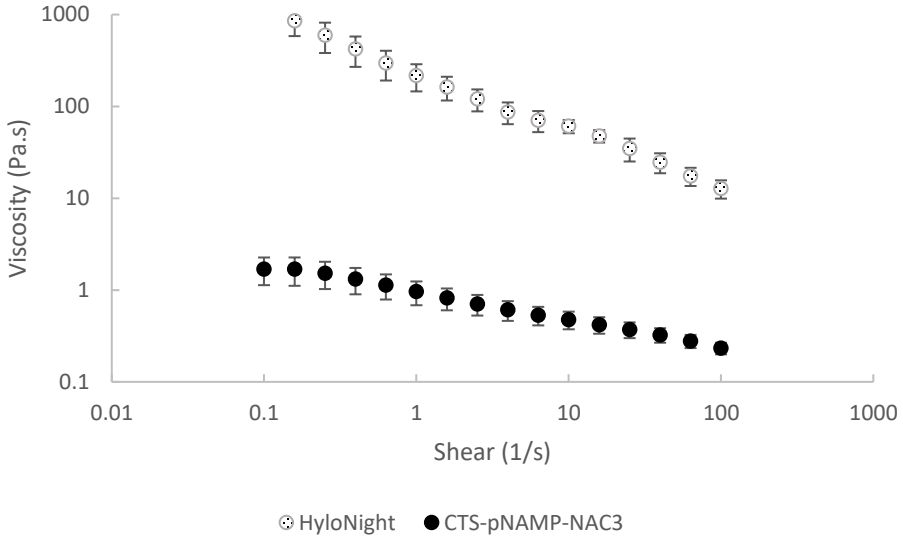

a)

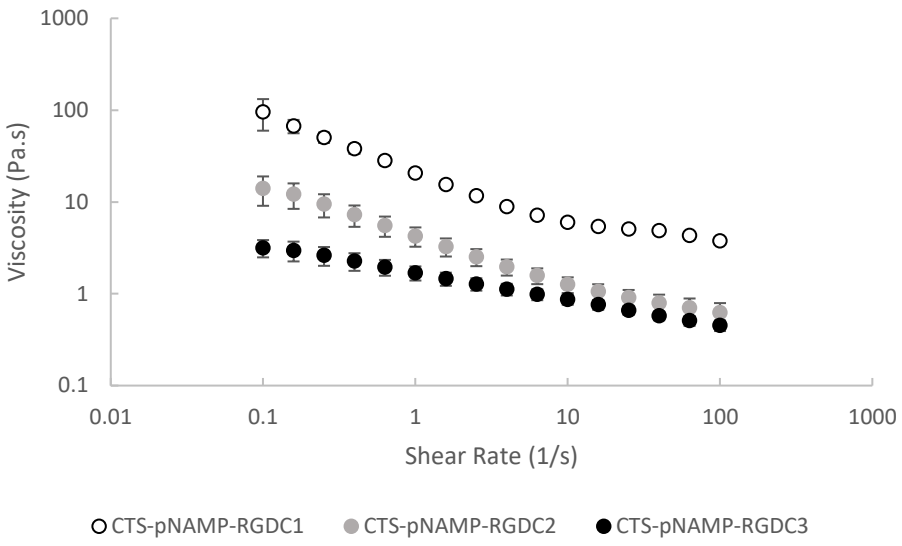

b)

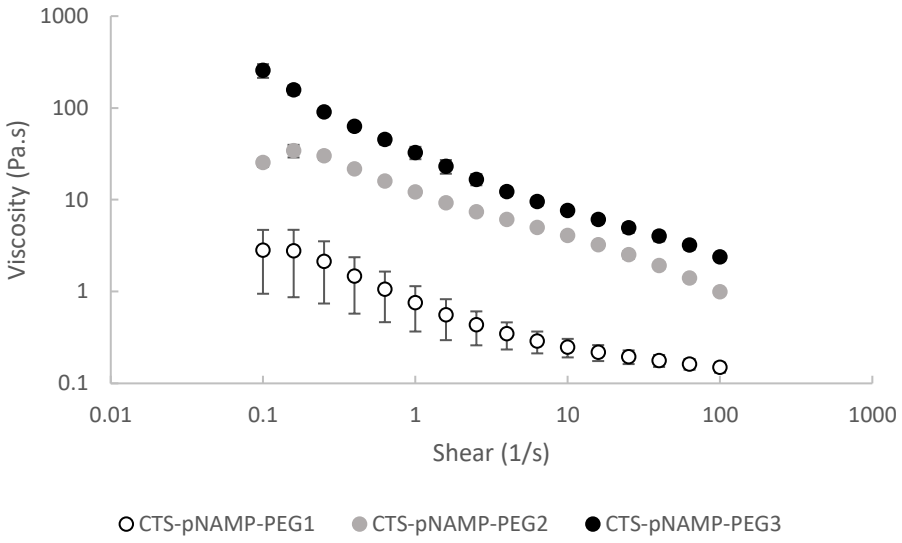

c)

Figure 5.3) Determination of formulation viscosity (4 ℃) for a) HYLO Night® NAC conjugated thermogels, b) RGDC conjugated thermogels and c) PEG conjugated thermogels. It was found that RGDC and PEG conjugated materials had an inverse relationship between solution viscosity and concentration of the conjugate. This result indicates that different small molecule conjugates will result in different optimal material properties based on their concentration. Data presented as mean ± SD (n = 3).

In this study, RGDC was selected for conjugation as a model peptide/protein. The successful conjugation of 1-3 mol% of RGDC suggests that the conjugation of larger proteins is possible although the solubility of such materials will likely need to be optimized. Peptide conjugation is less complicated as the peptide only needs to contain a cysteine residue. Regardless, there are several proteins which could be conjugated to these thermogels including an anti-vascular endothelial growth factor for treating corneal neovascularization [39], hepatocyte growth factor for corneal would healing applications [40], and proteoglycan 4 for treating dry eye [41]. However, some additional modification of these proteins may be required prior to conjugation to generate a free thiol capable of disulfide bridging which is not integral to protein folding. Cell penetrating peptides have been utilized for anterior ocular application and could be utilized with this designed thermogel [42]. The RGDC thermogels created in the current work may have applicability to be utilized for the delivery of cells to the anterior of the eye. Whether RGDC incorporation significantly increases the efficacy of the thermogels for cellular delivery, beyond the base chitosan crosslinked thermogel, requires further investigation.

Another possible conjugation would the utilization of a lubricating polymer. Thiomers, particularly thiolated hyaluronic acid could be conjugated to the developed thermogel and released slowly to the ocular surface to improve both thermogel wetting properties as well as stabilize the tear film for treating diseases such as dry eye.

5.4.3 Rheologic Determination of Gel Properties

Strain sweeps and frequency sweeps were conducted on the selected conjugated materials CTS-pNAMP-NAC3, CTS-pNAMP-RGDC3, and CTS-pNAMP-PEG2. The strain sweep analysis of the thermogels is shown in Figure 5.4a). From the strain sweep analysis, the thermogels can be seen to have a linear viscoelastic region (LVE) of up to 10% oscillation strain. The thermogels do not show a drastic decrease in material properties outside of LVE. For subsequent testing, an oscillation strain of 0.1% was utilized as it is well within the LVE of all the produced thermogels.

The frequency sweep analysis is shown in Figure 5.4b). It can be shown that CTS-pNAMP-NAC3 and CTS-pNAMP-RGDC3 thermogels have similar mechanical attributes. Not unexpectedly CTS-pNAMP-PEG2 had storage and loss modulus values greater than a full order of magnitude less than the other two materials due to the presence of PEG. PEG of similar molecular weight has been utilized in other thermogel studies to alter rheologic properties [9, 32, 33]. This is an important result as it demonstrates that the physical properties of this thermogelling platform can be altered depending on the small molecule to which it is conjugated, even at a low conjugate concentration. From the frequency sweep analysis, the damping factor could be calculated and is shown in Figure 5.4c). Again, CTS-pNAMP-NAC3 and CTS-pNAMP-RGDC3 display similar properties behaving more ideally viscous from 20 to approximately 45° with increasing angular frequency. Correspondingly, CTS-pNAMP-PEG2 displays a different trend

staying largely linear with increasing angular frequency at approximately 30-35°. Under the same testing conditions, the commercial HYLO Night® inferior fornix gel displayed a damping factor of 50-70°, demonstrating that these thermogels are more elastic compared to the commercial product.

Utilizing high speed cameras, the peak velocity of blinking during the closing phase has been shown to be 243 ± 9 mm/s and 157 ± 5 mm/s during the opening phase [43]. Based on the dimensions of the parallel plate utilized, these speeds correspond to approximately 12 and 8 rad/s, respectively. These values, which are the highest velocities achieved during blinking, are well within the 0.1 to 100 rad/s range tested in this study. From the frequency sweep analysis shown in Figure 5.4b) there is no reduction in material performance at max physiologic blink speed suggesting that these materials will operate as intended within the inferior fornix from a material property standpoint.

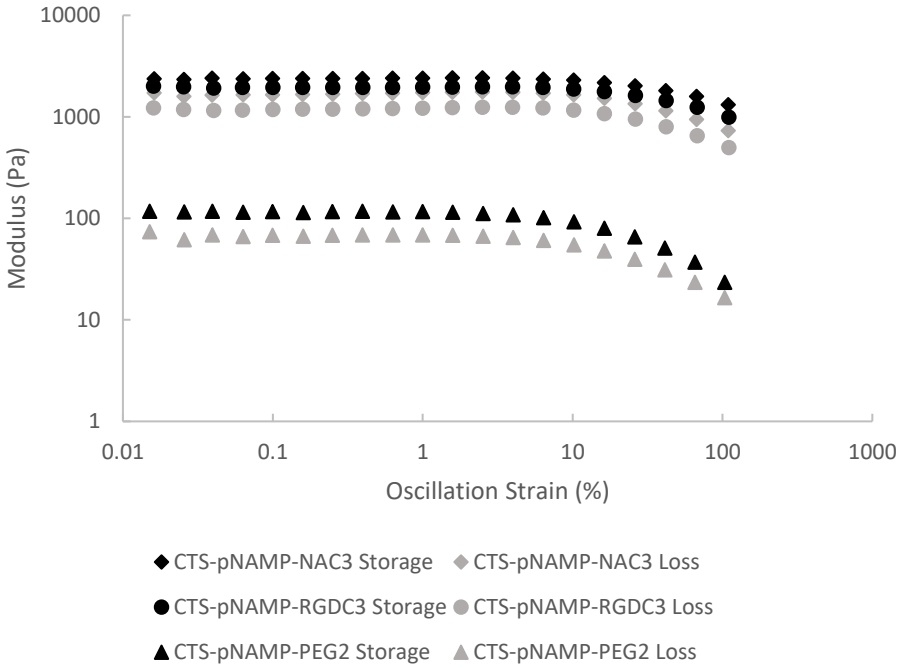
10000
1000
100
10
1
Modulus (Pa)
0.01
0.1
1
10
100
1000
Oscillation Strain (%)
CTS-pNAMP-NAC3 Storage
CTS-pNAMP-NAC3 Loss
CTS-pNAMP-RGDC3 Storage
CTS-pNAMP-RGDC3 Loss
CTS-pNAMP-PEG2 Storage
CTS-pNAMP-PEG2 Loss

a)

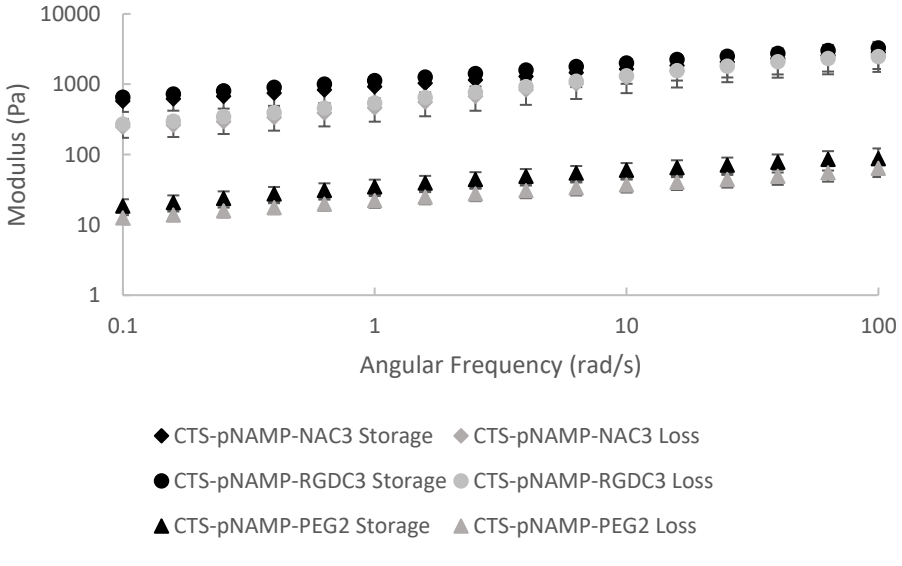
10000
1000
100
10
1
Modulus (Pa)
0.1
1
10
100
Angular Frequency (rad/s)
CTS-pNAMP-NAC3 Storage
CTS-pNAMP-NAC3 Loss
CTS-pNAMP-RGDC3 Storage
CTS-pNAMP-RGDC3 Loss
CTS-pNAMP-PEG2 Storage
CTS-pNAMP-PEG2 Loss

b)

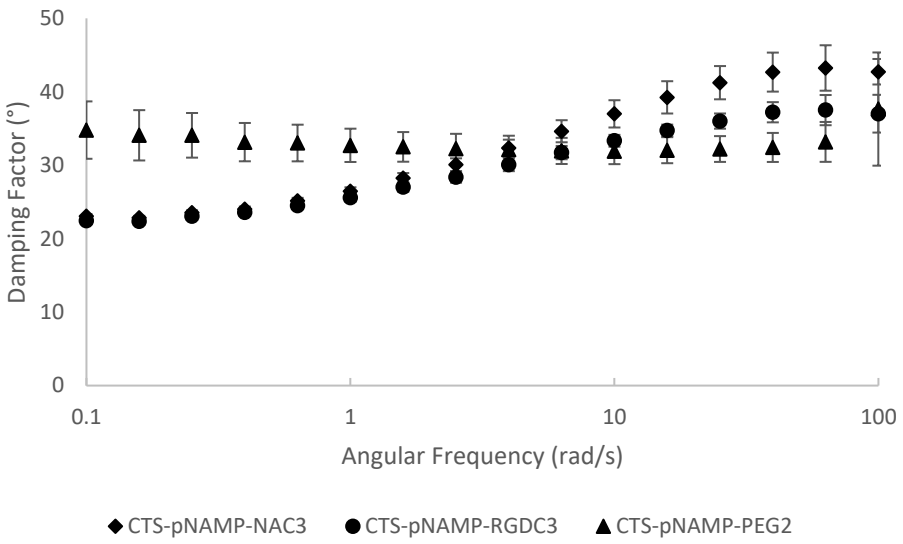

c)

Figure 5.4) Rheologic determination of CTS-pNAMP-NAC3, CTS-pNAMP-RGDC3, and CTS-pNAMP-PEG2. a) Strain sweep analysis b) Frequency sweep analysis and c) Damping factor as determined by frequency analysis. Conjugation with PEG results in approximately a full order of magnitude reduction in the storage and loss modulus across the testing region. Conjugating with PEG also yields materials with a more stable damping factor across the testing region. Data presented as mean ± SD (n = 3).

5.4.4 Thermogel EWC

The EWC after 24 hours of the three thermogels is shown in Figure 5.5. There is no difference in the water content ($p > 0.05$) between the thermogels, which all have an average EWC of 72-76%. Despite CTS-pNAMP-PEG2 being dissolved in 1x PBS and CTS-pNAMP-NAC3 and CTS-pNAMP-RGDC3 being dissolved in 1M NaCl, that difference in salt molarity did not significantly alter the swelling attributes.

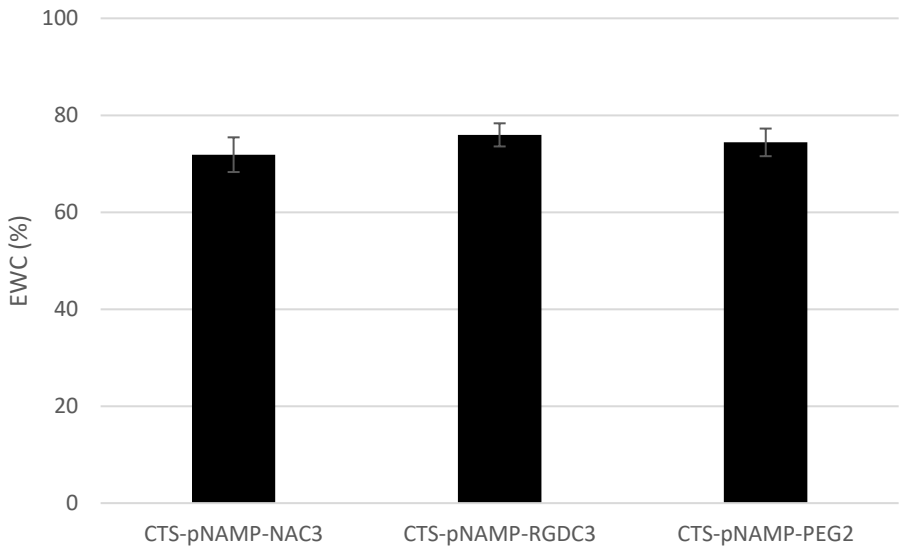

Figure 5.5) EWC of CTS-pNAMP-NAC3, CTS-pNAMP-RGDC3, and CTS-pNAMP-PEG2. The EWCs were not significantly different ($p > 0.05$) between the developed thermogels. Data presented as mean ± SD (n = 3), significance determined by single factor ANOVA analysis followed by Dunnett's post-hoc analysis comparing the thermo-gels.

5.4.5 Thermogel Degradation Analysis

The degradation profiles of the thermogels are shown in Figures 5.6 and 5.7. Figure 5.6 shows the gravimetric degradation profiles and Figure 5.7 displays the rheological analysis of the thermogel solutions following incubation with or without lysozyme. Measuring gravimetrically allows for the quantification of both enzymatic action as well as the effect of swelling and subsequent gel dissolution. From the gravimetric degradation profiles, all three materials were shown to degrade to a greater extent ($p < 0.05$) when incubated with the enzyme lysozyme as determined by a two-way ANOVA. The CTS-pNAMP-NAC3 and CTS-pNAMP-

RGDC3, which were dissolved in a higher molarity buffer, displayed significant swelling when incubated with the PBS supernatant. The gravimetric analysis of CTS-pNAMP-PEG2 thermogel displayed the lowest extent of degradation.

To assess just the effect of lysozyme without the influence of swelling, the material properties were measured by rheology following incubation with or without lysozyme as shown in Figure 5.7. From the rheologic analysis, CTS-pNAMP-NAC3 and CTS-pNAMP-RGDC3 both displayed a significant ($p < 0.05$) reduction in viscosity following incubation with lysozyme for 48 hours. This further substantiates the conclusion that lysozyme has an enzymatic effect on the materials. However, CTS-pNAMP-PEG2 did not display a significant reduction in solution viscosity following incubation with lysozyme for 48 hours ($p > 0.05$). Coupled with the gravimetric result of CTS-pNAMP-PEG2 degradation, these findings suggest that PEG conjugation hinders the enzymatic degradation by lysozyme which is likely attributable to the conjugated PEG sidechains limiting the successful docking of lysozyme to degrade the chitosan backbone. It is also important to consider that with various anterior ocular diseases, as well as aging, the concentration of lysozyme in the tear fluid may be reduced which can influence the degradation rate of the developed thermogels.

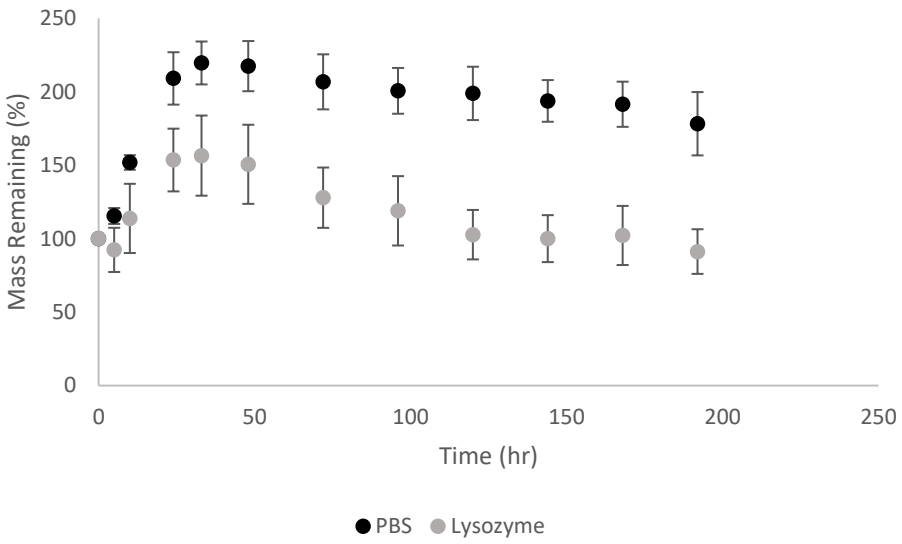
250
200
150
100
50
0
Mass Remaining (%)
0
50
100
150
200
250
Time (hr)
PBS
Lysozyme

a)

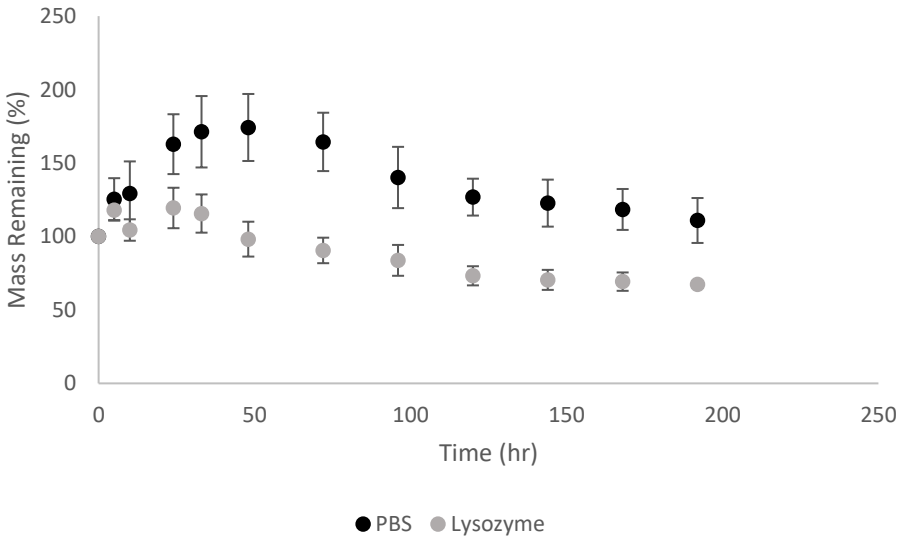
250
200
150
100
50
0
Mass Remaining (%)
0
50
100
150
200
250
Time (hr)
PBS
Lysozyme

b)

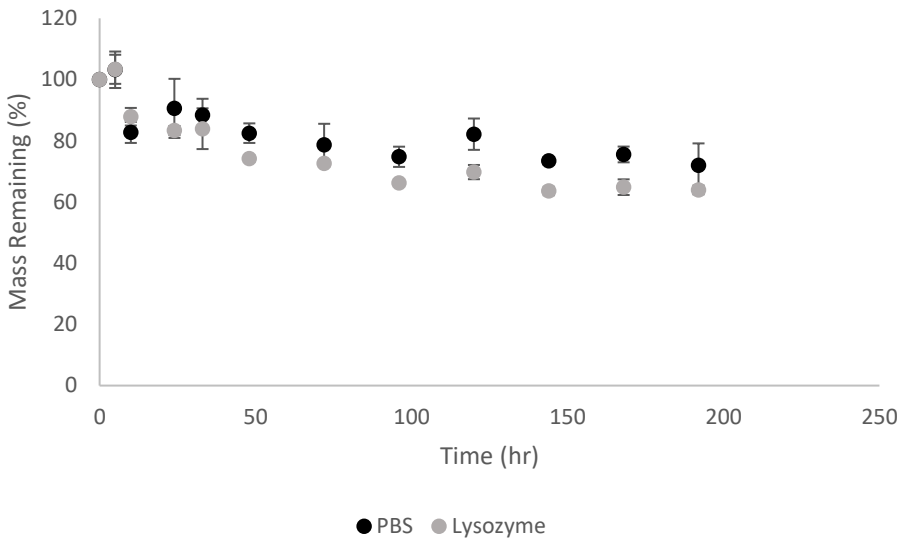

c)

Figure 5.6) Degradation Profiles of a) CTS-pNAMP-NAC3, b) CTS-pNAMP-RGDC3 and c) CTS-pNAMP-PEG2 incubated with or without lysozyme. All the developed thermogels demonstrated a significant increase in degradation following incubation with lysozyme ($p < 0.05$). Data presented as mean ± SD ($n = 3$), significance determined by two-way ANOVA analysis comparing incubation with or without lysozyme.

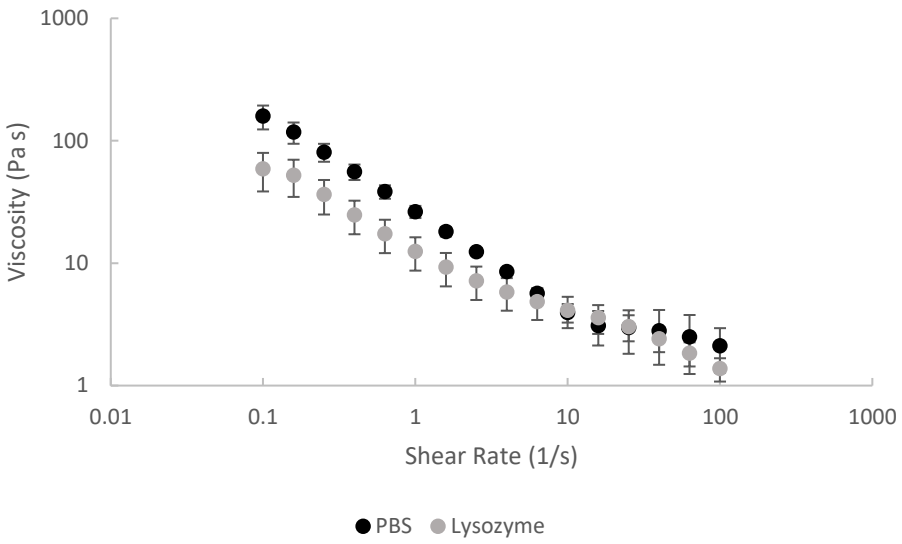
1000
100
10
1
Viscosity (Pa s)
0.01
0.1
1
10
100
1000
Shear Rate (1/s)
PBS
Lysozyme

a)

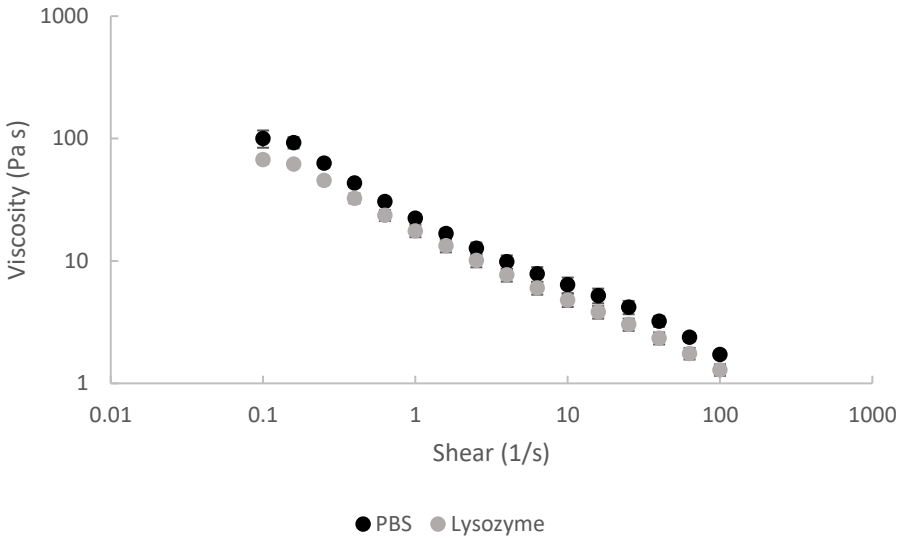
1000
100
10
1
Viscosity (Pa s)
0.01
0.1
1
10
100
1000
Shear (1/s)
PBS
Lysozyme

b)

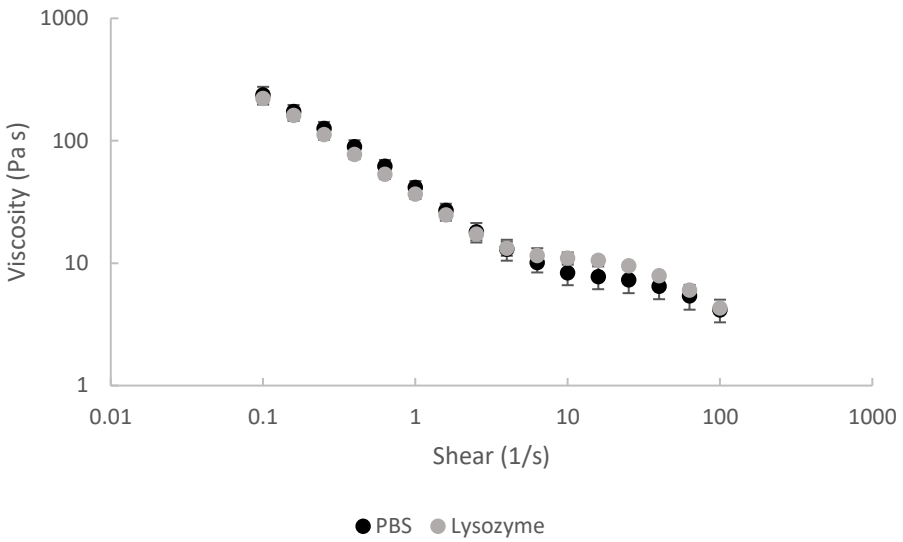

c)

Figure 5.7) Rheologic determination of degradation after following incubation with or without lysozyme of a) CTS-pNAMP-NAC3 b) CTS-pNAMP-RGDC3 and c) CTS-pNAMP-PEG2. CTS-pNAMP-NAC3 and CTS-pNAMP-RGDC3 thermogels demonstrated a significant decrease in solution viscosity following incubation with lysozyme for 48 hours ($p < 0.05$). CTS-pNAMP-PEG2 did not display a significant change in solution viscosity following incubation with lysozyme for 48 hours ($p > 0.05$). Data presented as mean ± SD ($n = 3$), significance determined by two-way ANOVA analysis comparing incubation with or without lysozyme.

5.4.6 Determination of Atropine Release Profiles

The release of atropine over five days from the CTS-pNAMP-NAC3, CTS-pNAMP-RGDC3, and CTS-pNAMP-PEG2 gels is shown in Figure 5.8. The thermogels displayed near-linear release of the hydrophilic atropine ($R^2 > 0.94$ for all materials) over the first 8 hours and plateaued after 24 hours. Overall, CTS-pNAMP-PEG2 released the greatest amount, on average, of loaded atropine at

96%, while CTS-pNAMP-NAC3 released 89%, and CTS-pNAMP-RGDC3 released the lowest amount over the five days at 74%. This demonstrates that the thermogels can release a loaded drug through diffusion while also expressing the respective conjugates by mucosal binding. The amount of drug released is demonstrated to be a function of the respective conjugate utilized. Based on the swelling properties of CTS-pNAMP-NAC3 and CTS-pNAMP-RGDC3, which were dissolved in 1M NaCl, it was hypothesized that they would have a much greater release compared to CTS-pNAMP-PEG2. However, CTS-pNAMP-PEG2 was found to display the greatest amount of atropine release over the testing period. Firstly, this may be a function of the lower rheological properties displayed by CTS-pNAMP-PEG2 compared to CTS-pNAMP-NAC3 and CTS-pNAMP-RGDC3. Secondly, atropine is hydrophilic, with a hydroxyl and tertiary amine; these groups can interact with the charged NAC and RGDC accounting for less of the drug released over time.

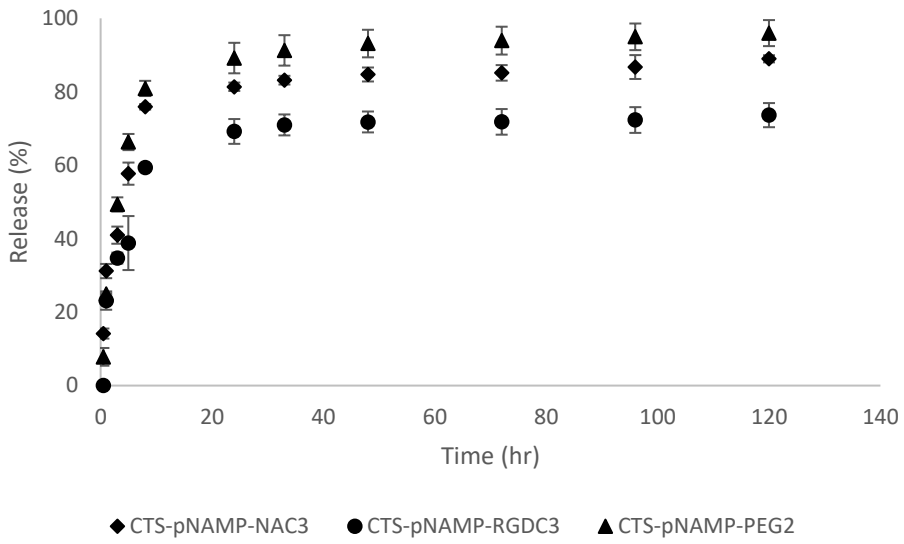

Figure 5.8) Atropine release from CTS-pNAMP-NAC3, CTS-pNAMP-RGDC3, and CTS-pNAMP-PEG2 over six days. The greatest release of atropine was noted from CTS-pNAMP-PEG2 while the lowest atropine release occurred from CTS-pNAMP-RGDC3. Data presented as mean ± SD (n = 3).

5.4.7 *In Vitro* Cytotoxicity

The MTT and Live/Dead assays using HCEC to demonstrate cell compatibility of the gels are shown in Figure 5.9. From the MTT analysis (Figure 5.9a), it was found that neither CTS-pNAMP-NAC3, CTS-pNAMP-RGDC3, nor CTS-pNAMP-PEG2 had a significantly different cellular viability compared to the positive control after 24 hours. From the Live/Dead staining shown in Figure 5.9b), there was no observable change in the concentration of live or dead cells or in the morphology of the cells. All images were taken from the left-hand side of the well for consistency. It was observed with CTS-pNAMP-RGDC3, and to a lesser extent

with CTS-pNAMP-NAC3, that there was lifting of cells in the centre of the wells directly underneath the well inserts. There are two possible explanations for this: either the higher ionic concentration of CTS-pNAMP-NAC3 and CTS-pNAMP-RGDC3 gels could result in localized cellular death and subsequent lifting or, especially with the CTS-pNAMP-RGDC3 formulation, cells may be attracted to the gel causing localized lifting. Despite the lifting, there was no statistical change in cellular viability as determined by the MTT assay or in the bulk of cellular growth as shown by the Live/Dead staining.

In this study, an acute *in vitro* cytotoxicity model was utilized, similar to our previous report [12]. An acute model was utilized to prevent cellular death from over confluence due to the doubling time of HCECs. Based on this acute model, as well as previous *in vivo* investigations on similar materials [18], the safety of the thermogels was further investigated *in vivo*.

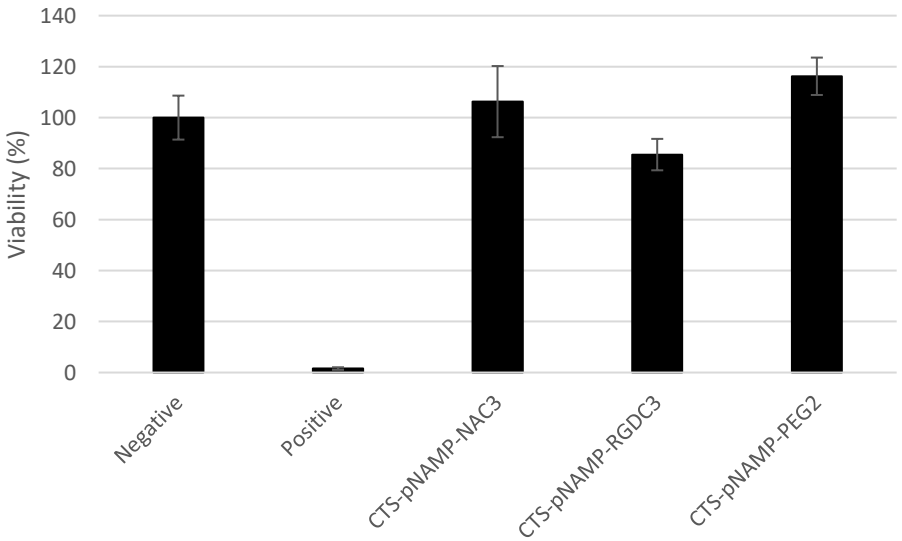

a)

b) 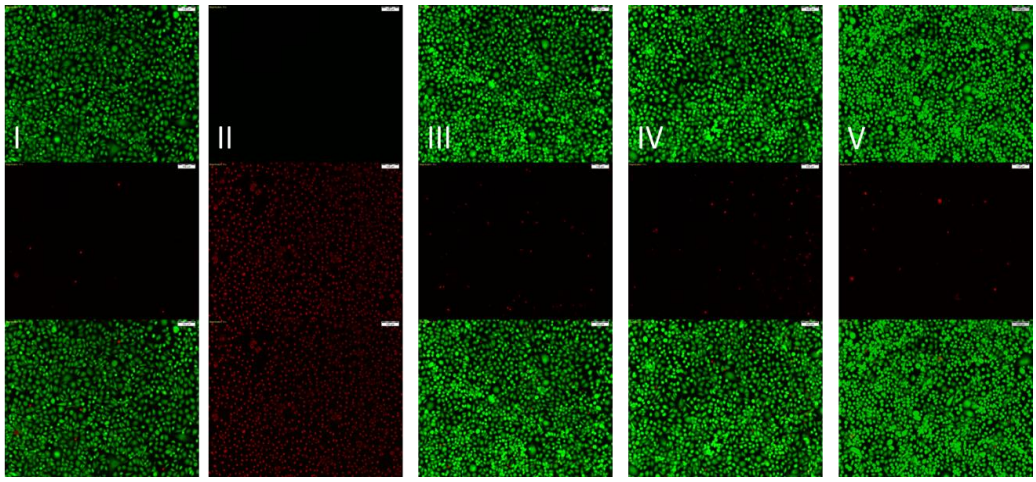

Figure 5.9a) MTT assay of HCECs following 24-hour incubation with the developed thermogels. No statistical difference ($p > 0.05$) in cellular viability between the negative control and CTS-pNAMP-NAC3, CTS-pNAMP-RGDC3, or CTS-pNAMP-PEG2. Data presented as mean ± SD (n = 3), significance determined by single factor ANOVA analysis followed by Dunnett's post-hoc analysis comparing the thermo-gels to the negative control. b) Live/Dead staining of HCECs following 24-hour incubation with negative control (I), positive control (II), CTS-pNAMP-NAC3 (III), CTS-pNAMP-RGDC3 (IV) and CTS-pNAMP-PEG2 (V). Top images live, middle dead, and bottom combined. All images taken at left-hand side of the well plate at a 10x magnification. Scale bars represent 100 µm.

5.4.8 *In Vivo* Safety Analysis

To assess the safety of the developed thermogels, 50 µL of each formulation was applied to the inferior fornix of the right eye. Suturing of the lid margin was necessary to ensure that the gels were not removed by the rabbits during grooming. During the experiment, one of the sutured eyes containing CTS-pNAMP-RGDC3, opened prematurely, and this animal was removed from the

study. The fluorescence staining of the corneal surfaces before and after the application of the thermogels is shown in Figure 5.10. Corneal staining is typically evaluated utilizing an Oxford staining score which relates area stained to a numerical score between 0 and 4 (0 indicating no staining and 4 significant staining). Greater corneal fluorescein staining indicates greater surface damage. From Figure 5.10, there is inconsistent results with fluorescein staining. CTS-pNAMP-NAC3 did result in a greater area of stain following thermogel treatment but greater staining was also observed with control eyes. CTS-pNAMP-RGDC3 resulted in a lower staining score following treatment while the control increased. Finally, CTS-pNAMP-PEG2 resulted in much greater staining in one case (5.10d) but not in another (5.10e). These results indicate the fluorescein staining alone cannot be utilized to indicate the safety profile of the materials with the given experimental design.

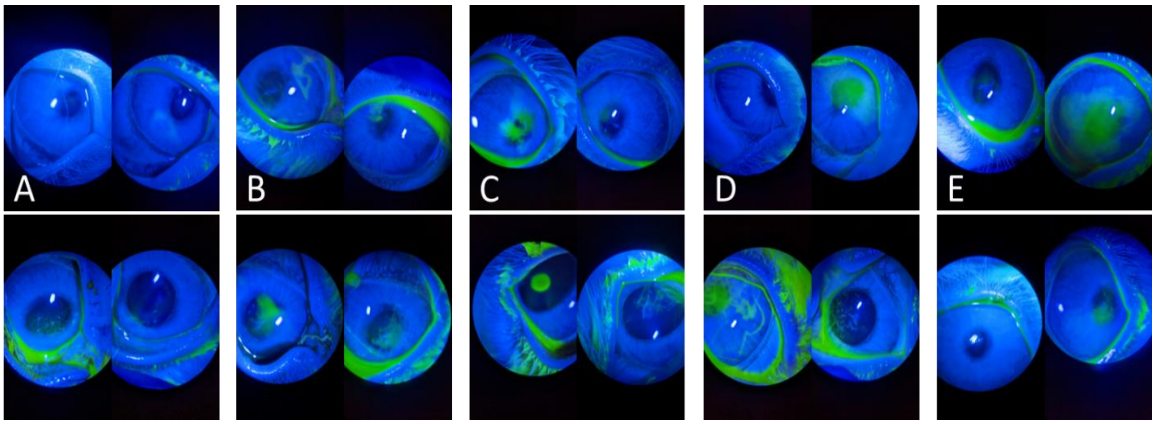

Figure 5.10) Fluorescein staining of corneal surfaces before and after thermogel application. Rabbit eyes were treated with CTS-pNAMP-NAC3 (A and B), CTS-pNAMP-

RGDC3 (C), and CTS-pNAMP-PEG2 (D and E). Eyes are grouped such that the treated right eye is first, and the control left eye is second. Baseline images are presented on the top and after 4-days on the bottom.

Anterior health was assessed by OCT before and after the treatment with the thermogels, as shown in Figure 5.11. Figure 5.11a) displays the anterior chamber, as captured by OCT, for eyes treated with CTS-pNAMP-NAC3 (I and IV), CTS-pNAMP-RGDC3 (II and V), and CTS-pNAMP-PEG2 (III and VI), both before (I, II, and III) and after (IV, V, and VI) thermogel application. Images are stacked with the untreated control eyes on top and the treated and partially closed eyes on the bottom. From the OCT analysis, the corneal epitheliums as well as the endothelium are intact. Furthermore, stromal integrity is apparent in all the images and there is no observable infiltration of inflammatory cells within the anterior chamber. From the OCT analysis, the corneal thickness can also be measured as shown in Figure 5.11b). The thermogel treated corneal thickness and untreated control corneal thickness displayed no significant change from one another ($p > 0.05$) following four-day treatment. The OCT analysis indicates that the materials do not cause corneal damage or an inflammatory response and are therefore well tolerated.

a)

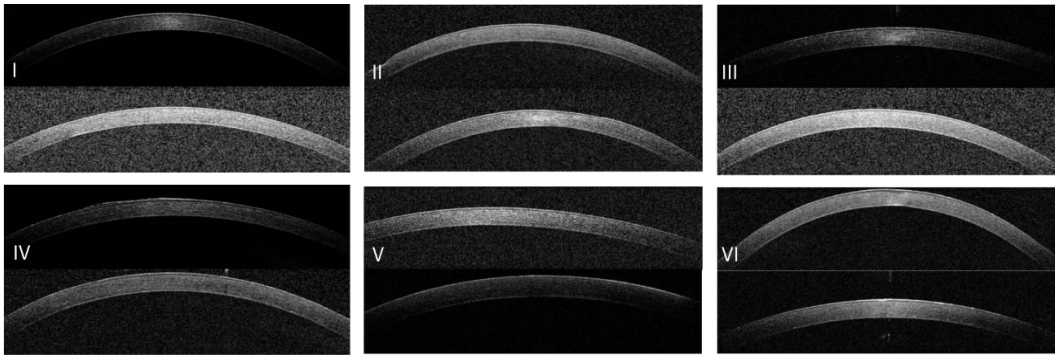

b)

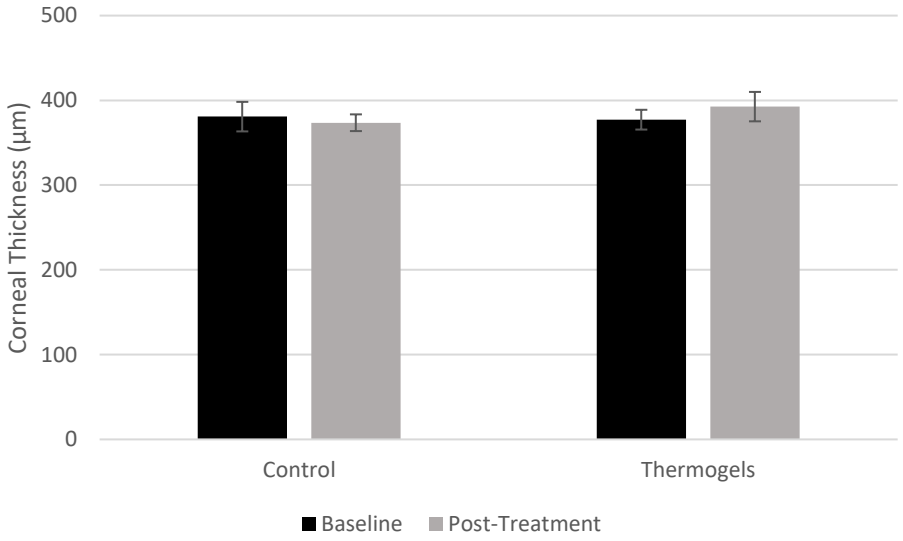

Figure 5.11a) OCT analysis of the anterior chamber before (I, II, and III) and after (IV, V, VI) 4-day treatment with CTS-pNAMP-NAC3 (I and IV), CTS-pNAMP-RGDC3 (II and V), or CTS-pNAMP-PEG2 (III and VI). For each thermogel tested at a given timepoint, the images are grouped with the untreated control eye on top and the partially closed and thermogel treated eye on the bottom. No corneal damage or infiltration of inflammatory cells within the anterior chamber was observed for any treatment. b) It was found that the corneal thickness did not significantly change from the baseline ($p > 0.05$) for either the control or thermogel-treated eyes. Data presented as mean ± SD ($n = 5$), significance

determined by Student T-test analysis using a two tailed distribution and unequal variance comparing the corneal thickness for a group between the two time points.

The histological analysis of the anterior of the rabbit eyes, specifically the cornea, following thermogel treatment and H&E staining is shown in Figure 5.12. From the histological analysis, there is no observable corneal damage from the gel application. Furthermore, complete stromal integrity is noted with no infiltration of inflammatory cells or neovascularization [44]. Along with the histological analysis, the fluorescein staining, and OCT imagery, these results indicate that the thermogel materials are safe and well tolerated and do not result in ocular damage following instillation.

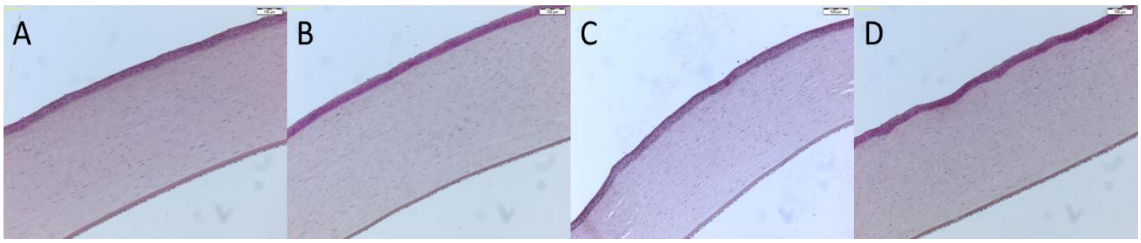

Figure 5.12) Histological H&E staining of rabbit corneas following four-day treatment with a) untreated control, b) CTS-pNAMP-NAC3, c) CTS-pNAMP-RGDC3, and d) CTS-pNAMP-PEG2. Images taken at 10x magnification; scale bars are 100 µm. No observable corneal damage or infiltration of inflammatory cells into the cornea.

5.5 Conclusions

A mucoadhesive and thermogelling platform eyedrop was investigated. This novel platform can be conjugated with various payloads to treat numerous ocular conditions. In this study, three different conjugates were chosen to demonstrate different possible applications of the thermogels. NAC was added to treat dry eye, RGDC was conjugated to model peptide/protein delivery to the front of the eye, and PEG was incorporated to control the rheologic properties. It was found that each of these conjugates could be incorporated into the base platform and that the properties, particularly the solution viscosity and LCST, could be modified based on the concentration of a given conjugate incorporated. All the thermogelling solutions had a lower viscosity compared to a commercial inferior fornix gel. Modifying with PEG was found to alter the rheologic properties compared to NAC or RGDC, but it interfered with the degradation of the gels by lysozyme. Significant reduction was noted with lysozyme for NAC or RGDC conjugated gels by gravimetric and rheologic analysis but not with PEG conjugation. In addition to the ability to release the three conjugated small molecules by disulfide bridging with mucin, the gels were also loaded with the model drug atropine which was released by diffusion. It was found that 70-90% of the loaded atropine was released after 24-hours depending on which conjugated material was utilized. The three determined optimal materials; CTS-pNAMP-NAC3, CTS-pNAMP-RGDC3, and CTS-pNAMP-PEG2 were tested both *in vitro* and *in vivo* to ensure safety. After 24 hours it was found that the thermogels had no significant effect on HCECs, as

assessed using an MTT analysis and Live/Dead imaging. *In vivo* the gels were instilled within the inferior fornix of rabbit eyes before being partially closed for four days. It was determined by fluorescein staining, OCT imagery, and histological analysis that the applied thermogels did not result in ocular surface damage underlying their safety. Future studies will explore utilizing other conjugates such as peptides for treating other ocular conditions as well as delivering multiple therapeutic payloads at once, exploring the ability for release by diffusion and through mucosal interaction to work synergistically in treating anterior ocular conditions.

Data Availability

The raw/processed data required to reproduce these findings cannot be shared at this time as the data also forms part of an ongoing study.

CRediT authorship contribution statement

Mitchell Ross: Conceptualization, Methodology, Data curation, Formal analysis, Investigation, Validation, Writing – original draft. **Lindsay Sheardown:** Investigation. **Benjamin Muirhead:** Methodology, Investigation. **Jonathan Mofford:** Methodology, Investigation. **Jennifer Tian:** Investigation. **Heather Sheardown:** Conceptualization, Supervision, Writing – review & editing.

5.6 Acknowledgements

We acknowledge The Natural Sciences and Engineering Research Council of Canada (NSERC Discovery) and Ontario Research Fund (C20/20 ORF-RE Round 8) for funding this research.

5.7 References

[1] R. D. Bachu, P. Chowdhury, Z. H. Al-Saedi, P. K. Karla, and S. H. Boddu, "Ocular drug delivery barriers—role of nanocarriers in the treatment of anterior segment ocular diseases," *Pharmaceutics,* vol. 10, no. 1, p. 28, 2018.

[2] A. S. Mundada and J. G. Avari, "In situ gelling polymers in ocular drug delivery systems: a review," *Critical Reviews™ in Therapeutic Drug Carrier Systems,* vol. 26, no. 1, 2009.

[3] B. Padmasri, R. Nagaraju, and D. Prasanth, "A Comprehensive Review on In Situ Gels," *International Journal of Applied Pharmaceutics,* pp. 24-33, 2020.

[4] Y. Cao, C. Zhang, W. Shen, Z. Cheng, L. L. Yu, and Q. Ping, "Poly(N-isopropylacrylamide)-chitosan as thermosensitive in situ gel-forming system for ocular drug delivery," *Journal of Controlled Release,* vol. 120, no. 3, pp. 186-94, Jul 31 2007, doi: 10.1016/j.jconrel.2007.05.009.

[5] Y. H. Cheng *et al.*, "Thermosensitive chitosan-based hydrogel as a topical ocular drug delivery system of latanoprost for glaucoma treatment," *Carbohydrate Polymers,* vol. 144, pp. 390-9, Jun 25 2016, doi: 10.1016/j.carbpol.2016.02.080.

[6] J. Y. Lai and L. J. Luo, "Chitosan-g-poly(N-isopropylacrylamide) copolymers as delivery carriers for intracameral pilocarpine administration," *European Journal Pharmaceutics Biopharmaceutics,* vol. 113, pp. 140-148, Apr 2017, doi: 10.1016/j.ejpb.2016.11.038.

[7] L. J. Luo, C. C. Huang, H. C. Chen, J. Y. Lai, and M. Matsusaki, "Effect of deacetylation degree on controlled pilocarpine release from injectable chitosan-g-poly(N-isopropylacrylamide) carriers," *Carbohydrate Polymers,* vol. 197, pp. 375-384, Oct 1 2018, doi: 10.1016/j.carbpol.2018.06.020.

[8] Y. C. Kim *et al.*, "Gelling hypotonic polymer solution for extended topical drug delivery to the eye," *Nature Biomedical Engineering,* vol. 4, no. 11, pp. 1053-1062, 2020.

[9] M. V. Fedorchak, I. P. Conner, J. S. Schuman, A. Cugini, and S. R. Little, "Long term glaucoma drug delivery using a topically retained gel/microsphere eye drop," *Scientific reports,* vol. 7, no. 1, pp. 1-11, 2017.

[10] J. Colter, B. Wirostko, and B. Coats, "Finite element design optimization of a hyaluronic acid-based hydrogel drug delivery device for improved retention," *Annals of Biomedical Engineering,* vol. 46, no. 2, pp. 211-221, 2018.

[11] S. Elliott, "More than meets the eye—estimating blinking shear rates," *RheoSense Inc,* ed, 2018.

[12] M. Ross, E. A. Hicks, T. Rambarran, and H. Sheardown, "Thermo-sensitivity and erosion of chitosan crosslinked poly [N-isopropylacrylamide-co-(acrylic acid)-co-(methyl methacrylate)] hydrogels for application to the inferior fornix," *Acta Biomaterialia*, vol. 141, pp. 151-163, 2022.

[13] T. Irimia *et al.*, "Chitosan-Based In Situ Gels for Ocular Delivery of Therapeutics: A State-of-the-Art Review," *Marine Drugs,* vol. 16, no. 10, Oct 9 2018, doi: 10.3390/md16100373.

[14] E. Aine and P. Morsky, "Lysozyme Concentration in Tears-Assessment of Reference Values in Normal Subjects," *Acta ophthalmologica,* vol. 62, no. 6, pp. 932-938, 1984.

[15] R. Sariri and H. Ghafoori, "Tear proteins in health, disease, and contact lens wear," *Biochemistry (moscow),* vol. 73, no. 4, pp. 381-392, 2008.

[16] J. Li, Y. Du, and H. Liang, "Influence of molecular parameters on the degradation of chitosan by a commercial enzyme," *Polymer Degradation and Stability,* vol. 92, no. 3, pp. 515-524, 2007.

[17] K. Tomihata and Y. Ikada, "In vitro and in vivo degradation of films of chitin and its deacetylated derivatives," *Biomaterials,* vol. 18, no. 7, pp. 567-575, 1997.

[18] M. Ross *et al.*, "Thermo-responsive and mucoadhesive gels for the treatment of cystinosis.," *Submitted to Biomaterials Advances on October 26th 2022*.

[19] B. M. Boddupalli, Z. N. Mohammed, R. A. Nath, and D. Banji, "Mucoadhesive drug delivery system: An overview," *Journal of advanced pharmaceutical technology & research,* vol. 1, no. 4, p. 381, 2010.

[20] R. Shaikh, T. R. R. Singh, M. J. Garland, A. D. Woolfson, and R. F. Donnelly, "Mucoadhesive drug delivery systems," *Journal of Pharmacy and Bioallied Sciences,* vol. 3, no. 1, p. 89, 2011.

[21] C. Federer, M. Kurpiers, and A. Bernkop-Schnürch, "Thiolated chitosans: a multi-talented class of polymers for various applications," *Biomacromolecules,* vol. 22, no. 1, pp. 24-56, 2020.

[22] I. A. Sogias, A. C. Williams, and V. V. Khutoryanskiy, "Why is chitosan mucoadhesive?," *Biomacromolecules,* vol. 9, no. 7, pp. 1837-1842, 2008.

[23] J. C. Cuggino, L. I. Tártara, L. M. Gugliotta, S. D. Palma, and C. I. A. Igarzabal, "Mucoadhesive and responsive nanogels as carriers for sustainable delivery of timolol for glaucoma therapy," *Materials Science and Engineering: C,* vol. 118, p. 111383, 2021.

[24] A. Sosnik *et al.*, "Mucoadhesive thermo-responsive chitosan-g-poly (N-isopropylacrylamide) polymeric micelles via a one-pot gamma-radiation-assisted pathway," *Colloids and Surfaces B: Biointerfaces,* vol. 136, pp. 900-907, 2015.

[25] X. Zhu, J. DeGraaf, F. Winnik, and D. Leckband, "pH-dependent mucoadhesion of a poly (N-isopropylacrylamide) copolymer reveals design rules for drug delivery," *Langmuir,* vol. 20, no. 24, pp. 10648-10656, 2004.

[26] L.-J. Luo, D. D. Nguyen, and J.-Y. Lai, "Long-acting mucoadhesive thermogels for improving topical treatments of dry eye disease," *Materials Science and Engineering: C,* vol. 115, p. 111095, 2020.

[27] E. Baloglu, S. Y. Karavana, Z. A. Senyigit, and T. Guneri, "Rheological and mechanical properties of poloxamer mixtures as a mucoadhesive gel base," *Pharmaceutical development and technology,* vol. 16, no. 6, pp. 627-636, 2011.

[28] S. B. D. S. Ferreira, J. B. Da Silva, F. B. Borghi-Pangoni, M. V. Junqueira, and M. L. Bruschi, "Linear correlation between rheological, mechanical and mucoadhesive properties of polycarbophil polymer blends for biomedical applications," *Journal of the mechanical behavior of biomedical materials,* vol. 68, pp. 265-275, 2017.

[29] J. Y. Chang, Y.-K. Oh, H.-g. Choi, Y. B. Kim, and C.-K. Kim, "Rheological evaluation of thermosensitive and mucoadhesive vaginal gels in physiological conditions," *International journal of pharmaceutics,* vol. 241, no. 1, pp. 155-163, 2002.

[30] Y. Eghtedari, L. J. Oh, N. Di Girolamo, and S. L. Watson, "The role of topical N-acetylcysteine in ocular therapeutics," *Survey of Ophthalmology,* 2021.

[31] S. Cohen, A. Martin, and K. Sall, "Evaluation of clinical outcomes in patients with dry eye disease using lubricant eye drops containing polyethylene glycol or carboxymethylcellulose," *Clinical ophthalmology (Auckland, NZ),* vol. 8, p. 157, 2014.

[32] E. Bellotti, M. V. Fedorchak, S. Velankar, and S. R. Little, "Tuning of thermoresponsive pNIPAAm hydrogels for the topical retention of controlled release ocular therapeutics," *Journal of Materials Chemistry B,* vol. 7, no. 8, pp. 1276-1283, 2019.

[33] J. Jimenez, M. A. Washington, J. L. Resnick, K. K. Nischal, and M. V. Fedorchak, "A sustained release cysteamine microsphere/ thermoresponsive gel eyedrop for corneal cystinosis improves drug stability," *Drug Delivery and Translational Research,* vol. 11, no. 5, pp. 2224-2238, 2021.

[34] M. Ross, N. Amaral, A. Taiyab, and H. Sheardown, "Delivery of Cells to the Cornea Using Synthetic Biomaterials," *Cornea,* p. 10.1097, 2022.

[35] N. Boehnke, “Degradable Hydrogels and Nanogels for the Delivery of Cells and Therapeutics*”*. University of California, Los Angeles, 2017.

[36] X. Huang, D. Appelhans, P. Formanek, F. Simon, and B. Voit, "Tailored synthesis of intelligent polymer nanocapsules: an investigation of controlled permeability and pH-dependent degradability," *ACS nano,* vol. 6, no. 11, pp. 9718-9726, 2012.

[37] K. Yamamoto *et al.*, "Effect of eyelid closure and overnight contact lens wear on viability of surface epithelial cells in rabbit cornea," *Cornea,* vol. 21, no. 1, pp. 85-90, 2002.

[38] H. Qi, L. Li, C. Huang, W. Li, and C. Wu, "Optimization and physicochemical characterization of thermosensitive poloxamer gel containing puerarin for ophthalmic use," *Chemical and pharmaceutical bulletin,* vol. 54, no. 11, pp. 1500-1507, 2006.

[39] J.-H. Chang, N. K. Garg, E. Lunde, K.-Y. Han, S. Jain, and D. T. Azar, "Corneal neovascularization: an anti-VEGF therapy review," *Survey of ophthalmology,* vol. 57, no. 5, pp. 415-429, 2012.

[40] H. Miyagi, S. M. Thomasy, P. Russell, and C. J. Murphy, "The role of hepatocyte growth factor in corneal wound healing," *Experimental eye research,* vol. 166, pp. 49-55, 2018.

[41] N. G. Menon *et al.*, "Proteoglycan 4 (PRG4) expression and function in dry eye associated inflammation," *Experimental Eye Research,* vol. 208, p. 108628, 2021.

[42] S. Pescina *et al.*, "Cell penetrating peptides in ocular drug delivery: State of the art," *Journal of Controlled Release,* vol. 284, pp. 84-102, 2018.

[43] K.-A. Kwon *et al.*, "High-speed camera characterization of voluntary eye blinking kinematics," *Journal of the Royal Society Interface,* vol. 10, no. 85, p. 20130227, 2013.

[44] J.-H. Chang, E. E. Gabison, T. Kato, and D. T. Azar, "Corneal neovascularization," *Current opinion in ophthalmology,* vol. 12, no. 4, pp. 242-249, 2001.

CHAPTER 6 – Conclusions

6.1 Project Goals

The goal of this thesis was to create a thermogelling system which can be used instead of topical eyedrops for treating anterior ocular conditions. It is well established that topical eyedrops are largely ineffective with greater than 95% of an applied dose being removed by the natural clearance mechanisms of the eye following instillation. This results in the need for frequent reapplication, systemic drug absorption, as well as comfort and compliance issues with patients. Despite this, topical eyedrops remain the mainstay treatment formulation for anterior ocular conditions. By developing a thermogel for application to the anterior of the eye, sustained drug release over multiple days can be achieved from a single dose, significantly improving patient burden and formulation efficacy.

There were three overarching goals for this thesis. Firstly, the thermogel should be designed to be instilled within the inferior fornix. Applying the thermogel to the inferior fornix allows for the formulation to be opaque while not obstructing vision. Furthermore, application to the inferior fornix is similar to simple topical application as compared to the more invasive routes of sub-conjunctival and intracameral injection of thermogels which have been explored in literature. The second goal of the thesis was to design the thermogel to undergo site specific degradation. The synthetic polymers which are often utilized in the production of thermogels are not degradable and would therefore need to be removed by the patient following drug release. However, hydrolysis, one of the most commonly

utilized modes of degradation in literature posses' difficulties when designing an aqueous thermogel formulation (especially with storage). Therefore, designing the thermogel to undergo site specific enzymatic degradation is of key interest. Finally, in order to have the developed thermogel be retained within the higher shear environment of the inferior fornix, it should be designed to adhere to the natural mucosal layers which coat the eye.

6.2 Summary of Completed Work

Chapter 2 reviews the thermogelling formulations which have been developed in literature for treating anterior ocular conditions. These thermogels can be broadly categorized as being based on pNIPAAm, PEG analogues/Poloxamers, and natural polymers. Particular emphasis was placed on the trends of incorporating degradation, mucoadhesion, and the development of thermo-composites which contain micro or nanoparticles dispersed within the thermogel matrix for improved drug release profiles or to prevent particle washout. Interestingly, Poloxamer based formulations have been shown to last for much shorter durations on the ocular surface or within the inferior fornix compared to pNIPAAm formulations. Despite some of the advantages which can be achieved utilizing fully natural thermogels, comparatively much less research has been done on these systems. Furthermore, gelling agents frequently need to be added to natural polymers to facilitate the production of thermogels which often compromises the perceived benefits.

The development of a chitosan crosslinked pNIPAAm based system was first explored in Chapter 3. Chitosan was utilized as it can be enzymatically degraded by lysozyme, the highest concentration protein found in tear fluid. pNAM was crosslinked with chitosan by either charge of through covalent chemistry. The degradation of these materials could be tailored from 1-4 days based on the method of chitosan incorporation although it was found that lysozyme did not have a statistical impact on degradation. Release of the anti-allergy drug Ketotifen Fumarate was studied as well as the safety profile of the developed thermogel *in vitro* and with an acute *in vivo* rat model. This study demonstrated that when incorporating chitosan, not only the polymer properties but also the degree of crosslinking needs to be optimized to produce thermogels capable of lysozyme mediated degradation.

The thermogel platform was further developed in Chapter 4 for the treatment of cystinosis. By utilizing a larger chitosan with less crosslinking, significantly increased degradation following incubation with lysozyme was demonstrated. By incorporating varying concentrations of the disulfide monomer PDSMA, the mucoadhesive properties of the developed thermogels could be modulated. Conjugating cysteamine to the disulfide bridge allowed for mucosal mediated drug release. Traditional cysteamine formulations for treating cystinosis suffer from several storage issues due to oxidation, by conjugating the cysteamine directly to the disulfide bridging component our system can effectively overcome these storage issues. The mucosal mediated release of the conjugated component

was estimated to be 6 to 10 µg over five days. The safety of the thermogels designed for treating cystinosis was studied *in vivo* utilizing a rat and rabbit model. With both models the thermogels did not result in adverse ocular side effects. However, whether increasing the mucoadhesive properties of the thermogels resulted in improved retention could not be delineated from the rabbit model utilized.

Cysteamine is not the only conjugate which can be applied to the developed thermogel system. Other therapeutic conjugates were explored in Chapter 5. Three conjugates were studied including NAC for treating dry eye, RGDC as a model peptide/protein, and PEG as a material property modifier. It was found that there were different optimal concentrations of these three conjugates based on solubility, LCST, and solution viscosity. It was found that the NAC and RGDC thermogels both displayed significantly greater degradation following incubation with lysozyme. However, the PEG conjugated thermogels did not show this increase in degradation following incubation with lysozyme, likely due to the resulting PEG brushes preventing enzyme docking. In addition to the release of conjugated components, the drug Atropine for treating myopia was released from the thermogel matrix with 70-90% release achieved over one day depending on the conjugate utilized. This result illustrates the ability of the thermogels to be loaded with multiple payloads with varying release kinetics. By *in vitro* testing utilizing HCECs, the thermogels were shown to not produce a significant cytotoxic effect following a one-day trial. A four-day safety studied on the three developed

formulations was conducted utilizing a rabbit model in which the eyes treated with the thermogel were partially closed to ensure gel retention. It was found that none of the formulations resulted in adverse effects on ocular health.

6.3 Significance of Research

This thesis describes the production of a modifiable, mucoadhesive, and enzymatically degradable thermogel for application to the inferior fornix in treating anterior ocular conditions. It was demonstrated that the mucoadhesive properties of the thermogel could be controlled based on crosslinking with chitosan as well as the varying the concentration of the incorporated disulfide bridging component. Furthermore, various therapeutic compounds could be conjugated to this incorporated disulfide bridge for mucosal mediated drug delivery in addition to diffusive drug delivery through the thermogel matrix. This system can be easily augmented to treat various diseases and achieve tailorable material properties. Finally, the thermogel was designed to be enzymatically degraded by lysozyme which is secreted by all submucosal glands. Therefore, the developed thermogel can be applied not only to the eye but any mucosal surface within the body.

6.4 Future Work

Although the safety of the developed thermogels have been extensively studied the efficacy has not. For the cysteamine conjugated thermogels described in Chapter 4, an *ex vivo* mouse eye model can be utilized to evaluate the removal

of cysteine crystals in the cornea. Currently, a mouse model (CTNS knockout) is the only cystinosis model which has been developed in literature, but the developed thermogels cannot be effectively tested *in vivo* with mice since the gel will be quickly removed from the ocular surface. Therefore, an *ex vivo* model will need to be produced and utilized for evaluating the efficacy of these thermogels for treating cystinosis. In contrast, a dry eye model could be utilized with rabbits to test the efficacy of the NAC conjugated thermogels described in Chapter 5. However, a different large animal model may need to be utilized as it has been shown in our studies that thermogel retention within the inferior fornix of rabbits is minimal without partial closure of the eyes. To this point, another key avenue of future research will be developing an *in vivo* model which can be used to effectively determine the influence of mucoadhesive properties and how those properties impact ocular retention.

From a materials standpoint, the developed thermogel platform can be further formulated with other conjugates for various therapeutic outcomes. Specifically, in Chapter 5 RGDC is utilized as a model for conjugating peptides or proteins to the thermogel. Several proteins have been proposed such as proteoglycan 4 for treating dry eye, hepatocyte growth factor for corneal wound applications, and an anti-vascular endothelial growth factor for treating corneal neovascularization. Two key limitations will need to be addressed in these future studies. Firstly, most thiols contained within proteins are structural and therefore the proteins will need to be modified with a free thiol prior to conjugation to not

compromise folding. Secondly, activity assays will have to be utilized showing that protein effectiveness is not compromised either by modification or subsequent conjugation.

It has been demonstrated that the developed thermogel can yield drug release both by diffusion and as a function of mucus interaction. An interesting future study would be to create a composite with the developed thermogel by dispersing either micro or nanoparticles within the matrix. This would improve drug release as a function of diffusion. By dispersing PLGA microparticles within the thermogel solution prior to application, improved release kinetics can be achieved, and a greater amount of drug can be incorporated. By creating a composite containing micelles or SLNs, the effective delivery of hydrophilic or lipophilic drugs can also be achieved.

Finally, an interesting iteration would be to graft disulfide bridges to chitosan directly to be used as an eyedrop. This formulation could be administered as an optically clear solution directly to the surface of eye. By incorporating the disulfide component directly to chitosan, the mucoadhesive properties of the solution could be easily altered as well as the solubility of chitosan improved. A therapeutic payload could then be conjugated as described in our previous studies. By utilizing this synthetic scheme, the release would be modulated by mucosal interaction rather than diffusion through the dilute solution. By using a dilute solution, the disulfide bridges should be readily accessible to bond with mucus, unlike those bonds which were situated in the core of the previously developed thermogels.

Once bound, the chitosan would be removed during natural mucosal turnover or enzymatically degraded. Overall, this system would release the therapeutic quicker than the thermogels but would be simpler to develop and easier for patients to use.